Mineral Solid Acid Catalysts in Environmentally Benign Fine Chemical Transformations

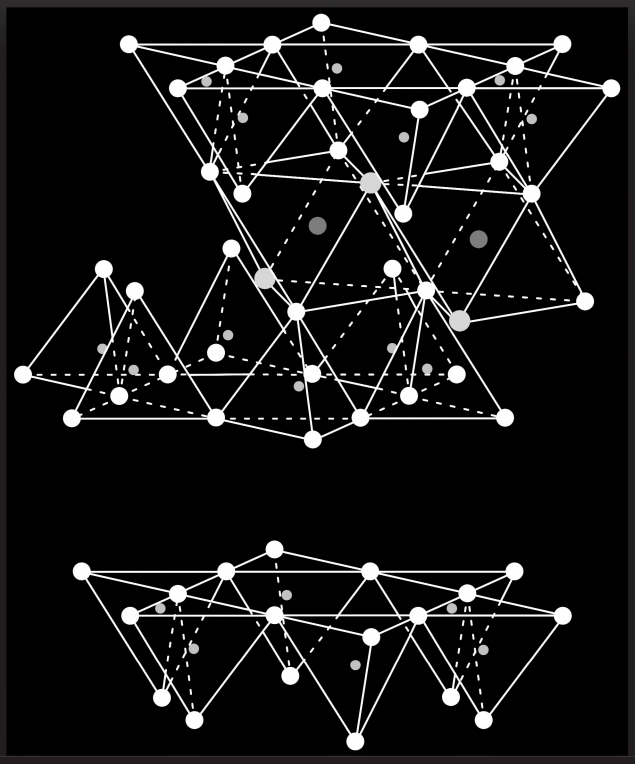

André Derksen

MINERAL SOLID ACID CATALYSTS IN ENVIRONMENTALLY BENIGN FINE CHEMICAL TRANSFORMATIONS

Een wetenschappelijke proeve op het gebied van de
Natuurwetenschappen, Wiskunde en Informatica

Proefschrift

ter verkrijging van de graad van doctor aan de Katholieke Universiteit Nijmegen,
volgens besluit van het College van Decanen in het openbaar te verdedigen op
dinsdag 14 maart 2000 des namiddags om 3.30 uur precies

door

Andries Johannes Derksen

Geboren op 6 september 1971
te Nijmegen

Promoter:	Prof. Dr. B. Zwanenburg
Co-promoter:	Dr. A.J.H. Klunder

Manuscriptcommissie:	Dr. M.J.G. Janssen (Exxon Chemical Europe Inc.)
	Prof. Dr. J.G. de Vries (DSM Research, Geleen)
	Dr. J.W. Scheeren

Ministerie van Economische Zaken

The research described in this thesis carried out as part of the
Innovation Oriented research Programme on Catalysis (IOP Katalyse, no. IKA 94068)
sponsored by the Netherlands Ministry of Economic Affairs.

ISBN 90-9013508-1

Voor mijn ouders

VOORWOORD

Een promotie en een proefschrift zijn een sluitstuk van een periode van onderzoek en studie. Deze periode heb ik als zeer prettig en leerzaam ervaren. Ik wil iedereen die hieraan heeft bijgedragen hartelijk bedanken, en zonder dat ik anderen tekort wil doen zal ik hieronder een aantal mensen met name noemen.

Allereerst bedank ik mijn promotor prof.dr. B. Zwanenburg voor het vertrouwen in mij en de grote mate van zelfstandigheid en vrijheid die hij mij heeft gegeven. Mijn co-promotor dr. Ton Klunder wil ik graag bedanken voor de stimulerende samenwerking, waarbij ik zijn niet aflatende stroom van enthousiaste ideeën zeer op prijs stelde. Ook mijn voorganger Adri van der Waals heeft een grote inbreng gehad in mijn promotie-onderzoek, aangezien ik verder kon gaan vanaf het punt dat hij had bereikt en ik hem voor tal van adviezen kon aanspreken.
Ook de voormalige en huidige Klunder-lab promovendi en post-docs André Volkers, Frank Bakkeren, René Gieling, René Ruinaard, dr. N.G. Ramesh, dr. Xue-shi Mao, Cyrus Afraz en Simona Müller dank ik voor de prettige en stimulerende samenwerking en fijne sfeer. Marieke van Ham wil ik bedanken voor de bijdrage die zij geleverd heeft aan het werk in hoofdstuk 7. Ook de overige studenten en promovendi van de afdeling ben ik dankbaar voor de goede onderlinge sfeer. De afdelingsstudiereizen naar Californië en Zuid-Afrika droegen hier enorm aan bij.
Mijn promotie-onderzoek was een IOP-Katalyse project waarbij er een samenwerking was met mede-IOP'ster drs. Meike Kerkhoffs en prof.dr. J.W. Geus van de afdeling anorganische chemie en heterogene katalyse van de Universiteit van Utrecht. Hierbij wil ik Meike bedanken voor de synthese van een aantal synthetische kleimaterialen en haar bijdrage aan de analyses van deze katalysatoren. De leden van de IOP-begeleidingscommissie dr. Marcel Janssen (Exxon Chemical Europe), dr.ir. W.T. Koetsier (Unichema), prof.dr. J.G. de Vries (DSM), dr. E. Kruissink (DSM), dr. F.T.B.J. van der Brink (DSM), dr. G.R. Meima (Dow Benelux), dr. M.H.G.M. Steijns (Dow Benelux), dr. C.R. Bayense (Engelhard De Meern), prof.dr.ir. W.J. Mortier (Exxon Chemical Europe), dr. J.J.L. Heinerman (AKZO Nobel Chemicals), dr. A.J.A. van der Weerdt (Quest), ing. J.J. Christiaanse (IFF), dr. C.M.A.M. Mesters (SRTCA), dr.ir. M.J. Groeneveld (SRTCA), drs. A.P.J. van Manen (PFW Aroma Chemicals) en ir. P.F. van den Oosterkamp (KTI) wil ik bedanken voor hun getoonde interesse, hun betrokkenheid en bijdragen aan de stimulerende discussies. De bijeenkomsten met deze specialisten hebben een grote invloed gehad op de richting van het onderzoek

en hebben mijn ogen geopend voor andere dan zuiver academische beweegredenen. De IOP-Katalyse bestuurders dr. Jan Oelderik, dr. Ward Mosmuller, drs. Jerry Kanhai en drs. Merlijn van Rijswijk wil ik bedanken voor hun inzet en prettige contacten.
Een speciaal woord van dank wil ik richten aan dr. Marcel Janssen (Exxon Chemical Europe) voor zijn hulp bij het opstarten van de experimenten met de micropuls unit (hoofdstuk 5), naar een voorbeeld uit zijn eigen laboratorium, en voor zijn hulp bij het leren uitvoeren en interpreteren van DRIFT-infrarood analyses (hoofdstuk 2). Bovendien kon ik bij hem terecht om typisch katalytische vraagstukken te bespreken. Dr. Kees Bayense van Engelhard De Meern wil ik bedanken voor het ter beschikking stellen van katalysatoren en voor zijn hulp bij het opstellen van een uniforme voor-behandelingswijze voor de gebruikte katalysatoren. Met de hulp van ing. J.J. Christiaanse en drs. J.-W. Slief (beide IFF) kon een grote verscheidenheid aan producten uitgaande van α-pineen oxide worden geïdentificeerd. Gerda Nachtegaal en dr. Arno Kentgens van de afdeling NMR spectroscopie wil ik bedanken voor hun hulp bij het uitvoeren en interpreteren van de aluminium MAS NMR metingen. De Röntgenanalyse uitgevoerd door dr. René de Gelder en Jan Smits van de afdeling Kristallografie verschafte essentiële informatie met betrekking tot de structuur van de onverwachte kooiverbinding uit hoofdstuk 7, zonder welke verder onderzoek aan dit onderwerp onmogelijk zou zijn geweest.
Van de afdeling Organische Chemie hebben Henk Regeling, Jan Dommerholt, Bertus Thijs, dr. Gerry Ariaans, dr. Gérard Nefkens en dr. Gordon Chittenden een bijdrage geleverd aan het werk uit dit proefschrift door hun interesse, discussies en suggesties. Ook een woord van dank aan Peter van Galen, Ad Swolfs, Helene Amatdjais-Groenen, Chris Kroon, Wim van Luyn en Pieter van der Meer voor hun analytische en/of technische steun. Jos Haerkens van de glasblazerij wil ik bedanken voor het altijd snel repareren of maken van onmisbare onderdelen. Voor de administratieve assistentie kon ik altijd weer terecht bij Jacky Versteeg, Sandra Tijdink en Nelly Weustink. Mijn paranimfen Ruud Titulaer en André Volkers wil ik bedanken voor onze prachtige vakantie-belevenissen in Zuid-Afrika.
Tenslotte wil ik mijn ouders bedanken voor de mogelijkheden die ze mij geboden hebben om me te ontwikkelen alsmede voor hun steun tijdens mijn studie en promotie-onderzoek. Helaas heeft mijn moeder de officiële afronding in de vorm van mijn promotie niet meer mogen meemaken.

André

CONTENTS

1 General Introduction

1.1 Heterogeneous catalysis in organic chemistry

Catalytic processes are involved in the manufacture of the majority of chemicals. Among the most frequently used catalysts are the acidic ones, which are generally applied in a homogeneous phase. The use of homogeneous acidic catalysts may have the following intrinsic drawbacks: *a.* a neutralization or washing step is usually required, which, depending on the amount of homogeneous catalyst to be used, may result in the formation of large amounts of waste salts. Disposal of these salts is usually expensive or entirely prohibited; *b.* separation of homogeneous catalysts from the reaction mixture is generally a difficult step; *c.* the use of Brønsted acids is often accompanied by corrosion of the process equipment; *d.* some of the applied catalysts are toxic or otherwise difficult to handle (air or water sensitive).

The aforementioned problems together with the increasing environmental concern and restrictive legislation have prompted research to find new effective catalysts, which avoid these drawbacks. Consequently, during the last decades solid acids are receiving increasing attention as catalysts in organic synthesis on laboratory and fine chemicals manufacturing scale.[1,2,3,4,5,6] Heterogeneous acid catalysts are of particular interest as they may have some intrinsic benefits: *a.* they can readily be separated from the reaction mixture; *b.* they are easier to handle, which enhances safety of operation; *c.* solid acids are less corrosive; *d.* many solid acids can be regenerated and reused, thus reducing the amount of effluents; *e.* solid acids may be adapted for use in a continuous flow reactor.

Many solid acid catalysts have already been developed, for example zeolites, clays and metal oxides, or supports impregnated with reagents such as BF_3. Despite their broad availability, the use of solid acid catalysts has so far been mainly limited to gas phase and bulk processes, such as (hydro)-cracking and (hydro)-isomerization.

Transport of the reactants to the active sites is generally not difficult for homogeneous catalysts. In heterogeneous catalysis, on the other hand, transport is an important issue, since the substrates have to migrate into the usually highly porous catalyst body in order to react and the reaction products should readily be released

from the catalyst into the bulk of the surrounding medium. In many acid-catalyzed reactions, however, one of the reactants may react to give compounds of higher molecular weight, which migrate slowly through the catalyst pores and which thus can block the active sites. Diffusion limitations are most important in the liquid phase, since diffusion coefficients in the liquid phase are approximately 10^4 times lower than in the gas phase. For this reason catalysts with long and narrow pores, such as zeolites, may suffer from a severe loss of activity in the liquid phase. Solid acids with pores considerably larger than those in zeolites are clays. Amorphous alumina and amorphous silica-aliminas may possess even larger pores, although the textural structures of these materials are less ordered than of the first two mentioned.
The desire to improve or alter the selectivity of a chemical process may be another important reason for selecting a solid catalyst. The structural and electronic properties of the solid catalyst can put constraints on the diffusion of molecules to and from active sites and on the geometric configuration of the transition state. These constraints may lead to kinetic control over reaction pathways, resulting in non-thermodynamic product compositions. However, the products formed from the primary reaction may also react in a secondary reaction, depending on the contact time and the strength of the interaction with the active site. It is therefore desirable that the products of the primary reaction desorb readily into the bulk of the surrounding medium. The contact time between catalysts and reactants and products may have a strong influence on the product selectivity.
The use of reduced pressure for reactions in the gas phase increases the driving force for desorption from the catalytic sites and thus decreases the residence times. This may lead to a decreased probability of undesired intermolecular reactions and consequently to an improved selectivity. The 'catalytic flash vacuum thermolysis' technique is a dynamic process in which a substrate in the gas phase is passed over a catalyst bed in a hot zone and the products are trapped afterwards.[6] The use of reduced pressures ensures a short residence time on the catalyst surface and in the hot zone. Elaborate (pumping) equipment and low mass transfers, however, reduce the economic viability of an industrial application of this technique. On the other hand, expensive reagents or laborious isolation procedures may become redundant.

1.2 IOP CATALYSIS

The Dutch Ministry of Economic Affairs promotes research in a number of promising fields in order to improve the competitive position of the industry in the Netherlands on the worldwide market. The Innovation Oriented research Programmes (IOPs) provide universities and (non-profit) research institutes with additional funding for research projects that are specifically aimed at meeting the short- and long-term

needs of Dutch industry. In addition, IOPs are intended to encourage collaboration between universities, research institutes and industry. Since 1989 several IOPs were initiated in a variety of fields and one of these programmes was aimed at strategic catalysis research: IOP Catalysis. The chemical industry generates 20-30% of the Gross National Product of the Netherlands and catalytic transformations are involved in the manufacture of approximately 80% of the total volume of chemicals. Hence, a solid knowledge base of catalysis is of strategic interest to the Dutch chemical industry.[7]

The central theme of the IOP catalysis is 'precision in chemical conversion'. This precision is required in order to save energy and feedstocks, as well as to avoid the formation of undesired by-products and waste. Catalysis is applied on a large scale in petroleum refining and in the production of bulk chemicals, but this is far less the case in the manufacture of fine chemicals where classical multi-step syntheses still play a much larger role. These classical procedures often involve lower selectivities, the use of undesirable, toxic, or corrosive reagents, the formation of by-products, and large amounts of waste. IOP Catalysis, therefore, directs its efforts to the introduction of novel catalytic routes in the fine chemical industry.

1.3 AIM AND OUTLINE OF THE THESIS

The aim of the research described in this thesis was to apply and develop catalysts for environmentally friendly fine chemical syntheses on the basis of amorphous aluminas and natural or synthetic clay materials.

In **Chapter 2** the chemical, textural and structural properties of solid acids, such as amorphous alumina, amorphous silica-alumina, clays and zeolites are described. In addition, the possible uses of these materials are briefly treated. Furthermore, the characterization of the solid acid catalysts used in this thesis is discussed.

Chapter 3 treats the use of various solid acid catalysts in the isomerization of epoxides to carbonyl compounds in liquid phase reactions (Scheme 1.1). The activity of the catalysts will be discussed with respect to their acidity and their porosity. In addition, attention will be given to the comparison of the catalytic activities of natural and synthetic clay materials. The epoxides used in this chapter have one or more aromatic substituents (viz. styrene oxide, *cis*- and *trans*-stilbene oxide and tetraphenyloxirane) or is a complex aliphatic epoxide (α-pinene oxide). The reactions of styrene oxide and α-pinene oxide to phenylacetaldehyde and campholenic aldehyde, respectively, are important fine chemical transformations and the industrial relevance of the present work is discussed.

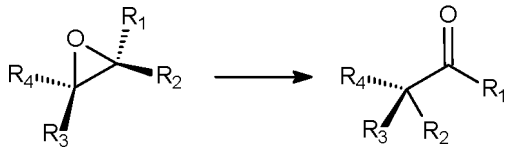

Scheme 1.1 *Isomerization of epoxides into carbonyl compounds*

In **Chapter 4**, the use of various solid acid catalysts in the isomerization of epoxides under catalytic flash vacuum thermolysis conditions is described. The substrates used to investigate the isomerization reaction were similar to those in Chapter 3, but, in addition, several aliphatic epoxides (viz. cyclohexene oxide and 1-octene oxide) and an epoxide having an additional polar functionality (viz. methyl 3-phenyl-2-oxiranecarboxylate) were used. As in Chapter 3, the industrial relevance of the conversions of styrene oxide into phenylacetaldehyde and of α-pinene oxide into campholenic aldehyde is discussed.

The application of various solid acid catalysts in a fixed reactor under normal pressure and flow conditions in the epoxy/carbonyl rearrangement reaction is treated in **Chapter 5**. A puls flow system incorporated in a gas chromatograph was employed as a model for a fixed bed reactor. The reactions of styrene oxide and α-pinene oxide, whose rearrangements are of industrial relevance, were investigated under these conditions.

Chapter 6 deals with the application of various solid acid catalysts in the pinacol rearrangement under catalytic flash vacuum thermolysis (Scheme 1.2). This rearrangement was studied, since it has mechanistic similarities with the epoxide rearrangement. A pronounced difference between these types of reactions is the formation of water during the pinacol rearrangement. However, it turned out that the water released does not hamper the catalytic performance under the conditions used. The diols used may be considered as the diol analogs of the epoxides used in Chapter 4 and a comparison is made between the results obtained in the pinacol rearrangement and the epoxy/carbonyl rearrangement. The industrial relevance of this work is discussed.

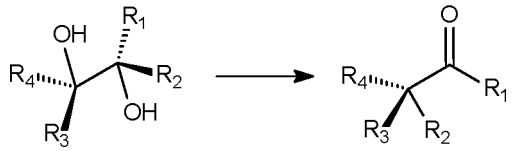

Scheme 1.2 *The pinacol rearrangement of diols into carbonyl compounds*

In **Chapter 7**, various solid acid catalysts were used in the liquid phase and under catalytic flash vacuum thermolysis conditions to study the retro Diels-Alder reaction. Surprisingly, in addition to this fragmentation reaction in both media an unexpected reaction product was found when more complex substrates were used (Scheme 1.3).

A reactive function in close proximity to the norbornene double bond proved to be essential in both cases. Mechanisms are proposed for both of these unexpected reactions. The structure of one of the compounds obtained under catalytic flash vacuum thermolysis conditions, was established by X-ray diffraction analysis.

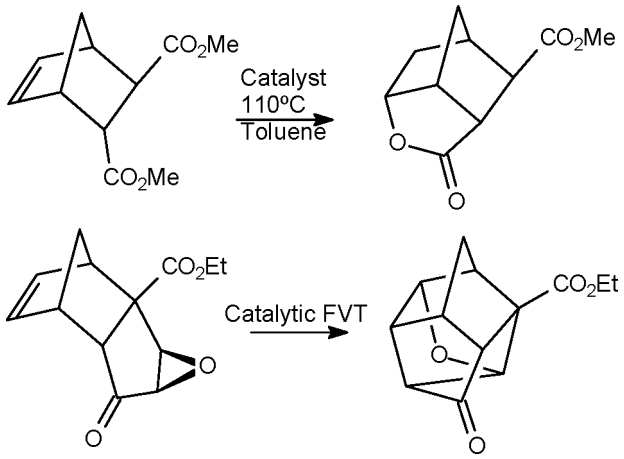

Scheme 1.3 *Unexpected reactions observed during the retro Diels-Alder reaction*

1.4 REFERENCES

1 Smith, K. Ed. *Solid Supports and Catalysts in Organic Synthesis*, Ellis Horwood Ltd., New York, 1992.

2 Izumi, Y.; Urabe, K.; Onaka, M. in *Zeolite, Clay and Heteropoly Acid in Organic Reactions*, VCH, Weinheim, 1992.

3 Balogh, M.; Laszlo, P. in *Organic Chemistry Using Clays*, Springer Verlag, Berlin, 1993.

4 Clark, J.H.; Kybett, A.P.; Macquarrie, D.J. in *Supported Reagents: preparation, analysis, and applications*, VCH, New York, 1992.

5 Laszlo, P. Ed. in *Preparative Chemistry using Supported Reagents*, Academic Press, San Diego, 1987.

6 Van der Waals, A.C.L.M. *Thesis*, University of Nijmegen, The Netherlands, 1997.

7 *IOP Catalysis, Book of factsheets*, Senter Den Haag, The Netherlands, 1998.

2 SELECTED SOLID ACIDS: THEIR CHARACTERISTICS, APPLICATIONS & PROPERTIES

2.1 INTRODUCTION

Solid catalysts have been used in organic chemistry for quite some time. Already at the beginning of the 20th century clay minerals were used as catalysts.[1] In 1911 Montaland[2] was granted an U.S. Patent for the isomerization of pinene to camphene employing various catalysts including the clay palygorskite. This mineral was also used by others authors to polymerize pentenes and hexenes to di- and trimers and higher polymers,[3] for the isomerization of terpenes[4], and the oxidation of alcohols to aldehydes.[4] The petrochemical industry started to use solid catalysts on a large scale as early as in the 1930s.[1,5] The use of oil as a feedstock to produce petroleum and gasoline was greatly enlarged when thermal and, later, catalytic cracking processes were developed. Initially, aluminum trichloride was used in a batch process, but severe problems were encountered in the disposal of spent catalyst dissolved in hydrocarbons. A major breakthrough came from the studies of Houdry who developed a fixed bed process, employing activated clays as the catalysts.[6] In this process the coke deposited on the used catalyst was removed by burning, thus enabling a continuous operation. Most of the aviation gasoline used during The Battle of Britain was produced in Houdry units.[5] At the beginning of the 1940s the Fluid Catalytic Cracking (FCC) technology was developed, which proved to be very successful. In this process the reactor and the regenerator consisted of fluidized beds and silica-alumina catalysts were used. The FCC process has been continuously improved with respect to the design of the process and the type of catalyst. Acid treated clays were replaced by silica-alumina catalysts, which in turn were replaced by zeolites in the early 60s. Their mechanical strength and thermal durability allowed further improvements in the FCC process.

During the last three decades solid acids are also receiving increasing attention for their use in organic synthesis on laboratory and fine chemicals manufacturing scale.[7,8,9,10,11,12] The growing interest in using solid acids in these areas finds its origin in some of the intrinsic benefits of these catalysts, namely, *a*) they can be removed easily from the reaction mixture by straightforward filtration or centrifugation,

which eliminates the necessity of an hydrolytic work-up procedure; *b*) they are easier to handle, which enhances safety of operation; *c*) solid acids are less corrosive; *d*) many solid acids can be regenerated and reused, thus reducing the amount of effluents; *e*) solid acids may be adapted for use in a continuous flow reactor.

Another important reason for selecting a solid catalyst is to improve or alter the selectivity of a chemical process. Due to the interaction with active sites at the surface or within the pores of the heterogeneous catalyst, the geometry of the adsorbed molecule is changed to such an extent that the activation energy barrier for a particular reaction pathway is altered (e.g. by protonation or dissociative chemisorption). The structural and electronic properties of the solid may also put constraints on the diffusion of molecules to and from active sites and on the geometric configuration of the transition state. These constraints may lead to kinetic control over reaction pathways, resulting in non-thermodynamic product compositions. However, the products formed from the primary reaction may undergo secondary reactions and undesired transformations, depending upon the contact time and the strength of the interaction with the active site. It is therefore desirable that the primary reaction products desorb back into the bulk of the surrounding medium. The contact time between catalysts and reactants and products may have a strong influence on the product selectivity. Generally, shorter contact times result in higher selectivities (at lower conversion) than long contact times when the selectivities are determined by primary reactions. Catalysts having long and narrow pores may, as a result, deactivate rapidly due to the accumulation of products in their cavities that then undergo secondary reactions. Diffusion of substrates to and products from active sites is less problematic when solid catalysts with short and wide pores are employed. This is most pronounced with large molecules and the ratio pore size : substrate size is important in this respect.

Solid acids are characterized by the presence of protons and/or coordinatively unsaturated cationic centers on their surfaces, resulting in Brønsted and Lewis acidity, respectively. The properties of solid acids are determined by *a*) the nature of the acidity (Brønsted or Lewis type); *b*) the number and strength of the acidic sites; *c*) the surface characteristics of the solid; *d*) the presence of coexisting acid and basic sites on the surface.

The decision to use a specific catalyst in an (industrial) application is also governed by factors such as thermal durability, mechanical strength, particle size and shape, attrition resistance, regenerability and cost.

2.2 SELECTED SOLID ACIDS: THEIR CHARACTERISTICS AND APPLICATIONS

Many types of solid acids are known. The most important groups of solid acids are acid resins, supported Brønsted and supported Lewis acids, solids containing activated water molecules (e.g. hydrated sulfates), solid super acids[13], activated carbons and silica aluminas. The last mentioned class of important porous inorganic solids can be subdivided into three morphological types:[7] *a*) amorphous solids with no long-range crystalline order containing random pores (e.g. amorphous silica-alumina and alumina); *b*) solids consisting of silicate sheets separated by interlamellar regions (e.g. clays); *c*) crystalline, microporous aluminosilicates with molecular-sized intracrystalline channels and cages (e.g. zeolites). In the next sections, the characteristics of these three types of silica aluminas will be treated in more detail.

2.2.1 Amorphous alumina

The term alumina refers to a series of solids having a general formula of $Al_2O_3 \bullet (H_2O)_n$, where n = 0 to 3, although none of them actually contains H_2O. Aluminas are prepared by heating natural or synthetic crystalline and amorphous $Al(OH)_3$ [$Al_2O_3 \bullet (H_2O)_3$] and AlO(OH) [$Al_2O_3 \bullet (H_2O)$]. When the materials are heated above 1100°C, the end point in the synthesis is corundum, which is the thermodynamically most stable form of Al_2O_3 and one of the hardest substances known. When heating at temperatures below 1100°C, amorphous aluminas or a series of transition aluminas can be prepared depending on the precursor, final temperature and the mode of heating. During thermolysis hydroxyl groups combine to generate H_2O, which is expelled from the solid. Heating to 600°C, yields the γ-alumina series with the formula $Al_2O_3 \bullet (H_2O)_n$, where n < 0.6. γ-Alumina, in which the Al^{3+} cations are partly tetrahedrally and partly octahedrally coordinated,[7] has a high surface area, a large mesopore volume and is thermally stable. Heating at higher temperatures between 800 and 1000°C, yields the δ series of aluminas. They contain very few OH groups and are more crystalline than aluminas of the γ series.

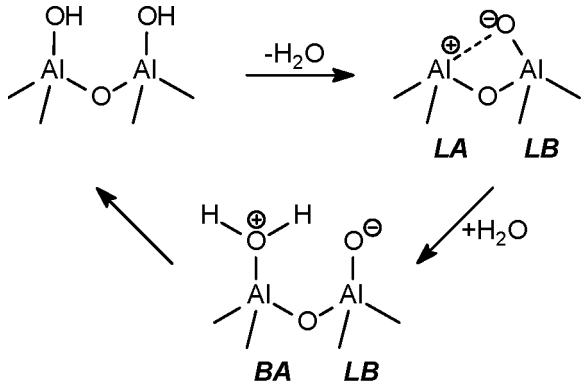

Scheme 2.1 *Acidic and basic sites on aluminas*[14] *(LA= Lewis acidic; LB= Lewis basic; BA= Brønsted acidic)*

The ideal surface of hydrated γ alumina, as proposed by Peri,[15] is ended by hydroxyl groups, each directly above an aluminum ion in the next layer of the crystallite. Upon heating, physisorbed water is lost and then adjacent hydroxyl groups react with one another by proton transfer to generate a bridging oxide and H_2O.[15,21] Thus, for every bridging oxide that is generated, an aluminum is exposed, resulting in the presence of three species on the surface: hydroxyls, bridging oxides and aluminum, as is depicted in Scheme 2.1. Their concentrations are correlated with each other and controlled by the activation temperature. Hence, the surface can exhibit a variety of properties: hydroxyls will act as a very weak Brønsted acid[16] (BA) or as a base (BB); bridging oxides will act as a strong base (LB) and nucleophile and exposed aluminum is a Lewis acid (LA). An activated alumina will, as a result, have strongly acidic and basic sites adjacent to each other, which may act cooperatively. Unactivated γ alumina is basic,[17] but neutral or acidic alumina may be prepared by treatment with an appropriate neutralizing or acidifying agent. Alumina is amphoteric. When it is brought into contact with a sufficiently basic solution, the surface hydroxyl groups are deprotonated and cations are placed onto the surface under reversible conditions. Contrarily, when the solid is contacted with a sufficiently acidic solution, the surface hydroxyl groups are protonated which puts anions on the surface.

The polar environment[18,19] of the surface of alumina is favorable for many ionic and heterolytic reactions. Organic substrates can interact with the surface by a variety of mechanisms, including hydrogen bond formation and acid-base reactions. Moreover, the presence of adjacent basic and acidic sites presents a reaction environment that is not possible in solution chemistry. In addition, a number of surface modified aluminas have found their applications in organic synthesis. These are often prepared by evaporation of an aqueous solution of a salt in the presence of the alumina to give a 'supporting reagent'.[7,10,11,13] Many salts have been employed in this fashion, of which the evaporation of KF in water onto alumina is a widely used one, giving a very basic solid containing no free fluoride ions.[13]

Aluminas and modified aluminas have been applied in a large variety of reactions.[20,21,22,23] Examples are: epoxide ring opening reactions, elimination and addition reactions, aromatic substitutions, nucleophilic substitution reactions, solvolysis reactions, condensation reactions and conjugate additions, isomerizations, rearrangements, protection and deprotection reactions, oxidation and reduction reactions and photochemical reactions.

2.2.2 Amorphous silica-alumina

The pure forms of alumina and silica exhibit only a weak acidity.[24] Silica-aluminas, however, show a pronounced acidity. The term silica-alumina (or aluminosilicates) refers to silicas in which a substantial fraction of the SiO_2 units are isomorphously substituted by AlO_2^- ions.[25] Since silicon is present in far greater numbers than aluminum, silanol groups and derivatives are abound at the surface of silica-aluminas. Hydrogen bonded water molecules are liberated in vacuum at ambient temperatures or at 150°C at normal pressures. When the temperature is increased (> 175°C) hydroxyl groups on the surface condense to form siloxane bonds by the expulsion of water (Scheme 2.2).[25]

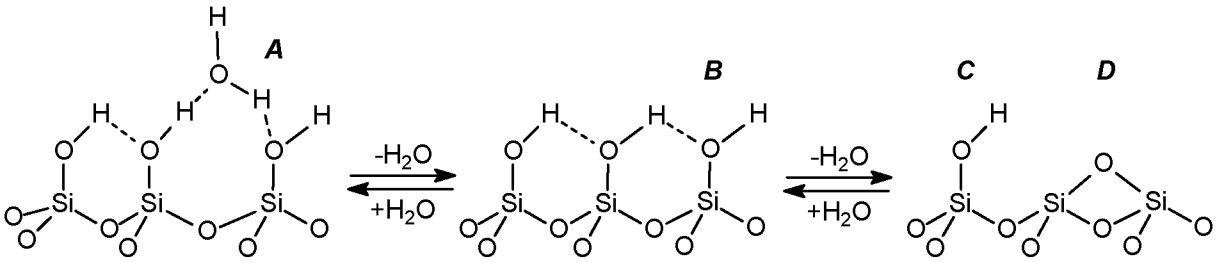

Scheme 2.2 *Types of hydroxyl groups on the surface of silica(-alumina)*

The types of hydroxyl groups that can be distinguished in Scheme 2.2 are: vicinal hydrated (***A***), vicinal anhydrous (***B***), isolated (***C***) and siloxane – dehydrated (***D***).
Since silica is the excess component in these materials, the fourfold coordination of silicon is enforced on the aluminum centers.[24] In a polymeric oxide structure aluminum has a coordination requirement of three, but the structure imposed by silica directs the coordination of the Al-O bonds of each aluminum into the tetrahedral configuration. The resulting vacant tetrahedral direction at the aluminum center presents a site, which can accept a pair of electrons: a Lewis acidic site (LA). This Lewis acid site can be converted into a Brønsted acid site by the interaction with a water molecule, as is shown in Scheme 2.3. By accepting the pair of electrons from the water molecule, the aluminum center can form a fourth bond. The complementary proton accepts electron density from one of the neighboring bridging oxygen atoms, forming a partial bond. This site can easily donate a proton: a Brønsted acidic site (BA), analogously to pure sulphuric acid. This model of silica-aluminas has been developed by theoretical investigations of prototype structures.[26] These show a substantial electron deficiency at the aluminum center in the Lewis acidic form and a relatively large positive charge of the proton which is attached to the bridging oxygen atom in the Brønsted acidic form.

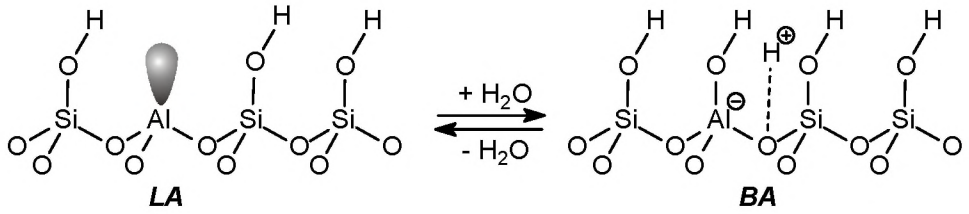

Scheme 2.3 *Acidity in silica-aluminas (LA= Lewis acidic; BA= Brønsted acidic)*

Amorphous silica-aluminas have been applied as catalysts in a number of reactions,[12,27] such as isomerizations of olefins and paraffins, alkylation of aromatics with alcohols and olefins, olefin polymerization and catalytic cracking.

2.2.3 Clays and clay minerals

The term 'clay' refers to naturally occurring materials composed primarily of fine-grained minerals, which are generally plastic at appropriate water contents and will harden when dried or fired.[28] Although clays usually contain a large amount of phyllosilicates, they may also contain other materials. The term 'clay minerals', on the other hand, refers to phyllosilicate minerals and to (other) minerals that cause plasticity to clay and which harden upon drying or firing.[28] The minerals that are presently known to give the plasticity to clays are phyllosilicates. Phyllosilicates are layered or two-dimensional silicates. Although the terms 'clays' and 'clay minerals' are not identical, in this thesis they are used interchangeably.

X-ray diffraction techniques have shown that clay minerals are crystalline.[29] Pauling[30] was the first to propose the crystal structure of a clay mineral, consisting of repeating layer structures. Most of the clay minerals are built up from two types of layers.[7] The first consists of a sheet of SiO_4^{4-} tetrahedra arranged in a hexagonal network. The SiO_4^{4-} tetrahedral sub-units are linked with its neighbors by sharing three of its four oxygen corners. The remaining fourth oxygen apex is shared with octahedra in an adjacent sheet. The second layer consists of edge-sharing octahedra, usually composed of either gibbsite $[Al_2(OH)_6]$ or brucite $[Mg_3(OH)_6]$ units. The octahedrons are arranged in a hexagonal configuration in such a manner that each oxygen atom is shared with two neighboring metal atoms. The resembling symmetry and almost identical dimensions of these tetrahedral and octahedral sheets permit them to be combined by sharing the apical oxygens of the silica layers with the successive octahedral layers.[31] This is accompanied by a slight distortion of the silica sub-units from a hexagonal to a ditrigonal symmetry. The octahedral layer may be further divided into a trioctahedral or dioctahedral type, depending upon their degree of occupancy of the octahedral sites. In trioctahedral layers all octahedral sites are occupied, generally by divalent ions (e.g. Mg^{2+}). In dioctahedral layers only 2/3

of the octahedral sites are filled, generally by trivalent ions (e.g. Al^{3+}), and 1/3 of their octahedral sites are vacant.

The sheet structures in clay minerals contain combinations of tetrahedral and octahedral layers.[7] A 1:1 clay mineral contains one layer of each type in a sheet (also called a TO sheet). In a 2:1 clay mineral one octahedral layer is 'sandwiched' by two tetrahedral layers in each TOT sheet. A 2:1:1 clay mineral contains alternating TOT sheets and gibbsite or brucite layers. 2:1 'inverted ribbon' clay minerals contain TOT sheets in which tetrahedra invert at regular intervals to cross-link octahedral layers, creating a three-dimensional structure. The structure of montmorillonite, a 2:1 phyllosilicate, is shown in Figure 2.1.[32]

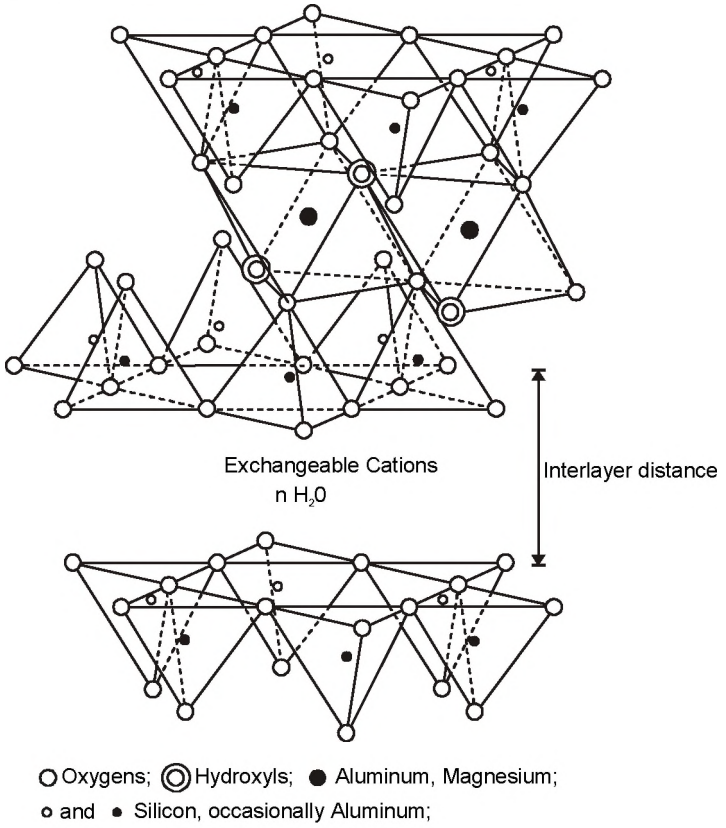

Figure 2.1 *Structure of montmorillonite (a 2:1 phyllosilicate)*

The cations in the tetrahedrons and octahedrons in clay sheets can sometimes be replaced by other cations, which is called isomorphous substitution.[7] Si^{4+} cations occupy most of the tetrahedral sites in clay minerals, but Al^{3+} may replace them to some extent. This substitution by Al^{3+} in the tetrahedral sheets must, however, comply with Loewenstein's rule[33] stating that only one of two connected tetrahedra can be occupied by aluminum. In dioctahedral clay minerals the octahedral sites are usually occupied by Mg^{2+}, which may be substituted by other divalent or monovalent cations (e.g. Fe^{2+}, Ni^{2+} or Li^{+}). In trioctahedral clays Al^{3+} predominantly occupies the octahedral sites. Substitution of Al^{3+} by other trivalent (e.g. Fe^{3+} or Cr^{3+}) or divalent cations (e.g. Mg^{2+} or Fe^{2+}) are common in 2:1 phyllosilicates. The isomor-

phous substitution of cations by lower valent cations results in a net negative charge of the sheets. This charge is compensated by interlayer cations (e.g. Na^+, K^+, Ca^{2+}, Mg^{2+}, etc) residing between adjacent sheets. When the interaction between the clay sheets is weak the interlayer cations are able to coordinate with water or other polar species causing swelling of the clay. This swelling can occur when there are enough interlayer cations present and the interlayer charge is not too large, since strong electrostatic forces would hold the alternating anionic layers and interlayer cations together. In Table 2.1 the most important 2:1 type clay minerals are collected, including their layer charges and idealized formulas.

Table 2.1 *Classification of 2:1 type clay minerals*[8,34]

Mineral group	**Subgroups**[a,b,c]	
(x = Layer charge)	Dioctahedral	Trioctahedral
Pyrophyllite-Talc ($x \cong 0$)	Pyrophyllite $[Al_4](Si_8)O_{20}(OH)_4$	Talc $[Mg_6](Si_8)O_{20}(OH)_4$
Smectite ($0.25 < x < 0.6$)	Montmorillonite $M^{n+}_{x/n}.yH_2O[Al_{4-x}Mg_x](Si_8)O_{20}(OH)_4$	Hectorite $M^{n+}_{x/n}.yH_2O[Mg_{6-x}Li_x](Si_8)O_{20}(OH)_4$
	Beidellite $M^{n+}_{x/n}.yH_2O[Al_4](Si_{8-x}Al_x)O_{20}(OH)_4$	Saponite $M^{n+}_{x/n}.yH_2O[Mg_6](Si_{8-x}Al_x)O_{20}(OH)_4$
		Stevensite $M^{n+}_{x/n}.yH_2O[Mg_{6-x}\bullet_x](Si_8)O_{20}(OH)_4$
Vermiculite ($0.6 < x < 0.9$)	Dioctahedral vermiculite $M^{n+}_{x/n}.yH_2O[Al_4](Si_{8-x}Al_x)O_{20}(OH)_4$	Trioctahedral vermiculite $M^{n+}_{x/n}.yH_2O[Mg_6](Si_{8-x}Al_x)O_{20}(OH)_4$
Mica ($x \cong 1$)	Muscovite $K_2[Al_4](Si_6Al_2)O_{20}(OH)_4$	Phlogopite $K_2[Mg_6](Si_6Al_2)O_{20}(OH)_4$
Brittle mica ($x \cong 2$)	Margarite $Ca_2[Al_4]Si_4Al_4)O_{20}(OH)_4$	Clintonite $Ca_2[Mg_4Al_2]Si_2Al_6)O_{20}(OH)_4$

[a] M^{n+} represents the interlayer cation. [b] • represents a vacant site. [c] cations in brackets occupy octahedral sites, cations in parentheses occupy tetrahedral sites.

Swelling can be used to exchange the interlayer cations by other simple cations or by large complex cation complexes to produce 'pillared clays'.[34,35] Pillaring allows the adjustment of the spacing between clay sheets, called interlayer distance, and hence the pore shape and volume. Moreover, pillared clays have a stabilized interlayer region that will not collapse as easily as in the case of non-pillared clays due to the (oxide) pillars forming a heat stable porous structure. The concentration of exchangeable cations is dependent on the layer charge and the type of cation present and is referred to as the cation exchange capacity, usually expressed in milli-equivalents per 100 g of dried clay.

Clays display both Lewis and Brønsted acidity. The occurrence of both types of acidity is governed by structural and environmental factors,[36] of which the water content is very important.[31,37,38] Adsorbed water is dissociated by the polarizing power of interlayer cations, which depends on the charge and size of the cation.[31,38] The destination of the resulting protons differs for tetrahedral and octahedral substituted smectites.[8] The strong Brønsted acidity in tetrahedrally substituted smectites is caused by the Si-OH···Al structure generated by the protonation at the Si-O-Al linkage in the tetrahedral sheet (cf. Scheme 2.4). The acidic site is thus formed at the surface. In the case of octahedrally substituted smectites the released protons migrate via a hexagonal window into the octahedral layer, since the surplus negative charge emanates from isomorphous substitution in this layer. The proton occupies there the site of a former vacancy and associates with the lattice oxygens, or becomes attached to the OH group located at the bottom of the hexagonal window (cf. Scheme 2.4). These acidic sites are located within silicate layers and access to these sites is very difficult since the entrance aperture of the hexagonal window is as small as an oxygen atom.[8]

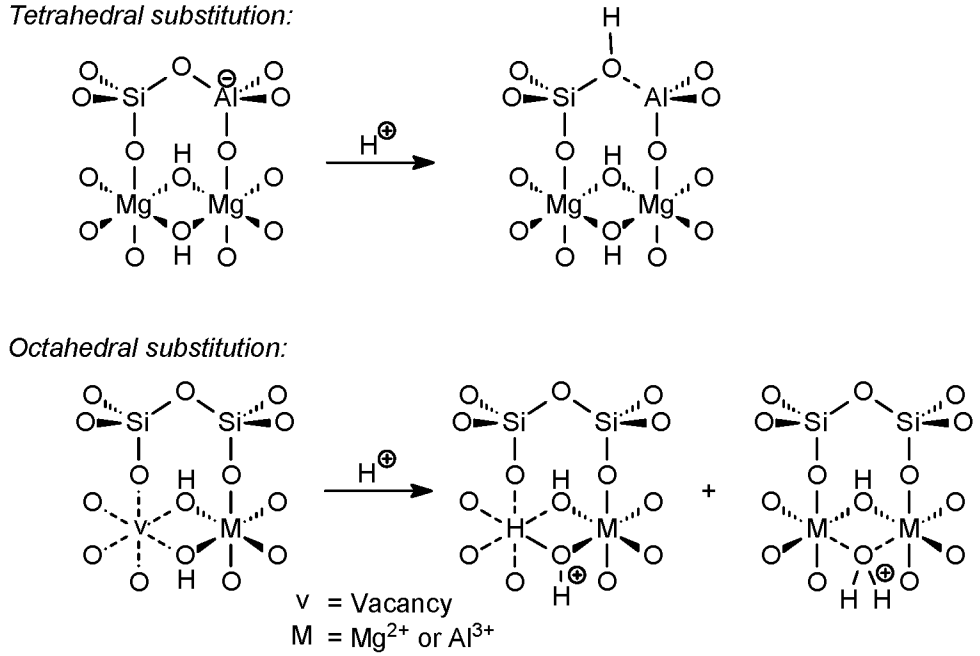

Scheme 2.4 *Brønsted acidity in clays*

When the water content of a clay is reduced to less than ~5% by weight, the acidity increases because the polarization by the cation is less dispersed.[39] However, removing all water from the clay, by calcination above 200°C, reduces the Brønsted acidity.[38] The clay adopts a more pronounced Lewis acidic character due to the transformation of Brønsted acidity into Lewis acidity[38] (cf. Scheme 2.5). A different type of Lewis acidity originates from exposed Al^{3+} centers at 'broken' crystallite

edges.[9,40] Such centers are coordinatively unsaturated and their dangling bonds constitute Lewis acidic sites (cf. Scheme 2.5).

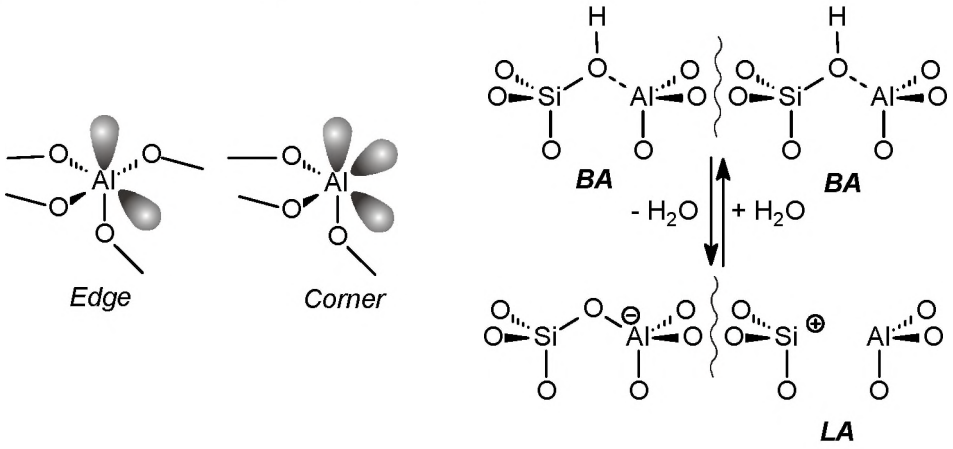

Scheme 2.5 *Lewis acidity in clays (LA= Lewis acidic; BA= Brønsted acidic)*

Smectite clays are often treated with mineral acids to give materials with high surface area (increasing from *ca* 60 m^2/g to *ca* 300 m^2/g). Fe^{3+} cations, causing a gray or yellow color of the clay, are removed by this acid activation process. This process involves harsh conditions (boiling for several hours in concentrated mineral acids) and destroys much of the layer structure as it leaches iron, aluminum and magnesium ions from the octahedral layer.[41] This causes the edges of the clay particles to become very disordered and consisting mainly of 'floppy' silica sheets,[31] as can be detected by scanning electron microscopy.[41] Mainly Al^{3+} and H^+ cations replace the exchangeable cations in the interlayer spacing during the acid treatment.

The application of natural clays is accompanied by some disadvantages that can be avoided using synthetic clay minerals. Synthetic clays can be prepared with a well-defined chemical composition and texture and the presence of impurities is prevented. In addition, clays may be synthesized with compositions that are not found in geological environments. A distinct morphologically difference between natural and synthetic clays is that in the latter the clay platelets are arranged in a 'house of cards' structure,[8,42] as is schematically drawn in Figure 2.2. The smaller dimensions of the clay platelets cause this deviating arrangement, but the type of interlayer cation and the method of drying are also of influence. The 'house of cards' structure gives these clays generally a higher surface area and an improved thermal stability.[8]

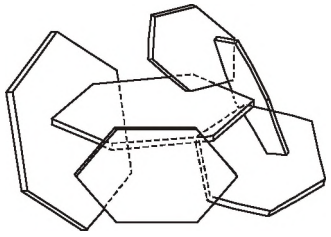

Figure 2.2 *Schematic representation of a 'house of cards' structure*

Long reaction times or high pressures and temperatures usually accompanied the synthesis of smectites.[35g] Recently, however, Vogels *et al.*[42,43,44] have developed a methodology by which synthetic saponites can be prepared under mild hydrothermal conditions (i.e. 10 h at 90°C and 1 atmosphere). Via this methodology saponites could be readily synthesized with various Si/Al ratios, various cations at octahedral positions (i.e. Mg^{2+}, Zn^{2+}, Ni^{2+}, Co^{2+} and combinations thereof) and a range of tetrahedral compositions (i.e. Si^{4+} substituted by Al^{3+}, Ga^{3+} or B^{3+}). These synthetic saponites exhibited promising results as catalysts in Friedel-Crafts alkylation[42,45] and cracking reactions.

Acid-treated natural clays were the solid catalysts of choice used in the petroleum refining in the early 1930s, but their lack of thermostability under high-temperature fluidized catalytic cracking (FCC) seriously affected their lifetime. In subsequent years they were replaced by the more stable synthetic silica-aluminas, which in turn were replaced by zeolites. However, a renewed interest in clays arose with the development of the more heat stable pillared clays, which are now considered as specialist FCC catalysts to deal with heavy crudes.[8]

The study of the potential application of clays as environmentally friendly solid acid catalysts in fine chemical and laboratory reactions has started in the 1970s. To date, there are numerous reports on the catalytic activity of clays and clay-based materials, in a large variety of organic transformations.[7,9,11,31,32,46,47] These include addition, Diels Alder, (de)protecting, condensation, elimination, electrophilic aromatic substitution, isomerization and oxidation reactions. In addition, clays have found widespread use as bifunctional or 'inert' supports (e.g. for metal complexes, enzymes, etc.) and as fillers to provide solid catalysts with certain required physical properties (e.g. attrition resistance, density, specific heat resistance).[7] Outside the field of catalysis, clays are in use in drilling fluids, as a bond for foundry sands and iron ore pellets, as a sealant in many engineering applications, as adsorbents and in structural ceramic products.[48]

2.2.4 Zeolites

Zeolites are three-dimensional crystalline aluminosilicates consisting of a framework of SiO_4 and AlO_4 tetrahedra, each with a silicon or aluminum in the center.[32] The oxygen atoms are shared between adjacent tetrahedra. A SiO_4 unit in a zeolite framework is electronically neutral, but since aluminum has a charge of +3, there must be a cation present for every aluminum tetrahedron to balance the resulting negative charge. A general formula[32] of a zeolite can be written as $M^{n+}_{x/n}(AlO_2)_x(SiO_2)_y \bullet mH_2O$, with M^{n+} as charge balancing cations. The number (m) of adsorbed water

molecules depends on the size of the cavities and pores and can be reduced by heating. The Si/Al ratio (*x/y*) varies from unity in certain synthetic zeolites to infinity in silicates with zeolite structures. Loewenstein's rule[33] prohibits a Si/Al ratio smaller than 1.

The tetrahedral units are arranged in a rigid three-dimensional network resulting in the occurrence of strictly regular cavities and pores with sizes of the same order of magnitude as molecular dimensions (3 – 15 Å).[27] Pore dimensions are dependent on the type of zeolite, of which, at present, approximately 98 structure types are known.[49] In addition to zeolites there are also many non-aluminosilicate molecular sieves, for example aluminophosphate or $AlPO_4$, a '3-5' analogue of the pure '4-4' SiO_2.

The water molecules occupying the cavities and pores of the zeolite can be reversibly removed by heating, leaving the zeolite structure intact. The resulting spaces are available for sorption of other molecules, and because of their uniform diameters they may discriminate between organic molecules on the basis of their size. When organic reactions take place in the channel and pore system of zeolites, size restrictions on the reactants, products or transition states may result in shape selectivity (cf. Scheme 2.6).[11,50,51]

The sorption properties and the acidity of zeolites is governed by the Si/Al ratio.[27] The electronic interactions of the charge balancing cations and the framework, and therefore the hydrophilicity and the affinity for polar molecules increase with an increasing aluminum content. Usually, Brønsted acidity is introduced using protons as charge balancing cations via ammonium exchange followed by thermal deammination. The origin of Brønsted and Lewis acidity in zeolites is similar as in clay minerals (see Scheme 2.4 and Scheme 2.5). Ionizable (bridging) hydroxyl groups and dissociation of water molecules by charge compensating cations give rise to Brønsted acidic sites,[7] which may be converted into Lewis acid sites by dehydration or dehydroxylation above 500°C.[52] The number of Brønsted sites is directly proportional to the concentration of framework aluminum.[11] The strength of the Brønsted acid sites depends on the number of aluminum tetrahedra in the next nearest neighbor positions.[55,53] The strongest acidity is reached when the aluminum sites are too far apart to interact with each other. This is achieved when none of the AlO_4 tetrahedra has another aluminum in its second coordination shell. Consequently, the strength of acidic sites increases inversely with the Si/Al ratio and reaches a maximum at a ratio of about ten.[11] Above this Si/Al ratio the acid strength is maximal and constant and only the number of acid sites determines the overall acidity of the zeolite. The structural properties of a zeolite are, however, also of influence on the acid

strength.[53] As a result, different zeolites with the same Si/Al ratio may display a remarkable difference in acid strength.[52]

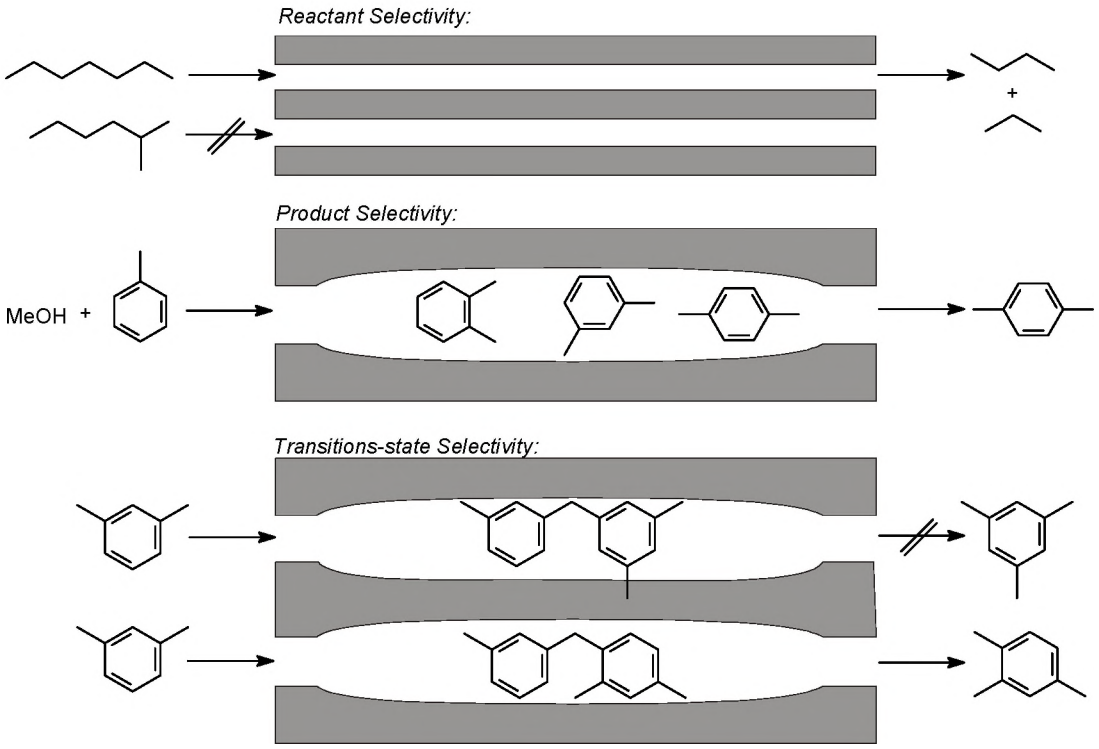

Scheme 2.6 *Various types of shape-selectivity in zeolite catalyzed reactions*[50]

(Synthetic) zeolites find their main applications as cation exchangers in detergent formulations, as selective adsorbents (molecular sieving) in drying and separations and as catalysts in the petrochemical industry.[54] In the latter their greatest use is in cracking of oil, isomerization and alkylation reactions.[55] The application of zeolites as solid acid catalysts in intermediate and fine chemical synthesis attracts increasing attention.[56] Several valuable applications have been reported.[7,8,11,27,54,57] However, for reactions involving large molecules the small pore sizes of zeolites have limited their use, although recent developments may overcome this. Zeolite-type materials with ultra-large pores have been synthesized,[56,58] which may expand their scope in fine chemical transformations.

2.3 SELECTED SOLID ACIDS: THEIR PROPERTIES

2.3.1 Type and origin of catalysts used in this thesis

Various types of catalytic materials were used in the present study. They were received as gifts from industrial suppliers, bought via regular channels or obtained through cooperation with the group of Prof. Geus, University of Utrecht. The catalytic materials used are listed according to their type in Table 2.2.

Table 2.2 *Types of catalytic materials used*

Amorphous alumina:	B698D-24
Amorphous silica-alumina:	B698D-25 and HA-SHPV
Commercial natural clays:	Montmorillonite K-10 and Montmorillonite KSF
Acid-treated natural clays:	F-1, F-13, F-105SF, F-24 and F-25
Synthetic clays:	Mg-Saponite\ Al^{3+}, Mg-Saponite\ H^{+}, Mg-Stevensite, Zn-Saponite\ Al^{3+}, Zn-Saponite\ H^{+}, Zn-Stevensite

The amorphous alumina B698D-24, the amorphous silica-alumina (ASA) B698D-25 and the acid-treated natural clays were received as generous gifts from Engelhard De Meern B.V. The amorphous silica-alumina HA-SHPV (High Amorphous Silica High Pore Volume) was obtained as a generous gift from AKZO Nobel Chemicals. Commercial natural clays Montmorillonite K-10 and Montmorillonite KSF are produced by Süd Chemie and were obtained via Aldrich Chemical Company. Prior to use the Montmorillonite K-10 was washed with hot demineralized water to remove any residual mineral acid that may be present due to the acid-treatment involved in its preparation. Synthetic clay materials were prepared and donated by the Department of Inorganic Chemistry and Heterogeneous Catalysis of the University of Utrecht (group of Prof.Dr. J.W. Geus). All saponites used had a Si/Al ratio of 7.9 and are described as M-Saponite\ C^{+}, where M represents the octahedral cation and C^{+} the interlayer cation.
The above mentioned amorphous (silica) aluminas, and natural and synthetic clays represent a broad and representative selection within these types of catalysts.

2.3.2 Nitrogen adsorption isotherms

The texture of solid catalysts can be determined by physical adsorption methods. The texture of a solid is considered to be known when its spatial architecture between 0.3 nm (lower limit) and 1 mm can be described. Generally, the texture of a solid is described in terms of surface area (S_A, m^2/g), the type of its pores (macro, meso and micro pores) and the pore volume (P_V, ml/g). The pores of solids can be classified according to their average width, i.e. the diameter of a cylindrical pore or the distance between the side of a slit-shaped pore. Micropores range from 0.2 to 3 nm; mesopores from 2 nm to 50 nm and macropores have pore widths of 50 nm up to about 10^5 nm.[5] Nitrogen is the most common adsorbent gas applied in determining the surface area and micro- and mesopore volumes. Mercury is used to determine the macroporosity of a solid, but this technique will not be discussed here.
The specific surface area (A) of a solid can be calculated from its monolayer capacity, using the equation:

$$A = n_m a_m N_A, \qquad \text{(Eqn 2.1)}$$

where a_m is the average area occupied by an adsorbate molecule in a completed monolayer; N_A is the Avogado constant and n_m is the monolayer capacity in moles of adsorbate per gram of adsorbent. The value of a_m for nitrogen can be derived from the density at its boiling point and has a value of 16.2 Å at -196°C.[5]

Adsorption isotherms are plots of the amount of gas (usually expressed as the mass of the gas or the volume of gas reduced to standard temperature and pressure (STP)) adsorbed at equilibrium as a function of the partial pressure p/p^o, at constant temperature. Several methods exist that translate the results from these plots into physical properties, each method having its own assumptions and limitations. A widely used model is the one developed by Brunauer, Emmet and Teller,[59] describing the multi-layer adsorption of gasses. The model is valid in the range of partial pressures from 0.05 to 0.3, often called the 'BET region' and is described by the BET equation:

$$\frac{p}{v(p^o - p)} = \frac{1}{v_m c} + \frac{c - 1}{v_m c} \cdot p/p^o \qquad \text{(Eqn 2.2)}$$

Here v is the volume of the gas (STP) adsorbed and v_m the volume of gas (STP) adsorbed in the monolayer. The relative pressure of the gas is p/p^o. The quantity c contains parameters for the heat of adsorption of the gas.[5] In the BET method a plot is made of $p/v(p^o\text{-}p)$ against p/p^o. The intercept and the tangent readily permit the calculation of v_m and c, and since n_m is deduced from v_m, the BET surface area can be calculated from Eqn 2.1. The pore radius and volume (distribution) can be derived from the relative pressure at which the pores are filled or emptied.[5]

Nitrogen adsorption analyses were carried out at the Department of Inorganic Chemistry and Heterogeneous Catalysis of the University of Utrecht. The experimental conditions are described in the Experimental Section. Two isotherms are displayed in Figure 2.3 that demonstrate the different isotherms arising from microporous and mesoporous materials. The isotherms of the amorphous silica-alumina HA-SHPV and the synthetic saponite Mg-saponite\Al^{3+} are given as examples for a mesoporous and a microporous solid, respectively.

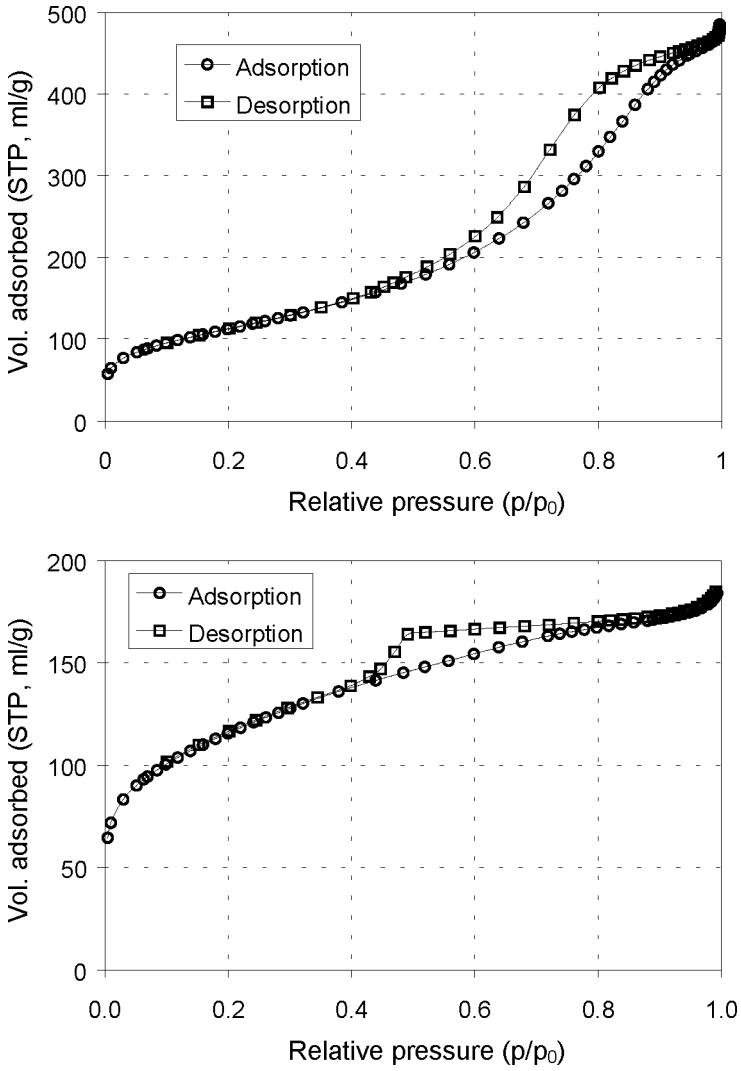

Figure 2.3 *Nitrogen adsorption-desorption isotherms of silica-alumina HA-SHPV (top) and synthetic clay Mg-saponite\Al^{3+} (bottom).*

A few observations can be made examining the displayed ad- and desorption isotherms. The adsorption and desorption curves are different for both materials, which indicates that capillary forces hold nitrogen in the pores of the solids when the relative pressure is decreased. The steep drop in the curve at a moderate relative pressure (*ca.* 0.47) in the desorption isotherm of the Mg-saponite\Al^{3+} clay corresponds to predominant micro- and mesoporosity of this catalyst material. The nicely converging adsorption and desorption curves indicate a primarily macro-porous structure of the HA-SHPV silica-alumina, as large pores are earlier emptied when decreasing the relative pressure.

The calculated specific surface areas, total pore volumes and average pore diameters of the solid catalysts analyzed are given in Table 2.3. External surface areas (S_E) were obtained from the difference between the total surface area (S_A) and micropore surface area (S_M), i.e. $S_E=S_A-S_M$.

Table 2.3 *Selected data on the texture of solid catalysts*

Catalyst[a]	Surface area (m^2/g)			Total pore volume	Average pore diameter
	Total (S_A)	Micropore (S_M)	External[c] (S_E)	(PV, ml/g)	(ϕ, nm)
B698D-24[b]	240	-	-	-	-
B698D-25[b]	421	-	-	-	-
HA-SHPV	403	0	403	0.75	7.4
F-1	261	1	260	0.29	4.5
F-13[b]	300	-	-	-	-
F-105SF[b]	318	-	-	0.51	-
F-24[b]	350	-	-	0.41	-
F-25[b]	369	0	369	0.41	4.4
Montmorillonite K-10[b]	220-270	2.5[d]	~220-270	0.32[d]	5.6[d]
Montmorillonite KSF[b]	20-40	1[d]	~20-40	0.01[d]	5.0[d]
Mg-saponite\ Al^{3+}	411	46	365	0.36	-
Zn-saponite\ Al^{3+}	244	54	190	0.29	-
Mg-saponite\ H^+	560	132	428	0.36	-
Zn-saponite\ H^+	206	37	159	0.37	-
Mg-stevensite	575	-	-	0.38	-
Zn-stevensite	165	-	-	0.19	-

[a] Data obtained through BET analysis, carried out at the University of Utrecht, unless mentioned otherwise. [b] Data provided by the respective suppliers. [c] $S_E=S_A-S_M$. [d] Data taken from ref. 60.

From the data in Table 2.3 a few trends can be recognized. The amorphous silica-aluminas have a relatively large BET-surface area, which is, at least for the HA-SHPV, made up of almost exclusively of meso- and macropores, since the surface area for micropores (S_M) is very small. The HA-SHPV has, in addition, also the highest pore volume of all catalytic materials listed. The acid-treated natural clays, the F-clays, have a surface area ranging from 261 to 369 m^2/g. The increase in surface area correlates with the increase in the thoroughness of the acid treatment to which these natural clays were subjected. The natural clay montmorillonite K-10 has a similar specific surface area and pore volume as the acid-treated natural clays mentioned earlier. The montmorillonite KSF, however, has a remarkably lower surface area of only 20-40 m^2/g and a very low pore volume. The synthetic saponite clay materials all have a considerable amount of micropore surface area (S_M). Generally, synthetic clay materials have a high specific surface area and pore volume because of the 'house of cards' structure and the limited size and stacking of the platelets of the clays prepared.[42] The synthetic clay materials, including the stevensites, with magnesium as the octahedral cation have a surface area that is much higher than the corresponding clays with zinc in the octahedral layer. This is due to the much smaller particle size of the former, as has been observed by TEM photography.[42]

2.3.3 Aluminum MAS NMR

Solid state 'magic angle spinning' (MAS) NMR is a technique sensitive to short-range order. The nucleus studied here is ^{27}Al, present in the solid acid catalysts used in this thesis, because oxygen-coordinated octahedral and tetrahedral aluminum centers can be easily distinguished by their large difference in chemical shift.[61] A slight drawback is that the signal around 0 ppm may be due to both octahedrally coordinated aluminum in the lattice as well as to hexahydrated Al^{3+} in non-framework sites. From the ^{27}Al MAS NMR spectra the ratio of the four- and sixfold coordinated aluminum may be determined. This is of importance since tetrahedral aluminum may be able to coordinate to additional electron demanding species, whereas octahedral aluminum is coordinatively saturated. Thus, only tetrahedral aluminum is capable to display Lewis acidic character. For clay materials the ratio of four- and sixfold coordinated aluminum will give information on the amount of aluminum incorporated in the tetrahedral or octahedral sheet.

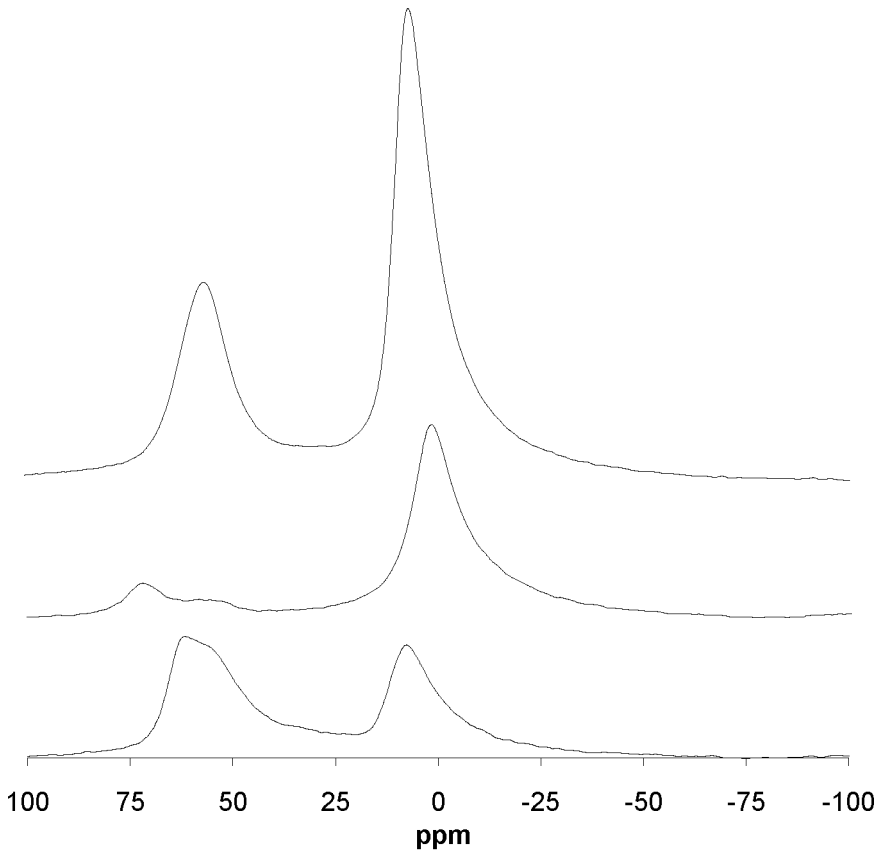

Figure 2.4 *^{27}Al MAS NMR spectra of three hydrated solid catalysts: HA-SHPV (top), Montmorillonite K-10 (middle) and Zn-saponite\Al^{3+} (bottom).*

The ^{27}Al MAS NMR spectra of three solid catalysts (the amorphous silica-alumina HA-SHPV, the natural clay Montmorillonite K-10 and the synthetic clay Zn-saponite\Al^{3+}) are displayed in Figure 2.4. The experimental conditions are described

in the Experimental Section. The chemical shifts of the Al^{oct} (octahedrally coordinated), Al^{tet} (tetrahedrally coordinated) resonances and the fractions of the Al^{tet} peak intensity are listed in Table 2.4.

Table 2.4 *^{27}Al MAS NMR data of solid catalysts*

Catalyst	Al^{oct} resonance (ppm)	Al^{tet} resonance (ppm)	Fraction Al^{tet} [b] (%)
B698D-24	7	55	36
B698D-25	8	55	7
HA-SHPV	7	56	34
F-1	1	58	21
F-13	0	56	6
F-105SF	2	59	25
F-24	0	57	5
F-25	1	56	6
Montmorillonite K-10	3	70, 55	17
Montmorillonite KSF	0	70, 59	13
Mg-saponite\Al^{3+}	4	62	73
Zn-saponite\Al^{3+}	8	62	60
Mg-saponite\H^{+}	5	65	74
Zn-saponite\H^{+}	8	63	62
Mg-stevensite[a]	1	54	33
Zn-stevensite[a]	8	65	15

[a] Very low amount of aluminum present. [b] Fraction Al^{tet} = Int[Al^{tet}]/(Int[Al^{oct}] + Int[Al^{tet}]).

All three spectra in Figure 2.4 show a clear resonance peak in the Al^{oct} region around 0 ppm and also the Al^{tet} resonance is present in the spectra in the 50-80 ppm region. The Montmorillonite K-10 spectrum shows predominantly six-fold coordinated aluminum, which is consistent with the composition and isomorphous substitution characteristics of this clay (cf. Table 2.1). For montmorillonites the cations in the octahedral sheet consist mainly of aluminum with some substitution by other cations, whereas the tetrahedral sheet consists mainly of silicon-centered tetrahedra. The synthetic clay Zn-saponite\Al^{3+} has a different structure, since most of the isomorphous substitution by aluminum replacing silicon in this type of material occurs in the tetrahedral sheet and only to a lesser extent in the octahedral sheet. This is clearly visible in the spectrum (bottom) in Figure 2.4, where the fraction of Al^{tet} is considerably larger than for the other two spectra shown. For saponite clays the acid sites at the surface (that can be accessed in acid-catalyzed reactions) are obtained by substitution of silicon by aluminum in the tetrahedral sheets. Since aluminum can also be incorporated in the interlayer or in the octahedral layer, the highest number of acid sites at the surface corresponds to the maximum amount of aluminum tetrahedrally coordinated within the clay sheets.[43]

Natural clay materials and the Mg-saponites have Al^{oct} peaks ranging from 0 to 5 ppm (Table 2.4). The Zn-saponites and the amorphous (silica)-aluminas show the

Al^{oct} peak at 7 or 8 ppm. The chemical shifts of the Al^{oct} resonances in Zn- and Mg-saponites are clearly different, whereas the Al^{tet} resonances are located at approximately the same position. Apparently, the neighboring Mg^{2+} or Zn^{2+} cations are affecting the Al^{3+} ions in the octahedral sheet significantly. The Al^{tet} resonance peaks occur in a range from 55 ppm for the amorphous alumina B698D-24 to 70 ppm for the Montmorillonites K-10 and KSF. The data for both stevensite materials should be interpreted with some reserve as the amount of aluminum present in these materials is considerably lower than in the other solids.

2.3.4 Infrared (DRIFT) analysis of adsorbed pyridine

Infrared spectroscopy is a powerful technique to determine the surface acidity of a solid, because the surface hydroxyls on a solid can be detected directly. Moreover, the interaction with basic molecules can be observed, allowing to establish whether they represent Brønsted and/or Lewis acidity and whether they are accessible to base molecules of varying sizes. However, the concentration of surface hydroxyl groups, and therefore the concentration of potential Brønsted acid sites, can only be estimated quantitatively from the intensity of the IR band when the extinction coefficients of the different types of contributing hydroxyls are known, which is seldom the case.[27] Different types of surface hydroxyls have been assigned on the basis of their O-H stretching frequency.[62] Vogels[42] was able to identify two distinct hydroxy groups in saponite clays by infrared spectroscopy of the plain samples. The strongest band (3610-3670 cm^{-1}) was assigned to the hydroxy group stretching frequency of the M-(OH) units in the octahedral sheet. The second band (3730-3735 cm^{-1}) was assigned to Si-OH species in the tetrahedral sheets at the external surface.
Due to the above mentioned difficulties, most of the information on the acidity of solids obtained by infrared spectroscopy comes from spectroscopic studies of adsorbed molecules. Various probe molecules have been employed:[27,63] pyridine, quinoline, ammonia and diazines as relatively strong bases, and CO, hydrogen sulfide or ethylene at low temperatures as very weak soft bases.
Pyridine is the most widely used probe molecule, since it allows the simultaneous determination of Brønsted and Lewis acid site concentrations. In addition, when infrared spectroscopy is combined with thermal desorption, it can provide an estimation of the acid strength distribution. The infrared bands from pyridine adsorbed on solid acids, along with their aromatic-ring mode assignments are collected in Table 2.5.[27,42]

Table 2.5 *Infrared bands (1400-1700 cm^{-1}) of pyridine adsorbed on solid acids*

Vibration Mode	Bronsted sites (Bpy) (pyridium ion)	Lewis sites (Lpy) (coordinatively bonded pyridine)	Hydrogen-bonded Pyridine
ν_{19b}	*1540*	*1447-1460*	1400-1477
ν_{19a}	1485-1500	1485-1503	1485-1490
ν_{8b}	1620	1580	1580-1590
ν_{8a}	1640	1600-1633	1590-1600

Upon the adsorption of pyridine on an acidic solid various bands appear, depending on the type of interaction of pyridine (i.e. protonated, coordinatively bound or hydrogen bonded) with the surface. Excess pyridine, physisorbed on non-acidic sites, may be detected by bands in the range of 1435-1440 cm^{-1} for montmorillonite clays,[64] or at higher frequencies for other solids.[65] Due to the overlap of various infrared adsorptions the most diagnostic infrared bands for the identification of Brønsted and Lewis acid sites are derived from the ν_{19b} vibration mode. Pyridine is not a small probe molecule and more acid sites might be accessible to a smaller probe molecule like NH_3, but the dimensions of the pyridine molecule are more representative for reactant or product molecules in many catalytic reactions. Studies with pyridine may therefore give information on the catalytically more relevant acid sites.

By measuring the intensity of the infrared bands of adsorbed pyridine it is possible to determine the ratio of Brønsted and Lewis acid sites that are capable of retaining pyridine at certain desorption temperatures. The absolute ratio and number of Brønsted and Lewis sites may be determined from the peak intensities when the extinction coefficients are known. These coefficients are dependent on the type of material and may therefore not be extrapolated for other materials without cautiousness. The integrated molar extinction coefficients for infrared adsorption bands of adsorbed pyridine were determined for a number of solid acids,[66] but clay materials were not among them. Even when the extinction coefficients are not known, useful information can still be obtained from the mentioned infrared measurements. For different samples the relative concentrations of Brønsted and Lewis acid sites may be calculated from the intensities or the areas of the respective signals[67] by normalizing the signals against the lattice Si-O combination band at 1860-1880 cm^{-1}.

By studying a probe molecule on a surface the most significant information can be obtained when only the surface and not the bulk of the solid is measured. Diffuse reflectance infrared Fourier transform (DRIFT) spectroscopy is a very suitable technique for such analyses. Infrared beams directed towards a solid are reflected in two ways: specular and diffusive. Specular (mirror-like) reflectance represents the

component of the radiation that has reflected directly from the sample and has not adsorbed energy. Diffuse reflectance is the radiation component that has penetrated and interacted with the sample before it was released. The latter can be collected with a set of ellipsoidal mirrors. Diluted samples of infinite depth (i.e. up to 3 mm) are used against the pure diluent to obtain the reflectance R_∞. The reflectance is related to the concentration c of the sample by the Kubelka-Munk equation:[68,69]

$$f(R_\infty) = \frac{(1 - R_\infty)^2}{2R_\infty} = \frac{2.303ac}{s} \qquad \text{(Eqn. 2.3)}$$

where a is the absorptivity and s the scattering coefficient. This equation can be considered as the diffuse reflectance analogue to the Beer's law for transmission measurements and is valid if an increase in depth of the sample does not appreciably change the spectrum[10].

DRIFT analyses of adsorbed pyridine were performed for several solid acid catalysts, according to the procedure described in the Experimental Section. At ambient temperature pyridine was adsorbed on the diluted sample and subsequently heated at 150°C under vacuum to remove pyridine that is physisorbed or coordinated to very weak acid sites. The spectra thus obtained are named '150°C-desorbed'. The '300°C-desorbed' spectra were recorded after heating the same sample at 300°C under vacuum.

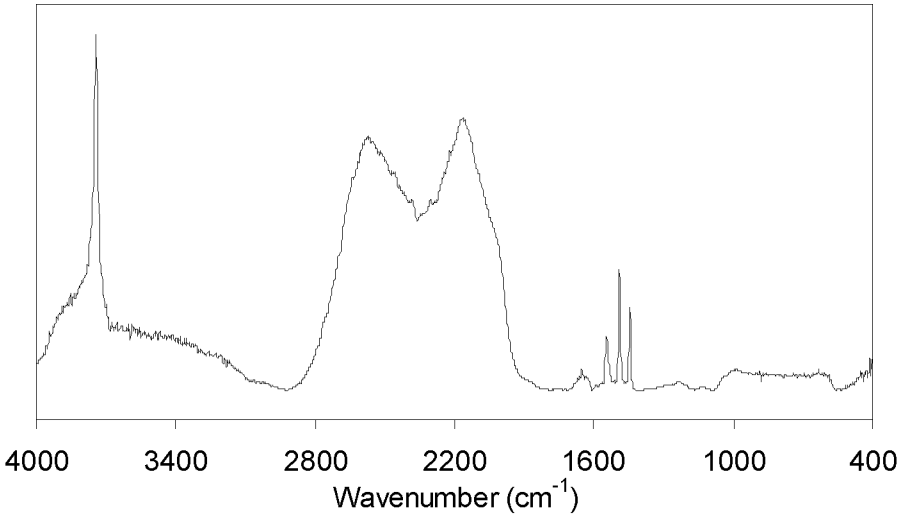

Figure 2.5 *IR spectrum of Mg-saponite\H⁺ after pyridine desorption at 150°C.*

The complete 150°C-desorbtion spectrum of Mg-saponite\H⁺ is displayed in Figure 2.5. In this spectrum the pyridine adsorption signals between 1400 and 1700 cm^{-1}, the big Si-O crystal lattice band around 1850-1900 cm^{-1} are clearly visible as well as a sharp peak at 3740 cm^{-1}, which is presumably due to stretching vibrations of OH^- groups in the sample. As was described earlier, the most diagnostic peaks to study

the acidity of the solid materials are located in the 1400-1700 cm^{-1} region and spectra in this region of the three selected 150°C and 300°C-desorbed solid acid catalysts are presented in Figure 2.6 and Figure 2.7, respectively. The intensity scales of the various spectra are not identical, allowing only a qualitative comparison.

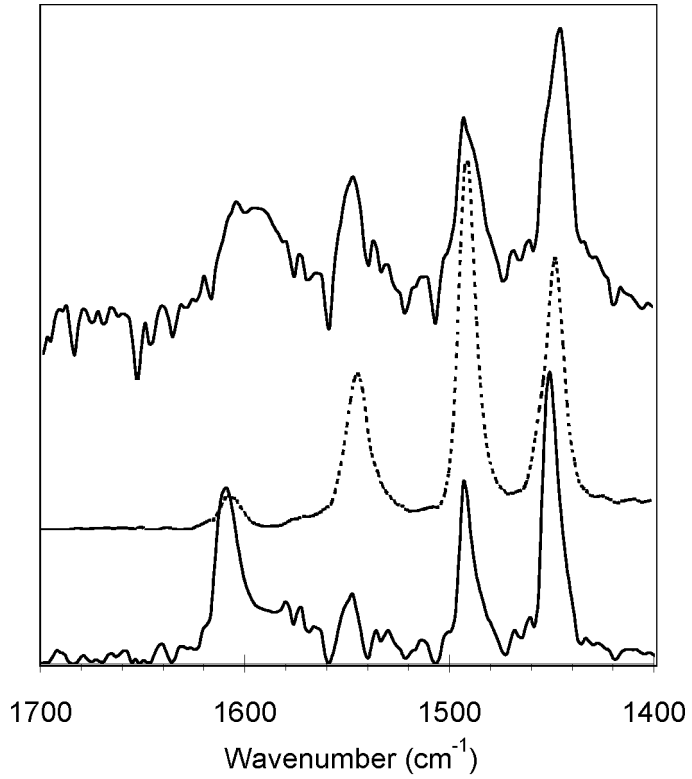

Figure 2.6 *IR spectra in the 1400-1700 cm^{-1} region after pyridine desorption at 150°C:Mg-saponite\$Al^{3+}$ (top), Mg-saponite\$H^{+}$ (middle) and Zn-saponite\$H^{+}$ (bottom).*

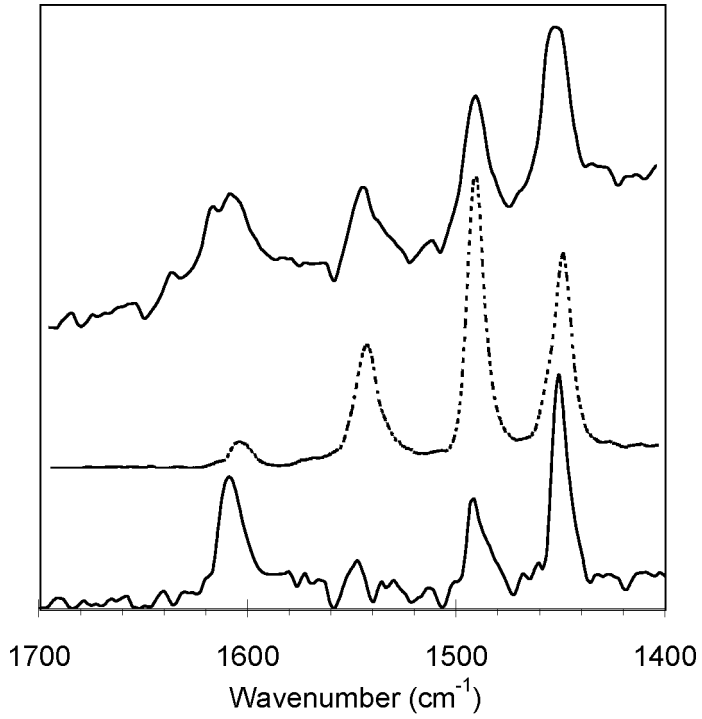

Figure 2.7 *IR spectra in the 1400-1700 cm^{-1} region after pyridine desorption at 300°C: Mg-saponite\$Al^{3+}$ (top), Mg-saponite\$H^{+}$ (middle) and Zn-saponite\$H^{+}$ (bottom).*

In the infrared spectra several adsorption peaks can be observed. The bands at *ca.* 1540 and *ca.* 1450 cm^{-1} are most diagnostic and correspond to pyridine adsorbed at Brønsted (Bpy) and Lewis (Lpy) acid sites, respectively. The band at *ca.* 1500 cm^{-1} is probably due to a combination of Bpy and Lpy.

Relative intensities (I_{rel}) were calculated for the bands due to pyridine adsorbed to Brønsted (Bpy) and Lewis sites (Lpy) by normalizing the absorption bands against the Si-O crystal vibration band at 1865 cm^{-1}. This allowed a correction for concentration differences between the samples. In Table 2.6 the relative intensities and the frequency maxima of the mentioned diagnostic pyridine adsorption peaks are listed. In deriving these relative intensities some assumptions were made that may not be necessarily valid. First, it was assumed that the molar extinction coefficients for both the Lpy and Bpy adsorptions were identical and, in addition, independent of temperature and the type of material studied. For a number of solids the integrated molar extinction coefficients for the Lpy and Bpy adsorptions were deduced,[66] but they have not been determined for the materials studied here. The second assumption is that desorption of pyridine proceeds with equal ease for all of the solid acids studied. Textural differences, however, between the solid catalysts may cause differences in the ease of desorption for materials with varying amounts of micro-, meso- and macropores.

The data in Table 2.6 provide valuable information on the acidity of the solid acid catalysts studied. The intensities of the respective Brønsted and Lewis bands of adsorbed pyridine (normalized against the lattice Si-O band) can be used to quantify the amount of acidic sites present. In addition, the ratio of the Bpy and Lpy intensities provides a good indication of the type of acidity that a certain solid exhibits. The catalysts that display a predominantly Lewis acidic character (L/B > ~2) are Montmorillonite K-10, Zn-saponite\$H^+$ and the F-1 clay. A distinct lower L/B ratio was observed for the F-1 clay at 300°C due to the decreased contribution from the Lpy signal, whereas the intensity of the Brønsted signal was largely unchanged. Catalysts that exhibit mainly Brønsted acidity (L/B < 1) are the ASA B698D-25 and, at 300°C, the F-25 and F-13 clays. The other solid acid catalysts listed exhibit principally Lewis acid character having a L/B ratio ranging from 1 to 2. Upon increasing the desorption temperature from 150 to 300°C the L/B ratio decreased for all the materials except for the silica-aluminas HA-SHPV and B698D-25 and the Mg-saponite\$Al^{3+}$. The L/B ratio remained more or less the same for the latter two, but increased for the HA-SHPV with an increase in desorption temperature. From the desorption temperatures necessary to remove pyridine from the surface sites it may be deduced that in most of the catalysts the Brønsted acid sites are stronger than

Lewis centers, since the L/B ratio is lower at higher desorption temperatures for most of the catalysts.

Table 2.6 *Relative intensities (I_{rel}) and frequency maxima (ν_{max}) of diagnostic pyridine adsorption bands from DRIFT analyses at 150 and 300°C desorption temperatures*

Catalyst	T_{des}	Lpy[a]		Bpy[a]		L/B[b]
	(°C)	($I_{rel}(\nu_{max})$)		($I_{rel}(\nu_{max})$)	ΣI_{rel} [c]	
B698D-25	150	3.11 (1456)		5.8 (1540)	5.8	0.54
	300	3.34 (1456)		6.3 (1540)	6.3	0.53
HA-SHPV	150	3.29 (1455)		2.62 (1540)	2.62	1.26
	300	1.83 (1455)		1.10 (1540)	1.10	1.66
F-1	150	2.27 (1441)		0.78 (1547)	0.78	2.91
	300	0.96 (1445)	0.05 (1527)	0.64 (1545)	0.69	1.39
F-13	150	1.52 (1443)	0.11 (1528)	0.73 (1545)	0.84	1.81
	300	0.71 (1446)		0.75 (1543)	0.75	0.95
F-105SF	150	2.33 (1442)	0.38 (1529)	0.79 (1548)	1.17	1.99
	300	0.75 (1448)		0.46 (1544)	0.46	1.63
F-25	150	1.12 (1443)	0.25 (1530)	0.48 (1547)	0.73	1.53
	300	1.11 (1446)	0.54 (1530)	0.93 (1545)	2.04	0.54
Montmorillonite K-10	150	2.06 (1443)	0.21 (1528)	0.37 (1548)	0.58	3.55
	300	1.02 (1445)	0.16 (1528)	0.25 (1547)	0.41	2.49
Mg-saponite\ Al^{3+}	150	3.71 (1444)	0.35 (1530)	2.12 (1547)	2.47	1.50
	300	2.02 (1449)		1.31 (1545)	1.31	1.54
Zn-saponite\ Al^{3+}	150	2.06 (1447)	0.18 (1528)	0.86 (1548)	1.04	1.98
	300	1.13 (1449)	0.18 (1531)	0.50 (1548)	0.68	1.66
Mg-saponite\ H^+	150	0.88 (1444)		0.58 (1546)	0.58	1.52
	300	0.70 (1447)		0.65 (1547)	0.65	1.08
Zn-saponite\ H^+	150	1.77 (1452)		0.52 (1540)	0.52	3.40
	300	1.01 (1452)		0.41 (1541)	0.41	2.46

[a] Lpy and Bpy refer to pyridine adsorbed onto Lewis and Brønsted acid sites, respectively. [b] $L/B = [I_{rel}(Lpy)]/[\Sigma I_{rel}(Bpy)]$. [c] ΣI_{rel} is the sum of the I_{rel}.

The sum of the peak intensities is for many of the catalysts of the same order of magnitude at a certain desorption temperature, but the lowest values were found for Mg-saponite\ H^+ and the F-13 clay materials. The synthetic clay Mg-saponite\ Al^{3+} and the amorphous silica-aluminas HA-SHPV and B698D-25 display the highest amount of acidity, and especially for the B698D-25 a very high intensity of the Bpy signal was observed. The silica-aluminas, however, are a totally different type of materials than the natural and synthetic clays (*vide supra*). The amount of silicon present and the intensity of the Si-O lattice vibration band may therefore be different, which may result in differences in the normalization step. Hence, it is conceivable that this causes the very high intensity of the Bpy peak of B698D-25. Other solids that clearly show a high intensity of the Bpy band are the Mg-saponite\ Al^{3+} (at 150°C) and F-25 (at 300°C) clays. Remarkably, the intensity of the pyridine adsorption bands

on the F-25 at 1530 and 1545 cm^{-1} increased as the desorption temperature was raised from 150 to 300°C. As was already described by Vogels[42] the release of protons from octahedral cavities to the surface of the clay platelets may be the reason for this observation. Pyridine that is released from other sites after increasing the desorption temperature may coordinate to these new surface acidic centers. A reverse phenomenon may be the origin of the surprisingly low Brønsted acidity observed for the synthetic saponites with H^+ as the interlayer cation as compared to their Lewis acidity. It is known[70] that during calcination of these materials, small interlayer cations such as protons are able to migrate through the hexagonal openings into the octahedral layers thereby occupying usually vacant sites. These migrated protons are then hardly accessible for the pyridine probe molecule or a substrate species. In addition, this autotransformation in H^+-exchanged saponites may induce some additional Lewis acidity.

The alumina B698D-24 is not listed in Table 2.6 because normalization of the signals against the Si-O vibration band was not possible because this material does not contain silicon. A comparison of pyridine adsorption intensities with other catalyst materials was therefore impracticable. Although the pyridine adsorption peaks could not be balanced against this reference peak, the pyridine adsorption peaks could nevertheless be compared with each other giving the L/B ratios: 0.88 (at 150°C desorption temperature) and 0.55 (at 300°C). Two synthetic clay materials are also not included in Table 2.6 because the signal to noise ratio of the spectra obtained was poor, which would introduce a large experimental error in values obtained. From other studies,[71] however, it is known that stevensites exhibit some acidity consisting of mainly Lewis nature. Stevensites, having no isomorphous substitution of silicon by aluminum in the tetrahedral layer, possess Lewis acid centers due to exposed metal cations at the edges of the clay sheets. Upon interaction with water these sites may also be transformed into Brønsted acid sites. Indeed, very small amounts of Brønsted sites were observed.[71]

2.4 CONCLUSIONS

Several solid acid catalysts were used during the study described in this thesis. Some of the typical characteristics of these materials were discussed together with a general description of the origin of their acidity. A number of analyses , viz. nitrogen adsorption, solid state aluminum NMR and infrared studies of adsorbed pyridine, were performed on these materials to obtain information about their textural and acidic features.

Nitrogen adsorption studies showed that the synthetic clays having magnesium as their octahedral cation, have a high surface area (S_A). This is due to the 'house of

cards' structure typical for synthetic clays and, when compared with zinc-containing synthetic clays, a small size of the clay particles. The amorphous silica-alumina HA-SHPV having a very high pore volume, displays an open mesoporous texture with an average pore diameter of 7.4 nm. The natural clays studied possess almost no microporosity, which points to amorphization as a result of the acid-treatment they all have undergone. Contrarily, synthetic clay materials, not acid-activated, possess a relatively high micropore surface area (S_M).

The aluminum MAS NMR spectra confirmed the presence of tetrahedrally and octahedrally coordinated aluminum centers. The Al^{tet} and Al^{oct} peaks for the various solid acids were each observed within a chemical shift range of a few ppm. This indicates that the structure and composition of the various materials have a distinct influence on the aluminum coordination. The amorphous silica-alumina B698D-25 and the F-13, F-24 and F-25 clays have only a very low fraction (5-7%) of tetrahedrally surrounded aluminum, which may point to a possible low Lewis acidic nature. A much larger Al^{tet} fraction was observed for the synthetic saponites, suggesting that these materials are able to display significant Lewis acidic characteristics.

Infrared studies of pyridine adsorbed on the solid acids showed that Montmorillonite K-10, Zn-saponite\$H^+$ and the F-1 clay possess predominantly Lewis acidic character. Catalytic materials that contain mainly Brønsted acid sites are the amorphous alumina B698D-25 and the F-13 and F-25 natural clays. Other materials that were studied possess slightly more Lewis acidic sites than Brønsted sites. Generally, the intensity of signals from adsorbed pyridine decreased at higher desorption temperatures, because only stronger acidic sites remain occupied. Only for the F-25 clay an increase in the intensity was observed which may be explained by autotransformation of protons from internal cavities to the clay surface. A (semi-) quantitative comparison of the signal intensities indicates that the relative amount of acidity was in the same order of magnitude for most of the catalysts at a given desorption temperature. The largest number of acidic sites is present in the amorphous silica-aluminas B698D-25 and HA-SHPV, and the synthetic clay Mg-saponite\$Al^{3+}$. The synthetic clay Mg-saponite\$H^+$ and the F-13 natural clay displayed lower acidity than the other solid catalysts studied.

2.5 EXPERIMENTAL SECTION

Nitrogen adsorption isotherms

Nitrogen adsorption-desorption analyses were carried out at the Department of Inorganic Chemistry and Heterogeneous Catalysis of the University of Utrecht using a Micrometrics ASAP 2400 apparatus. All powdered samples were degassed at 130°C under vacuum for at least 30 min before nitrogen adsorption-desorption analyses were recorded at -196°C. The

total surface areas (S_A) were calculated using the BET equation and the micropore surface areas (S_M) were determined from *t*-plots[5]. The external surface (S_E) is the difference between the former and the latter.

^{27}Al Magic Angle Spinning NMR

High-resolution solid-state MAS NMR measurements were performed on a Bruker AMX 500 spectrometer at the SON HF-NMR facility at the University of Nijmegen. ^{27}Al MAS NMR measurements were run at 130.32 MHz with a pulse length of 1 μs and a pulse interval of 0.25 s. The magic-angle sample rotation frequency was 22 to 24 kHz. Typically, 2000 scans were collected, although 16000 and 20000 scans were collected for the two stevensite samples. Chemical shifts were reported relative to an external standard of 1.0 M $Al(NO_3)_3$ in water at 0 ppm. The spectra were processed using the Bruker WINNMR and WINFIT software. Relative intensities were determined with a homemade fitting program that takes into account the distribution of the isotropic shift, the quadrupolar interaction and its distribution and an asymmetry parameter. All samples were stored in a water-saturated atmosphere for 24 h at ambient temperature prior to measurement.

Infrared (DRIFT) Spectroscopy of adsorbed pyridine

Infrared spectroscopy was performed using a BioRad FTS–25 spectrometer equipped with an in situ Diffuse Reflectance Infrared Fourier Transform (DRIFT) accessory. For each sample 64 scans were recorded with a resolution of 4 cm^{-1} using the Harrick DRA-2 'Praying Mantis' accessory in conjunction with an HVC-DR2 low pressure reaction chamber and an ATC-30D-2 automatic temperature controller.

Prior to the measurements the samples were stored at 120°C for 1 h in a furnace in order to adjust the degree of hydration. The solid was mixed with KBr (to *ca.* 10 wt% of solid in the mixture), placed in the low-pressure reaction chamber and heated at 150°C for 30 min under vacuum (1 mm Hg) to dehydrate the sample. Subsequently, background spectra were recorded under these conditions. Adsorption with pyridine was carried out by exposing the sample at room temperature for 30 min to a pyridine-N_2 flow. Excess (i.e. physisorbed) pyridine was removed by heating the sample under vacuum (1 mm Hg) at 150°C for 30 min and the '150°C desorption' spectrum was recorded. After heating the same sample for 30 min at 300°C under vacuum (1 mm Hg) the '300°C desorption' spectrum was recorded.

The assumption was made that no solid-state ionic exchange occurs under the conditions employed. The spectra were analyzed with the BioRad Win-IR software (version 2.04B) by mathematical transformation to Kubelka-Munk units. Multiple point baseline correction and Gaussian curve fitting were performed using Peakfit (version 4.0) from Jandel Scientific Software. Relative peak intensities (I_{rel}) of selected pyridine signals at 150°C and 300°C desorption temperature were calculated as normalized to the 1865 cm^{-1} Si-O crystal lattice band.

2.6 REFERENCES

[1] Rupert, J.P.; Granquist, W.T.; Pinnavaia, T.J. 'Catalytic Properties of Clay Minerals' in *Chemistry of Clays and clay minerals. Monograph No. 6,* Newman, A.C.D. ed., Longman Scientific & Technical, Harlow, 1987, p275.

[2] Montaland, L. US Pat. 999,667, 1911.

[3] Gurwitsch, L. *Z. Chemie Ind. Kolloide* **1912**, *11*, 17.

[4] Gurwitsch, L.*Z. Phys. Chem., Frankfurt* **1923**, *107*, 235.

[5] Moulijn, J.A.; Van Leeuwen, P.W.N.M.; Van Santen, R.A. Eds. in *Catalysis: An Intergrated Approach to Homogeneous, Heterogeneous and Industrial Catalysis*, Elsevier, Amsterdam, 1993.

[6] Houdry, E.; Burt, W.F.; Pew Jr., A.E.; Peters Jr., W.A. *Nat. Pet. News.* **1938**, *48*, R570.

[7] Smith, K. Ed. *Solid Supports and Catalysts in Organic Synthesis*, Ellis Horwood Ltd., New York, 1992.

[8] Izumi, Y.; Urabe, K.; Onaka, M. in *Zeolite, Clay and Heteropoly Acid in Organic Reactions*, VCH, Weinheim, 1992.

[9] Balogh, M.; Laszlo, P. in *Organic Chemistry Using Clays*, Springer Verlag, Berlin, 1993.

[10] Clark, J.H.; Kybett, A.P.; Macquarrie, D.J. in *Supported Reagents: preparation, analysis, and applications*, VCH, New York, 1992.

[11] Laszlo, P. Ed. in *Preparative Chemistry using Supported Reagents*, Academic Press, San Diego, 1987.

[12] Van der Waals, A.C.L.M. *Thesis*, University of Nijmegen, The Netherlands, 1997

[13] Clark, J.H. in *Catalysis of Organic Reactions by Supported Inorganic Reagents*, VCH, New York, 1994.

[14] Diddams, P. 'Inorganic supports and catalysts – an overview' in ref. 7, p3.

[15] Peri, J.B. *J. Phys. Chem* **1965**, *69*, 211, 220, 231.

[16] Cotton, F.A; Wilkinson, G *Advanced Inorganic Chemistry*, 4th ed., Wiley, New York, 1980.

[17] Parks, G.A. *Chem. Rev.* **1965**, *65*, 177.

[18] Michels, J.J.; Dorsey, J.G. *Langmuir* **1990**, *6*, 414.

[19] Pagni, R.M.; Kabalka, G.W.; Hondrogiannis, G.; Bains, S.; Anosike, P.; Kurt, R. *Tetrahedron* **1993**, *49*, 6743.

[20] Posner, G.H. *Angew. Chem.* **1978**, *90*, 527.

[21] Kabalka, G.W.; Pagni, R.M. *Tetrahedron* **1997**, *53*, 7999.

[22] Posner, G.H. 'Alumina and Alumina-supported Reagents' in ref. 11, p287.

[23] Some recent examples: a) Rood, G.A.; DeHaan, J.M.; Zibuck, R. *Tetrahedron Lett.* **1996**, *37*, 157. b) Yadav, V.K.; Kapoor, K.K. *Tetrahedron* **1996**, *52*, 3659. c) Mishani, E.; Dence, C.S.; McCarthy, T.J.; Welch, M.J. *Tetrahedron Lett.* **1996**, *37*, 319. d) Villemin, D.; Hachemi, M.; Lalaoui, M. *Synth. Commun.* **1996**, *26*, 2461. e) Lu, W.X.; Yan, C.G.; Yao, R. *Synth. Comm.* **1996**, *26*, 3719. f) McGinnis, M.B.; Vagle, K.; Green, J.F.; Tan, L.C.; Palmer, R.; Siler, J.; Pagni, R.M.; Kabalka, G.W. *J. Org. Chem.* **1996**, *61*, 3496. g) Avalos, M.; Babiano, R.; Bravo, J.L.; Cintas, P.; Jimenez, J.L.; Palacios, J.C.; Ranu, B.C. *Tetrahedron Lett.* **1998**, *39*, 2013. h) Kropp, P.J.; Breton, G.W.; Craig, S.L.; Crawford, S.D.; Durland, W.F.; Jones, J.E.; Raleigh, J.S. *J.Org.Chem.* **1995**, *60*, 4146.

[24] Campbell, I.M. in *Catalysis at surfaces*, Chapman and Hall Ltd., London, 1988.

[25] Iler, R.K. in *The chemistry of Silica; Solubility, Polymerization, Colloid and Surface Properties, and Biochemistry*, Wiley-Interscience, New York, 1979.

[26] Grabowski, W.; Misono, M.; Yoneda, Y. *J. Catal.* **1980**, *61*, 106.

[27] Corma, A. *Chem. Rev.* **1995**, *95*, 559.

[28] Guggenheim, S.; Martin, R.T. *Clay Minerals* **1995**, *30*, 257.

[29] Brindley, G.W., Brown, G. Eds. in *Crystal Structures of Clay Minerals and their X-ray Identification*, Mineralogical Society, London, 1980.

[30] Pauling, L. *Proc. Nat. Acad. Sci.* **1930**, *29*, 457.

[31] McCabe, R.W. 'Clay Chemistry' in *Inorganic Materials*, Bruce, D.W.; O'Hare, D. Eds., John Wiley & Sons, Chichester, 1992, p296.

[32] Tanabe, K.; Misono, M.; Ono, Y, Hattori, H. *Stud. Surf. Sci. Catal.* **1989**, *51*, 128.

[33] Loewenstein, W. *Am. Miner.* **1954**, *39*, 92.

[34] Pinnavaia, T.J. *Science* **1983**, *220*, 365.

[35] a) Butruille, J-R.; Pinnavaia, T.J. 'Alumina Pillared Clays: Methods of Preparation and Characterization' in *Characterization of Catalytic Materials*, Wachs, I.E. Ed., Butterworth-Heinermann, Boston, 1992, p 149. b) Figueras, F. *Catal. Rev. - Sci. Eng.* **1988**, *30*, 457. c) Plee, D.; Gatineau, L.; Fripiat, J.J. *Clays and Clay Minerals* **1987**, *35*, 81. c) Mokaya, R.; Jones, W. *J. Chem. Soc., Chem. Commun.* **1994**, 929. d) Mokaya, R.; Jones, W. *J. Catal.* **1995**, *153*, 76. e) Vaughan, D.E.W. *Catalysis Today* **1988**, *2*, 187. f) Yamanaka, S.; Hittori, M. *Stud. Surf. Sci. Cat.* **1991**, *60*, 89. g) Kloprogge, J.T. *Thesis*, University of Utrecht, The Netherlands, 1992.

[36] Mortland, M.M.; Raman, K.V. *Clays and Clay Miner.* **1968**, *16*, 393.

[37] Yariv, S. *Int. Rev. Phys. Chem.* **1992**, *11*, 345.

[38] Kellendonk, F.J.A.; Heinermann, J.J.L.; Van Santen, R.A. 'Clay Activated Isomerization Reactions', in ref. 11, p455.

[39] Theng, B.K.G. *Dev. Sedimentol.* **1982**, *35*, 197.

[40] Theng, B.K.G. in *The Chemistry of Clay-organic Reactions*, Adam Hilger, London, 1974.

[41] Kahn, R.; Blazek, J.J. *Clay Miner.* **1983**, *18*, 447.

[42] Vogels, R.J.M.J. *Thesis*, University of Utrecht, The Netherlands, 1996.

[43] Vogels, R.J.M.J.; Breukelaar, J.; Kloprogge, J.T.; Jansen, J.B.H.; Geus, J.W. *Clays and Clay Miner.* **1997**, *45*, 1.

[44] Vogels, R.J.M.J.; Kerkhoffs, M.J.H.V.; Geus, J.W. *Stud. Surf. Sci. Catal.* **1995**, *91*, 1153.

[45] Kerkhoffs, M.J.H.V.; Geus, J.W., IOP-Catalysis project IKA 94063, University of Utrecht, The Netherlands.

[46] Some reviews: a) Izumi, Y; Onaka, M. *Adv. Catal.* **1992**, *38*, 245. b) Cornélis, A.; Laszlo, P. *Synlett* **1994**, 155. c) Adams, J.M. *Appl. Clay Sci.* **1987**, 309. d) Chitnis, S.R.; Sharma, M.M. *React. Funct. Polym.* **1997**, *32*, 93. e) Onaka, M. J. *Syn. Org. Chem. Jpn.* **1995**, *53*, 392.

[47] Some recent examples: a) Jnaneshwara, G.K.; Deshpande, V.H.; Lalithambika, M.; Ravindranathan, T.; Bedekar, A.V. *Tetrahedron Lett.* **1998**, *39*, 459. b) Ponde, D.E.; Deshpande, V.H.; Bulbule, V.J.; Sudalai, A.; Gajare, A.S. *J. Org. Chem.* **1998**, *63*, 1058. c) Koster, R.M.; Bogert, M.; De Leeuw, B.; Poels, E.K.; Bliek, A. *J. Molec. Catal. A* **1998**, *134*, 159. d) Li, T.S.; Li, A.X. *J. Chem. Soc., Perkin Trans 1* **1998**, 1913. e) Zhang, Z.H.; Li, T.S.; Fu, C.C. *J. Chem. Res. (S)* **1997**, 174. f) Sampath Kumar, H.M.; Subba Reddy, B.V.; Mohanty, P.K.; Yadav, J.S. *Tetrahedron Lett.* **1997**, *38*, 3619. g) Chitnis, S.R.; Sharma, M.M. *J.Catal.* **1996**, *160*, 84. h) Shanmugam, P.; Nair, V. *Synth. Commun.* **1996**, *26*, 3007. i) Cativiela, C.; Garcia, J.I.; Garcia-Matres, M.; Mayoral, J.A.; Figueras, F.; Fraile, J.M.; Cseri, T.; Chiche, B. *Appl. Catal. A* **1995**, *123*, 273. j) Tateiwa, J.; Horiuchi, H.; Uemura, S. *J. Chem. Soc., Chem. Commun.* **1994**, 2567.

[48] Murray, H.H. *Appl. Clay Sci.* **1991**, *5*, 379.

[49] Meier, W.M.; Olson, D.H.; Baerlocher, C. *Atlas of Zeolite Structure Types*, 4th Ed., Elsevier, London, 1996.

[50] Csicsery, S.M. *Zeolites* **1984**, *4*, 202.

[51] Khouw, C.B.; Davis, M.E. 'Shape-Selective Catalysis with Zeolites and Molecular Sieves' in *Selectivity in Catalysis*, Khouw, C.B.; Davis, M.E. Eds., ACS Symposium series part 517, 1993, p 206.

[52] Ribeiro, F.R.; Alvarez, F.; Henriques, C.; Lemos, F; Lopes, J.M.; Ribeiro, M.F. *J. Mol. Catal. A* **1995**, *96*, 245.
[53] Barthomeuf, D. *Mater. Chem. Phys.* **1987**, *17*, 49.
[54] Van Bekkum, H.; Kouwenhoven, H.W. *Recl. Trav. Chim. Pays-Bas* **1989**, *108*, 283.
[55] Van Bekkum, H.; Flanigen, E.M.; Jansen, J.C. Eds. *Introduction to Zeolite Science and Practice*, Elsevier, Amsterdam, 1991.
[56] Venuto, P.B. *Microporous Mater.* **1994**, *2*, 297.
[57] Hölderich, W.; Hesse, M.; Näumann, F. *Angew. Chem.* **1988**, *100*, 232.
[58] Davis, M.E. *Acc. Chem. Res.* **1993**, *26*, 111.
[59] Brunauer, S.; Emmett, P.H.; Teller, E. *J. Am. Chem. Soc.* **1938**, *60*, 309.
[60] Békássy, S.; Cseri, T.; Bódás, Z.; Figueras, F. *New J. Chem.* **1996**, *20*, 357.
[61] Engelhard, G.; Michel, D. in *High Resolution Solid State NMR of Silicates and Zeolites*, Wiley, Chichester, 1987.
[62] Van Veen, J.A.R.; Veltmaat, F.T.G., Jonkers, G. *J. Chem. Soc., Chem. Commun.* **1985**, 1656.
[63] Kijenski, J.; Baiker, A. *Catal. Today* **1989**, *5*, 1.
[64] Swoboda, A.R.; Kunze, G.W. *Clays and Clay Min.* **1967**, *96*, 6729.
[65] a) Connell, G.; Dumesic, J.A. *J. Catal.* **1986**, *102*, 216. b) Martin, C.; Martin, I.; Rives, V. *J. Mol. Catal.* **1992**, *73*, 51.
[66] Emeis, C.A. *J. Catal* **1993**, *141*, 347.
[67] Bagshaw, S.A.; Cooney, R.P. *Chem. Mater.* **1993**, *5*, 1101.
[68] a) Kubelka, P.; Munk. F *Tech. Phys.* **1931**, *12*, 593. b) Duke, C.V.A.; Miller, J.M.; Clark, J.A.; Kybett, A.P. *Spectrochimica Acts* **1988**, *44A*, 1207.
[69] Harrick Inc., USA, Technical information bulletin concerning the 'Praying Mantis' DRIFT accessory.
[70] Calvet, R.; Prost, R. *Clays and Clay Min.* **1971**, *19*, 175.
[71] Leliveld, B.R.G.; Kerkhoffs, M.J.H.V.; Broersma, F.A.; van Dillen, J.A.J.; Geus, J.W.; Koningsberger, D.C. *J. Chem. Soc., Faraday Trans.* **1998**, *94*, 315.

3 Epoxide Rearrangement Reactions in Solution, Catalyzed by Solid Acids

3.1 Introduction

Epoxides are versatile building blocks for the synthesis of numerous intermediates and end products. The origin of their importance lies in their ample availability through a wide variety of methods[1] and their pronounced reactivity.[2] The bond angles of epoxides (average 60°) are far less[3] than the normal tetrahedral carbon angle of 109.5°. The inability to achieve maximum overlap of orbitals causes ring strain, which contributes, together with the polarity of the C-O bond, to the high reactivity of epoxides. Epoxides are susceptible to a variety of reaction types: nucleophilic additions, reductions and oxidations, and base or acid catalyzed rearrangement reactions.

The rearrangement of epoxides into carbonyl compounds (Scheme 3.1) is of commercial importance as is reflected in patent literature.[4] Moreover, at least one industrial process (ARCO) is operative[5] in which allyl alcohol is produced via isomerization of propylene oxide. The rearrangement of epoxides can be achieved photochemically,[6] thermally[7] or with acidic or basic catalysts.[1a,2,8] Base-catalyzed isomerization generally leads to allylic alcohols, whereas carbonyl compounds are the main products in the thermal or acid-catalyzed rearrangement of epoxides. In complex molecules (e.g. terpene oxides and steroids) also other types of products may be formed due to skeletal rearrangements. Photochemical isomerizations are reported only scarcely.

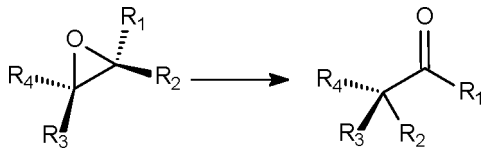

Scheme 3.1 *Rearrangement of epoxides into carbonyl compounds*

Acid-catalyzed rearrangement

Isomerization of epoxides can be carried out under mild conditions using a variety of acidic catalysts.[8] Unless there is a structural or a stereochemical bias, usually a

mixture of carbonyl products is obtained due to lack of regioselectivity in the ring opening step. In general, product formation in acid-catalyzed isomerization of epoxides is governed by two features: *i*) the regiochemistry of the ring opening, and *ii*) the relative migratory aptitude of substituent groups.

The direction of the ring opening depends on the relative ease of the heterolytic cleavage of the C-O bond (Scheme 3.2). Assuming the development of some electrophilicity on both carbons in the ring after initial protonation or coordination of the acid catalyst with the epoxide oxygen, electron-releasing substituents direct the ring opening towards the most stabilized carbocationic center. The rearrangement reaction may be a two-stage process with a rate-determining cleavage of the C-O bond followed by a fast migration of one of the substituents. However, it may also involve a concerted process in which bond breaking is more pronounced than bond forming. Factors that make the epoxide isomerization mechanism more complex include nucleophilic action of a conjugated base[1a] (protic acids), remote ligands[9] (Lewis acids), participating olefinic bonds or hydroxyl groups,[8] or steric effects caused by complexation with a catalyst.[2d]

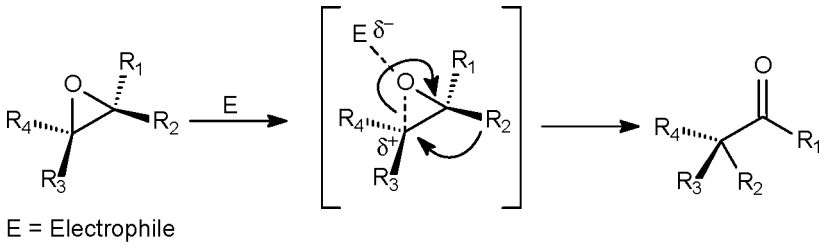

Scheme 3.2 *Acid-catalyzed epoxide rearrangement*

The relative migratory aptitude of substituent groups has been established from the many examples of the acid-catalyzed epoxide rearrangement reaction as aryl > acyl > hydride > ethyl > methyl.[1a,2a] This rule should, however, be used with care because this order is also dependent on steric effects,[1a] solvent and temperature.[10] An important aspect of the electron-releasing ability of aryl groups is the conceivable occurrence of a phenonium-ion[1a,11] intermediate, which may have both a steric and electronic influence[8] on the outcome of the rearrangement reaction.

The most commonly used (Lewis) acid to promote the acid-catalyzed rearrangement of epoxides is BF_3[8] (usually as the etherate), which is rather a reagent than a catalyst as it is often consumed or altered in the course of the reaction. Other catalysts that have also been employed include metal halides,[1a,2,8,12,13] various metal salts,[8,14] protic acids[8] and organometal[9,15] or transition metal[16] complexes. In addition, also solid acids have been used to carry out this rearrangement under mild conditions. These environmentally benign solid acids include alumina,[17,18] silica gel,[18,19] silica-alu-

mina,[20,21] (mixed) metal oxides,[22,23] heteropoly acids (HPAs),[13,24] zeolites[13,25] and clays.[13,20]

Catalysis of the epoxide rearrangement may occur in different ways, although in many instances a clear distinction is difficult to make. Solid acids may protonate or coordinate to the oxygen of the epoxide ring as is depicted in Scheme 3.2. This results after migration of an adjacent substituent, in a carbonyl product. In solids, however, acidic as well as basic sites are present. It is argued that in many cases the opening of epoxides is achieved by a cooperative action of electrophilic (acidic) and nucleophilic (basic) sites situated in close proximity on the catalyst surface. The outcome of the reaction may therefore depend upon the type, amount and strength of the acidic and basic sites present. If true, a controlled variation of these parameters can be used to direct the selectivity of the epoxide isomerization.[22a] Some authors[20,22b] have even suggested that the acidic or basic character of a catalyst may be established using the epoxide isomerization as a probe reaction.

The bifunctional action of solid acid catalysts in the rearrangement of epoxides has been proposed in a few qualitative working models,[18,23] but Ruiz-Hitzky and Casal[20] were the first to postulate a more detailed mechanism with a specific active site. Using natural silicates and amorphous silica-alumina, they proposed that the active center contains a Si(OH)-O-Al unit and that the isomerization of styrene oxide **1** to phenylacetaldehyde **2** proceeds via a series of steps as depicted in Scheme 3.3. After coordination of the electronegative epoxide oxygen to the electron deficient aluminum center, the silanol group opens the epoxide ring, which leads to a subsequent grafting reaction onto the surface. The second step involves the formation of a carbocation by transferring two electrons to the aluminum center. In the final step a carbonyl compound is formed by a rearrangement involving a hydride shift and which also regenerates the catalytic centers.

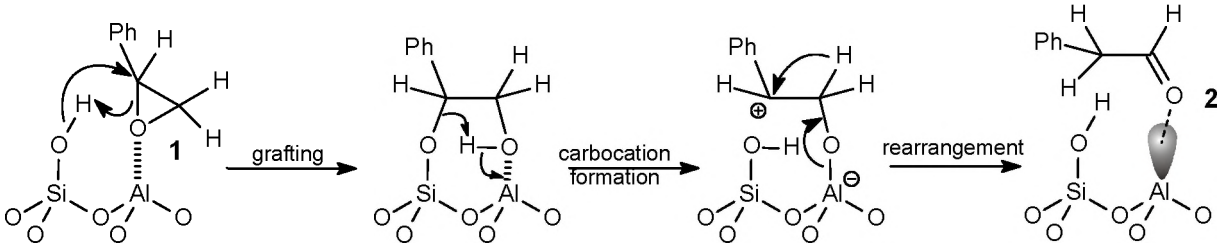

Scheme 3.3 *Mechanism[20] for the catalyzed isomerization of styrene oxide* **1** *into phenylacetaldehyde* **2**

Studies applying solid acids in the isomerization of epoxides have mainly focused on epoxides of the terpene series (e.g. 2- and 3-carene oxides, α- and β-pinene oxides, humulene oxide, limonene oxide, carvomenthene oxide, caryophyllene oxide), because rearrangement products of such terpene oxides are valuable as starting materials for perfumes, flavors and pharmaceutical products.[26,27] These isomeri-

zations are usually not limited to the epoxide moiety since skeletal rearrangements are frequently observed as well. An example is the rearrangement of α-pinene oxide **3** into campholenic aldehyde **4**, which has been studied extensively because campholenic aldehyde is a widely used intermediate in the flavor and fragrance industry.[28] It is used as a building block for sandalwood odorants and is produced by a number of companies and has a market value of *ca.* \$10/kg.[29,30] Industrially, campholenic aldehyde **4** is prepared from α-pinene oxide **3** in a yield of about 87% applying $ZnCl_2$ as the catalyst in benzene.[31] The desire to replace conventional Lewis acids by solid acids for environmental, economic and handling reasons (cf. Chapter 2) has prompted the study described in this thesis. Scheme 3.4 displays the main reaction pathways and the reaction products for the isomerization of α-pinene oxide **3**.[32] Coordination of a Lewis acid or protonation by a protic acid facilitates the fission of a C-O bond, yielding the most stable (tertiary) carbocation intermediate **5**. Starting from intermediate **5** several reaction pathways are possible. The acidic site may be released in a concerted process in which a hydride migrates and a carbonyl group is formed (pathway i), giving pinocamphone **7**. In most cases, however, intermediate **5** undergoes subsequent skeletal rearrangements in which first the strain energy of the four-membered ring is released (pathways ii and iii), giving intermediates **6** and **8**. Carbonyl formation then gives the desired campholenic aldehyde **4** or its isomer 2-(2,2,4-trimethyl-3-cyclopentenyl)acetaldehyde **9**. The selectivity of this reaction is strongly determined by the stability of the intermediate carbocations. In addition, electronic and steric interactions with the (solid) acid and/or the counter ion effect play a role in the preference for a specific reaction sequence.

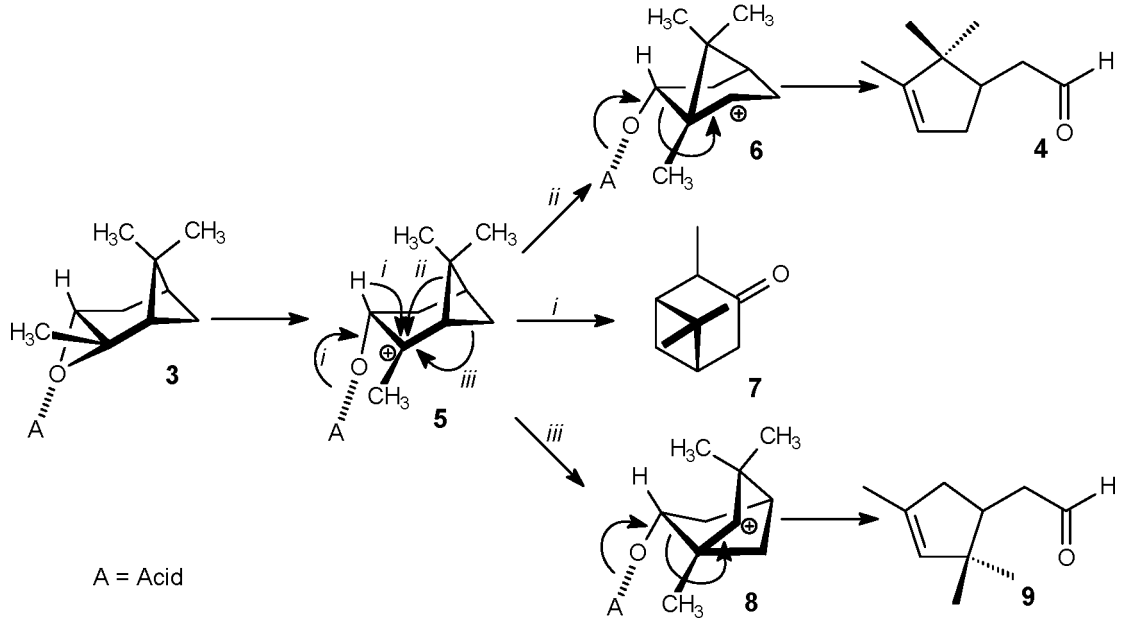

Scheme 3.4 *Main routes in the isomerization of α-pinene oxide*

Using kinetic measurements Whittaker[33] *et al.* demonstrated that Brønsted acid-catalyzed opening of the epoxide ring of α-pinene oxide does not proceed by an initial C-O bond fission. Instead, they suggested that the reaction starts by fission of the C_x-C_y bond to give a heterocyclic cationic intermediate **10**, which then ring opens and subsequently undergoes ring expansion of the cyclobutane ring to give a mixture of **4** and **9** (Scheme 3.5).

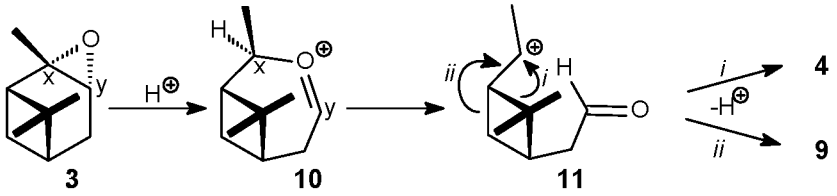

Scheme 3.5 *Isomerization of α-pinene oxide via a C-C bond fission mechanism*[33]

Nomura *et al.*[25d] have reported high selectivities (up to 86%) in the reaction from **3** to **4** using Zn^{2+} exchanged zeolites under flow pyrolysis conditions at reduced pressure. Van Bekkum *et al.*[13], however, were unable to reproduce these results. In an elaborate study they obtained the highest product selectivity (85%) for **4** using $ZnCl_2$ in 1,2-dichloroethane. This high selectivity was rationalized by the assumption that zinc chloride can stabilize the carbocation ion intermediate (similar to **5**) by coordination of the metal to the oxygen and an interaction between a chloride and the carbocation. In addition, they also tested various solid acids (e.g. HPAs, zeolites and natural clays) which proved to be quite active but inferior in terms of selectivity towards **4**.

Besides terpene oxides and some less complex aliphatic epoxides (e.g. cyclohexene oxide,[34] (cyclo)octene oxide[22c,24]) also aryl-substituted oxiranes have been studied in solid acid catalyzed isomerization reactions. These include stilbene oxides,[15c,d,21] chalcone oxide **12**,[19b] styrene oxide **1**[4c,20] and derivatives[19a] applying silica gel,[19] silica-aluminas,[20] zeolites,[25b] metal oxides,[20] immobilized organometal catalysts[15c,d] and organoboron compounds.[9] The presence of aryl substituents has a profound influence on the epoxide-carbonyl isomerization. Firstly, through their electron releasing capacity the regiochemistry of C-O bond cleavage is directed towards the carbon to which the aryl groups are attached. Secondly, migration of an aryl group may occur quite readily compared to a hydride or alkyl-shift, owing to the intermediacy of a phenonium-ion.[1a,11] Some examples of solid acid catalyzed isomerizations of aryl-substituted epoxides are given in Scheme 3.6. A notable example of an aryl-substituted epoxide isomerization of industrial and commercial interest constitutes the transformation of styrene oxide **1** into phenyl acetaldehyde **2**. Industrially, **2** is prepared by oxidation of 2-phenylethanol, however, the purity of the final product never exceeds 85%[35] since **2** is rather labile and usually trimerizes or polymerizes rapidly under homogeneous acidic conditions.

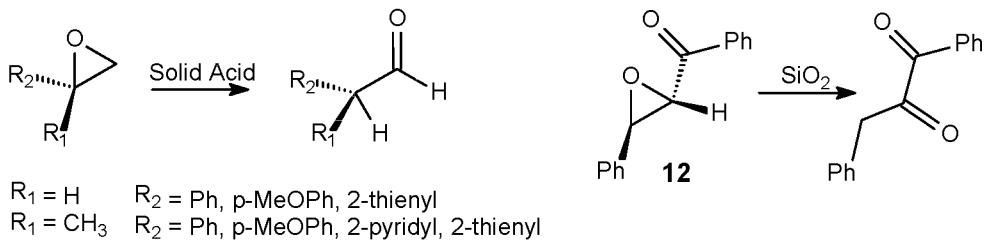

Scheme 3.6 *Examples of solid acid catalyzed isomerizations of aryl-substituted epoxides*

Objective and approach

Clay minerals of the smectite type (e.g. bentonite or montmorillonite) are powerful solid acid catalysts for a large variety of organic transformations (cf. Chapter 2). So far, however, these clays have only been scarcely used for the conversion of epoxides into carbonyl compounds. The aim of the study presented in this Chapter is to investigate the isomerization of epoxides using solid acid catalysts in solution phase reactions. The application of solid acid catalysts in the isomerization of epoxides to carbonyl compounds in the gas phase is reported in Chapter 4. The activity of the catalysts will be discussed with respect to their acidity and their porosity. In addition, the catalytic activities of natural and synthetic clay materials will be compared. The epoxides used in this chapter comprise four epoxides having one or more aromatic substituents (e.g. styrene oxide **1**, *cis*- **18** and *trans*-stilbene oxide **15** and tetraphenyloxirane **21**) and one complex aliphatic epoxide (α-pinene oxide **3**). The reactions of styrene oxide **1** to phenylacetaldehyde **2** and of α-pinene oxide **3** to campholenic aldehyde **4** are important fine chemical transformations. The other aromatically substituted epoxides were chosen to study the effect of the steric bulk on the solid acid-catalyzed epoxy/carbonyl rearrangement.

3.2 CATALYZED REARRANGEMENT REACTIONS OF EPOXIDES

3.2.1 Rearrangement of styrene oxide

Styrene oxide **1** was taken as the model substrate, as its rearrangement leads to the commercially interesting phenylacetaldehyde **2** (Scheme 3.7). This product is rather acid labile and usually trimerizes or polymerizes rapidly under homogeneous acidic conditions.

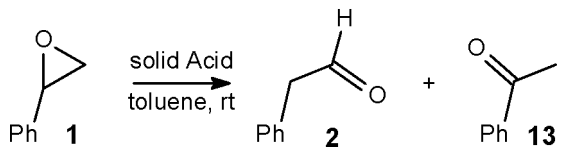

Scheme 3.7 *Isomerization of styrene oxide* **1** *into phenylacetaldehyde* **2**

In Table 3.1, Table 3.2 and Table 3.3 the results obtained with natural clays, synthetic clays and amorphous (silica) aluminas as environmentally benign solid acid catalysts in the isomerization of styrene oxide **1** are collected.

With the exception of montmorillonite KSF, all natural clays tested were effective catalysts. When a solution of styrene oxide **1** in toluene was treated with 1 mass equivalent of clay or 0.1 mass equivalent of montmorillonite K-10 or F-105SF at room temperature, a rapid conversion into phenylacetaldehyde **2** was observed (Table 3.1). With 1 mass equivalent of clay, the conversions were generally extremely high after a short reaction time but often at the expense of selectivity towards **2**. Particularly, montmorillonites K-10 and KSF, when used without any pre-treatment, led to considerable amounts of higher molecular weight products (entries 18 and 25 in Table 3.1). The formation of these condensation products could, however, be dramatically reduced by using these catalysts in a 0.1 mass ratio and by drying the clay prior to use (see Experimental Section). A selectivity of up to 99% with 100% conversion was now realized (entry 23) with the montmorillonite K-10. However, after a certain reaction time the conversion dropped considerably, although for some clays the conversions remained at a useful level. Interestingly, the F-105SF clay gave a similar efficient rearrangement when 1 mass equivalent of (not pre-treated) catalyst was applied (entry 7). In contrast to montmorillonite K-10, the selectivity dropped when this catalyst was dried prior to use (entry 10). By reviewing the results listed in Table 3.1, it may be concluded that the activity of a catalyst is considerably lower when not dried prior to use. Physisorbed water will be present in the cavities and pores of the catalysts, thus blocking the access of organic species to the active sites. Drying at 125°C at ambient pressure will remove most of this physisorbed water, whereas drying at 400°C at 0.05 mbar (applied for catalysts in Table 3.2, and used throughout Chapter 4 in catalytic flash vacuum thermolysis experiments) results in a complete removal of any physisorbed water present at the catalytic surface. In the literature, however, many authors have employed clay catalysts without any conditioning or pre-treatment,[36,39b,41b,c] which makes the comparison of our results with those previously reported quite difficult. Other natural clay catalysts, viz. F-1, F-13, F-24 and F-25, also displayed a considerable activity; the conversion reached completion when a catalyst to substrate mass ratio of 1.0 was employed. Under these experimental conditions the selectivities observed ranged from 78 to 88%. When a lower amount of these catalysts was used the selectivities were notably higher, but the conversions remained low after prolonged reaction times. The results shown in Table 3.1 reveal that the best results are obtained with the catalysts F-105SF (entry 7) and montmorillonite K-10 (entry 23).

Table 3.1 *Rearrangement of styrene oxide* **1** *catalyzed by natural clays*

Entry	Catalyst[a]	Mass Ratio[b]	Reaction Time (h)	Conversion[c] (%)	Selectivity[c,d] (%)
1	F-1	1	0.1	47	95
2		1	1	100	83
3		0.1	3	27	98
4	F-13	1	0.1	95	80
5		1	1	100	78
6		0.1	3	38	84
7	F-105SF[e]	1	0.1	100	99
8		0.1	1	95	77
9		0.01	1	23	71
10	F-105SF	0.1	1	73	79
11		0.1	3	99	87
12	F-24	1	0.1	31	94
13		1	1	100	88
14		0.1	3	18	95
15	F-25	1	0.1	68	92
16		1	1	100	81
17		0.1	3	29	86
18	Montmorillonite K-10[e]	1	0.1	100	67
19		0.1	1	83	65
20		0.01	1	23	86
21	Montmorillonite K-10	1	0.1	100	74
22		0.1	2	73	99
23		0.1	3	100	99
24	Montmorillonite KSF[e]	1	0.1	20	99
25		1	21	100	84
26	Montmorillonite KSF	1	0.1	10	71
27		1	3	45	62
28		0.1	3	6	99
29		0.1	20	28	97

[a] Catalysts were dried at 125 °C for 1 h prior to use, unless stated otherwise. [b] Mass ratio stands for the ratio [mass catalyst]/[mass substrate]; 100 mg of substrate was used. [c] Conversions and selectivities determined by GC against an internal standard. [d] Selectivity towards **2**; [e] Catalyst used as received.

Table 3.2 summarizes the results for the isomerization of styrene oxide **1** using synthetic clay materials and amorphous (silica) aluminas as solid acid catalysts. The catalyst Mg-saponite\Al^{3+} is listed three times in the table (entries 1-9), viz. as a powder and as a sieve fraction of 150-425 μm both pretreated at 400°C at 0.05 mbar and as a powder pre-treated at 125°C at ambient pressure (*vide infra*).

The method of pre-treatment has a significant influence on the catalytic performance, since the conversion after a certain reaction time and the selectivity were different for the two types of pre-treated catalysts (compare entries 6, 10 and 22 with 9, 14 and 23, respectively, in Table 3.2). The selectivity towards **2** was usually somewhat lower using catalysts pre-treated at 400°C and 0.05 mbar. This trend in selectivity indicates that during the conditioning at 400°C and 0.05 mbar more catalytic sites were made available. The strongest catalytic sites will hold adsorbed water most firmly and only

a strong desorption force will release this water. It should be noted, however, that these strongest sites most likely give rise to side-reactions (e.g. condensation reactions). The observed conversions after a certain reaction time was inconsistent for the two types of pre-treated catalysts: in some cases the conversion was lower using the catalysts pre-treated at 400°C and 0.05 mbar (entries 4 and 10 compared to entries 7 and 14, respectively, in Table 3.2), but also the reverse was observed (entries 20 and 22 vs entries 21 and 23, respectively, in Table 3.2).

Table 3.2 *Rearrangement of styrene oxide* **1** *catalyzed by synthetic clays*

Entry	Catalyst[a]	Mass Ratio[b]	Reaction Time (h)	Conversion[c] (%)	Selectivity[c,d] (%)
1	Mg-saponite\Al^{3+}	1	0.1	25	37
2	(150-425 µm)[f]	1	1	52	59
3		1	3	73	64
4	Mg-saponite\Al^{3+}	1	0.1	88	64
5		1	1	100	67
6		0.1	3	29	52
7	Mg-Saponite\Al^{3+} [e]	1	0.1	100	69
8		0.1	1	91	67
9		0.1	3	100	70
10	Zn-saponite\Al^{3+}	1	3	29	54
11		0.1	3	27	53
12		0.1	23	41	53
13	Zn-saponite\Al^{3+} [e]	1	0.1	30	55
14		1	3	87	71
15		0.1	3	17	51
16	Mg-saponite\H^{+}	1	0.1	75	71
17		1	1	100	72
18		0.1	3	18	43
19	Zn-saponite\H^{+}	1	3	32	51
20	Zn-stevensite	1	3	24	46
21	Zn-stevensite[e]	1	3	13	27
22	Mg-stevensite	1	3	47	68
23	Mg-stevensite[e]	1	3	28	41

[a] Catalysts were dried (15 minutes) at 400 °C at 0.05 mbar prior to use, unless stated otherwise. [b] Mass ratio stands for the ratio [mass catalyst]/[mass substrate]; 100 mg of substrate was used. [c] Conversions and selectivities determined by GC against an internal standard. [d] Selectivity towards **2**. [e] Catalysts were dried at 125 °C for 1 h prior to use. [f] Sieve fraction of 150-425 µm, other materials were used as powder.

Diffusion from the catalytic surface through the catalyst particles also plays an important role. This is exemplified by the comparison of the results using a powdered catalyst (entries 4-6 in Table 3.2) and using the same catalyst in a sieve fraction of 150-425 µm (entries 1-3 in Table 3.2). With the larger catalyst particles the conversion after a certain reaction time was drastically lower and, in addition, also the selectivities towards **2** were lower. The substantial differences in the conversion due to differences in catalyst particle size, point to accessibility as the rate-determining step, i.e. diffusion controlled reactions.

Generally, the selectivity towards **2** increased as the reaction time was prolonged. Apparently, the initial selectivity was relatively poor but increased considerably with time, since the overall selectivity towards **2** increased. This observation may find its origin in diffusion limitations, which leads to longer residence times for the substrate or the product(s) at the active sites of the catalyst which may result in consumption of the initially formed products. These undesired secondary reaction product(s) may block the most active sites rapidly and irreversibly, thus inhibiting these side reactions considerably as the reaction proceeds and hence increasing the selectivity towards **2**.

Reviewing the performance of the synthetic clay materials listed in Table 3.2 the Mg-saponite\$Al^{3+}$ gave the highest conversions after a certain time of reaction (entries 7 and 9), followed by the Mg-saponite\$H^{+}$ for which the reaction reached also completion after 1 h when 1.0 mass equivalent of catalyst was used (entry 17). For other synthetic clays, e.g. the Zn-saponites and the stevensites, modest activity was observed. Only after prolonged reaction times a substantial conversion was observed only for Zn-saponite\$Al^{3+}$ (entry 14). The selectivities towards **2** using synthetic clays as catalysts ranged from 27 to 71%. Generally, the highest selectivities were found in the fastest reactions.

Comparison of the data shown in Table 3.1 and Table 3.2 clearly demonstrates that the natural clays outperform the synthetic clays.

Table 3.3 *Rearrangement of styrene oxide* **1** *catalyzed by amorphous (silica) aluminas*

Entry	Catalyst[a]	Mass Ratio[b]	Reaction Time (h)	Conversion[c] (%)	Selectivity[c,d] (%)
1	B698D-24	1	1	57	99
2		1	3	78	98
3		1	21	100	91
4	B698D-25	1	1	66	99
5		1	3	84	99
6		1	19	100	94
7	HA-SHPV	1	1	45	99
8		1	3	90	99
9		1	19	98	93

[a] Catalysts were dried at 125 °C for 1 h prior to use. [b] Mass ratio stands for the ratio [mass catalyst]/[mass substrate]; 100 mg of substrate was used. [c] Conversions and selectivities determined by GC against an internal standard. [d] Selectivity towards **2**.

Besides natural and synthetic clay materials, two amorphous silica-aluminas and one amorphous alumina were also used as catalysts in the rearrangement reaction of styrene oxide **1** (Table 3.3). These materials were pre-treated at 125°C at ambient pressure. Using these three catalysts in a mass ratio of 1.0 the conversions after a certain reaction time were comparable or somewhat lower than with clay catalysts. The selectivities observed were very high, namely ranging from 91 to 99%. The

selectivity was 99% for all three catalysts after a reaction time of 1 h, but after longer reaction times it dropped to 91-94%.

As an overall conclusion it may be concluded that the highest conversion rates were found with montmorillonite K-10 and Mg-saponite\Al^{3+}. With this latter catalyst, however, the selectivity towards the desired phenylacetaldehyde was no more than 70%, whereas with the former catalyst a selectivity of 99% could be achieved. Thus montmorillonite K-10 is the best catalyst in the rearrangement of styrene oxide **1** into phenylacetaldehyde **2** in the solution phase.

The type and amount of acidic sites of the various solid catalysts has been semi-quantitatively determined using infrared analyses of adsorbed pyridine (cf. Chapter 2). These studies showed that montmorillonite K-10, Zn-saponite\H^{+} and the F-1 clay possess predominantly Lewis acidic character, whereas amorphous alumina B698D-25 and the F-13 and F-25 natural clays contained mainly Brønsted acidity. The other materials studied contain a slightly larger number of Lewis acidic sites. The relative acidity was of the same order of magnitude for most of the catalysts. The largest acidity was observed for the amorphous silica-aluminas B698D-25 and HA-SHPV and the synthetic clay Mg-saponite\Al^{3+}. The synthetic clay Mg-saponite\H^{+} and the F-13 natural clay displayed lower acidity than the other solid catalysts studied. Stevensites have a considerably lower relative acidity, and it is known[37] that this (low) acidity is mainly of the Lewis type. It should be mentioned, however, that the temperatures applied to study the desorption of pyridine from the solid acids are not the same as those used during the pre-treatment prior to the catalytic experiments. This may affect the interpretation of the correlation between the results of both series of experiments. The current desorption temperatures were chosen at the indicated values to enable an easy comparison with desorption results obtained in a previous study.[21b]
The results listed in Table 3.1 and Table 3.2 only partly reflect these acidic properties. The B698D-25 amorphous silica-alumina has the strongest acidity and has the largest number of acidic sites, but this material is by no means the most catalytically active one. The highest conversions after a certain reaction time were observed with montmorillonite K-10 and the F-105SF, followed by the Mg-saponites, the F-1, F-13, F-24 and F-25. No consistent correlation could be found between this order of catalytic activity and the order of the total acidity of the respective catalysts (e.g. Lewis or Brønsted acidity).
Some correlation was found for the synthetic clay catalysts. The clay that displayed the highest total acidity (Mg-saponite\Al^{3+}) also gave the highest conversions. The

order of acidity for the other synthetic clays correlates also quite well, although not entirely; viz. Zn-saponite\$Al^{3+}$ > Mg-saponite\$H^+$ > Zn-saponite\$H^+$ > stevensites.
In contrast, there is no clear correlation between the acidity and the conversions for the natural clays. Most of the natural clay catalysts that lead to a high conversion of styrene oxide **1** are relatively acidic (see Chapter 2), however, F-1, that has a similar total acidity showed a considerably lower rate of conversion.
In summary, it may be concluded that there is no consistent correlation between the acidic properties of the catalysts used and their catalytic activity. An acceptable correlation was only found for the synthetic clay materials. No such correlation was found for the various natural clays. The high total acidity found for the amorphous silica-aluminas was not reflected in their catalytic activity.

The results suggest that the active surface area may also play a role in the rearrangement of **1** to **2**. KSF montmorillonite with an active surface area of only 20-40 m^2/g has a considerably lower catalytic activity than the other natural clay catalysts, all of which have an active surface area larger than 200 m^2/g. This considerably lower surface area of montmorillonite KSF might outweigh any other feature effecting its catalytic activity in this epoxy/carbonyl rearrangement. The differences in surface area between the other catalysts are much smaller (e.g. a multiplication factor of 2 to 3 instead of 10) and therefore other factors are still important to understand the differences in their catalytic activity.

The high selectivities observed for some of the catalysts indicate that their active sites retain their catalytic activity throughout the process, implying a large turnover number. This was confirmed by reusing the catalyst (e.g. montmorillonite K-10 and F-105SF), after washing and drying, in a second batch with styrene oxide **1**. Hardly any loss of catalytic activity was observed.

Larger scale isomerization of styrene oxide

The selectivities listed in Table 3.1 and Table 3.2 were determined by sampling directly from the reaction mixture without removal of the solvent upon isolation. In general, however, the fraction of the aldehyde in the mixture decreased somewhat when the solutions were concentrated. Apparently, the higher concentration led to unwanted (condensation) reactions of the product. This was also observed when the isomerization reaction of **1** using montmorillonite K-10 was repeated at larger scale (Table 3.4). In one case the amounts of catalyst and substrate were 100 times larger (viz. 10 g of **1** and 1.0 g of catalyst), but the amount of solvent was only 6 times larger (Table 3.4, entries 1-3). In this case the selectivity for **2** was only 65%, after a reaction

time of 3 h, which is considerably lower than observed for the same reaction at small scale (Table 3.1, entry 23). However, when the amounts of substrate, catalyst and also the amount of solvent were enlarged by the same factor, viz. 10, a much higher selectivity for **2** was observed (83% after 20 h, Table 3.4, entry 6).

Table 3.4 *Isomerization of styrene oxide* ***1*** *at a larger scale using montmorillonite K-10*

Entry	Amount of 1 (g)	Amount of montm. K-10[a] (g)	Amount of toluene (ml)	Reaction time (h)	Conversion[b] (%)	Selectivity[b,c] (%)
1	10	1	90	0.1	58	60
2	10	1	90	1	78	62
3	10	1	90	3	85	65
4	1	0.1	140	1	45	94
5	1	0.1	140	3	54	94
6	1	0.1	140	20	100	83

[a] Catalyst was dried at 125 °C for 1 h prior to use. [b] Conversions and selectivities determined by GC analysis. [c] Selectivity towards **2**.

Tandem reactions starting with the isomerization of styrene oxide

Handling of phenylacetaldehyde **2** is quite troublesome because of its acid lability and it easily gives rise to unwanted self-condensation reactions (*vide infra*). It was therefore considered to trap phenylacetaldehyde **2** immediately after its formation from styrene oxide **1**, thus circumventing the necessity to isolate **2**. Two types of conversions were studied: a Wittig type reaction and an acetalization reaction (Scheme 3.8). The Wittig reaction was carried out with methyl 2-(1,1,1-triphenyl-λ^5-phosphanylidene)acetate as the phosphor ylide, which was added to the reaction mixture 15 minutes after the isomerization reaction had started. The solvents used were toluene and hexane. When 1.0 mass equivalent of montmorillonite K-10 was used with toluene as the solvent methyl (E)-4-phenyl-2-butenoate **13** could be isolated in 46% yield (cis:trans ≈ 1:1). With hexane as the solvent the reaction proceeded quite sluggishly and gave only 34% of **13** after 6 days. About 27% of the epoxide could still be recovered. This observation indicates that the epoxy/carbonyl isomerization is inhibited by the highly polar phosphor ylide, which is thought to coordinate strongly with the surface of the solid acid. It would therefore probably be better to carry out the epoxide isomerization and remove the solid catalyst from the reaction mixture before the phosphor ylide is added.

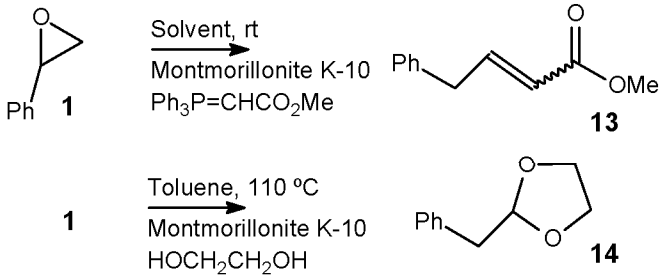

Scheme 3.8 *Follow-up reactions carried out after isomerization*

The acetalization reaction was carried out with 1,2-ethanediol and 1.0 mass equivalent montmorillonite K-10 in refluxing toluene. 2-Benzyl-1,3-dioxolane **14** was obtained in an acceptable yield of 65% after a reaction time 2 h. Various authors have studied the application of solid acid catalysts in the protection[38] of carbonyl compounds with diol and thiols and also the deprotection[39] has been studied rather extensively. These studies showed that protection of an aldehyde with a diol might be accomplished quite readily. High yields of up to 99% of the 1,3-dioxolane products were obtained, but the labile phenylacetaldehyde **2** was not used as a substrate in these studies.[38] In the present work it was established that this protection with a diol may also be accomplished immediately following an epoxide rearrangement reaction.

3.2.2 Rearrangement of stilbene oxides

Stilbene oxides, *trans*- **15** and *cis*- **18**, are two aromatically substituted epoxides of which epoxy/carbonyl isomerizations have been studied rather extensively. With BF_3-etherate as the homogeneous Lewis acidic catalyst, diphenylacetaldehyde **16** was obtained as the only product from the isomerization reaction of both *cis*- and *trans*-stilbene oxide.[40] However, when using $MgBr_2$ a mixture of **16** and deoxybenzoin **17** was obtained starting from *trans*-stilbene oxide **15**, whereas **16** appeared the sole product from the isomerization of *cis*-stilbene oxide **18**[40]. Isomerization of both **15** and **18** with $[(\eta^5\text{-}C_5H_5)Fe(CO)_2(THF)]^+BF_4^-$ as a the Lewis acid afforded **16** as the only product,[15a] while **17** was the sole product using $Pd(OAc)_2$-PPh_3 as the catalyst.[15b] These results show that the catalyst used has a profound effect on the regiochemistry of the rearrangement, which must be attributed to different reaction paths.[40] Therefore, these stilbenes are excellent substrates to compare the catalytic behavior of various solid acids. In addition, the impact of stereochemistry on the isomerization, viz. *cis*- vs. *trans*-, can be established.

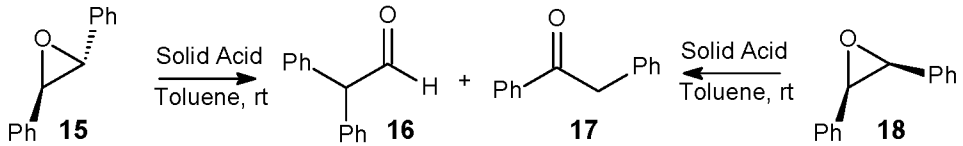

Scheme 3.9 *Isomerization of trans-stilbene oxide* **15** *and cis-stilbene oxide* **18**

The results obtained for the isomerization of *trans*-stilbene oxide **15** applying natural and synthetic clays are collected in Table 3.5. All clays, except the two stevensites, were effective catalysts in this isomerization reaction. When a solution of **15** in toluene was treated with 1 mass equivalent of clay catalyst a rapid conversion into diphenylacetaldehyde **16** was observed. With most catalysts, used in a mass ratio of 1.0, an almost 100% conversion was achieved after about 5 min. However, when the

amount of catalyst was only 0.1 mass equivalent, a more diverse picture was observed, viz. much more dependent on the catalyst used. After a reaction time of 1 h conversions higher than 95% were found for montmorillonite K-10, F-13, F-105SF, F-25 and Mg-saponite\Al^{3+} catalysts. The montmorillonite K-10 and Mg-saponite\Al^{3+} catalysts turned out to be the most reactive ones as the conversions observed after ca. 5 min were considerably higher than for other catalysts (viz. 68-69%). Zn-stevensite was the least reactive catalyst in this reaction since, with a catalyst:substrate ratio of 1.0, still only a very low conversion (23%) was observed after a reaction time of 120 h. The selectivity towards **16** ranged for the more reactive catalysts from 86% (Mg-saponite\Al^{3+}, entry 28) to 100% (montmorillonite K-10, entry 21). With the stevensites, which gave the lowest conversions, diphenylacetaldehyde **16** was formed with very low selectivity or not at all (Zn-stevensite, Table 3.5, entries 38-39). With all catalysts studied no deoxybenzoin **17** was observed in the reactions with *trans*-stilbene oxide **15**.

Catalysts that were not pre-treated at 125°C gave, in general, a somewhat lower conversion (Table 3.5, compare entries 7 and 9); and a substantially lower selectivity (Table 3.5, entries 7, 8, 18-20). These un-pre-treated catalysts contain an appreciable amount of physisorbed water (see Section 3.2.1). As the result, the adsorbed water functions as a nucleophile, yielding a considerable amount of 1,2-diphenyl-1,2-ethanediol **19**, which was isolated from the reaction mixtures. The nucleophilic ring opening of epoxides is a very common reaction, and several reports discuss the application of solid acid catalysts in this type of reaction.[41] In fact, isomerization of epoxides only proceeds well in the absence of strong nucleophiles. Another side-product that could be isolated and characterized was 2,4,6-tribenzhydryl-1,3,5-trioxane **20**, which is formed by a trimerization of diphenylacetaldehyde **16**. This product **20** was obtained when 1.0 mass equivalent of montmorillonite K-10 was used (Table 3.5, entries 18 and 19). The amount of **20** increased (9% to 37%) when stirring of the reaction mixture was continued after complete consumption of the epoxide **15**. This trimerization of diphenylacetaldehyde **16** was only observed for un-pre-treated montmorillonite K-10. The side-products **19** and **20** were not found at all, when pre-treated catalysts were used. The synthesis of 1,3,5-trioxanes using solid acids has been reported earlier using a bentonitic earth as catalyst.[42]

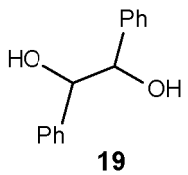

19

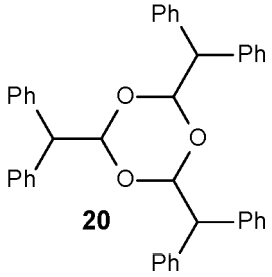

20

The data in Table 3.5 reveal that the best catalysts for the isomerization of *trans*-stilbene oxide **15** into diphenylacetaldehyde **16** are montmorillonite K-10, F-1 and Zn-saponite\Al^{3+}.

Table 3.5 *Rearrangement of trans-stilbene* **15** *catalyzed by natural and synthetic clays*

Entry	Catalyst[a]	Mass Ratio[b]	Reaction Time (h)	Conversion[c] (%)	Selectivity[c] (%) 16
1	F-1	1	0.1	100	94
2		0.1	1	71	99
3		0.1	3	97	99
4	F-13	1	0.1	98	87
5		0.1	0.1	16	99
6		0.1	1	98	93
7	F-105SF[d]	1	0.1	56	58[e]
8		1	1.3	100	67[e]
9	F-105SF	1	0.1	98	88
10		0.1	0.1	45	99
11		0.1	1	98	91
12	F-24	1	0.1	82	92
13		0.1	1	42	99
14		0.1	3	89	93
15	F-25	1	0.1	98	88
16		0.1	0.1	12	95
17		0.1	1	98	94
18	Montmorillonite K-10[d]	1	0.1	100	91[g]
19		1	1	100	73[h]
20		0.1	0.5	95	81[f]
21	Montmorillonite K-10	1	0.1	100	100
22		0.1	0.1	69	88
23		0.1	1	100	91
24	Montmorillonite KSF	1	1	66	94
25		1	3	99	93
26		0.1	1	44	97
27		0.1	3	94	92
28	Mg-Saponite\Al^{3+}	1	0.1	100	86
29		0.1	0.1	68	99
30		0.1	1	100	91
31	Zn-Saponite\Al^{3+}	1	0.1	86	99
32		1	1	100	99
33		0.1	1	67	95
34		0.1	3	90	98
35	Mg-Stevensite	1	3	33	73
36		1	120	100	73
37		0.1	18	5	48
38	Zn-Stevensite	1	120	23	0
39		0.1	18	8	0

[a] Catalysts were dried at 125 °C for 1 h prior to use, unless stated otherwise. [b] Mass ratio stands for the ratio [mass catalyst]/[mass substrate]; 100 mg of substrate was used. [c] Conversions and selectivities determined by GC against an internal standard. [d] Catalyst used as received. [e] also 30% of 1,2-diphenyl-1,2-ethanediol **19**. [f] also 18% of 1,2-diphenyl-1,2-ethanediol **19.**; [g] also 9% of 2,4,6-tribenzhydryl-1,3,5-trioxane **20**. [h] also 37% of 2,4,6-tribenzhydryl-1,3,5-trioxane **20**.

The results obtained for the isomerization of *cis*-stilbene oxide **18** are collected in Table 3.6. Only natural clays were used since these proved to be the most active ones in the rearrangement reactions of styrene oxide **1** and *trans*-stilbene oxide **15**.

Table 3.6 *Rearrangement of cis-stilbene* **18** *catalyzed by natural clays*

Entry	Catalyst[a]	Mass Ratio[b]	Reaction Time (h)	Conversion[c] (%)	Selectivity[c] (%)	
					16	17
1	F-1	1	0.1	100	78	9
2		0.1	0.1	20	64	20
3		0.1	1	70	79	14
4	F-13	1	0.1	100	83	9
5		0.1	0.1	52	69	13
6		0.1	1	100	73	11
7	F-105SF	1	0.1	100	73	8
8		0.1	0.1	56	70	13
9		0.1	1	100	76	10
10	F-24	1	0.1	100	82	9
11		0.1	0.1	24	28	13
12		0.1	1	85	73	12
13	F-25	1	0.1	100	80	9
14		0.1	0.1	29	52	22
15		0.1	1	91	70	12
16	Montmorillonite K-10	1	0.1	100	77	11
17		0.1	1	100	68	12
18	Montmorillonite KSF	1	1	15	80	7
19		1	3	76	77	16
20		0.1	1	10	41	12
21		0.1	3	16	73	12

[a] Catalysts were dried at 125 °C for 1 h prior to use. [b] Mass ratio stands for the ratio [mass catalyst]/[mass substrate]; 100 mg of substrate was used. [c] Conversions and selectivities determined by GC against an internal standard.

The majority of the clays tested were effective catalysts in the isomerization of *cis*-stilbene oxide **18**. Upon treatment of a solution of **18** in toluene with 1 mass equivalent of clay catalyst generally led to a rapid conversion into diphenylacetaldehyde **16**. Most of the catalysts gave, under these conditions, a conversion of a 100% after 5 min. When the amount of catalyst was reduced to 0.1 mass equivalents a different picture was observed, namely that the conversion was more dependent on the catalyst. After 5 min, conversions higher than 95% were found for montmorillonite K-10, F-13 and F-105SF as the catalysts. Montmorillonite KSF (Table 3.6, entries 18-21) gave substantially lower conversions. Comparison of the conversions of *cis*-stilbene oxide **18** with those of *trans*-stilbene oxide **15** immediately shows that the former are much higher. This greater reactivity of **18** is not surprising, since this isomer experiences a greater degree of intrinsic steric strain, which is released upon isomerization to a carbonyl compound. Moreover, the *cis*-isomer encounters less steric hindrance in approaching an active site on the catalyst surface than the *trans*-isomer. In *cis*-stilbene oxide **18** one of the stereotopic faces is considerably less bulky,

whereas in *trans*-stilbene oxide **15** the steric bulk caused by a phenyl group is the same for both faces.
Interestingly, in contrast to *trans*-stilbene oxide **15**, *cis*-stilbene oxide **18** gave not only diphenylacetaldehyde, but also deoxybenzoin **17** as one of its reaction products. The ketone **17** was obtained with selectivities ranging from 7 to 22%. In general, the selectivity towards the aldehyde **16** is lower than for *trans*-stilbene oxide **15** and is 83% at the maximum (Table 3.6, entry 4).

The results listed in Table 3.5 and Table 3.6 reflect only partly the acidic properties of the catalysts (see Chapter 2 and Section 3.2.1). The highest conversions were observed with montmorillonite K-10 and the Mg-saponite\Al^{3+} (only tested for *cis*-**18**) followed by the F-105SF, F-13 and F-25 clays. A satisfactory correlation between conversion values and acidity (Lewis or Brønsted acidity) is absent. Nevertheless, the clay that displayed the highest and strongest acidity (Mg-saponite\Al^{3+}) also gave the highest conversion values, while the clays with the lowest acidity, viz. the stevensite clays, showed the lowest conversions.

Also here the active surface area seems to play a role in the rearrangement of *cis*-stilbene oxide **18**, since KSF montmorillonite with a much lower active surface area has a considerably lower catalytic activity than the other natural clay catalysts. In the rearrangement of *trans*-stilbene oxide **15** this effect was less pronounced. This considerably lower surface area of montmorillonite KSF might outweigh any other feature that affects its catalytic activity in this epoxy/carbonyl rearrangement.

The catalysts that show the highest conversions rates (namely montmorillonite K-10, Mg-saponite\Al^{3+}, F-105SF, F-13 and F-25 clays) in the rearrangement of the stilbene oxides **15** and **18** are, with the exception of F-25, also the most active ones in the isomerization of styrene oxide **1**. The fact that the acidity of the catalysts is only partly reflected in their catalytic performance in the rearrangement of *cis*- **15** and *trans*-stilbene oxide **18** was also observed for the isomerization of styrene oxide **1**.

3.2.3 Rearrangement of 2,2,3,3-tetraphenyloxirane

In order to investigate the effect of steric bulk on the acid catalysis of aromatically substituted epoxides applying solid acids, 2,2,3,3-tetraphenyloxirane **21** was chosen as the substrate. Obviously, the epoxy/carbonyl rearrangement can only produce triphenylacetophenone **22** as the product. The results obtained in the isomerization of 2,2,3,3-tetraphenyloxirane **21** using natural clays are listed in Table 3.7. Only natural

clays were used since these proved to be the most active ones in the rearrangement reactions of styrene oxide **1** and *trans*-stilbene oxide **15**.

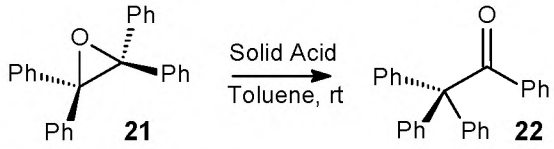

Scheme 3.10 *Isomerization of 2,2,3,3-tetraphenyloxirane* **21**

Table 3.7 *Rearrangement of 2,2,3,3-tetraphenyloxirane* **21** *catalyzed by natural clays*

Entry	Catalyst[a]	Mass Ratio[b]	Reaction Time (h)	Conversion[c] (%)	Selectivity[c,d] (%)
1	F-1[e]	1	20	27	100
2	F-1	1	0.1	52	98
3		1	1	100	98
4		0.1	3	12	84
5	F-13[e]	1	20	33	100
6	F-13	1	0.1	100	98
7		0.1	3	20	96
8	F-105SF[e]	1	20	93	100
9	F-105SF	1	0.1	99	97
10		0.1	3	20	97
11	F-24	1	0.1	76	100
12		0.1	3	22	99
13	F-25[e]	1	20	8	100
14	F-25	1	0.1	86	98
15		1	1	100	95
16		0.1	3	24	98
17	Montmorillonite K-10[e]	1	1	38	100
18	Montmorillonite K-10	1	0.1	71	100
19		1	1	100	100
20		0.1	1	17	100
21		0.1	18	60	100
22	Montmorillonite KSF[e]	1	1	4	100
23	Montmorillonite KSF	1	1	9	100
24		1	23	89	100

[a] Catalysts were dried at 125 °C for 1 h prior to use, unless stated otherwise. [b] Mass ratio stands for the ratio [mass catalyst]/[mass substrate]; 100 mg of substrate was used. [c] Conversions and selectivities determined by GC against an internal standard. [d] Selectivity towards **22**; [e] Catalyst used as received.

The isomerization of **21** proceeded generally quite fast when a pre-treated clay was employed in a mass ratio of 1.0. Most of the catalysts used led to a conversion of about 100% after 1 h. When the mass ratio was reduced to 0.1 the conversions were substantially lower. After 3 h less than 25% of **21** had reacted. Just as for the other aromatic epoxides montmorillonite KSF proved again an exception and gave substantially lower conversions, also at a mass ratio of 1.0 (Table 3.7, entries 22-24).

The effect of pre-treatment of the clay on the conversions of **21** was large. The isomerization reaction proceeded several orders of magnitude slower when untreated catalysts were used (Table 3.7, compare entries 1, 5, 8, 13 and 17 with

entries 2, 6, 9, 14 and 18, respectively). Apparently, the bulky molecule **21** is effectively blocked from access to the reactive surface sites by physisorbed water.
The selectivity towards 1,2,2,2-tetraphenyl-1-ethanone **22** is extremely high. In most cases it was the only product and the lowest selectivity observed was still 84%. This shows that the product is not labile towards the solid acids applied.
As for other aromatically substituted epoxides (Section 3.2.2) no good correlation was obtained between the conversion rates and the acidity of the catalysts. Natural clay catalysts that gave a relatively fast conversion are also the most acidic ones (see Chapter 2), however, with the exception of F-1.
The conversion rates for 2,2,3,3-tetraphenylethene oxide **21** were considerably lower than those for stilbene oxides **15** and **18** and styrene oxide **1**. This confirms that the steric bulk of the four phenyl groups of **21** reduces the reactivity significantly in the epoxy/carbonyl isomerization catalyzed by solid acids.
Besides toluene also other solvents have been used, such as dichloromethane, hexane and ethanol. The results obtained with dichloromethane and hexane as solvent were similar to those obtained in toluene, but with the much more polar solvent ethanol the conversions were considerably lower. This is not surprising because the hydroxyl group of ethanol is a strong competitor of the epoxide moiety for the coordination on the active surface site.

3.2.4 Rearrangement of α-pinene oxide

Several studies have been reported on the rearrangement of α-pinene oxide **3** into campholenic aldehyde **4**, which is a widely used intermediate in the flavor and fragrance industry (see Section 3.1). The main reaction pathways and the reaction products (**4**, **7** and **9**) from this acid-catalyzed isomerization of α-pinene oxide **3** are shown in Scheme 3.4.
In Table 3.8 the results obtained for the isomerization **3** using natural and synthetic clays are listed. Most of the catalysts used turned out to be very effective and the conversions were generally very high even after a short reaction time. Reactions proceeded much faster with α-pinene oxide **3** than with the aromatically substituted epoxides described earlier in this Chapter, confirming that **3** is a much more reactive molecule. When a solution of epoxide **3** was treated with 1 mass equivalent of clay catalyst in toluene a rapid conversion was observed. Generally, the desired campholenic aldehyde **4** was the major component in the product mixtures. With most catalysts, when used in a mass ratio of 1.0, a complete conversion was achieved after 5 min. When the amount of catalyst was reduced to one-tenth mass ratio a more differentiated picture was observed with more dependance on the nature of the catalyst. After 0.1 h the highest conversions were found for montmorillonite K-10

(entry 17), F-13 (entry 5) and F-105SF (entry 8). The stevensite catalysts were the least reactive ones in this reaction (entries 31-36).

Table 3.8 *Rearrangement of α-pinene oxide* **3** *catalyzed by natural and synthetic clays*

Entry	Catalyst[a]	Mass Ratio[b]	Reaction Time (h)	Conversion[c] (%)	Selectivity[c] (%)									
					4	**7**	**9**	**23**	**24**	**25**	**26**	**27a**[d]	**27b**[d]	**Others**[e]
1	F-1	1	0.1	100	34	6	7	8	6		15	11	10	3
2		0.1	0.1	41	37	5	9	7			11	15	15	1
3		0.1	1	100	31	6	7	6	4		13	13	15	5
4	F-13	1	0.1	100	32	7	7	8	10	4	16	6	1	9
5		0.1	0.1	90	32	5	8	6	3		11	13	15	7
6		0.1	1	100	31	6	7	6	5		13	12	13	7
7	F-105SF	1	0.1	100	35	7	6	9	8	3	15	10	7	
8		0.1	0.1	80	30	5	6	6	3		10	12	14	14
9		0.1	1	100	29	6	6	6	4	1	11	12	13	12
10	F-24	1	0.1	100	34	6	7	7	5		14	11	12	4
11		0.1	0.1	38	35	4	9	6	3		10	14	14	5
12		0.1	1	100	30	5	8	5	3		12	13	14	10
13	F-25	1	0.1	100	34	6	6	7	6	2	14	9	8	8
14		0.1	0.1	65	34	5	9	6	4		14	14	14	
15		0.1	1	100	29	6	8	6	5	1	13	12	11	9
16	Mont. K-10	1	0.1	100	38	6	7	8	7	3	13	12	6	
17		0.1	0.1	100	34	4	7	7	4		11	15	14	4
18	Mont. KSF	1	1	100	36	4	10	5	2		9	18	13	3
19		0.1	1	34	40		12	5			7	19	13	4
20		0.1	3	99	34	3	11	5	1		8	16	11	11
21	'Clayzic'[f]	1	0.1	84	65	3	3	4			4	3	4	14
22		1	1	100	63	4	3	3			4	3	4	16
23		0.1	3	21	60		6					7	6	21
24	Mg-Sapo-	1	0.1	99	34	2	11	10	1	1	2	17	5	17
25	nite\Al^{3+}	0.1	0.1	32	42		11	5		6		21	7	8
26		0.1	1	93	39	2	13	6	1	2	2	25	8	2
27	Zn-Sapo-	1	0.1	81	37	2	12	8	1	2	3	22	8	5
28	nite\Al^{3+}	1	1	99	35	2	12	12	2	1	3	15	4	14
29		0.1	1	27	39		12	6		6	2	19	6	10
30		0.1	3	54	47	2	12	6		2	2	22	7	
31	Mg-Steven-	1	0.1	33	52	2	5	4	2	5	2	12	7	9
32	site	1	1	61	55	3	4	5	2	2	3	10	8	8
33		0.1	3	24	47	2	5	3	1	6	2	12	7	15
34	Zn-Steven-	1	0.1	18	41		7	3		8		14	4	23
35	site	1	1	21	46	1	6	3	1	7	1	13	6	16
36		0.1	3	18	38	1	7	3	1	8	1	15	6	20

[a] Catalysts dried at 125 °C for 1 h prior to use. [b] 'Mass ratio' refers to the ratio [mass catalyst]/[mass substrate]; 100 mg of substrate was used. [c] Conversions and selectivities determined by GC against an internal standard. [d] **27a** and **27b** are *cis*- and *trans*-isomers of the allylic alcohol **27**. [e] 'others' refers to various unidentified products. [f] Zinc chloride impregnated on montmorillonite K-10[43].

From the data in Table 3.8 it is evident that besides **4**, **7** and **9** a number of other products were obtained. Some of these could be identified, such as *p*-cymene **23**, pinol **24**, pinocarveol **25**, camphor **26** and carveol **27**. Both acidic and basic sites on a catalytic surface (i.e. bifunctionality) play an important role in the formation of pinocarveol **25**. In a mechanism (Scheme 3.11) that possibly explains the formation of

25, the epoxide oxygen attaches itself to an acidic surface site to give a carbocation upon opening of the epoxide. An adjacent basic surface site may assist in abstracting a proton and its subsequent transfer to the oxygen to produce the allylic alcohol **25**.

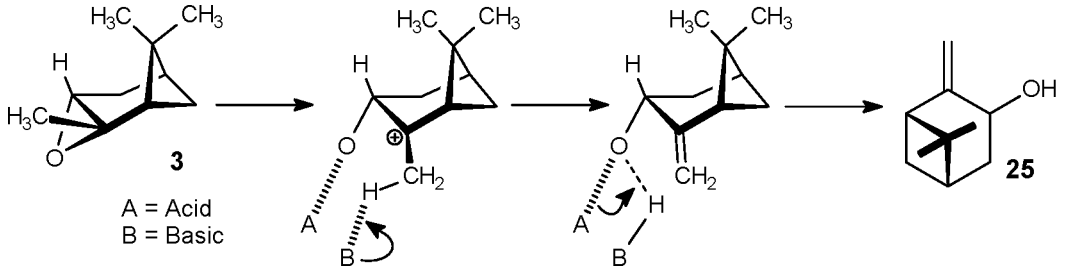

Scheme 3.11 *Mechanism for the formation of pinocarveol* **25** *from α-pinene oxide* **3**

Conceivable mechanisms for the formation of *p*-cymene **23**, pinol **24**, camphor **26** and carveol **27** from α-pinene oxide **3** are shown in Scheme 3.12. Coordination of a Lewis or Brønsted surface acidic site to the epoxide oxygen atom facilitates the fission of a C-O bond of α-pinene oxide **3**, yielding the relatively stable (tertiary) carbocation **5**. Intermediate **5** may, amongst others, rearrange via an alkyl migration (route *i*) to form **8**, which then via a 1,5 H-shift and subsequent formation of a carbonyl unit gives product **26**. Intermediate **28** may be formed by release of strain energy from **5** via the carbocation rearrangement of route *ii*. Pinol **24** may be formed from **28** via a diol intermediate by addition of water, epimerization of the hydroxyl groups and elimination of water. Proton elimination from **28** and detachment from the acidic site would result in the formation of carveol **27** as its *trans*-isomer. The hydroxyl group may, however, epimerize on interaction with acid and water, yielding the *cis*-isomer of **27** as well. Water elimination from **27** followed by a double bond rearrangement is an accepted route[13] to the aromatic compound **23**.

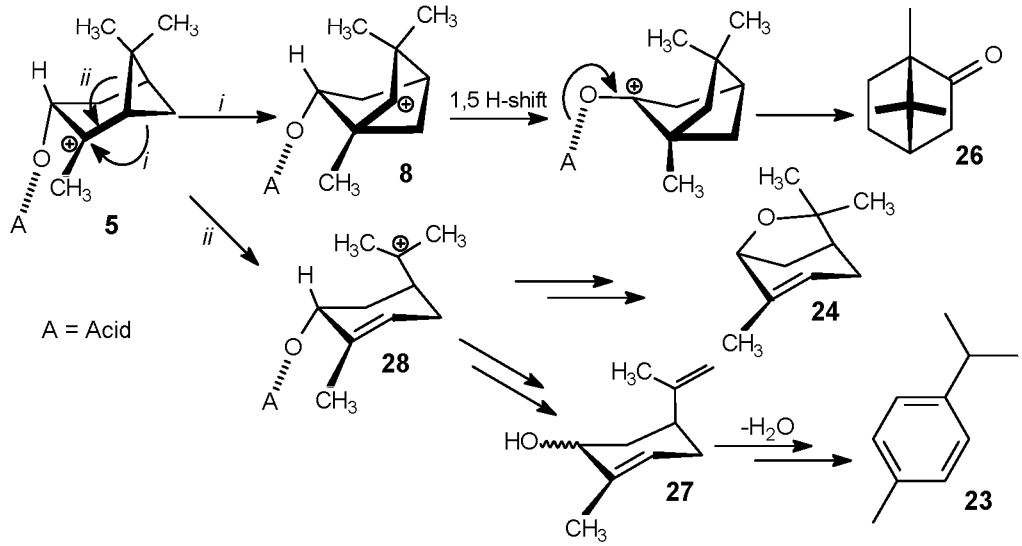

Scheme 3.12 *Mechanisms for the formation of* **23**, **24**, **26** *and* **27** *from α-pinene oxide* **3**

The selectivity towards the desired campholenic aldehyde **4** ranged between 29 and 40% for the natural clays and between 34 and 55% for the synthetic clays. The largest

fraction of **4** (60-65%, entries 21-23) was found using 'clayzic' as the catalyst; this is montmorillonite K-10 impregnated with $ZnCl_2$.[43] Basically, the clay serves here as a solid support to improve handling properties of the Lewis acid $ZnCl_2$. Clayzic has been used with great success in Friedel-Crafts alkylations[44] and acylations.[45] The application of clayzic in the present reaction is, however, accompanied with uncertainty, because possible leaching of $ZnCl_2$ from the solid support. It has been reported that $ZnCl_2$ in benzene affords **4** with a selectivity of 85%.[13] More study is necessary to exclude this possibility of homogeneous catalysis when using clayzic.
Apart from clayzic, Mg-stevensite showed the highest selectivity towards the desired **4** (55%), but the rate of conversion was notably lower than that for the more active clay catalysts. Also other catalysts (viz. Zn-stevensite and Zn-saponite\Al^{3+}) that displayed lower conversion rates in this reaction gave a somewhat larger fraction of **4** in the product mixtures.
2,2,4-Trimethyl-3-cyclopentene **9** (Scheme 3.4), which is an isomer of **4**, is formed as a side-product in all reactions with a selectivity of 6 to 13%. Both Zn-saponites and montmorillonite KSF afforded **9** with a selectivity of 11-13%, whereas the fraction of **9** did not exceed a value of 9% for the other clays. Using natural clay catalysts the camphor **26** was formed in appreciable amounts (11-15%), while it was hardly produced with synthetic clays. Contrarily, pinocarveol **25** was found in limited amounts (up to 8%) mainly with synthetic clays, whereas only traces were formed with natural clays. Shape-selective effects cannot be excluded here. The *cis*- and *trans*-isomers of carveol **27** made up the largest fraction of the side-products. The combined selectivity ranged from 33% (entry 26) to 7% (entries 4, 21 and 22). The largest yields were obtained when 0.1 mass ratios of catalyst were used with relatively slow rearrangement of **3** (entries 4, 7, 13, 16). Pinocamphone **7** was almost absent when synthetic clays (0-2%) were applied but was found in somewhat larger amounts with natural clay catalysts (3-7%). All product mixtures contained *p*-cymene **23** in moderate amounts of up to 12%.

The results listed in Table 3.8 reflect only partly the acidic properties of the various solid acids (see Chapter 2 and Section 3.2.1). The highest conversions were observed using montmorillonite K-10, the Mg-saponite and F-13 followed by F-105SF. Other catalysts showed distinctly lower conversions when used in a mass ratio of 0.1. Unfortunately, again no satisfactory correlation could be found between conversions and product formations, and the acidity of the solid acids. However, again the clay that was most acidic (Mg-saponite\Al^{3+}) gave the highest conversion. In addition, the solids that exhibited only modest acidity (viz. the stevensites) gave the lowest conversions.

Synthetic clays having magnesium as their octahedral cation cause a more rapid conversion of α-pinene oxide. This might be accounted for by the difference in their acidic properties, but the large difference in surface area also seems of influence. The magnesium-clays have a much larger active surface area (411-575 m^2/g) than their zinc-counterparts (244-165 m^2/g) (see Chapter 2). Similarly, the natural clay with a very low active surface area (20-40 m^2/g) (montmorillonite KSF), showed catalytic activities that were considerable lower than those found for other natural clays.
No satisfactory correlation could be established between the catalytic activity and the relative acid site density, which was calculated as the ratio of the relative intensity of the Brønsted or the Lewis acid sites (cf. Section 2.3.4) and the total surface area (cf. Section 2.3.2). A correlation with the micropore volume (see Section 2.3.2) was observed neither.

3.3 CONCLUSIONS

The rearrangement of epoxides using solid acid catalysts in solution phase reactions was investigated. Various natural and synthetic clay materials were tested and, in addition, also amorphous (silica) aluminas were employed. Some representative epoxides containing aryl substituents and an epoxide from the terpene series were studied.
Styrene oxide **1** rearranged to the rather labile phenylacetaldehyde **2** as the major product. The best results, in terms of fast reactions and high product selectivities, were achieved with montmorillonite K-10 as the catalyst. Similarly high conversions, but distinctly lower product selectivities were obtained using Mg-saponite\Al^{3+}. Montmorillonite K-10 was therefore selected to study this rearrangement also on a larger scale. These experiments showed that the selectivity towards **2** dropped when the substrate concentration was increased, due to an increase of secondary reaction products at these higher concentrations.
The best performing catalysts in the rearrangement of both *cis*-stilbene oxide **15** and *trans*-stilbene oxide **18** were montmorillonite K-10, F-13, F-105SF and Mg-saponite\Al^{3+}. *Cis*-stilbene oxide **18** gave both diphenylacetaldehyde **16** and deoxybenzoin **17** as products, whereas compound **17** was the only isomerization product of its *trans*-isomer **15**. The selectivity towards **16** was generally very high starting from **15** and it was also the major product in the isomerization of the *cis*-isomer **18**.
The steric bulk of tetraphenylethene oxide **21** reduced the conversion rates considerably in comparison with those of stilbene oxides **15** and **18** and styrene oxide **1**. The highest conversion rates were found with F-13 and F-105SF as the catalysts. Epoxide **21** was rearranged into triphenylacetophenone **22** as its sole product.

The rearrangement of the highly reactive α-pinene oxide **3** resulted in a broad spectrum of products. Campholenic aldehyde **4** was the major product with a maximum selectivity of 55% using Mg-stevensite. With various natural clay catalysts the selectivity did not exceed 40%. With $ZnCl_2$ impregnated montmorillonite K-10 a selectivity of 65% was achieved, but leaching of $ZnCl_2$ may interfere here. Reactions proceeded much faster with α-pinene oxide **3** than with the aromatically substituted epoxides, confirming that **3** is a much more reactive molecule. The catalysts that led to the fastest conversions of **3** were montmorillonite K-10 and F-13. These catalysts exhibited moderate selectivities towards **4** (up to 38%).
As an overall conclusion, it can be stated that the highest catalytic activity was displayed by montmorillonite K-10, followed by F-13 and F-105SF catalysts.

The nature and number of acidic sites of the various solid catalysts has been semi-quantitatively determined using infrared analyses of adsorbed pyridine (cf. Chapter 2). The results obtained in the isomerization of epoxides reflect only partly the established acidic properties of the catalysts. The highest conversions were observed using montmorillonite K-10, Mg-saponite\$Al^{3+}$ and F-105SF clays. Indeed, Mg-saponite\$Al^{3+}$ exhibits the highest total acidity. Although montmorillonite K-10 and F-105SF did not differ much in their acidic properties from other catalysts they are much more effective catalysts. The solid acids that are considerably less acidic (viz. the stevensites) gave also the lowest conversions.

Accessibility to catalytic surface sites is very important and this is reflected in some cases. Magnesium saponites have a much larger active surface area than their zinc-counterparts. In accordance herewith a more rapid conversion was observed with the Mg-saponites in comparison with Zn-saponites. Although the difference in their acidity may explain the differences in catalytic activity, their unequal surface areas must also be taken into account. Similarly, the natural clay with a very low active surface area, montmorillonite KSF, showed conversions that were considerably lower than those observed for other natural clays.

Industrial perspective

Two transformations were studied that are of particular interest in fine chemical industry, viz. the isomerization of styrene oxide **1** into phenylacetaldehyde **2** and of α-pinene oxide **3** into campholenic aldehyde **4**.
Phenylacetaldehyde **2** could be prepared from **1** in high yields (99%) using montmorillonite K-10 as the catalyst. With this best performing catalyst a few larger scale reactions were carried out. These showed that at higher substrate concen-

trations the reaction time to achieve high conversions was longer and that the selectivity towards desired **2** was lower due to an increased formation of secondary reaction products. Industrially, phenylacetaldehyde **2** is prepared by the oxidation of 2-phenylethanol but the maximum purity of the final product never exceeds 85%[35] since **2** is labile and usually trimerizes or polymerizes rapidly under homogeneous acidic conditions. The method described in this chapter allows the synthesis of phenylacetaldehyde **2** with much higher purities and with a mere filtration as the only work-up step. Moreover, no oxidants are required, which facilitates the handling operations during the manufacturing process, and no waste salts are produced.

The isomerization of α-pinene oxide **3** using clay catalysts afforded campholenic aldehyde **4** as its major product with a maximum selectivity of 55%. The catalysts that provided very high conversion rates (i.e. the natural clays) gave only moderate selectivities of up to 40%. In the present commercial homogeneous process, using $ZnCl_2$ in benzene, campholenic aldehyde **4** is obtained in 87% yield.[31] This process, however, is accompanied by the formation of considerable amounts of waste products (inorganic salts) and suffers from laborious work-up procedures. The method described in this chapter allows the synthesis of campholenic aldehyde **4** avoiding the use of a classical Lewis acid and with filtration as the only work-up step, thus reducing the amounts of waste. In addition, the handling properties of clays are better than those of $ZnCl_2$, which is beneficial for the safety of the manufacturing operation.

3.4 EXPERIMENTAL SECTION

General remarks

Reported percentages are molar percentages (% $^{m}/_{m}$). Gas chromatographic (GC) analyses were performed on a Hewlett-Packard HP5890II gas chromatograph, using a capillary column (HP-1, 25 m x 0.31 mm x 0.17 µm), nitrogen at 2ml/min (0.5 atm) as the carrier gas, and a temperature program from 75°C (5 minutes isothermal)-250°C at 15°C/min followed by 3 min at 250°C (isothermal) or from 100°C to 250°C at 15°C/min followed by 10 min at 250°C (isothermal). FT-IR spectra were recorded on a Biorad FTS-25 spectrophotometer. ^{1}H- and ^{13}C-NMR spectra were recorded on a Bruker AM-400 and a Bruker AC-100 at T=298 K. Chemical shifts were reported against $Si(CH_3)_4$. Mass spectrometric (MS) analyses were measured with a double focussing VG Analytical 7070E mass spectrometer or a Varian Saturn II GC-MS set-up equipped with an HP-1 capillary column and Varian 8100 autosampler.

Column chromatography at ambient pressure was carried out using Merck Kieselgel 60. Thin layer chromatography (TLC) was carried out on Merck precoated silicagel 60 F254 plates

(0.25 mm) using the eluents indicated. Spots were visualized with UV or molybdate spray. Toluene was distilled from sodium, hexane from calciumhydride and ethyl acetate from potassium carbonate. Commercially available starting materials were used as received.

Origin of the catalysts

Amorphous alumina B698D-24, amorphous silica-alumina B698D-25 and the acid-treated natural F-clays were received as generous gifts from Engelhard De Meern B.V. Amorphous silica-alumina HA-SHPV was obtained as a generous gift from AKZO Nobel Chemicals. Commercial natural clays montmorillonite K-10 and montmorillonite KSF are produced by Süd Chemie and were purchased from Aldrich Chemical Company. Prior to use the montmorillonite K-10 was washed in hot demineralized water and subsequently dried to remove any residual mineral acid that may have been remained after the acid-treatment during its preparation. Synthetic clay materials were donated by the Department of Inorganic Chemistry and Heterogeneous Catalysis of the University of Utrecht. All saponites used had a Si/Al ratio of 7.9 and are described as M-saponite\C^+, where M represents the octahedral cation and C^+ the interlayer cation.

General procedure for the isomerization of epoxides with catalysts pretreated at 125°C

An amount of catalyst was weighed into a glass round-bottom flask, which was closed with a calcium chloride tube and subsequently placed in an oven at 125°C for 1 h. The flask and catalyst were allowed to cool to room temperature under a nitrogen flow. Toluene, a fixed amount of a toluene solution of the internal standard and a fixed amount of a toluene solution of the epoxide were then added successively. The mixture was stirred magnetically. The reaction was monitored by taking small aliquots, which were, after filtration, subjected to GC analysis. After completion the reaction mixture was filtered and concentrated *in vacuo*, and analyzed for its composition.

General procedure for the isomerization of epoxides with catalysts pretreated at 400°C and 0.05 mbar

An amount of catalyst was placed on a quartz porous filter in the middle of a quartz tube. Using the catalytic-Flash Vacuum Thermolysis set-up (See Chapter 4) the catalyst was equilibrated at a temperature of 400°C and a pressure of 0.05 mbar. The hot catalyst was then transferred into a glass flask, which had been heated in an oven at 125°C for 1 h. The flask and catalyst were subsequently allowed to cool to room temperature under a nitrogen flow. Then, the general procedure as described above for the pretreatment at 125°C was followed.

Isomerization of styrene oxide ***1***

Experiments were carried out according to the general procedures described above. To the catalyst (10 or 100 mg) were successively added toluene (5 ml) and toluene solutions of styrene oxide **1** (100 mg in 5 ml) and 1,2,3,4-tetrahydronaphtalene (100 mg in 5 ml; as internal standard). Samples were analyzed, after filtration, using gas chromatography. Results are collected in Table 3.1, Table 3.2 and Table 3.3.

Methyl 4-phenyl-2-butenoate ***13*** *via isomerization of styrene oxide* ***1*** *in toluene*

Montmorillonite K-10 (120 mg) was weighed into a glass round-bottom flask, which was closed with a calcium chloride tube and subsequently placed in an oven at 125°C for 1 h. The flask and catalyst were allowed to cool to room temperature under a nitrogen flow. Toluene (5 ml) and a toluene solution of **1** (120 mg in 5 ml) were successively added. The mixture was stirred magnetically. After 5 min a toluene solution of methyl 2-(1,1,1-triphenyl-λ^5-phosphanylidene)acetate (335 mg in 5 ml) was added. The reaction was monitored by taking small aliquots, which were subjected, after filtration, to GC analysis. After 66 h the reaction mixture was filtered and concentrated *in vacuo*. Hexane was added and the mixture was filtered and concentrated *in vacuo*. Pure **14** (81 mg, 46%; cis:trans ≈ 1:1) was obtained by column chromatography (hexane : ethyl acetate = 40:1) as a light-yellow oil.
Analytical data were in agreement with those reported in the literature.[46]

Methyl 4-phenyl-2-butenoate ***13*** *via isomerization of styrene oxide* ***1*** *in hexane*

Montmorillonite K-10 (120 mg) was weighed into a glass round-bottom flask, which was closed with a calcium chloride tube and subsequently placed in an oven at 125°C for 1 h. The flask and catalyst were allowed to cool to room temperature under a nitrogen flow. Hexane (5 ml) and a hexane solution of **1** (120 mg in 5 ml) were successively added. The mixture was stirred magnetically. After 15 min a hexane solution of methyl 2-(1,1,1-triphenyl-λ^5-phosphanylidene)acetate (325 mg in 5 ml) was added. The reaction was monitored by taking small aliquots, which were subjected, after filtration, to GC analysis. After 6 days the reaction mixture was filtered and concentrated *in vacuo*. Pure **13** (60 mg, 34%; cis:trans ≈ 1:1) was obtained by column chromatography (hexane : ethyl acetate = 40:1) as a light-yellow oil.
Analytical data were in agreement with those reported in the literature.[46]

2-Benzyl-1,3-dioxolane ***14*** *via isomerization of styrene oxide* ***1***

Montmorillonite K-10 (120 mg) was weighed into a glass round-bottom flask, which was closed with a calcium chloride tube and subsequently placed in an oven at 125°C for 1 h. The flask and catalyst were allowed to cool to room temperature under a nitrogen flow. Toluene (5 ml), a toluene solution of **1** (120 mg in 5 ml) and a toluene solution of 1,2-ethanediol (130 mg in 5 ml) were added successively. The mixture was stirred magnetically at 110°C. The reaction was monitored by taking small aliquots, which were subjected, after filtration, to GC analysis. After 1 h the reaction mixture was filtered, washed (2x) with a 5% aqueous solution of KOH, dried (Na_2SO_4) and concentrated *in vacuo*. The crude product (yield 65%) was not purified further.
Analysis of the crude product by NMR, IR and mass spectroscopy confirmed the structure of **14** and these analytical data were in agreement with those reported in the literature.[47]

Isomerization of trans-*stilbene oxide* ***14*** *or* cis-*stilbene oxide* ***18***

Experiments were carried out according to the general procedure described above. To the catalyst (10 or 100 mg) were successively added toluene (5 ml) and toluene solutions of a

stilbene oxide (100 mg in 5 ml) and phenantrene (100 mg in 5 ml; as internal standard). Samples were analyzed, after filtration, using gas chromatography. Results are collected in Table 3.5 and Table 3.6.

1,2-Diphenyl-1,2-ethanediol ***19***

The procedure for the isomerization of *trans*-stilbene oxide was followed, using 100 mg of F-105SF or 10 mg of montmorillonite K-10 catalyst. The catalyst was, however, not pretreated at 125°C. An analytically pure sample of **19** was obtained by column chromatography (hexane : ethyl acetate = 19:1) of the crude reaction mixture.

Analytical data were in agreement with those reported in the literature.[48]

2,4,6-Tribenzhydryl-1,3,5-trioxane ***20***

The procedure for the isomerization of *trans*-stilbene oxide was followed, using 100 mg of montmorillonite K-10 catalyst. The catalyst was, however, not pretreated at 125°C. An analytically pure sample of **20** was obtained by column chromatography (hexane : ethyl acetate = 3:2) of the crude reaction mixture.

^{1}H-NMR (100 MHz, $CDCl_3$, ppm): δ 7.55-7.15 (m, 27H, arom), 7.07-6.85 (m, 3H, arom), 6.12 and 4.56 (ABq, J_{AB}=156 Hz, 3H, 3x -O-C<u>H</u>-O), 4.70 and 4.31 (ABq, J_{AB}=8.0 Hz, 3H, 3x –C<u>H</u>$(Ph)_2$-). ^{13}C-NMR (25 MHz, $CDCl_3$, ppm): δ 129.9, 128.6, 128.4, 128.2, 127.1, 126.3 (arom), 106 (-O-<u>C</u>H-O), 55 (–<u>C</u>H$(Ph)_2$-). IR (CCl_4, cm^{-1}): ν 3066, 3034 (C-H arom), 1162 (C-O-C). EI/GC-MS: *m/e* (%) 225 (12, M^+ - CH-$CHPh_2$, - CHO_2-CH-$CHPh_2$), 197 (100, $^+$CHO-CH-$CHPh_2$ +1), 180 (30, $^+$CH-CH-$CHPh_2$), 165 (33, $^+$CH-$CHPh_2$).

Isomerization of 2,2,3,3-tetraphenyloxirane ***21***

Experiments were carried out according to the general procedure described above. Toluene (5 ml) was added to the catalyst (10 or 100 mg) followed by successively adding toluene solutions of 2,2,3,3-tetraphenyloxirane (100 mg in 5 ml) and phenantrene (100 mg in 5 ml; as internal standard). Samples were analyzed, after filtration, using gas chromatography. Results are collected in Table 3.7.

Isomerization of α-pinene oxide ***3***

Experiments were carried out according to the general procedure described above. Toluene (5 ml) was added to the catalyst (10 or 100 mg) followed by successively adding toluene solutions of α-pinene oxide (100 mg in 5 ml) and 1,2,3,4-tetrahydronaphtalene (100 mg in 5 ml; as internal standard). Samples were analyzed, after filtration, using gas chromatography. Results are collected in Table 3.8. Selected samples were analyzed using GC-MS configured with an appropriate library at IFF.

3.5 REFERENCES

1 a) Parker, R.E.; Isaacs, N.S. *Chem. Rev.* **1959**, *59*, 737. b) Schwartz, N.N.; Blumbergs, J.H. *J. Org. Chem.* **1964**, *29*, 1976. c) Fringuelli, F.; Germani, R.; Pizzo, F.; Savelli, G. *Tetrahedron Lett.* **1989**, *30*, 1427. d) Ishizuka, N. *J. Chem. Soc., Perkin Trans. 1* **1990**, 813.

2 a) Smith, J.G. *Synthesis* **1984**, 629. b) Rao, A.S.; Paknikar, S.K.; Kirtane, J.G. *Tetrahedron* **1983**, *39*, 2323. c) Rosowsky, A. in *Heterocyclic Compounds with 3- and 4-membered Rings; The Chemistry of Heterocyclic Compounds*, Weisberger, A. Ed., Part 1, Interscience, New York, 1964, p231. d) Bartók, M.; Láng, K.L. in *Small Ring Heterocycles; The Chemistry of Heterocyclic Compounds*, Hassner, A. Ed., Vol. 42, Part 3, Interscience, New York, 1985, p65.

3 Morrison, R.T.; Boyd, R.N. in *Organic Chemistry* 5th edn., Allyn and Bacon, Newton, 1987, p715.

4 a) JP patent 79 154735, Noi, R.; Suzuki, M.; Kurozumi, S.; Hashimoto, Y. *to* Teijin Ltd., 6 Dec. 1979; *Chem. Abstr.* **1980**, *93*, 25989n. b) USSR Patent 513966, Koshel, G.N.; Farberov, M.I.; Antonova, T.N.; Glazyrina, I.I., 15 May 1976; *Chem. Abstr.* **1976**, *85*, 176936d. c) JP Patent 74 51233, Wachi, T., 18 May 1974; *Chem. Abstr.* **1974**, *81*, 120220r.

5 Hölderich, W.F. in *New Frontiers in Catalysis*, Guczi, L. *et al.* Eds., *Proc. 10th Int. Conf. Catal.*, 19-24 July 1992, p127.

6 Huisgen, R. *Angew. Chem.* **1977**, *89*, 589.

7 Brown, R.F.C. in *Pyrolytic Methods in Organic Chemistry: Application of flow and flash vacuum pyrolytic techniques; Organic Chemistry Monographs*, Vol. 41, Academic Press, New York, 1980.

8 Rickborn, B. 'Acid-catalyzed Rearrangements of Epoxides' in *Comprehensive Organic Synthesis; Carbon-Carbon σ-Bond Formation*, Trost, B.M. Ed., Vol. 3, Pergamon Press, Oxford, 1991, Section 3.3.

9 Ishihara, K.; Hanaki, N.; Yamamoto, H. *Synlett* **1995**, 721.

10 Kagan, J.; Agdeppa, D.A.; Singh, S.P.; Mayers, D.A.; Boyajina, C.; Poorker, C.; Firth, B.E. *J. Am. Chem. Soc.* **1976**, *98*, 4581.

11 Carey, F.A.; Sundberg, R.J. in *Advanced Organic Chemistry, Part A: Structure and Mechanisms* 3rd edn., Plenum Press, New York, 1990, p311.

12 Ranu, B.C.; Jana, U. *J. Org. Chem.* **1998**, *63*, 8212.

13 Kaminska, J.; Schwegler, M.A.; Hoefnagel, A.J.; Van Bekkum, H. *Recl. Trav. Chim. Pays-Bas* **1992**, *111*, 432.

14 a) Sudha, R.; Malola Narasimhan, K.; Geetha Saraswathy, V; Sankararaman, S. *J. Org. Chem.* **1996**, *61*, 1877. b) Lopez, L.; Mele, G.; Fiandanese, V.; Cardelicchio, C.; Nacci, A. *Tetrahedron* **1994**, *50*, 9097. c) Coxon, J.M.; McDonald, D.Q. *Tetrahedron Lett.* **1988**, *29*, 2575. d) Miyashita, A.; Shimada, T.; Sugawara, A.; Nohira, H. *Chem. Lett.* **1986**, 1323.

15 a) Picione, J.; Mahmood, S.J.; Gill, A.; Hilliard, M.; Hossain, M.M. *Tetrahedron Lett.* **1998**, *39*, 2681. b) Kulasegaram, S.; Kulawiec, R.J. *J. Org. Chem.* **1997**, *62*, 6547. c) Nagahara, S.; Maruoka, K.; Yamamoto, H. *Chem. Lett.* **1992**, 1193. d) Maruoka, K.; Nagahara, S.; Ooi, T.; Yamamoto, H. *Tetrahedron Lett.* **1989**, *30*, 5607.

16 a) Pálinkó, I.; Ocskó, J. *J. Mol. Catal. A* **1996**, *104*, 261. b) Cabrera, A.; Mathé, F.; Castanet, Y.; Mortreux, A.; Petit, F. *J. Mol. Catal.* **1991**, *64*, L11.

17 a) Dev, S.; Joshi, V.S. *Tetrahedron* **1977**, *33*, 2955. b) Joshi, V.S.; Damodaran, N.P.; Dev, S. *Tetrahedron* **1968**, *24*, 5817. c) Nigam, I.C.; Levi, L. *Can. J. Chem.* **1968**, *46*, 1944.

18 Dev, S. *J. Scient. Ind. Res.* **1972**, *31*, 60.

19 Lemini, C.; Ordoñez, M.; Pérez-Flores, J.; Cruz-Almanza, R. *Synth. Commun.* **1995**, *25*, 2695. b) Bharati Rao, T.; Madhusudana Rao, J. *Synth. Commun.* **1993**, *23*, 1527. d) Paparatto, G.; Gregorio, G. *Tetrahedron Lett.* **1988**, *29*, 1471.

[20] Ruiz-Hitzky, E.; Casal, B. *J. Catal.* **1985**, *92*, 291.
[21] a) Van der Waals, A.C.L.M.; Klunder, A.J.H.; Van Buren, F.R.; Zwanenburg, B. *J. Mol. Catal. A* **1998**, *134*, 179. b) Van der Waals, A.C.L.M *Thesis*, University of Nijmegen, The Netherlands, 1997.
[22] a) Molnár, A.; Bucsi, I.; Bartók, M. *Stud. Surf. Sci. Catal.* **1991**, *25*, 549. b) Molnár, A.; Bucsi, I.; Bartók, M. *J. Catal* **1991**, *129*, 303. c) Arata, K.; Nakamura, H.; Nakamura, Y. *Bull. Chem. Soc. Jpn.* **1994**, *67*, 2351. d) Arata, K, Bledsoe, J.O.; Tanabe, K. *J. Org. Chem.* **1978**, *43*, 1660.
[23] Jayasree, J.; Narayanan, C.S. *Bull. Chem. Soc. Jpn.* **1995**, *68*, 89.
[24] Yadav, G.D.; Satoskar, D.V. *J. Chem. Tech. Biotechnol.* **1997**, *69*, 438.
[25] a) Sheldon, R.A.; Elings, J.A.; Lee, S.K., Lempers, H.E.B.; Downing, R.S. *J. Mol. Catal. A* **1998**, *134*, 129. b) Hölderich, W.F; Goetz, N. in *Zeolite Catalyzed Rearrangements of Epoxides and Glycidic Esters*, Ballmoos, R. *et al* Eds., *Proc. Int. Zeolite Conf. 9th, Montreal 1992*, Butterworth-Heinemann, Boston, 1993, p309. c) Nomura, M.; Fujihara, Y.; Takata, H. *Chem. Express* **1993**, *8*, 693. d) Nomura, M.; Fujihara, Y. *Chem. Express* **1992**, *7*, 121. e) Brunel, D.; Chamoumi, M.; Geneste, P.; Moreau, P. *J. Mol. Catal.* **1993**, *79*, 297.
[26] Verghese, J. Ed. *Terpene Chemistry*, Tata McGraw-Hill, New Delhi, 1982.
[27] Arata, K.; Tanabe, K. *Catal. Rev. Sci. Eng.* **1983**, *25*, 365.
[28] Chapuis, C.; Brauchli, R. *Helv. Chim. Acta* **1992**, *75*, 1527.
[29] Among the industrial suppliers are Fragrance Resources Inc. (CH), Glidco Organics (USA) and Harting SA (Chile). Sources: a) Perfume Material Performance (PMP) Database; b) Allured Flavor & Fragrance Materials Database.
[30] a) PL patent 125694 B2, Derdzinski, D.; Wawrzenczyk, C.; Czeslaw, Z.; Andrzej, G.J. *to* Politechnika Wroclawska, 15 May 1984. b) US patent 4052341, Naipawer, R.E., Easter, W.M. *to* Givaudan Corp., 14 Oct. 1977. c) JP patent 54 125645, Toroko, K.; Kobayashi, T.; Muraki, S.; Tsuruta, H.; Yoshida, T. *to* Takasago Perfumery Co. Ltd., 17 March 1978.
[31] Personal communication by Dr. A.J.A. van der Weerdt (Quest International).
[32] Erman, W.F. 'Chemistry of the Monoterpenes' in *Studies in Organic Chemistry*, Vol. 11, Part B, Marcel Dekker Inc., New York, 1985, p969.
[33] Carr, G.; Dosanjh, G.; Millar, A.P.; Whittaker, D. *J. Chem. Soc., Perkin Trans. 2* **1994**, 1419.
[34] a) Arata, K.; Akutagawa, S.; Tanabe, K. *J. Catal.* **1976**, *41*, 173. b) Arata, K.; Akutagawa, S.; Tanabe, K. *Bull. Chem. Soc. Jpn.* **1975**, *48*, 1097.
[35] Personal communication by Dr. J.G. de Vries (DSM)
[36] Ishii, A.; Jin, Y.N.; Hoshino, M.; Nakayama, J. *Heteroatom Chem.* **1995**, *6*, 161.
[37] Leliveld, B.R.G.; Kerkhoffs, M.J.H.V.; Broersma, F.A.; van Dillen, J.A.J.; Geus, J.W.; Koningsberger, D.C. *J. Chem. Soc., Faraday Trans.* **1998**, *94*, 315.
[38] Some recent examples: a) Ponde, D.E.; Deshpande, V.H.; Bulbule, V.J.; Sudalai, A.; Gajare, A.S. *J. Org. Chem.* **1998**, *63*, 1058. b) Ponde D.; Borate, H.B.; Sudalai, A.; Ravindranathan, T.; Deshpande, V.H. *Tetrahedron Lett.* **1996**, *37*, 4605. c) Li, T.S.; Li, S.H.; Li, H.Z. *J. Chem. Res. (S)* **1997**, 26. d) Choudary, B.M.; Sudha, Y. *Synth. Commun.* **1996**, *26*, 2993.
[39] Some recent examples: a) Gautier, E.C.L.; Graham, A.E.; McKillop, A.; Standen, S.P.; Taylor, R.T.K. *Tetrahedron Lett.* **1997**, *38*, 1881. b) Hirano, M.; Ukawa, K.; Yakabe, S.; Clark, J.H.; Morimoto, T. *Synthesis* **1997**, 858. c) Li, T.S.; Li, S.H. *Synth. Commun.* **1997**, *27*, 2299. d) Varma, R.S.; Saini, R.K. *Tetrahedron Lett.* **1997**, *38*, 2623.
[40] House, H.O. *J. Am. Chem. Soc.* **1955**, *77*, 3070.
[41] Some examples: a) Onaka, M.; Kawai, M.; Izumi, Y. *Chem. Lett.* **1985**, 779. b) Krishna Maiti, A.; Biswas, G.K.; Bhattacharyya, P. *J. Chem. Research (S)* **1993**, 325. c) Cabrera, A.; Rosas, N.; Marquez, C.; Salmon, M.; Angeles, E.; Miranda, R.; Lozano, R. *Gazz. Chim. It.* **1991**, *121*, 127. d) Biswas, G.K.; Bhattacharyya, P. *Synth. Commun.* **1991**, *21*, 569.

[42] Camarena, R.; Cano, A.C.; Delgado, F.; Zuniga, N.; Alvarez, C. *Tetrahedron Lett.* **1993**, *34*, 6857.
[43] Clark, P.D.; Kirk, A.; Kydd, R.A. *Catal. Lett.* **1994**, *25*, 163.
[44] Cornélis, A.; Dony, C.; Laszlo, P.; Nsunda, K.M. *Tetrahedron Lett.* **1991**, *32*, 2903.
[45] Cornélis, A.; Gerstmans, A.; Laszlo, P.; Mathy, A.; Zieba, I. *Catal. Lett.* **1990**, *6*, 103.
[46] Kato, K.; Saino, T.; Nishizawa, R.; Takita, T.; Umezawa, H. *J. Chem. Soc. Perkin Trans 1* **1980**, 1618.
[47] Arnold, D.R.; Lamont, L.J. *Can. J. Chem.* **1989**, *67*, 2119.
[48] Itoh, K.; Nakanishi, S.; Otsuji, Y. *Bull. Chem. Soc. Jpn.* **1991**, *64*, 118.

4 Epoxide Rearrangement Reactions via Catalytic Flash Vacuum Thermolysis using Solid Acids

4.1 Introduction

Isomerization of epoxides into various products is of commercial importance as is reflected in patent literature.[1] Moreover, at least one industrial process (ARCO) is operative[2] in which allyl alcohol is produced via isomerization of propylene oxide. The rearrangement of epoxides (Scheme 4.1) can be achieved photochemically,[3] thermally[4] or with acidic or basic catalysts.[5,6,7] Base-catalyzed isomerization generally leads to allylic alcohols, whereas carbonyl compounds are the main products in the thermal or acid-catalyzed rearrangement of epoxides (see Chapter 3). In complex molecules (e.g. terpene oxides and steroids) also other types of products may be formed due to skeletal rearrangements.

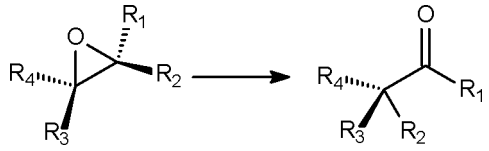

Scheme 4.1 *Rearrangement of epoxides into carbonyl compounds*

Most thermal rearrangement studies of epoxides suggest that diradical intermediates are involved. The pyrolytic rearrangement of norbornene oxide is a typical example.[8] Many products are formed but the suggested major reaction pathways are shown in Scheme 4.2. Substitution has a profound effect on the activation energy and product selectivity of product reactions. For example, a trimethylsilyl group in α,β-epoxy-silanes facilitates rearrangement, while a phenyl substituent has an effect on the direction of the epoxide ring opening. Heterolytic cleavage of the C-O bond is facilitated by strong electron-withdrawing substituents, such as phenyl or cyano groups. Many earlier studies[6c,d] investigated the thermolytic behavior of simple epoxides like norbornene oxide[8], cyclohexene oxide and styrene oxide,[9] and because of their industrial relevance also terpene oxides and steroid epoxides, under static conditions.

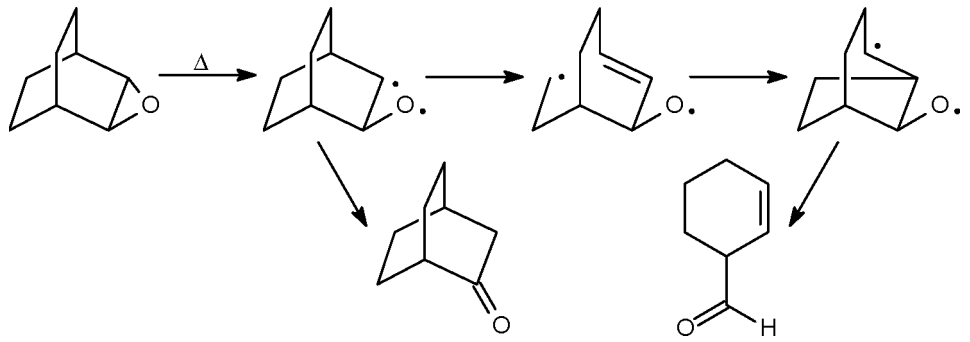

Scheme 4.2 *Suggested reaction pathways in the rearrangement of norbornene oxide under pyrolytic conditions*

Recently, a detailed study[10] has appeared on the gas-phase thermolysis of various alkyl- and aryl-substituted as well as cyclic epoxides. Most of the compounds studied proved to be quite inert up to a reaction temperature of about 600°C. The much higher reactivity of cyclo-octene oxide compared to cyclohexene oxide and cyclopentene oxide was attributed to its higher strain energy.

Van der Waals[11] has combined thermal reactions at reduced pressures (flash vacuum thermolysis) and heterogeneous catalysis into 'catalytic flash vacuum thermolysis'. Using this methodology he studied retro Diels-Alder reactions, isomerizations of α-pinene oxide and stilbene oxides and epoxide dehydratations.[11,12] It turned out that variation of the amount of catalyst and the reaction temperature allowed the tuning of the product selectivity in the reactions of *cis*- **1** and *trans*-stilbene oxides **2**. At low temperatures (100-250°C) diphenylacetaldehyde **3** or deoxybenzoin **4** were obtained as the main reaction products. At an elevated temperature (500°C) and using larger amounts of catalyst diphenylacetylene **5** was produced in high yields (Scheme 4.3). He was able to demonstrate that **5** could also be produced from **3** and **4**, which suggested a common surface-intermediate. Van der Waals has also extensively studied the isomerization of α-pinene oxide **16** because of its commercial importance (cf. Chapter 3). The highest yield of the desired campholenic aldehyde **18** was 45% with amorphous (silica)alumina catalysts. This is no improvement to the current industrial liquid-phase process which yields 87% of campholenic aldehyde.[22]

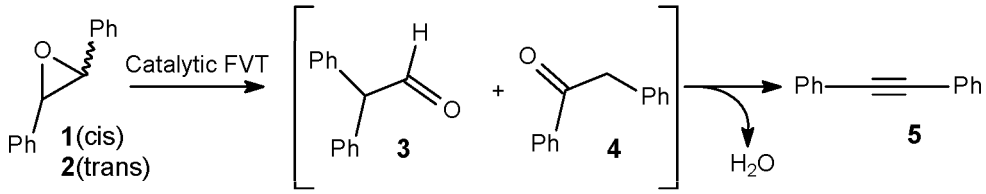

Scheme 4.3 *Isomerization of stilbene oxides* **1** *and* **2** *and dehydration to diphenylacetylene* **5** *under catalytic Flash Vacuum Thermolysis conditions*

Objective and approach

Clay minerals of the smectite type (e.g. bentonite or montmorillonite) are powerful solid acid catalysts for a large variety of organic transformations (cf. Chapter 2). So far, however, these clays have only scarcely been used for the conversion of epoxides to carbonyl compounds. The aim of the study presented in this Chapter is to investigate the rearrangement of epoxides using solid acid catalysts under flash vacuum thermolysis conditions. A study of similar liquid-phase reactions catalyzed by solid acids has been described in Chapter 3. Various natural and synthetic clay materials were tested and, in addition, also amorphous (silica) aluminas have been employed. The activity of the catalysts will be discussed in terms of their acidity and porosity. In addition, the catalytic activities of natural and synthetic clay materials will be compared with each other. The epoxides used in this chapter comprised one aromatically substituted epoxide (viz. styrene oxide **6**), one complex aliphatic epoxide (viz. α-pinene oxide **16**), two simple aliphatic epoxides (viz. cyclohexene oxide **10** and 2-hexyloxirane **13**) and one epoxide having both a phenyl and an ester group (viz. methyl 3-phenyl-2-oxiranecarboxylate **30**). The reactions of styrene oxide **6** and α-pinene oxide **16** to phenylacetaldehyde **7** and campholenic aldehyde **18**, respectively, are important fine chemical transformations. The other epoxides were chosen to study the effect of the various substituents on the solid acid-catalyzed epoxy/carbonyl rearrangement.

4.2 REARRANGEMENT OF EPOXIDES VIA CATALYTIC FVT

Epoxide rearrangement reactions were carried out using the catalytic flash vacuum thermolysis set-up described in the Experimental section. Experiments were performed at 0.05 mbar with 100 mg of a fractured catalyst (150-425 μm), which was pre-treated at 400°C and 0.05 mbar prior to use in order to remove physisorbed water from the catalyst. Epoxides were vaporized at an appropriate temperature (see Experimental section) in about 45 min. Typically, a series of runs was performed using the same catalyst batch while the reaction temperature was varied according to a hysteresis loop, going from 400°C to 150°C and back to 400°C. In this manner a possible deactivation of the catalyst will be detectable by comparing the results of two experiments carried out at the same reaction temperature. Deactivation was visibly observed by blackening of the catalyst after use. Control experiments were performed under identical condition without a catalyst.

4.2.1 Rearrangement of styrene oxide

Styrene oxide **6** was taken as the model substrate, as rearrangement of this epoxide leads to the commercially interesting phenylacetaldehyde **7**. This compound is rather acid labile and usually rapidly trimerizes or polymerizes under homogeneous acidic conditions.

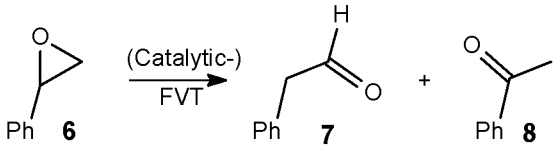

Scheme 4.4 *Isomerization of styrene oxide* **6** *under (Catalytic-) FVT conditions*

The thermal reactivity of styrene oxide **6** was determined in some control experiments (Table 4.1). Styrene oxide **6** proved to be quite stabile as only 29% was converted at 500°C to give phenylacetaldehyde **7**. The conversion approached completion (97%) at a reaction temperature of 700°C (entry 5). The main product was aldehyde **7** but in some cases the selectivity towards this compound was only moderate while also higher molecular weight products were formed.

Table 4.1 *Rearrangement of styrene oxide* **6** *under FVT conditions (without catalyst)*

Entry	Catalyst	Temp.[a] (°C)	Conversion[b] (%)	Selectivity[b] (%)	
				7	8
1	none	200	11	40.7	-
2		400	18	100.0	-
3		500	29	97.9	-
4		600	66	84.8	-
5		700	97	92.6	-

[a] Oven temperature; The substrate was vaporized at room temperature.
[b] Conversions and selectivities determined by GC.

Table 4.2, Table 4.3 and Table 4.4 list the results obtained with natural clays, synthetic clays and amorphous (silica) aluminas as environmentally benign solid acid catalysts in the rearrangement of styrene oxide **6** under catalytic FVT conditions. All these materials proved to be effective catalysts in this transformation as the conversions were considerably higher than in the absence of a catalyst at the selected temperatures (400°C at the highest).

A series of runs was performed using the same catalyst batch while the reaction temperature was varied according to a hysteresis loop, going from 400°C to 150°C and back to 400°C. In the first run with a certain catalyst at the highest temperature (400°C) the conversions were generally very high, reaching in most cases 100%. Only in the case of Zn-stevensite a somewhat lower conversion (92%) was observed. However, when this temperature was used again in the seventh run with the same catalyst batch the conversions were notably lower. This was most striking with synthetic clays as catalysts (Table 4.3), but also other catalysts showed signs of deacti-

vation after several consecutive experiments. A similar effect was noticed by comparing the second and sixth run (300°C) and the third and fifth run (200°C). At these lower reaction temperatures the difference in the conversions was more pronounced than at 400°C. The amorphous alumina B698D-24 and the amorphous silica-alumina HA-SHPV (Table 4.4) were the only two catalysts that gave complete conversions during all seven runs with the same batch of catalyst. Another catalyst that proved to be very active was the natural clay F-1 showing a conversion of 98% at 150°C (entry 11 in Table 4.2). A somewhat lower activity was displayed by the montmorillonite K-10, and the F-25, F-105SF and F-24 clays (Table 4.2) which all gave conversions larger than 50% at this lowest reaction temperature. The lowest conversion values were observed with the Zn-stevensite and the saponites having H^+ as the interlayer cation (Table 4.3).

The selectivity towards the desired phenylacetaldehyde **7** was usually very high and often exceeded 99%. The rearrangement of styrene oxide **6** proceeds with a high selectivity as the direction of the ring opening depends on the relative ease of the heterolytic cleavage of the respective C-O bonds (See Scheme 3.2). Assuming the development of some electrophilicity on both carbons in the three-membered ring after initial protonation or coordination of the acid catalyst with the epoxide oxygen, electron-releasing substituents, like a phenyl group, direct the ring opening towards the most stabilized carbocationic center. After migration of an adjacent hydride to this positive center and release of the product from the surface the catalytic center may be regenerated (cf. Scheme 3.2). Acetophenone **8** is the additional product in the catalytic rearrangement of styrene oxide **6**. The formation of ketone **8** can be explained by generating the electron deficient center at the other carbon of the epoxide ring. From this intermediate two products can be formed: aldehyde **7** after a hydride shift and ketone **8** after a phenyl migration. Since the migratory aptitude of an aryl group is larger than that of a hydride (See Chapter 3), the major product from this last intermediate will be acetophenone **8**. The results listed in Table 4.2, Table 4.3 and Table 4.4 reveal that the selectivity towards **8** is always quite low (max 4%, Table 4.2, entry 46), thus confirming that the phenyl group strongly directs the outcome of the catalyzed rearrangement of **6**.

Table 4.2 *Rearrangement of styrene oxide* **6** *under Catalytic FVT conditions using natural clays*

Entry[d]	Catalyst[a]	Temp.[b] (°C)	Conversion[c] (%)	Selectivity[c] (%)	
				7	8
1	F-1	400	100	95.4	0.5
2		300	100	93.4	0.8
3		200	97	99.3	0.7
4		150	61	98.0	1.6
5		200	66	98.8	1.2
6		300	88	99.2	0.8
7		400	99	99.2	0.8
8	F-13	400	100	94.1	0.6
9		300	100	99.4	0.6
10		200	99	99.5	0.4
11		150	98	99.6	0.4
12		200	97	99.6	0.4
13		300	99	99.3	0.7
14		400	100	99.1	0.9
15	F-105SF	400	100	95.4	0.5
16		300	100	93.4	0.8
17		200	97	99.3	0.7
18		150	61	98.0	1.6
19		200	66	98.8	1.2
20		300	88	99.2	0.8
21		400	99	99.2	0.8
22	F-24	400	100	96.6	0.5
23		300	100	99.4	0.6
24		200	98	99.5	0.5
25		150	58	98.8	1.2
26		200	76	98.7	0.9
27		300	92	97.5	0.7
28		400	99	99.0	0.8
29	F-25	400	100	96.2	0.7
30		300	100	99.0	0.6
31		200	97	99.4	0.5
32		150	66	99.1	0.9
33		200	59	99.0	1.0
34		300	88	99.2	0.8
35		400	97	99.6	0.4
36	Montmorillonite K-10	400	100	97.9	0.7
37		300	100	99.5	0.5
38		200	97	98.6	0.5
39		150	83	99.3	0.6
40		200	77	99.2	0.8
41		300	90	99.4	0.6
42		400	99	99.2	0.7
43	Montmorillonite KSF	400	99	99.3	0.7
44		300	97	99.7	0.3
45		200	83	99.6	0.4
46		150	22	89.7	4.0
47		200	22	95.9	3.2
48		300	62	98.9	1.1
49		400	85	99.1	0.9

[a] 100 mg of catalyst was used and 100 mg of substrate per run. [b] Oven temperature; The substrate was vaporized at room temperature; 0.05 mbar pressure. [c] Conversions and selectivities determined by GC. [d] The best results are marked by shading of the entry number.

Table 4.3 *Rearrangement of styrene oxide* **6** *under Catalytic FVT conditions using synthetic clays*

Entry[d]	Catalyst[a]	Temp.[b] (°C)	Conversion[c] (%)	Selectivity[c] (%)	
				7	8
1	Mg-saponite\ Al^{3+}	400	100	99.9	0.1
2		300	98	99.5	0.5
3		200	79	99.4	0.6
4		150	22	96.8	3.2
5		200	41	100.0	1.5
6		300	79	99.0	0.9
7		400	92	98.9	1.0
8	Zn-saponite\ Al^{3+}	400	100	99.5	0.5
9		300	98	98.7	0.7
10		200	83	99.9	0.1
11		150	14	95.8	4.2
12		200	38	97.4	0.5
13		300	81	99.8	0.2
14		400	96	99.8	0.2
15	Mg-saponite\ H^{+}	400	100	95.0	0.4
16		300	97	97.9	0.4
17		200	65	98.3	0.6
18		150	9	87.6	4.5
19		200	21	90.7	2.0
20		300	64	96.9	0.6
21		400	97	99.3	0.6
22	Zn-saponite\ H^{+}	400	100	99.8	0.2
23		300	98	99.4	0.6
24		200	63	99.2	0.8
25		150	9	97.8	2.2
26		200	15	98.7	1.3
27		300	60	99.7	0.3
28		400	90	99.8	0.2
29	Mg-Stevensite	400	98	99.8	0.2
30		300	80	99.8	0.3
31		200	59	99.8	0.2
32		150	17	99.4	0.6
33		200	20	99.5	0.5
34		300	55	98.7	1.1
35		400	83	99.0	1.0
36	Zn-Stevensite	400	92	99.3	0.5
37		300	60	99.2	0.8
38		200	19	97.9	2.1
39		150	7	100.0	2.9
40		200	13	100.0	1.5
41		300	48	98.7	1.1
42		400	72	99.0	1.0

[a] 100 mg of catalyst was used and 100 mg of substrate per run. [b] Oven temperature; The substrate was vaporized at room temperature; 0.05 mbar pressure. [c] Conversions and selectivities determined by GC. [d] The best results are marked by shading of the entry number.

Table 4.4 *Rearrangement of styrene oxide* **6** *under Catalytic FVT conditions using amorphous (silica) aluminas*

Entry[d]	Catalyst[a]	Temp.[b] (°C)	Conversion[c] (%)	Selectivity[c] (%)	
				7	8
1	B698D-24	400	100	51.3	0.2
2		300	100	86.2	0.4
3		200	100	96.1	0.4
4		150	100	99.7	0.2
5		200	100	99.8	0.1
6		300	100	96.8	0.6
7		400	100	81.9	0.5
8	B698D-25	400	100	89.4	0.8
9		300	98	97.0	0.5
10		200	81	90.4	0.5
11		150	33	96.7	1.2
12		200	48	93.3	0.8
13		300	85	96.1	0.8
14		400	98	97.1	0.7
15	HA-SHPV	400	100	43.8	0.2
16		300	100	85.7	0.4
17		200	100	97.3	0.5
18		150	100	99.1	0.4
19		200	100	99.5	0.4
20		300	100	93.0	0.5
21		400	100	76.4	0.4

[a] 100 mg of catalyst was used and 100 mg of substrate per run. [b] Oven temperature; The substrate was vaporized at room temperature; 0.05 mbar pressure. [c] Conversions and selectivities determined by GC. [d] The best results are marked by shading of the entry number.

In a series of runs with the same catalyst batch, the first run at 400°C generally shows a somewhat lower selectivity for **7**. This is most evident for the application of amorphous (silica) aluminas (Table 4.4) where the selectivity in the first run was only 51, 89 and 44% for B698D-24, B698D-25 and the HA-SHPV, respectively, whereas much higher values were obtained during later runs. Catalytic sites that are only present on the surface of these fresh catalysts may effect the formation of higher molecular weight products during the first run. At subsequent runs the selectivities for **7** were much higher which points to a rapid and irreversible deactivation of these specific catalytic sites. A similar effect on the selectivity for **7** was observed employing natural clay catalysts (Table 4.2). For the amorphous (silica) aluminas also the last runs (at 400°C) show a low(er) selectivity (entries 7 and 21 in Table 4.4), which suggests that at this temperature the deactivating species on these catalytic surfaces may be partly removed.

The highest yields of phenylacetaldehyde **7** at moderate reaction temperatures were obtained using the F-clays, montmorillonite K-10, B698D-24, HA-SHPV and the sapo-

nite clays. With these catalysts very high selectivities (>99%) and (nearly) complete conversions were combined at reaction temperatures of 200 or 300°C.

In order to establish the durability of the catalytic activity of a catalyst, a series of 11 runs (each with 100 mg of **6**) was performed at the same reaction temperature using one catalyst batch (100 mg) for this experiment. Montmorillonite K-10 was used at a reaction temperature of 250°C. The conversions and selectivities obtained are displayed in Figure 4.1. The conversion decreased slowly from 100% in the first run to 88% in the eleventh run. The selectivity for phenylacetaldehyde **7** was only 98.7% in the first run, but subsequent runs displayed selectivities between 99.5 and 99.9%. The lower selectivity during the first run may be ascribed to deactivation of certain catalytic surface sites, as discussed above.

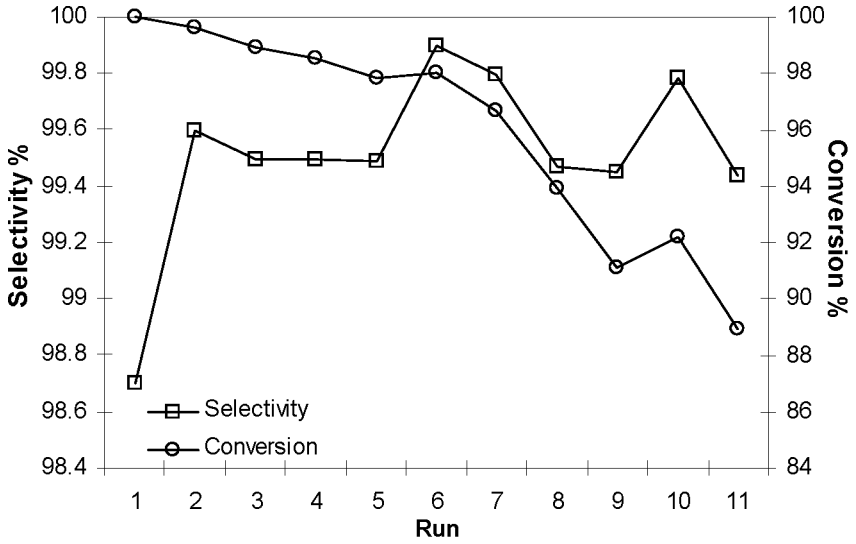

Figure 4.1 *Conversions (%) and selectivities (%) in the isomerization of styrene oxide* **6** *(100 mg) into phenylacetaldehyde* **7** *under catalytic FVT conditions using the same batch of montmorillonite K-10 (100 mg) in a series of 11 runs at a reaction temperature of 250°C.*

These results show that montmorillonite K-10 may be utilized to isomerize styrene oxide **6** into phenylacetaldehyde **7** in a substrate/catalyst ratio that is much higher than unity. Apart from using the same batch of montmorillonite K-10 during 11 runs of 100 mg each, also some catalytic FVT experiments were carried out in which 1.0 or 2.0 g of **6** was passed over a mixture of 100 mg of montmorillonite K-10 and 400 mg of quartz powder. In these experiments conversions of 99 and 90% and selectivities of 99 and 97% were obtained, respectively. A drawback of the experimental set-up used (See Experimental section) is, however, that the flow rate over the catalyst bed is rather limited. Using an evaporation temperature of 80°C, it took 1.5 hours to pass 2.0 g of **6** over the abovementioned catalyst mixture (i.e. 13.3 g/h.g).

The type and amount of acidic sites of the various solid catalysts has been semi-quantitatively determined using infrared analyses of adsorbed pyridine (cf. Chapter 2). These studies showed that montmorillonite K-10, Zn-saponite\H$^+$ and the F-1 clay possess predominantly Lewis acidic character, whereas the amorphous alumina B698D-25 and the F-13 and F-25 natural clays exhibit mainly Brønsted acidity. Other materials studied contain a slight larger number of Lewis acidic sites. The relative acidity was of the same order of magnitude for most of the catalysts. The highest acidity was observed for the amorphous silica-aluminas B698D-25 and HA-SHPV and the synthetic clay Mg-saponite\Al^{3+}. The synthetic clay Mg-saponite\H$^+$ and the F-13 natural clay have a lower acidity than the other solid catalysts studied. Stevensite materials have a considerable lower relative acidity, and it is known[13] that this (low) acidity is mainly of the Lewis type.
These acidic properties are only partly reflected in the results obtained for the rearrangement of **6**. The B698D-25 amorphous silica-alumina has the highest acidity and the highest number of acidic sites, but this material is by no means the most catalytic active one. The highest conversions at a certain reaction temperature were observed for the B698D-24 and HA-SHPV catalysts, followed by the F-clays, montmorillonite K-10, and the saponite clays. HA-SHPV has a relative strong Lewis acidity, but a material with similar acidic properties (Mg-saponite\Al^{3+}) showed a distinctly lower catalytic activity than HA-SHPV. No consistent correlation was found between this order of catalytic activity and of the total acidity of the catalysts (e.g. Lewis or Brønsted acidity).
Some correlation was found for the synthetic clay catalysts, since the clay with the highest total acidity (Mg-saponite\Al^{3+}) also gave the highest conversion at a certain temperature. The order of acidity for the other synthetic clays correlates also rather well (e.g. Zn-saponite\Al^{3+} > Mg-saponite\H$^+$ > Zn-saponite\H$^+$ > stevensites).
In summary, it may be concluded that there is no consistent correlation between the acidic properties of the various classes of catalysts and their catalytic activity. An acceptable correlation was only found for the synthetic clay materials. No such correlation was found for the natural clay catalysts. The high number and strength of acidic sites measured for the amorphous silica-aluminas was only partly reflected in their catalytic activity.

The results do not indicate that the active surface area is an important factor in the rearrangement of **6** to **7**. KSF montmorillonite with a low active surface area (20-40 m^2/g) displayed a comparable catalytic activity as the other natural clay catalysts, all of which have a larger active surface area (> 200 m^2/g). The magnesium clays have a much larger active surface area (411-575 m^2/g) than their zinc-counterparts (244-165

m^2/g), but their catalytic activities were quite similar. The differences in the surface area must therefore be outweighed by other factors effecting the catalytic activity in this epoxy/carbonyl rearrangement under FVT conditions.

When higher reaction temperatures were employed also another product was observed which was identified as phenylacetylene **9**. The results with styrene oxide **6** at higher reaction temperatures using various catalysts are collected in Table 4.5. Using montmorillonite K-10 as the solid acid catalyst only 0.4% of phenylacetylene **9** was found at 600°C, but with the F-105SF clay and the amorphous silica-alumina HA-SHPV **9** was obtained in 1.4 and 3.6%, respectively, at this temperature. Increasing the reaction temperature to 650 and 700°C resulted in a boost of the fraction of **9** to 8.6 and 14.7%, respectively, for the HA-SHPV catalyzed reaction.

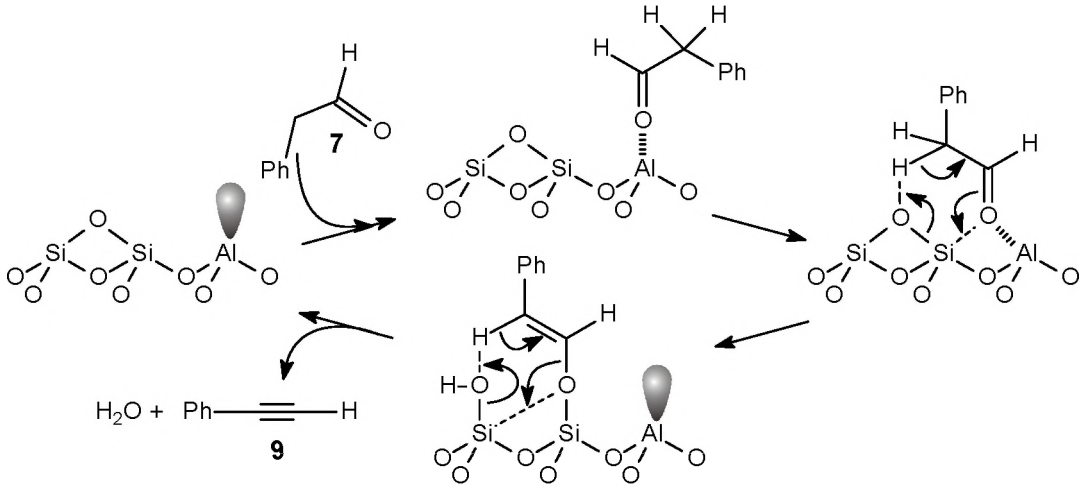

Scheme 4.5 *Dehydration mechanism leading to phenylacetylene 9*

Van der Waals observed a similar dehydration reaction for *cis*- and *trans*-stilbene oxides when subjected to catalytic FVT conditions.[11,12] Depending on the amount of catalyst diphenylacetaldehyde **3** or deoxybenzoin **4** was obtained as the main reaction product at temperatures in the range of 100-250°C. However, at an elevated temperature (500°C) and using larger amounts of catalyst diphenylacetylene **5** was produced in high yields (Scheme 4.3). In addition, it was shown that **5** could also be produced from **3** and **4**, suggesting a common surface-intermediate.[11,12] The involvement of such a common surface-intermediate species was confirmed in the present study. Phenylacetylene **9** was also obtained from phenylacetaldehyde **7** using HA-SHPV as the catalyst. At 600°C the product mixture consisted of 77% unreacted **7** and 4% phenylacetylene **9**; at 650°C these percentages were 74 and 6, respectively. The mechanism explaining the formation of phenylacetylene **9** from phenylacetaldehyde **7** will be analogous to that proposed for the conversion of desoxybenzoin **4** into diphenylacetylene **5** as is depicted in Scheme 4.5.

Table 4.5 *Rearrangement of styrene oxide* **6** *under Catalytic FVT conditions at higher reaction temperatures using various catalysts*

Entry[d]	Catalyst[a,b]	Temp.[c] (°C)	Conversion[d] (%)	Selectivity[d] (%)		
				7	8	9
1	Montmorillonite K-10	400	100	96.8	0.6	-
2		500	100	98.2	0.9	-
3		600	100	97.2	1.1	0.4
4	F-105SF	500	100	91.8	0.7	0.2
5		550	100	95.2	0.8	0.5
6		600	100	92.4	1.4	1.4
7		650	100	91.2	2.3	2.9
8		700	100	85.0	2.0	4.6
9		800	100	52.1	4.3	6.3
10	HA-SHPV	500	100	45.2	-	0.3
11		550	100	67.6	-	1.7
12		600	100	94.2	-	3.6
13		650	100	78.0	-	8.6
14		700	100	74.0	-	14.7

[a] 100 mg of catalyst was used and 100 mg of substrate per run. [b] Catalyst pre-treated at 600°C and 0.05 mbar prior to use. [c] Oven temperature; The substrate was vaporized at room temperature; 0.05 mbar pressure. [d] Conversions and selectivities determined by GC. [d] The best results are marked by shading of the entry number.

In conclusion, phenylacetaldehyde **7** can be prepared in high yields from styrene oxide **6** using various solid acid catalysts under catalytic flash vacuum thermolysis conditions. It was demonstrated for montmorillonite K-10, that it may be used in a substrate/catalyst ratio up to 20 to effectively isomerize **6** into **7**. Using the current experimental set-up, however, a large-scale preparation of **7** from **6** would take considerable time. At moderate temperatures the thermolysis results in phenylacetaldehyde **7** (up to 99.9%) as the main product and a small quantity of acetophenone **8**, but at higher reaction temperatures also some phenylacetylene **9** was observed (up to 15%). The occurrence of a common surface intermediate is highly probable in the formation of these products since **9** could also be obtained starting from **7**.

4.2.2 Rearrangement of cyclohexene oxide

Alicyclic epoxides are more sensitive to rearrangement reactions than acyclic ones due to the extra ring strain. Cyclohexene oxide **10** is a suitable substrate to investigate the influence of ring annulation on the outcome of the reactions under catalytic flash vacuum thermolysis conditions. This substrate **10** may serve as a model compound for the more complex α-pinene oxide **16** (See Section 4.2.4).

Control experiments, applying flash vacuum thermolysis in the absence of catalysts, showed that cyclohexene oxide **10** is quite inert under thermal conditions, as only 9% is converted at 400°C, whereas at 500°C conversions is still rather poor, viz. 30% (Table 4.6). The main products were identified as cyclohexanone **11** and cyclopentanecarbaldehyde **12** (Scheme 4.6).

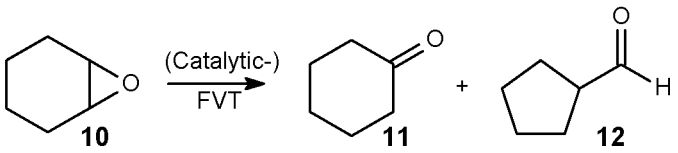

Scheme 4.6 *Rearrangement of cyclohexene oxide* **10** *under (Catalytic-) FVT conditions*

The results obtained using natural clays, synthetic clays and amorphous (silica) aluminas as solid acid catalysts in the rearrangement of cyclohexene oxide **10** under catalytic FVT conditions are listed in Table 4.7, Table 4.8 and Table 4.9, respectively.

A series of runs was performed using the same batch of catalyst while the reaction temperature was varied according to a hysteresis loop, going from 400°C to 150°C. In the first run with a certain catalyst at the highest temperature (400°C) the conversions were usually higher than in the final run (at the same temperature). This was the case for all catalysts, except the F-clays. Such indications of deactivation may also be noticed by comparing the second and sixth runs (300°C). The amorphous silica-alumina HA-SHPV was the only catalyst that gave complete conversion (Table 4.9, entries 15, 16 and 21). Other catalyst materials exhibited a much lower activity, but B698D-25, montmorillonite K-10 and the F-clays nevertheless showed a fair activity. The lowest conversions were observed for montmorillonite KSF and the synthetic clay materials.

Table 4.6 *Rearrangement of cyclohexene oxide* **10** *under thermal FVT conditions*

Entry	Catalyst	Temp.[a] (°C)	Conversion[b] (%)	Selectivity[b] (%)	
				11	12
1	none	200	0.3		
2		300	1		
3		400	9	36	
4		500	30	42	12

[a] Oven temperature; The substrate was vaporized at room temperature; 0.05 mbar pressure. [b] Conversions and selectivities determined by GC.

The selectivity observed for the products **11** and **12** depended strongly on the reaction temperature. At higher temperatures ketone **11** was the major component in the product mixture, whereas at lower temperatures also aldehyde **12** was formed in considerable amounts. This isomerization proceeded in a much lower selectivity than that of styrene oxide **6** (Section 4.2.1). Cyclohexene oxide **10** does not contain a strongly directing group as is present in styrene oxide **6**. The outcome of the rearrangement of cyclohexene oxide **10** is governed by the relative migratory aptitude of a hydride versus an alkyl substituent with a preference for the former (See Chapter 3). This may explain why cyclohexanone **11** is preferably formed from **10**.

Table 4.7 *Rearrangement of cyclohexene oxide* **10** *under Catalytic FVT conditions using natural clays*

Entry[d]	Catalyst[a]	Temp.[b] (°C)	Conversion[c] (%)	Selectivity[c] (%)	
				11	**12**
1	F-1	400	32	81	19
2		300	68	27	35
3		200	16	13	32
4		150	11	14	34
5		200	13	11	29
6		300	35	25	32
7		400	52	56	26
8	F-13	400	69	62	11
9		300	60	35	51
10		200	58	7	26
11		150	19	10	27
12		200	43	7	27
13		300	68	20	39
14		400	62	77	21
15	F-105SF	400	76	63	15
16		300	60	25	38
17		200	27	11	32
18		150	8	12	27
19		200	20	11	31
20		300	35	22	36
21		400	76	57	22
22	F-24	400	54	84	22
23		300	62	27	38
24		200	33	9	31
25		150	7	16	47
26		200	20	10	32
27		300	49	25	35
28		400	56	50	26
29	F-25	400	60	67	15
30		300	66	23	38
31		200	25	10	34
32		150	10	10	26
33		200	18	11	33
34		300	50	20	31
35		400	72	57	21
36	Montmorillonite K-10	400	83	60	23
37		300	51	29	23
38		200	11	15	47
39		150	3	0	45
40		200	9	13	40
41		300	32	25	25
42		400	55	48	14
43	Montmorillonite KSF	400	51	57	22
44		300	18	32	34
45		200	5	16	31
46		150	0	-	-
47		200	3	16	28
48		300	12	33	30
49		400	20	50	23

[a] 100 mg of catalyst was used and 100 mg of substrate per run. [b] Oven temperature; The substrate was vaporized at room temperature; 0.05 mbar pressure. [c] Conversions and selectivities determined by GC. [d] The best results are marked by shading of the entry number.

Table 4.8 *Rearrangement of cyclohexene oxide* **10** *under Catalytic FVT conditions using synthetic clays*

Entry[d]	Catalyst[a]	Temp.[b] (°C)	Conversion[c] (%)	Selectivity[c] (%)	
				11	**12**
1	Mg-saponite\ Al^{3+}	400	70	52	19
2		300	13	38	27
3		200	1	-	-
4		150	1	-	-
5		200	1	-	-
6		300	12	35	21
7		400	40	47	15
8	Zn-saponite\ Al^{3+}	400	62	51	18
9		300	25	37	33
10		200	3	34	55
11		150	1	-	-
12		200	3	30	44
13		300	20	35	30
14		400	41	53	20
15	Mg-saponite\ H^+	400	37	49	23
16		300	5	44	31
17		200	1	-	-
18		150	1	-	-
19		200	3	-	-
20		300	3	45	26
21		400	11	47	23
22	Zn-saponite\ H^+	400	45	44	20
23		300	3	41	29
24		200	1	-	-
25		150	1	-	-
26		200	2	-	-
27		300	3	32	19
28		400	17	46	21
29	Mg-Stevensite	400	21	67	13
30		300	3	55	15
31		200	0	-	-
32		150	0	-	-
33		200	1	-	-
34		300	1	44	22
35		400	6	60	14
36	Zn-Stevensite	400	75	65	10
37		300	16	76	7
38		200	3	65	
39		150	2	14	
40		200	1	-	-
41		300	9	55	19
42		400	28	75	13

[a] 100 mg of catalyst was used and 100 mg of substrate per run. [b] Oven temperature; The substrate was vaporized at room temperature. [c] Conversions and selectivities determined by GC. [d] The best results are marked by shading of the entry number.

Table 4.9 *Rearrangement of cyclohexene oxide* **10** *under Catalytic FVT conditions using amorphous (silica) aluminas*

Entry[d]	Catalyst[a]	Temp.[b] (°C)	Conversion[c] (%)	Selectivity[c] (%)	
				11	**12**
1	B698D-24	400	18	52	5
2		300	65	32	20
3		200	16	23	26
4		150	11	14	9
5		200	25	11	14
6		300	41	33	22
7		400	59	52	22
8	B698D-25	400	89	55	20
9		300	27	33	25
10		200	3	27	40
11		150	15	2	2
12		200	6	9	20
13		300	12	34	30
14		400	47	39	17
15	HA-SHPV	400	100	65	0
16		300	100	70	14
17		200	93	17	33
18		150	39	13	22
19		200	70	14	42
20		300	96	58	26
21		400	100	83	7

[a] 100 mg of catalyst was used and 100 mg of substrate per run. [b] Oven temperature; The substrate was vaporized at room temperature. [c] Conversions and selectivities determined by GC. [d] The best results are marked by shading of the entry number.

The results obtained for the rearrangement of cyclohexene oxide **10** do not reflect the acidic properties of the respective catalysts (cf. Chapter 2 and Section 4.2.1). At a given reaction temperature the highest conversions were observed with HA-SHPV, followed by montmorillonite K-10 and the F clays. The clay that has the strongest acidity (Mg-saponite\Al^{3+}) displayed only moderate activity in the rearrangement of **10** under catalytic FVT conditions. The clay materials that displayed the weakest acidity, the stevensite clays, were not the least active ones. No correlation was observed between the catalytic activity and the total acidity of the catalysts.
As found for the rearrangement of styrene oxide **7**, there is no indication that the active surface area plays a role in this rearrangement of cyclohexene oxide **10**.

4.2.3 Rearrangement of 2-hexyloxirane

The acid-catalyzed rearrangement of aliphatic epoxides usually leads to a wide product distribution without any specific selectivity. A recent review on the use of zeolites as catalysts in the isomerization of aliphatic epoxides pinpoints this poor selectivity.[14] The liquid phase rearrangement of 2-hexyloxirane **13** gives octanal **14** as the main product.[15] Octanal (caprylaldehyde) **14** finds use in artificial citrus oils and

in perfumery as an additive in eau de cologne.[15] In addition, octanal may be useful as precursor for the production of 1-octanol by hydrogenation. In a recent study $ZnCl_2$, H_3PO_4 and dodecatungstophosphoric acid (HPA) on various supports and zeolites were used in the liquid phase rearrangement of 2-hexyloxirane **13** at atmospheric and superatmospheric pressures.[16] A variety of products was obtained which contained octanal **14** in about 50-60% together with several allyl alcohols, depending on the catalyst. The aim of the present study was to investigate whether catalytic FVT using various solid acids would lead to a different product distribution.

FVT control experiments, without catalysts, 2-hexyloxirane **13** to be fairly inert under thermal conditions, as only 2% was converted at 400°C and 25% at 600°C (Table 4.10). The main products were identified as octanal **14**, 2-octanone **15** and 1-octyne **16** (Scheme 4.7).

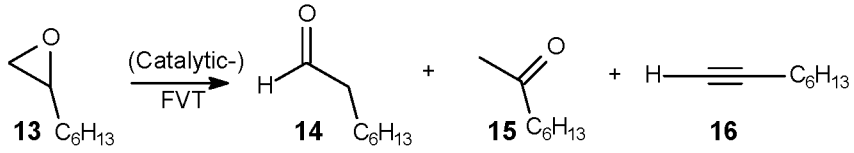

Scheme 4.7 *Reaction of 2-hexyloxirane* **13** *under (Catalytic-) FVT conditions*

In Table 4.11, Table 4.12 and Table 4.13 the data obtained for the rearrangement of 2-hexyloxirane **13** under catalytic FVT conditions using natural clays, synthetic clays and amorphous (silica) aluminas solid acid catalysts are collected.

Table 4.10 *Rearrangement of 2-hexyloxirane* **13** *under FVT conditions (without catalyst)*

Entry	Catalyst	Temp.[a] (°C)	Conversion[b] (%)	Selectivity[b] (%)		
				14	15	16
1	none	200	0			
2		300	0.4	100		
3		400	2	75		8
4		500	12	62	2	2
5		600	25	65	2	4

[a] Oven temperature; The substrate was vaporized at room temperature. [b] Conversions and selectivities determined by GC.

A series of runs was performed using the same batch of catalyst while the reaction temperature was varied according to a hysteresis loop, going from 400°C to 150°C and back to 400°C. In the first run at the highest temperature (400°C) the conversions were usually higher than in the seventh run (at the same temperature). This was the case for all the catalysts. Such indications of deactivation may also be noticed by comparing the second and sixth run (300°C). The amorphous silica-alumina HA-SHPV and the amorphous alumina B698D-24 were the only catalysts that gave a complete conversion (Table 4.13, entries 1, 15, 16 and 21). Other catalysts displayed a much lower activity, but montmorillonite K-10 and the F-clays are reasonably active. The lowest conversions were observed for the stevensites.

Table 4.11 *Rearrangement of 2-hexyloxirane 13 under Catalytic FVT conditions using natural clays*

Entry[d]	Catalyst[a]	Temp.[b] (°C)	Conversion[c] (%)	Selectivity[c] (%)		
				14	**15**	**16**
1	F-1	400	90	55	2	15
2		300	51	51	5	11
3		200	10	62	4	11
4		150	2	82		15
5		200	6	68	5	11
6		300	23	55	3	14
7		400	52	57	3	17
8	F-13	400	99	42	1	9
9		300	86	47	5	12
10		200	34	52	6	10
11		150	8	53	5	7
12		200	22	49	5	8
13		300	64	51	6	15
14		400	85	55	2	14
15	F-105SF	400	98	58	1	11
16		300	88	58	2	5
17		200	42	55	3	9
18		150	13	62	6	4
19		200	21	70	4	7
20		300	64	59	2	11
21		400	88	63	1	16
22	F-24	400	95	50	3	16
23		300	64	52	6	6
24		200	17	48	7	10
25		150	4	59	8	10
26		200	11	43	5	5
27		300	32	55	6	12
28		400	67	62	3	19
29	F-25	400	93	63		13
30		300	64	56	2	10
31		200	15	62	3	9
32		150	4	89		
33		200	7	79		7
34		300	33	64	6	16
35		400	66	62	3	22
36	Montmorillonite K-10	400	92	58	1	18
37		300	65	57	2	10
38		200	17	62	4	7
39		150	3	91	9	
40		200	7	72	4	7
41		300	34	60	2	10
42		400	67	67	1	13
43	Montmorillonite KSF	400	60	72	2	10
44		300	23	80	3	4
45		200	7	100		
46		150	5	100		
47		200	2	100		
48		300	9	80	4	2
49		400	25	73	2	6

[a] 100 mg of catalyst was used and 100 mg of substrate per run. [b] Oven temperature; The substrate was vaporized at room temperature; 0.05 mbar pressure. [c] Conversions and selectivities determined by GC. [d] The best results are marked by shading of the entry number.

Table 4.12 *Rearrangement of 2-hexyloxirane* **13** *under Catalytic FVT conditions using synthetic clays*

Entry[d]	Catalyst[a]	Temp.[b] (°C)	Conversion[c] (%)	Selectivity[c] (%)		
				14	**15**	**16**
1	Mg-saponite\ Al^{3+}	400	83	63		8
2		300	36	51	2	4
3		200	5	60	4	4
4		150	2	55	10	5
5		200	2	74	5	5
6		300	14	60	3	6
7		400	32	60	2	13
8	Zn-saponite\ Al^{3+}	400	55	58	3	15
9		300	14	55	6	8
10		200	1	-	-	
11		150	1	-	-	-
12		200	1	-	-	
13		300	8	63	4	10
14		400	28	59	2	16
15	Mg-saponite\ H^{+}	400	72	53	1	9
16		300	18	52	2	7
17		200	1	-	-	-
18		150	1	-	-	-
19		200	1	-	-	-
20		300	2	78	39	4
21		400	33	61	1	8
22	Zn-saponite\ H^{+}	400	93	23	1	6
23		300	4	60	5	7
24		200	1	-	-	-
25		150	0	-	-	-
26		200	0	-	-	-
27		300	1	-	-	-
28		400	18	60	2	15
29	Mg-Stevensite	400	47	51		19
30		300	10	61		12
31		200	2	72		
32		150	1	-		-
33		200	1	-		-
34		300	3	85		15
35		400	18	59		7
36	Zn-Stevensite	400	14	59	2	7
37		300	2	100		
38		200	1	-	-	-
39		150	1	-	-	-
40		200	1	-	-	-
41		300	1	-	-	-
42		400	5	72		6

[a] 100 mg of catalyst was used and 100 mg of substrate per run. [b] Oven temperature; The substrate was vaporized at room temperature; 0.05 mbar pressure. [c] Conversions and selectivities determined by GC. [d] The best results are marked by shading of the entry number.

The selectivity for the products **14**, **15** and **16** has some correlation with the reaction temperature. Octanal **14**, the main product in most cases, was formed with a selectivity ranging from 14 to 100%, but the typical selectivity for this compound was 50-65% at relatively high temperatures. 2-Octanone **15** was only obtained in very low

quantities and the selectivity for this compound was lowest in the higher temperature range. However, when the selectivity for **14** and **15** was high, the conversion was rather low and accordingly the quantities of these compounds were modest. 1-Octyne **16** was formed in considerable amounts, especially at the high reaction temperatures. At lower temperatures 1-octyne **16** was hardly formed at all. The mechanism of the dehydratation process leading to **16** is similar to that proposed for the formation of phenylacetylene **9** from styrene oxide **6** (Scheme 4.5). It is of interest to note that the formation of a decent amount of acetylene occurred at lower temperature (300-400°C) for 1-octyne **16** than for phenylacetylene **9** (600-700°C). A rationale for this observation cannot be given. Obviously, cyclohexene oxide **10** cannot form an acetylene and consequently, the main products are cyclohexanone **11** and cyclopentanecarbaldehyde **12**. The selectivity observed for the rearrangement of cyclohexene **10** and 2-hexyloxirane **13** is much lower than that of for styrene oxide **6**, which is attributable to the absence of a strongly directing substituent as is present in the latter epoxide.

Table 4.13 *Rearrangement of 2-hexyloxirane* **13** *under Catalytic FVT conditions using amorphous (silica) aluminas*

Entry[d]	Catalyst[a]	Temp.[b] (°C)	Conversion[c] (%)	Selectivity[c] (%)		
				14	**15**	**16**
1	B698D-24	400	100	24		13
2		300	97	47	1	24
3		200	56	61	3	11
4		150	19	65	4	3
5		200	29	65	4	6
6		300	91	56	2	22
7		400	99	52		21
8	B698D-25	400	68	60	3	13
9		300	28	53	6	14
10		200	3	59	3	9
11		150	1	-	-	-
12		200	2	68	11	5
13		300	11	59	5	5
14		400	33	59	3	10
15	HA-SHPV	400	100	14		10
16		300	100	41	1	12
17		200	89	56	5	18
18		150	54	64	5	4
19		200	79	53	4	10
20		300	99	53	5	8
21		400	100	34		8

[a] 100 mg of catalyst was used and 100 mg of substrate per run. [b] Oven temperature; The substrate was vaporized at room temperature; 0.05 mbar pressure. [c] Conversions and selectivities determined by GC. [d] The best results are marked by shading of the entry number.

The application of solid acid catalysts in combination with the flash vacuum thermolysis technique has a distinct influence on the outcome of the reaction in comparison

with liquid phase reactions. In the liquid phase[16] 2-hexyloxirane **13** gives in the presence of various (supported) solid acids at 180°C a mixture of products consisting for 50-60% of 1-octanal **14** and several allylic alcohols. In the present study, it is shown that catalytic FVT leads to a much higher selectivity for 1-octanal **14**. In addition, the dehydratation product 1-octyne **16** is obtained that was completely absent in the liquid phase reactions.

It is relevant to note that there is no correlation between the catalytic activity and the total acidity of the catalysts in the rearrangement of 2-hexyloxirane **13** under catalytic FVT conditions. The same holds for cyclohexene oxide **10**. As with the other substrates there is no indication that the active surface area plays a distinctive role in this rearrangement of **13**.

4.2.4 Rearrangement of α-pinene oxide

Several studies appeared on the rearrangement of α-pinene oxide **17** into campholenic aldehyde **18**, which is widely used as an intermediate in the flavor and fragrance industry (cf. Chapter 3). Scheme 4.8 displays respective pathways to the main reaction products from the isomerization of α-pinene oxide **17**.[17] Coordination of a Lewis acid or protonation by a protic acid facilitates the fission of a C-O bond, yielding the most stable (tertiary) carbocation intermediate **25**. Starting from this intermediate several reactions are conceivable. The acidic site may be released in a concerted process in which a hydride migrates and a carbonyl group is formed giving pinocamphone **22t** (pathway i). In most cases, however, intermediate **25** undergoes subsequent skeletal rearrangements in which first the strain energy of the four-membered ring is released (pathways ii and iii), giving intermediates **26** and **27**. Carbonyl formation then gives the desired campholenic aldehyde **18** or its isomer 2-(2,2,4-trimethyl-3-cyclopentenyl)acetaldehyde **20**.

Table 4.14 *Rearrangement of α-pinene oxide* **16** *under FVT conditions (without catalyst)*

Entry	Temp.[a] (°C)	Conversion[b] (%)	Selectivity[b] (%)							
			18	**19**	**20**	**21**	**22t**	**22c**	**23**	**Others[c]**
1	200	6	34		5	22	22			16
2	300	16	43		3	15	34			5
3	400	85	40	0	3	12	39	2		1
4	500	100	38	1	4	3	36	8	1	6
5	600	100	39	1	7	1	32	10	1	7

[a] Oven temperature; The substrate was vaporized at room temperature; 0.05 mbar pressure. [b] Conversions and selectivities determined by GC. [c] 'others' refers to various unidentified products.

The gas phase stability of α-pinene oxide **17** has been investigated applying the FVT methodology as described in the Experimental section. No catalyst was applied. The results are collected in Table 4.14. Substantial conversion was observed at 300°C and higher, but the selectivity for the desired campholenic aldehyde **18** was only moderate with a maximum of 43% (entry 2). A mixture of products was obtained containing twp other main components, viz. *trans*-pinocamphone **22t** and pinovarveol **21**.

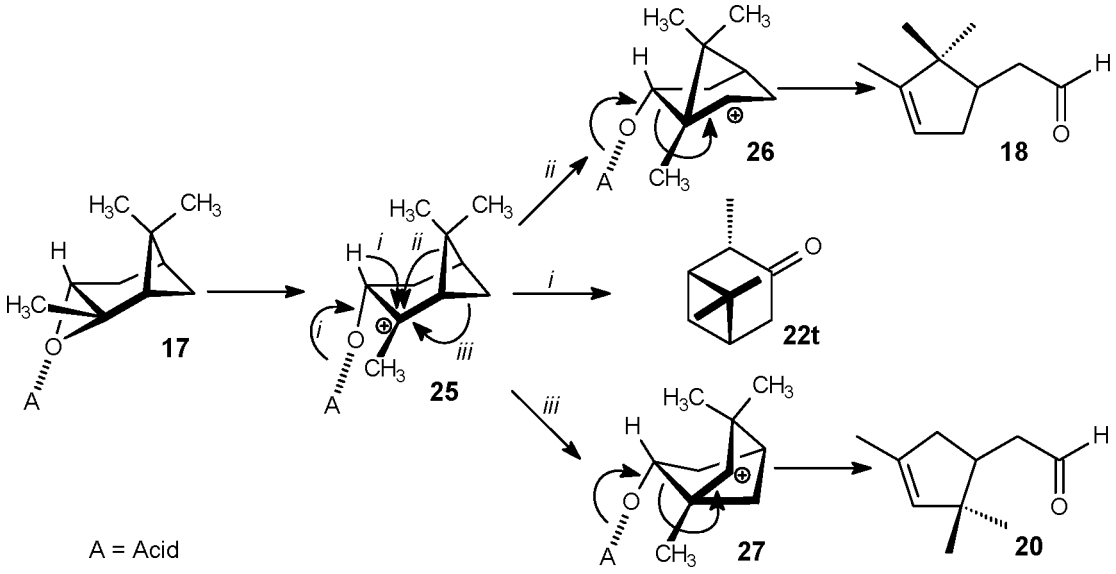

Scheme 4.8 *Main routes in the isomerization of α-pinene oxide* **17**

In the Table 4.15, Table 4.16 and Table 4.17 the results obtained for the catalytic FVT of α-pinene oxide **17** using natural and synthetic clays, and amorphous (silica) aluminas as solid acid catalysts are compiled. For all catalysts the conversions were substantially higher than in the absence of a catalyst.

The conversions were usually satisfactory at all temperatures (150-400°C). Considerable lower conversion at lower temperatures was only observed for some catalysts, viz. the F-1, F-24, F25, montmorillonite KSF, the saponites and the stevensites. For the latter two catalyst the dependence of the conversion on the reaction temperature was most pronounced. A very high conversion throughout the entire temperature hysteresis loop was observed for F-13, F105SF, montmorillonite K-10 and the amorphous (silica) aluminas. However, complete conversions were achieved only when using B698D-24 amorphous alumina (Table 4.17, entries 1, 4 and 5) and the synthetic clay Zn-saponite\H$^+$ (Table 4.16, entry 28).

From the data in the three tables it is evident that besides the three compounds **18**, **20** and **22t**, a number of other products were formed as well. Some of them could be identified. These products include *p*-cymene **19**, pinocarveol **21**, *iso*-pinocamphone **22i**, and exo-isocamphanone **23**. Both acidic and basic sites on a catalytic surface (e.g. bifunctionality) may play an important role in the formation of pinocarveol **21**. In the

mechanism (Scheme 4.9) that explains the formation of **21**, the epoxide oxygen attaches itself to an acidic surface site forming a carbocation upon opening of the epoxide, while an adjacent basic surface site may assist in abstracting and transfer of a proton in the formation of the allylic alcohol **21**.

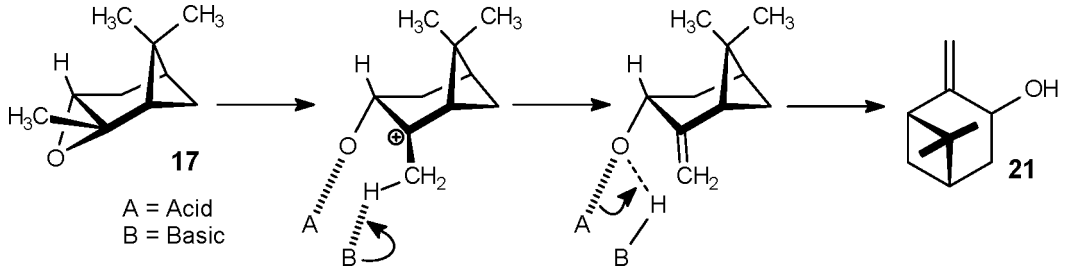

Scheme 4.9 *Mechanism for the formation of pinocarveol* **21** *from α-pinene oxide* **17**

Conceivable mechanisms for the formation of *p*-cymene **19**, carveol **24** and exo-isocamphanone **23** from α-pinene oxide **17** are shown in Scheme 4.10. Coordination of a Lewis or Brønsted surface acidic site to the epoxide oxygen promotes the fission of a C-O bond of α-pinene oxide **17**, yielding again the relatively stable (tertiary) carbocation **25**. This intermediate **25** may, amongst others, rearrange via an alkyl migration to form **28**. Proton elimination from **28** and release of the acidic site then results in the formation of carveol **24** as its *trans*-isomer. The hydroxyl group may, however, epimerize on interaction with acid and water, producing the *cis*-isomer of **24** as well. Water elimination from **24**, followed by a rearrangement is an accepted route[18] to the aromatic compound **19**. Intermediate **26** may lead to campholenic aldehyde **18** (cf. Scheme 4.8) but may also undergo an alkyl shift to the tertiary carbocationic intermediate **29**, which can react to give *exo*-isocamphanone **23** via carbonyl formation and a stereoselective 1,3 hydride shift (Scheme 4.10).

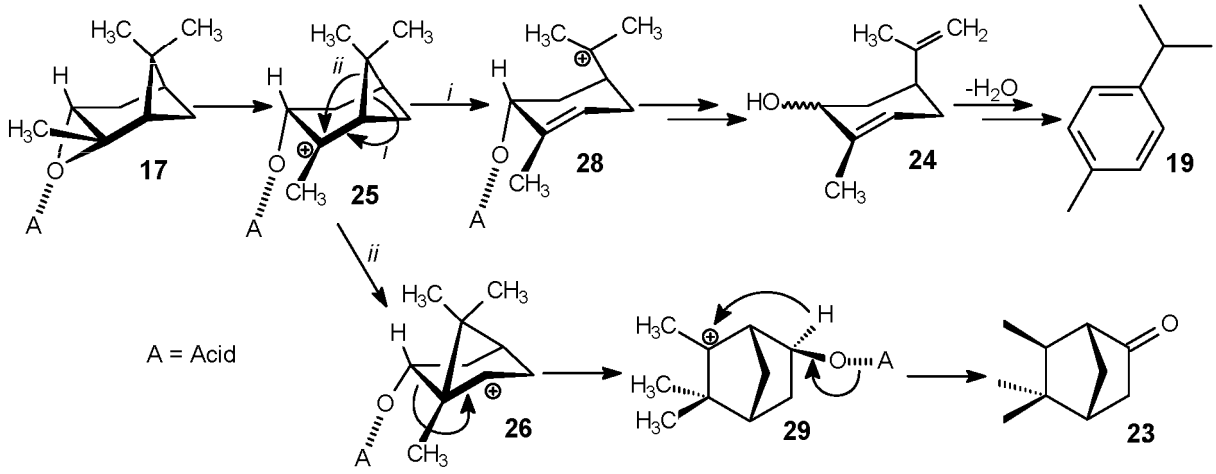

Scheme 4.10 *Mechanisms for the formation p-cymene* **19**, *carveol* **24** *and exo-isocamphanone* **23**

Table 4.15 *Rearrangement of α-pinene oxide* **17** *under Catalytic FVT conditions using natural clays*

Entry[e]	Catalyst[a]	Temp.[b] (°C)	Conversion[c] (%)	Selectivity[c] (%)							
				18	19	20	21	22t	22i	23	Others[d]
1	F-1	400	95	17	19	4		21	5	12	22
2		300	91	31	17	7		23	4	7	10
3		200	84	44	11	12	1	19	2	1	9
4		150	66	19	4	7	1	6	1		63
5		200	61	42	9	16	2	15	1	2	13
6		300	89	41	10	9	1	24	3	3	8
7		400	96	29	13	6	1	27	5	9	11
8	F-13	400	98	5	34	2		15	1	8	35
9		300	86	15	25	4		19	5	18	16
10		200	85	36	15	7		22		5	15
11		150	94	48	14	10		17	2	1	8
12		200	92	44	14	9		21	3	2	7
13		300	89	23	18	5		22	6	15	11
14		400	93	12	27	3		18	4	15	22
15	F-105SF	400	95	8	31	3		17	3	11	29
16		300	86	20	22	4		22	6	14	12
17		200	86	37	17	9		22	3	3	9
18		150	94	45	17	13		15	2		8
19		200	93	45	14	11		20	3	2	6
20		300	92	31	14	6		24	6	11	8
21		400	94	18	20	4		23	6	17	12
22	F-24	400	94	17	26	5		25	6	16	7
23		300	89	30	17	6		25	6	10	6
24		200	90	48	12	8		25		3	4
25		150	71	43	12	13		14	3		15
26		200	81	47	9	10		21	2	1	9
27		300	93	40	11	7		27	4	6	5
28		400	96	26	14	5		26	6	14	8
29	F-25	400	94	14	25	4		24	5	16	12
30		300	89	28	14	5		26	6	13	8
31		200	91	46	12	8		23	3	3	6
32		150	75	45	12	13		15	3		12
33		200	80	52	11	13		21			2
34		300	94	39	12	7		26	4	6	5
35		400	96	26	16	5		28	7	15	3
36	Montmo-	400	95	14	25	3		21	4	14	19
37	rillonite K-10	300	89	25	19	6		22	5	12	12
38		200	93	40	14	12		20	2	2	9
39		150	91	42	12	18	1	15	2	1	9
40		200	92	44	12	15	1	19	1	1	7
41		300	94	41	13	9		27	3	5	2
42		400	96	28	12	6		28	7	13	7
43	Montmo-	400	98	31	8	6		31	5	11	9
44	rillonite KSF	300	98	46	5	8		31	2	2	5
45		200	86	47	6	15	1	23	1		6
46		150	47	44	4	15	2	21	2		11
47		200	63	47	4	14	2	25	2		7
48		300	90	47	3	8	1	33	2		5
49		400	99	41	2	6	1	36	5	4	6

[a] 100 mg of catalyst and 100 mg of substrate per run. [b] Oven temperature; The substrate was vaporized at room temperature; 0.05 mbar pressure. [c] Conversions and selectivities determined by GC. [d] 'others' refers to various unidentified products. [e] The best results are marked by shading of the entry number.

Table 4.16 *Rearrangement of α-pinene oxide* **17** *under Catalytic FVT conditions using synthetic clays*

Entry[e]	Catalyst[a]	Temp.[b] (°C)	Conversion[c] (%)	Selectivity[c] (%)								
				18	**19**	**20**	**21**	**22t**	**22i**	**23**	**24[d]**	**Others[e]**
1	Mg-sapo-	400	93	14	28	4		21	5	12		13
2	nite\ Al^{3+}	300	95	20	29	15		15	3	6		9
3		200	98	24	19	31	2	12	2	2		8
4		150	65	26	11	34	5	11			7	6
5		200	68	27	6	30	6	15	1		9	4
6		300	96	28	14	20	2	18	3	2	3	8
7		400	97	27	19	9		27	5	7		5
8	Zn-sapo-	400	97	24	12	5		28	7	11		11
9	nite\ Al^{3+}	300	97	34	16	11		24		4		6
10		200	95	35	16	25		16			1	42
11		150	48	41	4	18	3	21			10	4
12		200	67	42	4	19	3	25			5	3
13		300	94	40	8	12	1	29	2	1	1	5
14		400	98	33	6	6		35	8	7		3
15	Mg-sapo-	400	89	13	28	4		24	7	7		14
16	nite\ H^{+}	300	92	15	36	14		13	3	4		14
17		200	98	21	22	33	2	10	1		1	10
18		150	34	24	10	37	6	10			9	4
19		200	55	23	7	35	6	12			10	7
20		300	97	23	21	24	2	14	3	1	1	10
21		400	96	23	22	10		25	6	5		8
22	Zn-sapo-	400	98	34	7	5		39	7	5		2
23	nite\ H^{+}	300	96	30	27	18		19				7
24		200	95	26	17	32	2	10	2		3	9
25		150	14	25	6	25	5	9			25	5
26		200	43	27	5	31	4	13			16	4
27		300	91	31	10	19	2	22	2		4	9
28		400	100	34	4	6	2	43	5	3		2
29	Mg-Steven-	400	91	38	1	4	6	38	6		1	7
30	site	300	42	35		4	6	41	3		1	8
31		200	14	30		4	10	31	3			21
32		150	7	26	1	3	14	25	3			28
33		200	16	26	1	6	8	16	2		5	36
34		300	27	34	1	4	10	41	3		1	6
35		400	68	35	1	4	7	45	3		1	4
36	Zn-Steven-	400	98	41	2	5	3	40	8			2
37	site	300	67	40	1	5	4	44	3			3
38		200	24	47		6	5	43				
39		150	15	48		5	5	36				6
40		200	16	46		5	5	40				4
41		300	39	38		5	7	51				
42		400	84	36	1	5	5	43	5	1	2	1

[a] 100 mg of catalyst was used and 100 mg of substrate per run. [b] Oven temperature; The substrate was vaporized at room temperature; 0.05 mbar pressure. [c] Conversions and selectivities determined by GC. [d] *Cis* and *trans* isomers of **24** [e] 'others' refers to various unidentified products. [e] The best results are marked by shading of the entry number.

The selectivity for the desired campholenic aldehyde **18** ranged from 8 to 60%. In general, the selectivity for **18** was poor at high reaction temperatures, but much higher at lower temperatures. This was observed for all the catalysts, but was most pronounced for the amorphous (silica) aluminas. With these catalysts the selectivity

for **18** was very poor at 400°C, but relatively high at the lowest temperature (150°C). In fact, the selectivity achieved under these conditions was the highest observed in the present study. It should be noted that for these catalysts the conversion remained high at this low reaction temperature, which implies that the yields of **18** are also the highest, namely 52-60% (Table 4.17, entries 4, 11 and 18). With saponites having aluminum as their interlayer cation and natural clays a similar correlation between the reaction temperature and the selectivity for **18** was observed, i.e. higher selectivities for **18** at lower temperatures.

Table 4.17 *Rearrangement of α-pinene oxide* **17** *under Catalytic FVT conditions using amorphous (silica) aluminas*

Entry[e]	Catalyst[a]	Temp.[b] (°C)	Conversion[c] (%)	Selectivity[c] (%)							
				18	**19**	**20**	**21**	**22t**	**22i**	**23**	**Others[d]**
1	B698D-24	400	100	12	46			17		3	23
2		300	95	8	22			9		30	31
3		200	95	24	8	3		26	7	25	5
4		150	100	60	3	4		27	3	2	1
5		200	100	46	4	4		27	6	9	3
6		300	96	15	15	3	2	20	6	32	4
7		400	95	6	34	3	3	15	2	11	27
8	B698D-25	400	96	5	36	1	2	14	2	7	32
9		300	91	21	22	4		19	5	14	12
10		200	94	40	11	6		23	5	5	7
11		150	95	53	6	8		25	3	1	3
12		200	95	46	8	7		26	4	3	5
13		300	93	28	15	5		23	6	14	6
14		400	94	15	29	4		20	5	15	12
15	HA-SHPV	400	97	13	42	2		17		6	19
16		300	96	10	21	2		15	4	29	16
17		200	96	37	8	4		25	6	15	5
18		150	99	54	4	4		26	4	4	4
19		200	98	42	6	4		27	6	12	3
20		300	96	16	15	2	3	18	5	29	9
21		400	96	6	31	2	3	15		12	29

[a] 100 mg of catalyst was used and 100 mg of substrate per run. [b] Oven temperature; The substrate was vaporized at room temperature; 0.05 mbar pressure. [c] Conversions and selectivities determined by GC. [d] 'others' refers to various unidentified products. [e] The best results are marked by shading of the entry number.

The isomer of **18**, 2-(2,2,4-trimethyl-3-cyclopentenyl)acetaldehyde **20**, is another main product (Scheme 4.8) and its formation is similarly dependent on the temperature as observed for **18**. The selectivity for **20** ranged from 0 to 37%. With amorphous (silica) aluminas only minute amounts of **20** were obtained at a maximum selectivity of 8% (Table 4.17). On the other hand, relative large quantities of **20** were produced using the saponites, where a maximum selectivity of 37% was reached (entry 18 in Table 4.16).

A third major product is *trans*-pinocamphone **22t** (Scheme 4.8), which was formed generally at higher reaction temperatures. The selectivities for **22t** ranged from 6 to

51%, with the highest values for the stevensites, Zn-saponite\H^+ and montmorillonite KSF at 300-400°C. These catalysts gave relatively poor conversions of α-pinene oxide **17** at low reaction temperatures, which points to a poorer catalytic activity. At all temperatures *iso*-pinocamphone **22i** was also found in minor amounts. Compound **22i** cannot be produced directly from carbocationic intermediate **25** but may be formed via epimerization of **22t**. This is quite likely since carbonyl compounds are susceptible to enolization on solid acidic and basic surfaces,[19] which in the case of **22** would imply the epimerization of the methyl group.

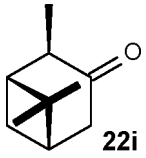

22i

p-Cymene **19** was produced from α-pinene oxide **17** in moderate quantities practically in all cases except when the two stevensite clays were applied. A maximum selectivity for **19** was observed using the B698D-24 and HA-SHPV, viz. 46% (Table 4.17, entry 1) and 42% (Table 4.17, entry 15), respectively. The selectivity for **19** showed a partial correlation with the reaction temperature. During the first two runs (at 400 and 300°C) a relative large amount of **19** was obtained, but at the end of the temperature hysteresis loop the amounts were notably lower at identical reaction temperatures. This was observed most clearly for the F-105SF, F-24, F-25, montmorillonite K-10 and Zn-saponite\Al^{3+} catalysts. This suggests that at higher temperatures the complex isomerization pathway to **19** becomes more competitive, but also that in later runs this pathway is partly obstructed. Apparently, some of the catalyst active surface sites responsible for the formation of **19** become deactivated during the process.

Pinocarveol **21** was only observed in a few cases and in low amounts. In fact, noticeable quantities were only obtained when one of the saponites was used. Carveol **24** was found in small amounts using the saponites and Zn-stevensite as solid catalysts.

Exo-isocamphanone **23** was another by-product that could be identified. It was formed at higher reaction temperatures only and the highest selectivities for this by-product were observed using the B698D-24 and HA-SHPV catalysts. With these two catalysts the reaction temperature has a great influence on product selectivity. At 400°C the main product is *p*-cymene **19**, by lowering the temperature to 300°C the main component of the product mixture is *exo*-isocamphanone **23** and at 150°C the selectivity for campholenic aldehyde **18** is at its maximum.

The results for the rearrangement of α-pinene oxide **17** do not indicate a correlation between the catalytic activity and the total acidity of the catalysts under catalytic FVT conditions. This corresponds to the thermal behavior of cyclohexene oxide **10** and 2-hexyloxiran **13** applying the FVT methodology.
In the case of α-pinene oxide **17** the active surface area seems to have some influence on the rearrangement. The synthetic Mg-saponites have a much larger active surface area (411-575 m^2/g) than their zinc-counterparts (244-165 m^2/g) (cf. Chapter 2). The Mg-catalysts show generally higher conversions than the Zn-catalysts. This may be accounted for by the difference in their acidic properties but their different surface areas may also be a factor. Similarly, the natural clay montmorillonite KSF with a very low active surface area (20-40 m^2/g) gave considerably lower conversions than observed using other natural clays with larger surface areas.

4.2.5 Rearrangement of methyl 3-phenyl-2-oxiranecarboxylate

The epoxides studied in the preceding sections only have either aromatic or aliphatic substituents. This implies that coordination with the acidic catalyst will primarily take place with the epoxide oxygen atom. It is of interest to investigate functionalized epoxides in which a competing coordinating site for the catalyst is present. For this purpose, an ester unit was chosen to functionalize the epoxide, as present in substrate **30**. It is worth noting that the rearranged product, viz. methyl 2-oxo-3-phenylpropanoate **31**, has industrial relevance for the preparation of phenylalanine[20].

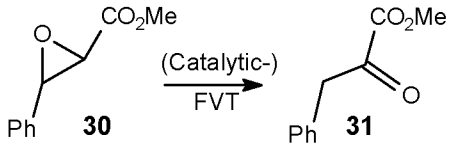

Scheme 4.11 *Rearrangement of* **30** *under (Catalytic-) FVT conditions*

The results obtained for the rearrangement reactions of methyl 3-phenyl-2-oxirane-carboxylate **30** using catalytic FVT are represented in Figure 4.2. The thermal reactivity of **30** was marginal, as at 400°C a conversion of only 0.5% was observed. Methyl 2-oxo-3-phenylpropanoate **31** was identified as the only product. At lower reaction temperatures (e.g. 200-300°C) only starting material was recovered.
When solid acid catalysts were applied much higher conversions were achieved ranging from 0 to 100%, whereby product **31** was essentially the only product. The selectivity for **31** was always at least 98%, in most cases 100%. Two natural clays, two synthetic clays and one amorphous silica-alumina were applied as catalysts. The highest activity was observed for the natural clays F-105SF and montmorillonite K-10, while almost no conversion was noticed for Mg-stevensite. The HA-SHPV gave a very high conversion of 95% during the first run at 400°C but considerably lower

values were obtained during consecutive runs. At 300°C (second run) only 45% and 25% (fourth run) of **30** had reacted and in the last run at 400°C, 70% of **30** was recovered. A similar trend can be seen for Mg-saponite\ Al^{3+} (Figure 4.2). The conversions obtained in later runs at identical temperatures were in most cases considerably lower (Figure 4.2), which indicates a significant deactivation of the catalytic surface sites of the catalysts. This deactivation effect was most pronounced with the HA-SHPV and and Mg-saponite\ Al^{3+}.

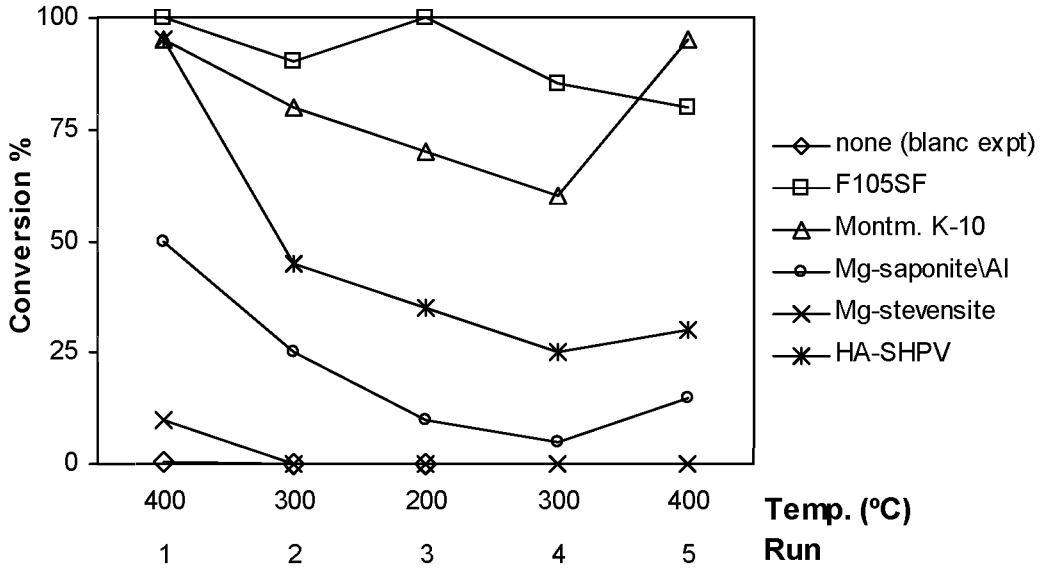

Figure 4.2 *Conversions (%) as a function of the reaction temperature and the run number in the rearrangement reactions of* **24** *under Catalytic FVT conditions using various solid acid catalysts*

In conclusion, methyl 3-phenyl-2-oxiranecarboxylate **30** can conveniently be isomerized into methyl 2-oxo-3-phenylpropanoate **31** using various solid acid catalysts under catalytic FVT conditions. The trends observed for these conversions are quite similar to those observed for the epoxides with only aromatic or aliphatic substituents. The selectivity for **31** was always very high. However, there is considerable deactivation of the catalyst in most cases. Thus, it may be concluded that the presence of another electronegative group in the epoxide substrate does not impede the epoxy/carbonyl rearrangement reaction when solid acid catalysts are used under flash vacuum thermolysis conditions.

4.3 CONCLUSIONS

The isomerization of epoxides using solid acid catalysts was investigated under flash vacuum thermolysis conditions. Various natural and synthetic clays, and some amorphous (silica) aluminas were tested.

Styrene oxide **6** gave the rather labile phenylacetaldehyde **7** as its major product upon rearrangement. The highest catalytic activity was observed for B698D-24, HA-

SHPV, followed by the F-clays and montmorillonite K-10. The selectivity for **7** was very high, typically between 97 and 99.5%. Acetophenone **8** was a by-product usually formed with a selectivity below 1.5%. At more elevated reaction temperatures also some phenylacetylene **9** was produced via a dehydration mechanism. For montmorillonite K-10 it was shown that the rearrangement can be used to prepare phenylacetaldehyde **7** in a substrate/catalyst ratio of up to 20.
Catalytic FVT of cyclohexene oxide **10** resulted in two main products, viz. cyclohexanone **11** and cyclopentanecarbaldehyde **12**. The ketone was formed especially at high reaction temperatures whereas at lower temperatures also considerable amounts of the aldehyde were produced. The best conversions at a suitable temperature were obtained using HA-SHPV, followed by montmorillonite K-10 and the F-clays.
Rearrangement of 2-hexyloxirane **13** afforded three products: octanal **14**, 2-octanone **15** and 1-octyne **16** of which the aldehyde and the acetylene were formed in the largest amounts. The selectivities are dependent on the reaction temperature. Aldehyde **14** was formed with the highest selectivity at low temperatures while the best selectivities for **16** were observed at high temperatures. The best catalysts were B698D-24, HA-SHPV, followed by the F-clays and montmorillonite K-10.
Rearrangement of the sensitive α-pinene oxide **17** resulted in a broad spectrum of products. Campholenic aldehyde **18** was the principal product, for which a maximum selectivity of 60% was attained using the B698D-24 amorphous alumina at 150°C. The selectivity for **18** usually reached a maximum at the lowest possible reaction temperature. Very high conversions were obtained for most of the catalysts, the best ones being B698D-24, HA-SHPV, B698D-25, the F-clays, montmorillonite K-10 and Mg-saponite\ Al^{3+}.
Methyl 3-phenyl-2-oxiranecarboxylate **30** was smoothly isomerized into methyl 2-oxo-3-phenylpropanoate **31** with a very high selectivity. Apparently, the presence of an electronegative function in the epoxide does not impede the epoxide rearrangement reaction using solid acid catalysts. Unfortunately, considerable deactivation of the catalysts was observed in several cases.

Overviewing the results of the catalytic FVT experiments with all epoxides studied, it may be concluded that the highest conversions at the most suitable reaction temperature are obtained for B698D-24 and HA-SHPV followed by the F-clays, montmorillonite K-10, and the saponite clays as the solid acid catalysts.

The nature and number of acidic sites of the various solid catalysts has been semi-quantitatively determined using infrared analyses of adsorbed pyridine (cf. Chapter

2). However, no consistent correlation was found between the catalytic activity and the acidity of the catalysts.

In general, the active surface area does not play a major role in the performance of the catalysts; an exception may be the rearrangement of α-pinene oxide **17**, where there seems to be an effect of the surface area.

Industrial perspective

Two transformations were studied that are of interest in fine chemical industry, namely the isomerization of styrene oxide **6** into phenylacetaldehyde **7** and of α-pinene oxide **17** into campholenic aldehyde **18**.

Phenylacetaldehyde **7** could be prepared from styrene oxide **6** in very high yields (99%) using various solid acid catalysts at moderate reaction temperatures. Experiments with montmorillonite K-10 as the catalyst showed that the present method can be utilized to prepare product **7** in a substrate/catalyst ratio of up to 20. The yield and purity of **7** obtained here is much higher (99%) than in the commercial process, which involves the oxidation of the corresponding alcohol. The labile nature of the product under these homogeneous oxidative conditions limits the maximum purity to 85%.[21]

Campholenic aldehyde **18** was the major product from the isomerization of α-pinene oxide **17**. The highest yield observed was 60% using B698D-24 as the catalyst. In the current commercial homogeneous process ($ZnCl_2$ in benzene) aldehyde **18** is produced in a much higher yield (85%[22]) than here, but the formation of considerable amounts of waste products (i.e. salts) is a considerable drawback here.

Benefits of the flash vacuum thermolysis technique in combination with solid acid catalysts as used in the two transformations mentioned above are the high yield and selectivity for phenylacetaldehyde **7**, and no additional reagents are needed. These aspects improve the ease and safety of operations. Moreover, with the methodology described here no waste salts are produced.

Flash Vacuum Thermolysis, however, is not a technique that is hitherto implemented anywhere on a larger than laboratory-scale. However, when products are considered with a high added value and by taking into account that the desired compounds can be obtained with very high purity, that no solvents are used and that waste, such as salts, are minimal, a thorough study aimed at the implementation of the Flash Vacuum Thermolysis technique in combination with solid acids on an industrial base is certainly worthwhile. It should be added, however, that in many cases high vacuum is probably not needed to achieve selective thermal transformations. If true, this would considerably reduce the cost of an industrial set-up, as this would involve

a gas flow system applying a fixed bed reactor. In Chapter 5 it is investigated whether the reactions of epoxides studied with the catalytic FVT technique, can be conducted under normal pressure and flow conditions. As a model for such a continuous flow reactor type, a 'micropuls reactor unit' was used, in which a solid catalyst is mounted in a fixed bed in the flow system.

4.4 EXPERIMENTAL SECTION

General remarks

Reported percentages are molar percentages (% $^{m}/_{m}$). Gas chromatographic (GC) analyses were performed on a Hewlett-Packard HP5890II gas chromatograph (flame ionization detector, FID) equipped with an HP-3396II integrator, using a capillary column (HP-1, 25 m x 0.31 mm x 0.17 µm) and nitrogen at 2 ml/min (0.5 atm) as the carrier gas or on a Hewlett-Packard HP6890 gas chromatograph (flame ionization detector, FID) equipped with an HP-6890 integrator, using a capillary column (HP-1, 25 m x 0.32 mm x 0.17 µm) and hydrogen at 3.2 ml/min (0.53 atm) as the carrier gas. The GC temperature programs employed were either from 75°C (5 min isothermal) to 250°C at 15°C/min followed by 3 min at 250°C (isothermal) or from 100°C to 250°C at 15°C/min followed by 10 min at 250°C (isothermal). FT-IR spectra were recorded on a Biorad FTS-25 spectrophotometer. ^{1}H- and ^{13}C-NMR spectra were recorded on a Bruker AM-400 and a Bruker AC-100 at T=298 K. Chemical shifts were reported against $Si(CH_3)_4$. Mass spectrometric (MS) analyses were measured with a double focussing VG Analytical 7070E mass spectrometer or a Varian Saturn II GC-MS set-up equipped with an HP-1 capillary column and Varian 8100 autosampler.

Column chromatography at ambient pressure was carried out using Merck Kieselgel 60. Thin layer chromatography (TLC) was carried out on Merck precoated silicagel 60 F254 plates (0.25 mm) using the eluents indicated. Spots were visualized with UV or molybdate spray. Dichloromethane was distilled from calciumhydride. Commercially available starting materials were used as received.

Origin of the catalysts

Amorphous alumina B698D-24, amorphous silica-alumina B698D-25 and the acid-treated natural F-clays were received as generous gifts from Engelhard De Meern B.V. Amorphous silica-alumina HA-SHPV was obtained as a generous gift from AKZO Nobel Chemicals. Commercial natural clays montmorillonite K-10 and montmorillonite KSF are produced by Süd Chemie and were obtained via Aldrich Chemical Company. Prior to use montmorillonite K-10 was washed in hot demineralized water and subsequently dried to remove any residual mineral acid that may have been present due to the acid-treatment during its preparation. Synthetic clay materials were prepared and donated by the Department of Inorganic Chemistry and Heterogeneous Catalysis of the University of Utrecht. All saponites used had a Si/Al ratio of 7.9 and are described as M-saponite\C^{+}, where M represents the octahedral cation and C^{+} the interlayer cation.

All catalysts were pressed (3 tons), sieved into the desired particle size (150-425 μm), and stored at ambient pressure. Catalysts were used after a pre-treatment: An amount of catalyst was placed on a quartz porous filter in the middle of a quartz (FVT-)tube. Using the catalytic Flash Vacuum Thermolysis set-up (*vide infra*) the catalyst was equilibrated at a temperature of 400°C and a vacuum of 0.05 mbar during 15-20 min to remove physisorbed water.

Catalytic Flash Vacuum Thermolysis set-up

The Catalytic Flash Vacuum Thermolysis apparatus, as developed at the Department of Organic Chemistry of the University of Nijmegen, is schematically depicted in Figure 4.3.
The pyrex bulb contains the substrate and may be heated with a sublimation oven (Buchi TO 50) to bring the substrate into the gas phase. All connections are Rotulex cups and balls. The pressure in the system is controlled by means of needle valves near the manometer and the sample flask. The sample flask is connected to the quartz oven tube with an internal diameter of 16 mm, a length of 18 cm and a quartz filter in the middle of the tube. A solid acid can be placed upon this filter. In this way a fixed bed type reactor can be obtained with the added feature of reduced pressure in the system. A tubing connection between the substrate flask and the vacuum pump proved to be a prerequisite in order to prevent the catalyst particles from being blown out of the tube when the system is evacuated. Once the desired pressure in the system is achieved the valve on the substrate flask is closed making this temporary connection irrelevant to the actual experiment. The oven tube is heated by a Heraeus BR 1.6/18 oven equipped with a Heraeus RK 42 control unit. Connected at the other side of the receiving cooler are the manometer to measure the pressure and a double cold trap system to protect the vacuum pump (Edwards, E2M8).

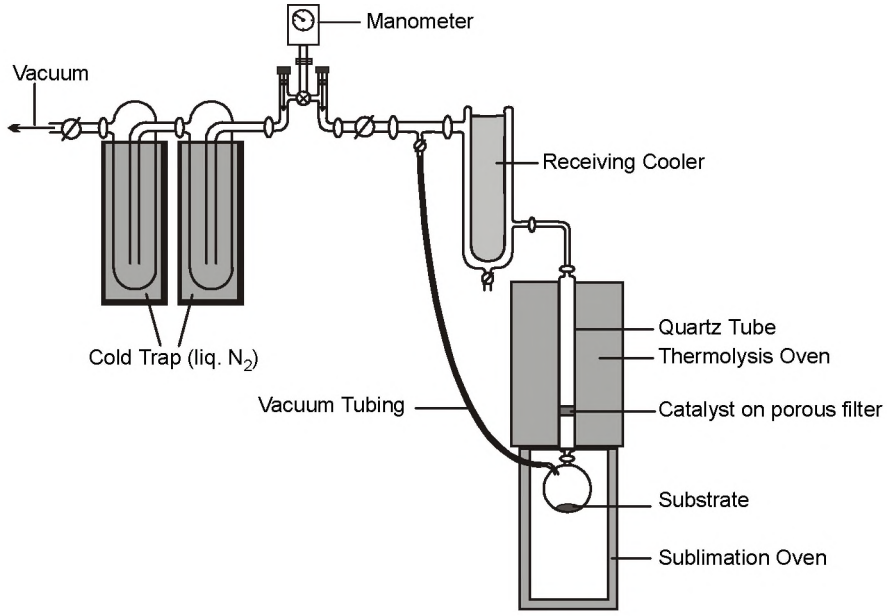

Figure 4.3 *Schematic representation of the Catalytic Flash Vacuum Thermolysis set-up*

General procedure for catalytic flash vacuum thermolysis experiments

The Catalytic Flash Vacuum Thermolysis set-up described above was used. Typically, 100 mg of a fractured catalyst with a sieve fraction of 150-425 μm was placed on a porous filter in

the center of the quartz tube. The catalyst was equilibrated at a temperature of 400°C and a vacuum of 0.05 mbar during 15-20 min to remove physisorbed water. The thermolysis oven was brought to the desired temperature and the substrate was weighted into the substrate flask. The vacuum gauge was carefully opened until maximum vacuum was achieved after which the receiving cooler was filled with CO_2/acetone (-78°C). The substrate (usually 50 or 100 mg) was vaporized at room temperature or with the aid of a sublimation oven, at such a rate that evaporation was complete in 45 min. After another 10 min, the system was flushed with nitrogen. Products were rinsed from the receiving cooler with an appropriate solvent and analyzed by gas chromatography. Thermal control experiments were carried out under identical conditions, however, without employing a catalyst.

Catalytic-FVT of styrene oxide ***6***

Experiments were carried out according to the general procedure described above. Styrene oxide **6** was vaporized at room temperature and thermolyzed over 100 mg of catalyst in about 40 min. The products were rinsed from the receiving cooler with dichloromethane and analyzed by gas chromatography. Results are collected in Table 4.1, Table 4.2, Table 4.3 and Table 4.4.

Catalytic-FVT of cyclohexene oxide ***10***

Experiments were carried out according to the general procedure described above. Cyclohexene oxide **10** was vaporized at room temperature and thermolyzed over 100 mg of catalyst in about 40 min. The products were rinsed from the receiving cooler with dichloromethane and analyzed by gas chromatography. Results are collected in Table 4.6, Table 4.7, Table 4.8 and Table 4.9.

Catalytic-FVT of 2-hexyloxirane ***13***

Experiments were carried out according to the general procedure described above. 2-Hexyl-oxirane **13** was vaporized at room temperature and thermolyzed over 100 mg of catalyst in about 40 min. The products were rinsed from the receiving cooler with dichloromethane and analyzed by gas chromatography. Results are collected in Table 4.10, Table 4.11, Table 4.12 and Table 4.13.

Catalytic-FVT of α-pinene oxide ***17***

Experiments were carried out according to the general procedure described above. α-Pinene oxide **17** was vaporized at room temperature and thermolyzed over 100 mg of catalyst in about 40 min. The products were rinsed from the receiving cooler with dichloromethane and analyzed by gas chromatography. Selected samples were analyzed using GC-MS configured with an appropriate library at IFF. Results are collected in Table 4.14, Table 4.15, Table 4.16 and Table 4.17.

Catalytic-FVT of methyl 3-phenyl-2-oxiranecarboxylate ***30***

Experiments were carried out according to the general procedure described above. Methyl 3-phenyl-2-oxiranecarboxylate **30** was vaporized at 75°C and thermolyzed over 100 mg of catalyst in about 60 min. The products were rinsed from the receiving cooler with dichloromethane and analyzed by gas chromatography and ^{1}H-NMR. Analytical data of product **31** were in agreement with those of a sample of **31** that was prepared via an independent route[23]. Results are collected Figure 4.2.

4.5 REFERENCES

1 a) JP patent 79 154735, Noi, R.; Suzuki, M.; Kurozumi, S.; Hashimoto, Y. *to* Teijin Ltd., 6 Dec. 1979; *Chem. Abstr.* **1980**, *93*, 25989n. b) USSR Patent 513966, Koshel, G.N.; Farberov, M.I.; Antonova, T.N.; Glazyrina, I.I., 15 May 1976; *Chem. Abstr.* **1976**, *85*, 176936d. c) JP Patent 74 51233, Wachi, T., 18 May 1974; *Chem. Abstr.* **1974**, *81*, 120220r.

2 Hölderich, W.F. in *New Frontiers in Catalysis*, Guczi, L. *et al.* Eds., *Proc. 10th Int. Conf. Catal.*, 19-24 July 1992, p127.

3 Huisgen, R. *Angew. Chem.* **1977**, *89*, 589.

4 Brown, R.F.C. in *Pyrolytic Methods in Organic Chemistry: Application of flow and flash vacuum pyrolytic techniques; Organic Chemistry Monographs*, Vol. 41, Academic Press, New York, 1980.

5 Parker, R.E.; Isaacs, N.S. *Chem. Rev.* **1959**, *59*, 737.

6 a) Smith, J.G. *Synthesis* **1984**, 629. b) Rao, A.S.; Paknikar, S.K.; Kirtane, J.G. *Tetrahedron* **1983**, *39*, 2323. c) Rosowsky, A. in *Heterocyclic Compounds with 3- and 4-membered Rings; The Chemistry of Heterocyclic Compounds*, Weisberger, A. Ed., Part 1, Interscience, New York, 1964, p231. d) Bartók, M.; Láng, K.L. in *Small Ring Heterocycles; The Chemistry of Heterocyclic Compounds*, Hassner, A. Ed., Vol. 42, Part 3, Interscience, New York, 1985, p1.

7 Rickborn, B. 'Acid-catalyzed Rearrangements of Epoxides' in *Comprehensive Organic Synthesis; Carbon-Carbon σ-Bond Formation*, Trost, B.M. Ed., Vol. 3, Pergamon Press, Oxford, 1991, Section 3.3.

8 Garin, D.L. *Can. J. Chem.* **1969**, *47*, 4071.

9 Watson, J.M.; Young, B.L. *J. Org. Chem.* **1974**, *39*, 116.

10 Oyewale, A.O.; Aitken, R.A. *Russ. Che. Bull.* **1995**, *44*, 919.

11 Van der Waals, A.C.L.M *Thesis*, University of Nijmegen, The Netherlands, 1997.

12 Van der Waals, A.C.L.M.; Klunder, A.J.H.; Van Buren, F.R.; Zwanenburg, B. *J. Mol. Catal. A* **1998**, *134*, 179.

13 Leliveld, B.R.G.; Kerkhoffs, M.J.H.V.; Broersma, F.A.; van Dillen, J.A.J.; Geus, J.W.; Koningsberger, D.C. *J. Chem. Soc., Faraday Trans.* **1998**, *94*, 315.

14 Brunnel, D.; Mostafa, C.; Patrick, G. *J. Mol. Catal.* **1993**, *79*, 297.

15 Bauer, K.; Garbe, D.; Surburg, H. in *Common Fragrance and Flavour Materials; Preparation, Properties and Uses*, 2nd Ed., VCH, Weinheim, 1990.

16 Yadav, G.D.; Satoskar, D.V. *J. Chem. Tech. Biotechnol.* **1997**, *69*, 438.

17 Erman, W.F. 'Chemistry of the Monoterpenes' in *Studies in Organic Chemistry*, Vol. 11, Part B, Marcel Dekker Inc., New York, 1985, p969.

18 Kaminska, J.; Schwegler, M.A.; Hoefnagel, A.J.; Van Bekkum, H. *Recl. Trav. Chim. Pays-Bas* **1992**, *111*, 432.

19 Posner, G. *Angew. Chem.* **1978**, *90*, 527.

20 Information from DSM, The Netherlands.

[21] Personal communication by Dr. J.G. de Vries (DSM).
[22] Personal communication by Dr. A.J.A. van der Weerdt (Quest International).
[23] Deol, B.S.; Ridley, D.D.; Simpson, G.W. *Aust. J. Chem.* **1976**, *29*, 2459.

5 EPOXIDE REARRANGEMENT REACTIONS IN A FIXED BED REACTOR USING SOLID ACID CATALYSTS

5.1 INTRODUCTION

In the preceding chapter it was shown that epoxides can efficiently be isomerized into carbonyl compounds using the catalytic Flash Vacuum Thermolysis technique. However, the experimental conditions of this technique cannot easily be adopted in an industrial process. The vacuum applied and the low WHSV (weight hour space velocity: unit of substrate per unit time and unit catalyst) would make a scale-up of the catalytic FVT conditions virtually impossible. However, when chemicals would be manufactured with a high added value and in much higher purity, or with any other advantages, it might be worthwhile to study the possibility to implement flash vacuum thermolysis in combination with solid acids on small industrial (pilot) scale. On a large scale, however, the use of catalytic FVT technique may be impractical or economically undesirable. As in particular the use of vacuum is the key problem, it was decided to investigate whether the reactions of epoxides studied with the catalytic FVT technique, can be conducted under normal pressure and flow conditions. As a model for such a continuous flow reactor type, a 'micropuls reactor unit' was used. At Exxon Chemical Europe a similar experimental set-up has been in use with great success.[1] In addition, pulse experiments in a gas chromatograph have been used at AKZO Nobel to study the cracking of gas oil as a function of the reaction time and the oil partial vapor pressure.[2]

The 'micropuls reactor unit' used in the present study is essentially a gas chromatograph (GC) apparatus in which the solid catalyst is mounted in a fixed bed in the flow system. A solution of the substrate and an internal standard is injected into the GC-flow system over this fixed bed and an immediate product analysis is carried out.

Experiments at Exxon Chemical Europe indicated that results obtained under these conditions allow a fair and ready comparison of various catalysts. It was shown that the obtained internal order of catalyst performances was similar to that obtained

using more elaborate experimental systems.[1] Coopmans[2] *et al.* compared the information obtained using the pulse methodology with that of a continuous stream of feed in the cracking of gas oil over zeolitic catalysts. As a model for the two extremes pulses were used in which the concentration decreased exponentially and pulses that had a block form. The latter can be considered as a cut-off from a continuous stream of reactants. It was concluded from these results and the kinetic expressions derived therefrom that the kinetic scheme did not depend on the character of the pulses in these experiments. Hence, it was concluded that results using pulse experiments will not differ significantly from those derived from continuous flow reactors.
The use of a 'micropuls reactor unit' thus constitutes an elegant and simple method to derive a general order of the catalytic performances of a variety of solid catalysts and this order is expected to be valid under large(r) scale conditions as well.

5.2 REARRANGEMENT OF EPOXIDES USING A MICROPULS REACTOR UNIT

Epoxide rearrangement reactions were carried out using the micropuls reactor unit set-up described in the Experimental Section. Experiments were performed using a fractured catalyst (150-425 μm), which was pre-treated at 400°C in the micropuls reactor unit prior to use, to remove physisorbed water from the catalyst.
In the current experimental set-up, the pre-column of a gas chromatograph (GC) was equipped with a solid catalyst, diluted in quartz. On top of this mixture an amount of inert material (quartz) was placed to act as a preheating section and mixing device. A solution of the epoxide and an internal standard was injected with a syringe into the GC-flow system just above the catalyst bed (nitrogen as the carrier gas). An immediate product analysis was carried out using the analytical column of the GC. With an attached autosampler a large series of consecutive injections could be carried out in order to study the deactivation of various catalysts as a function of the amount of substrate being applied.

5.2.1 Styrene oxide

Styrene oxide **1** was taken as the model substrate, as rearrangement of this epoxide leads to the commercially interesting phenylacetaldehyde **2**. This product is rather acid labile and usually rapidly polymerizes under homogeneous acidic conditions. The isomerization of **1** using solid acid catalysts has already been studied in toluene solutions (cf. Chapter 3) and under catalytic flash vacuum thermolysis conditions (cf. Chapter 4). The solution phase experiments (Chapter 3) showed that fast conversions and product selectivities for **2** of up to 99% could be achieved. However, when the

substrate concentration was increased the formation of secondary reaction products caused a drop in the product selectivity. Catalytic FVT experiments (Chapter 4) showed that the selectivity for **2** was very high, typically between 97 and 99.5% and a series of small-scale experiments and some larger scale catalytic FVT experiments demonstrated that this method could be utilized to prepare product **2** in a substrate/catalyst ratio of up to 20. However, if these high yields of **2** could be achieved under normal pressure and flow conditions implementation in an industrial setting would have a better feasibility. The rearrangement of styrene oxide **1** into phenylacetaldehyde **2** was therefore also studied using solid acid catalysts in the micropuls reactor unit.

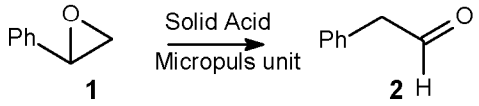

Scheme 5.1 *Isomerization of styrene oxide* **1** *to phenylacetaldehyde* **2** *using the micropuls reactor unit*

Figure 5.1 and Figure 5.2 display the conversions and selectivities obtained for the isomerization of styrene oxide **1** into phenylacetaldehyde **2** using various solid acid catalysts in the micropuls reactor unit at temperatures of 200 and 300°C. Consecutive 2 µl injections of a 10% (Figure 5.1) or 20% (m/m) (Figure 5.2) hexane solution of **1** and 2-methylnaphtalene as internal standard (1:1) were passed over a mixture of catalyst (5 mg) and quartz (20 mg).

For the first injections over the fresh catalyst only little amounts of unreacted substrate **1** were found in the product mixture, but for some catalysts the conversions values dropped severely with consecutive injections. It should be mentioned that the amount of substrate which is passed over the catalyst is small: 0.2 or 0.4 mg of substrate **1** in the case of 2 µl of a 10% or 20% solution, respectively. As the amount of catalyst used in the pre-column of the system was 5 mg, diluted with 20 mg of quartz, the catalyst to substrate ratio is very high. For multiple injections, however, the ratio of catalyst to substrate passed over the catalyst decreases linearly and the performance of the catalyst may be determined as a function of the amount of substrate passed over it.

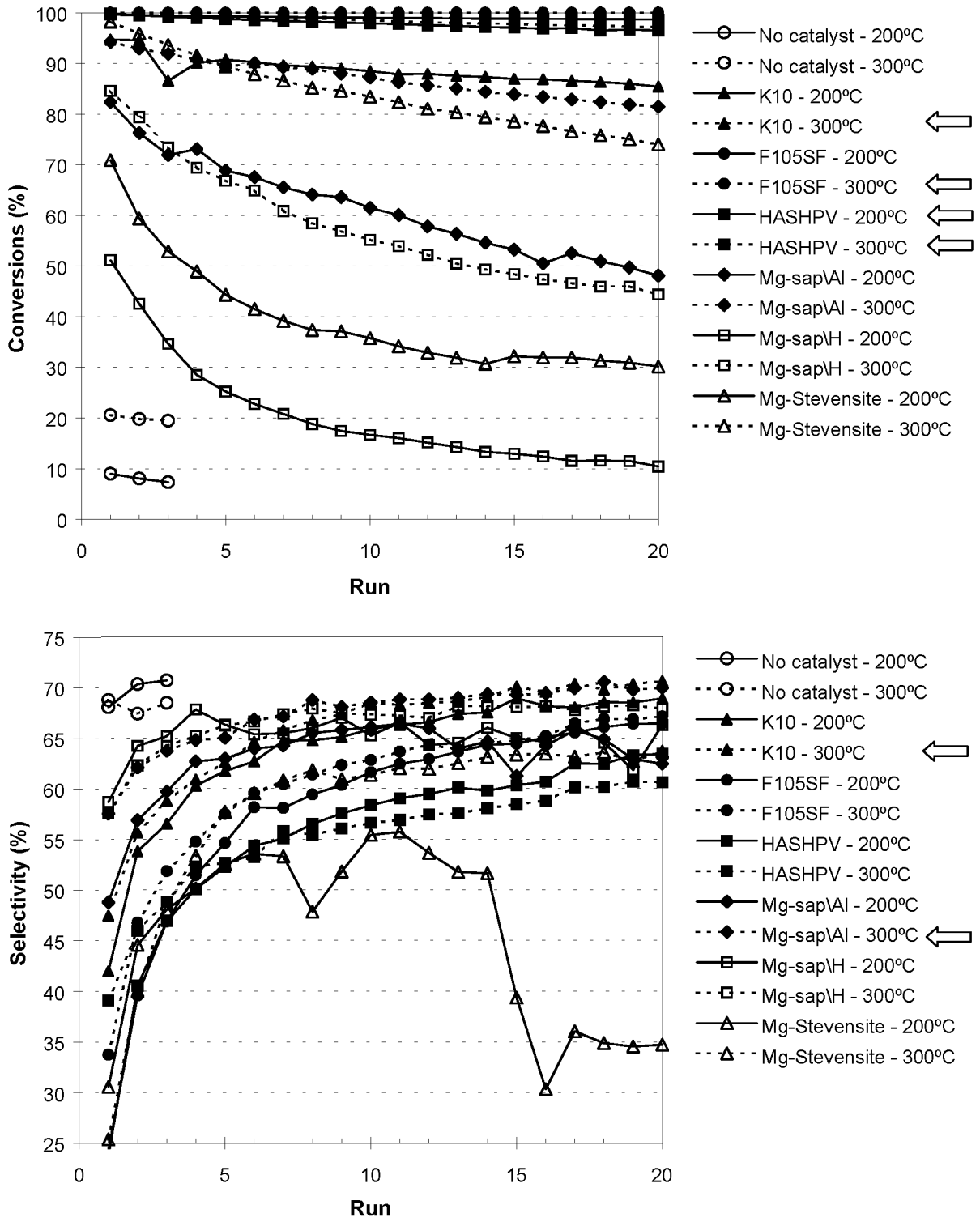

Figure 5.1 *Conversions (%) and selectivities (%) in the isomerization of styrene oxide* **1** *into phenylacetaldehyde* **2** *using various solid acid catalysts in the micropuls reactor unit. 20 consecutive 2 µl injections of a 10% (m/m) hexane solution of* **1** *and 2-methylnaphtalene as internal standard (1:1) were passed over a mixture of catalyst (5 mg) and quartz (20 mg). Reaction temperatures were 200 and 300°C. Arrows indicate the best results.*

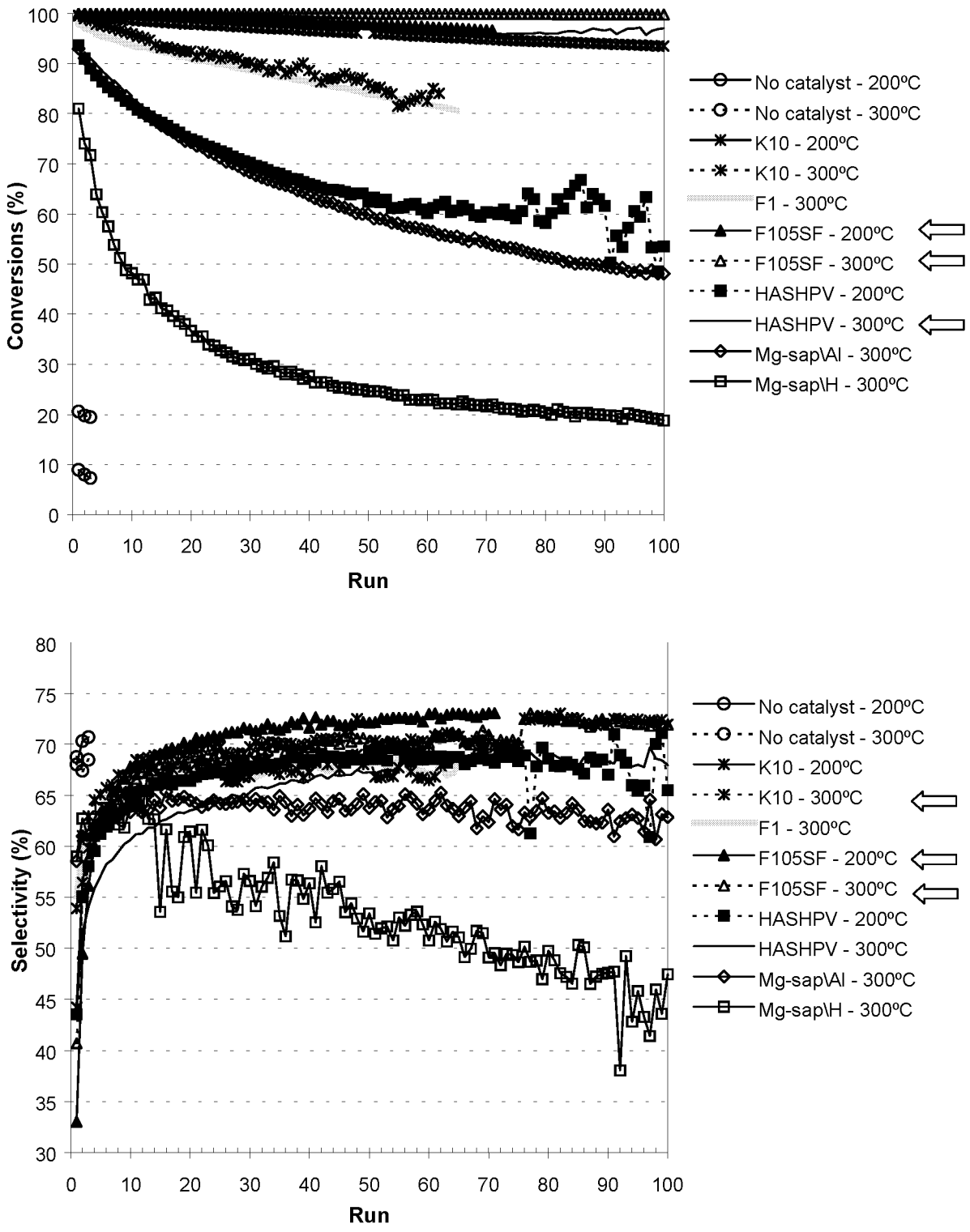

Figure 5.2 *Conversions (%) and selectivities (%) in the isomerization of styrene oxide* **1** *into phenylacetaldehyde* **2** *using various solid acid catalysts in the micropuls reactor unit. Up to 100 consecutive 2 µl injections of a 20% (m/m) hexane solution of* **1** *and 2-methylnaphtalene as internal standard (1:1) were passed over a mixture of catalyst (5 mg) and quartz (20 mg). Reaction temperatures were 200 and 300°C. Arrows indicate the best results.*

From the catalysts used the natural clay F-105SF and the amorphous silica-alumina HA-SHPV turned out to be the most active ones. Using F105SF at a reaction temperature of 300°C gave complete conversions for both the 10% (Figure 5.1) and

the 20% (Figure 5.2) substrate solutions after 20 and 100 injections (runs), respectively. At 200°C not all the runs yielded complete conversions, but still very high values were obtained: 99% (10% solution, 20 runs) and 97% (20% solution, 71 runs). At a reaction temperature of 300°C very high conversions were also observed using the HA-SHPV as values of 99% (10% solution, 20 runs) and 96% (20% solution, 100 runs) were obtained in the last runs of the series. At the lower reaction temperature of 200°C, however, a major difference was found for the two different substrate concentrations. For the 10% solution a conversion of 96% was obtained in the twentieth run, but for the 20% solutions conversions decreased drastically upon increasing the number of runs. After 20 runs the conversion amounted to only 75% and after 100 runs to a mere 54%. This decrease in conversion with the HA-SHPV catalyst at 200°C may be caused by several factors. At 200°C the reactivity of the surface catalytic sites is lower and the release of an organic species from the surface occurs less readily. Furthermore, the amount of available catalytic sites is limited and may be insufficient to accommodate a doubling of the amount of styrene oxide **1** when at this temperature (200°C) the residence time of each organic species is longer than at a more elevated temperature (e.g. 300°C).

The catalyst that displayed the next best catalytic activity was montmorillonite K-10. At 300°C high conversions were observed: 97% (10% solution, 20 runs) and 93% (20% solution, 100 runs); at 200°C somewhat lower values were obtained: 85% (10% solution, 20 runs) and 84% (20% solution, 61 runs). The only other natural clay catalyst tested, F-1, gave clearly lower conversions as at 300°C. Only values of 80% were obtained after 65 runs. In addition to the above-mentioned catalysts several synthetic clay materials were employed. These included Mg-stevensite and Mg-saponites having both aluminum and protons as their interlayer cations. The conversions obtained with these catalysts were notably lower than with the catalysts described above and, in addition, the differences in the conversion values for the two reaction temperatures used, viz. 200 and 300°C, were much more pronounced (Figure 5.1). The synthetic clay Mg-saponite\$Al^{3+}$ displayed the highest catalytic activity as conversions of 81% (10% solution, 20 runs) and 48% (20% solution, 100 runs) were observed at a reaction temperature of 300°C. Mg-saponite\$H^{+}$ showed the lowest activity (19% after 100 runs at 300°C, 20% solution) and the activity of the Mg-stevensite is between the catalytic activity of both saponites.

The conversions decreased with the number of runs, whereas the selectivity for phenylacetaldehyde **2** usually increased with the number of runs for a given catalyst batch until a maximum value for the selectivity was reached. During the first few runs the increase in the selectivity for **2** was at its steepest. Catalytic sites that are only present on the surface of the fresh catalysts may effect the formation of higher

molecular weight products during the first runs. The fact that during subsequent runs the selectivities for **2** is much higher, points to a rapid and irreversible deactivation of these specific catalytic sites. An additional factor may be the low substrate to catalyst ratio (*vide supra*). If the adsorption of organic species is relatively strong with the consequence that the residence times are fairly long then it may be expected that the amount of product **2** found in the not adsorbed product mixture is low. The conversions and selectivities are, after all, determined using an internal standard, which possesses no heteroatoms and which is therefore less readily adsorbed on the surface. After more injections (runs) an equilibrium of the surface occupancy will be established and the adsorption and release of organic species to and from the catalytic surface will reach a steady-state situation. Indeed, the values for the selectivity for **2** remain at a certain maximum level once this has been reached. As can be deduced from Figure 5.1 and Figure 5.2 this required more than 20 injections and the maximum level in selectivity was achieved for most of the catalysts after ca. 40 runs. The selectivities for **2** ranged, after 100 runs, from 45 to 73%. At the top of this range in selectivities are the natural clay catalysts F-105SF (72-73%), F-1 (68%) and montmorillonite K-10 (67-72%), at the bottom Mg-saponite\$H^+$ (ca. 45%) and in the middle Mg-saponite\$Al^{3+}$ (63%) and the amorphous silica-alumina HA-SHPV (65-71%).

Using the catalytic flash vacuum thermolysis (FVT) technique (cf. Chapter 4) the highest yields of phenylacetaldehyde **2** from styrene oxide **1** at moderate reaction temperatures were obtained using the F-clays, montmorillonite K-10, HA-SHPV and the saponite clays. Moreover, with these catalysts very high selectivities (>99%) were combined with (nearly) complete conversions at reaction temperatures of 200 or 300°C. Using the micropuls reactor unit the values for the conversions varied within a much broader range and the selectivities were considerably lower than observed with the catalytic FVT technique. The use of normal pressure instead of a vacuum of 0.05 mbar is the most probable factor to account for these differences. At normal pressure the driving force for desorption of organic species will be lower and as a result the residence times will be longer. Longer residence times may result in a complete coverage of the catalytic surface leaving no site open for unreacted substrate, which has a negative effect on the conversion. In addition, longer residence times may give rise to an enhanced concentration of organic species at the surface. Such higher surface concentrations increase the likelihood that organic species undergo intermolecular reactions. Hence, longer residence times may promote the formation of higher molecular weight products and accordingly give rise to a lower selectivity for the desired isomerization product **2**.

5.2.2 α-Pinene oxide

Several studies appeared in the literature on the rearrangement of α-pinene oxide **3** into campholenic aldehyde **4** because of its use as an intermediate in the flavor and fragrance industry (cf. Chapter 3). The main reaction pathways leading to the various products resulting from the isomerization of α-pinene oxide **3** are displayed in Chapters 3 (Scheme 3.3) and 4 (Scheme 4.7). One of the major reaction products is the desired campholenic aldehyde **4**, which is formed through a skeletal rearrangement with a concomitant release of the strain energy of the four-membered ring in α-pinene oxide **3**. Besides campholenic aldehyde **4** also a wide range of other rearrangement products were found. These include aldehydes, allylic alcohols, *p*-cymene and others (cf. Chapters 3 and 4).

The isomerization of **3** using solid acid catalysts was studied in toluene solutions (cf. Chapter 3) and under catalytic flash vacuum thermolysis conditions (cf. Chapter 4). The solution phase experiments (Chapter 3) showed that fast conversions could be achieved but that the selectivity for **4** did not exceed 55% when using clay catalysts. Also catalytic FVT experiments (Chapter 4) applying the sensitive α-pinene oxide **3** resulted in a broad spectrum of products of which campholenic aldehyde **4** was the principal product. The selectivity for **4** usually reached a maximum at the lowest reaction temperature. A maximum selectivity for **4** of 60% was achieved using the B698D-24 amorphous alumina at 150°C.

If high selectivities for **4** could be achieved under normal pressure and flow conditions then implementation of solid acid catalysts in an industrial gas phase thermolysis setting would probably be feasible. The rearrangement of **3** into **4** using solid acid catalysts was therefore also studied in the micropuls reactor unit (Scheme 5.2). The conversions and selectivities obtained for the isomerization of α-pinene oxide **3** into campholenic aldehyde **4** using various solid acid catalysts in the micropuls reactor unit at temperatures of 200 and 300°C are displayed in Figure 5.3 and Figure 5.4. Consecutive 2 µl injections of a 20% (m/m) hexane solution of **3** and 2-methylnaphtalene as internal standard (1:1) were passed over a mixture of catalyst (5 mg) and quartz (20 mg).

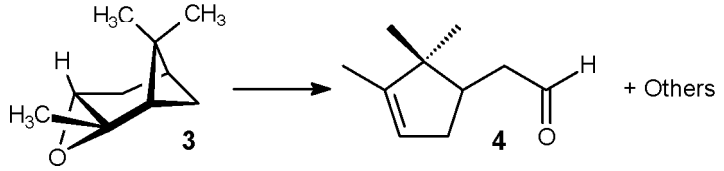

Scheme 5.2 *Isomerization of α-pinene oxide* **3** *to campholenic aldehyde* **4**

The first injections over the fresh catalyst gave very high conversions, but they dropped drastically for many of the catalysts by continuation of injection. It should

be mentioned that the amount of substrate passed over the catalyst is small: 0.4 mg of substrate **3** in a 20% hexane solution. As the amount of catalyst used was 5 mg, diluted in 20 mg of quartz, the initial catalyst to substrate ratio is very high. After multiple injections, however, the ratio of catalyst to substrate passed over the catalyst decreases linearly and the performance of the catalyst may be determined as a function of the amount of substrate passed over.

The natural clays montmorillonite K-10 and F-105SF turned out to be the most active ones, followed by the amorphous silica-alumina HA-SHPV. Using montmorillonite K-10 at 300°C gave a conversion of 86% after 100 injections (runs). For F-105SF and HA-SHPV conversions of 80 and 73% were obtained, respectively. Reduction of the reaction temperature to 200°C caused a severe drop in the conversions to 52% (K-10), 28% (F-105SF) and 54% (HA-SHPV) after 100 runs. The fact that at this temperature the conversions with the HA-SHPV catalyst are so much lower may be attributed to several (unknown) factors. As was discussed earlier for styrene oxide, it is likely that at 200°C the reactivity of the surface catalytic sites is lower than at 300°C.

Also two synthetic clays (Mg-saponite\$H^+$ and Mg-saponite\$Al^{3+}$), an amorphous alumina (B698D-24) and an amorphous silica-alumina (B698D-25) were used in the micropuls reactor. The conversions obtained with these catalysts were notably lower than those described above, although a fair conversion of 49% was achieved for B698D-24 after 100 runs at 200°C.

While the conversions decreased with the number of runs, the selectivities for campholenic aldehyde **4** usually increased for a given catalyst batch until a maximum value for the selectivity was reached. During the first runs the increase in the selectivities for **4** was very pronounced. An explanation for this increase was given in the preceding section. The selectivity for **4** remained reasonably constant when a certain maximum level had been reached. A similar trend had been observed for the formation of phenylacetaldehyde **2** from styrene oxide **1**. The selectivities for **4** ranged, after 100 runs, from 18 to 58%. The amorphous (silica-) aluminas HA-SHPV (58-49%), B698D-25 (56-51%) and B698D-24 (52%) ranked highest in this range of selectivities, the natural clay catalysts F-105SF (46-48%) and montmorillonite K-10 (46-47%) in the middle and Mg-saponite\$H^+$ (18-36%) and Mg-saponite\$Al^{3+}$ (34-40%) lowest.

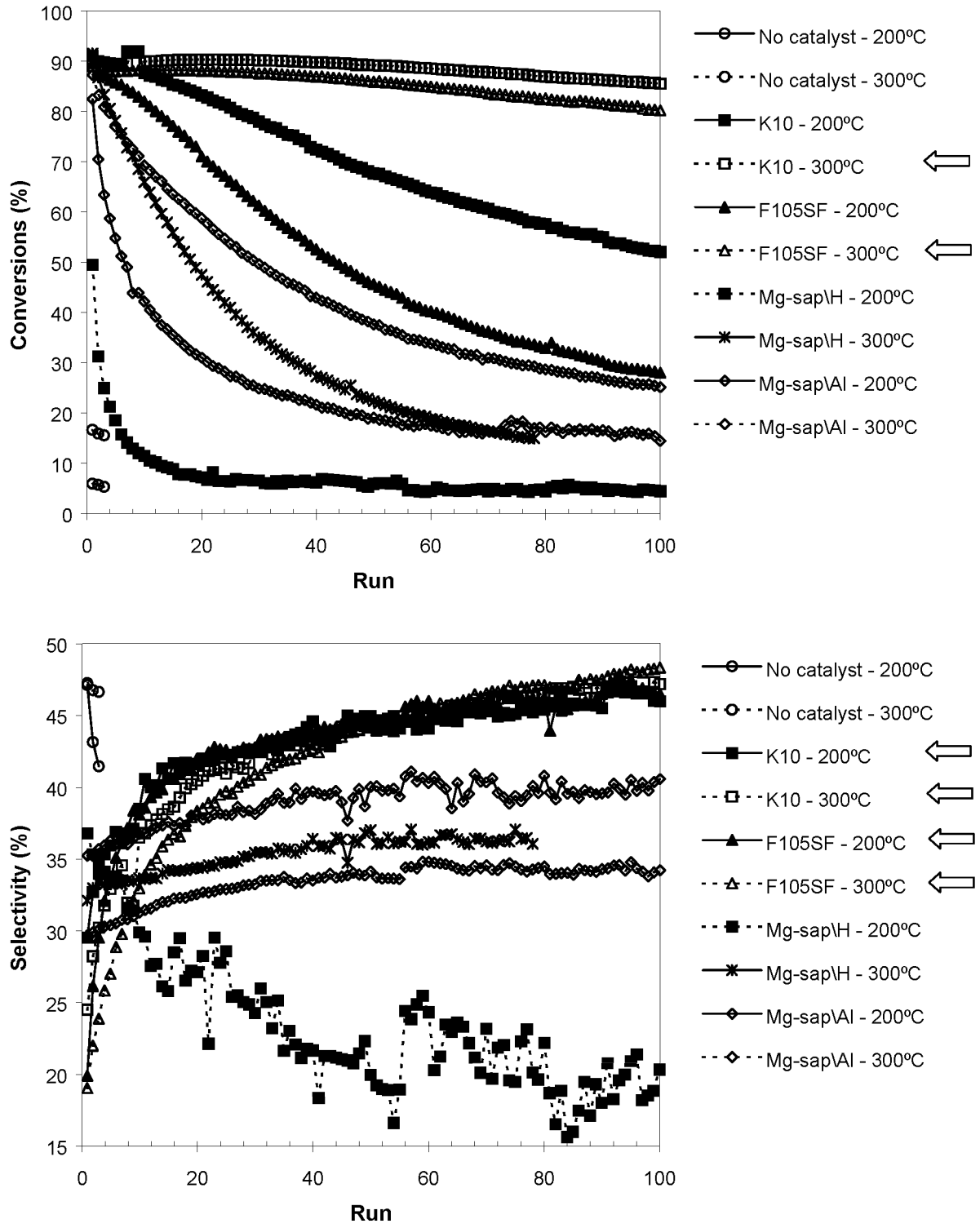

Figure 5.3 *Conversions (%) and selectivities (%) in the isomerization of α-pinene oxide* **3** *into campholenic aldehyde* **4** *using various clay catalysts in the micropuls reactor unit. Up to 100 consecutive 2 µl injections of a 20% (m/m) hexane solution of* **3** *and 2-methylnaphtalene as internal standard (1:1) were passed over a mixture of catalyst (5 mg) and quartz (20 mg). Reaction temperatures were 200 and 300°C. Arrows indicate the best results.*

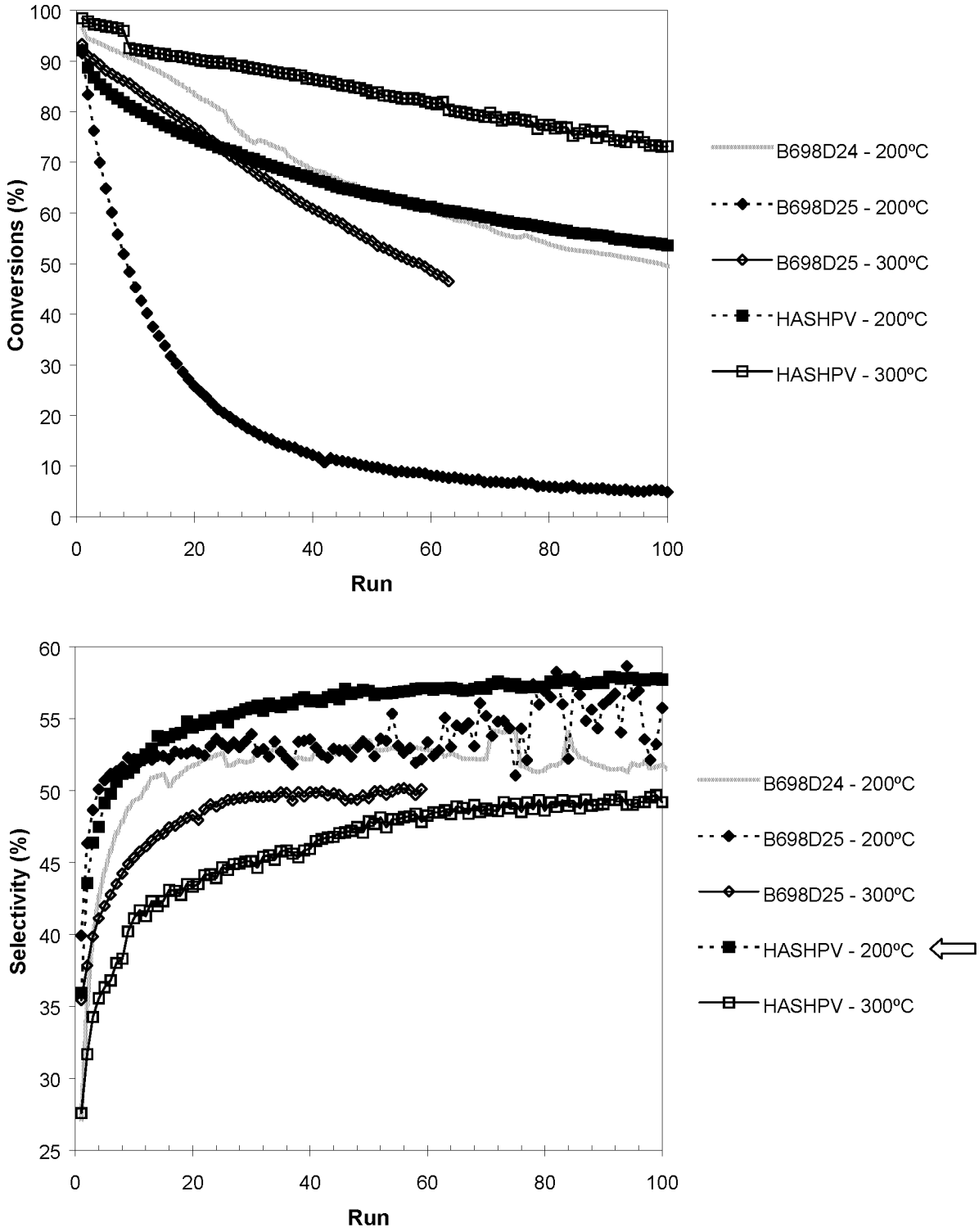

Figure 5.4 *Conversions (%) and selectivities (%) in the isomerization of α-pinene oxide* **3** *into campholenic aldehyde* **4** *using various amorphous (silica-) aluminas in the micropuls reactor unit. Up to 100 consecutive 2 µl injections of a 20% (m/m) hexane solution of* **3** *and 2-methylnaphtalene as internal standard (1:1) were passed over a mixture of catalyst (5 mg) and quartz (20 mg). Reaction temperatures were 200 and 300°C. Arrows indicate the best results.*

Using the catalytic flash vacuum thermolysis (FVT) technique (cf. Chapter 4) very high conversions were obtained at moderate reaction temperatures for most of the catalysts. However, in most cases, the selectivity for **4** was only moderate, but a

maximum of 60% was obtained for B698D-24 at 150°C. Using the micropuls reactor unit the conversions were notably lower but the maximum selectivities (up to 56%) were in the same order of magnitude as observed for the catalytic FVT technique. The use of normal pressure instead of a vacuum of 0.05 mbar is the probably the responsible factor for this difference in conversions. At normal pressure the driving force for desorption of organic species will be lower, leading to longer residence times leaving less sites vacant at a given time for the unreacted substrate, which results in a lower conversion. The longer residence times at the catalytic surface did not decrease the selectivity for **4**. This observation is in sharp contrast to the effect of pressure on the selectivities towards phenylacetaldehyde **2** (Section 5.2). Here a considerable drop in selectivity is observed. Apparently, campholenic aldehyde **4** is less prone to bimolecular reactions than phenylacetaldehyde **2** under these conditions.

5.3 CONCLUSIONS

The isomerization of epoxides using solid acid catalysts under normal pressure and flow conditions was investigated using the micropuls reactor unit. Various natural and synthetic clay materials were tested and, in addition, also amorphous (silica-) aluminas have been employed. Two epoxides were studied, namely styrene oxide **1** and α-pinene oxide **3**.

The conversion of **1** into phenylacetaldehyde **2** was dependent on the type of catalyst, the reaction temperature and the amount of substrate. At the highest temperature (300°C) the conversions were optimal. For some catalysts (F-105SF and HA-SHPV) complete conversions were still obtained after 100 runs. A lower amount of substrate per run resulted in higher conversions, although for some catalysts this difference was hardly noticeable. The selectivity for **2** increased with the number of runs until a maximum was reached, which ranged from 45 to 73% (F-105SF).

Rearrangement of α-pinene oxide **3** resulted in a broad spectrum of products of which campholenic aldehyde **4** was the principal component. As with styrene oxide, the conversions of **3** decreased with the number of runs, but the percentage of conversion was significantly lower. The selectivity for **4** increased by increasing the number of runs and a maximum of 58% was reached after 100 runs using HA-SHPV as the catalyst.

A comparison of the results obtained by the catalytic FVT methodology and the micropuls reactor shows that there is a profound effect of pressure. Using the micropuls reactor unit the conversions for both styrene oxide **1** and α-pinene oxide **3** varied within a much broader range than applying the catalytic FVT experiments.

The selectivities for campholenic aldehyde **4** were in the same order of magnitude as observed when using the catalytic FVT technique, but the selectivity for phenylacetaldehyde **2** was dramatically lower.

Industrial perspective

The use of a micropuls reactor unit is valuable method for a fast evaluation of catalysts at ambient pressure and provides useful information for employing the catalysts in a fixed bed reactor under normal pressure and flow conditions. As stated in chapter 4, the industrial prospect of catalytical FVT on a larger (industrial, pilot) scale is rather limited because of the scaling-up problems. The evaluation of the catalysts using the micropuls reactor shows that the desired epoxide rearrangement reactions can be performed at ambient pressure. Thus, the fixed bed reactor is the best option for scaling up, although for the production of phenylacetaldehyde **2** from styrene oxide **1** the advantages typical for the catalytic FVT method, viz. much higher product purity, low waste production, high conversion and selectivity, cannot completely be reached. For the conversion of α-pinene oxide **3** the outcome of the reaction under ambient pressure is in the same range as was accomplished under catalytic FVT conditions. Here a fixed bed reactor seems an attractive option.

5.4 EXPERIMENTAL SECTION

Origin of the catalysts

Amorphous alumina B698D-24, amorphous silica-alumina B698D-25 and the acid-treated natural F-clays were received as generous gifts from Engelhard De Meern B.V. Amorphous silica-alumina HA-SHPV was obtained as a generous gift from AKZO Nobel Chemicals. Commercial natural clays montmorillonite K-10 and montmorillonite KSF are produced by Süd Chemie and were obtained via Aldrich Chemical Company. Prior to use montmorillonite K-10 was washed in hot demineralized water and subsequently dried to remove any residual mineral acid that may have been present due to the acid-treatment during in its preparation. Synthetic clay materials were prepared and donated by the Department of Inorganic Chemistry and Heterogeneous Catalysis of the University of Utrecht. All saponites used had a Si/Al ratio of 7.9 and are described as M-saponite\C$^+$, where M represents the octahedral cation and C$^+$ the interlayer cation.

All catalysts were pressed (3 tons), sieved into the desired particle size (150-425 μm), and stored at ambient pressure. Catalysts were used after a pre-treatment: Prior to the start of the experiments the catalysts were kept at 400°C inside the micropuls reactor unit.

Micropuls reactor unit set-up

The micropuls reactor unit apparatus, as used at the Department of Organic Chemistry of the University of Nijmegen, is schematically depicted in Figure 5.5. The micropuls reactor unit

consists of a Hewlett-Packard HP5890 gas chromatograph (flame ionization detector, FID), a HP-3393A integrator and a HP-7673A automatic sampler. The pre-column of the GC was equipped with a fixed bed of the catalyst and quartz. This fixed bed consists of a solid catalyst, diluted by quartz (150-425 μm) and a portion of quartz (425-850μm) on top of that, placed in the pre-column of the GC. These plugs of catalyst and quartz were held in place by small amounts of DMCS treated glass wool (Chrompack). The gas flows at the injection point and at the split were 2.7 and 83 ml/min, respectively. A capillary column (HP-Ultra 1, 25 m x 0.32 mm x 0.52 μm), nitrogen at 2.7 ml/min as the carrier gas, and a temperature program from 75°C (5 min isothermal) to 250°C at 15°C/min followed by 3 min at 250°C (isothermal) or from 100°C to 250°C at 15°C/min followed by 10 min at 250°C (isothermal) were used for analysis of the reaction products.

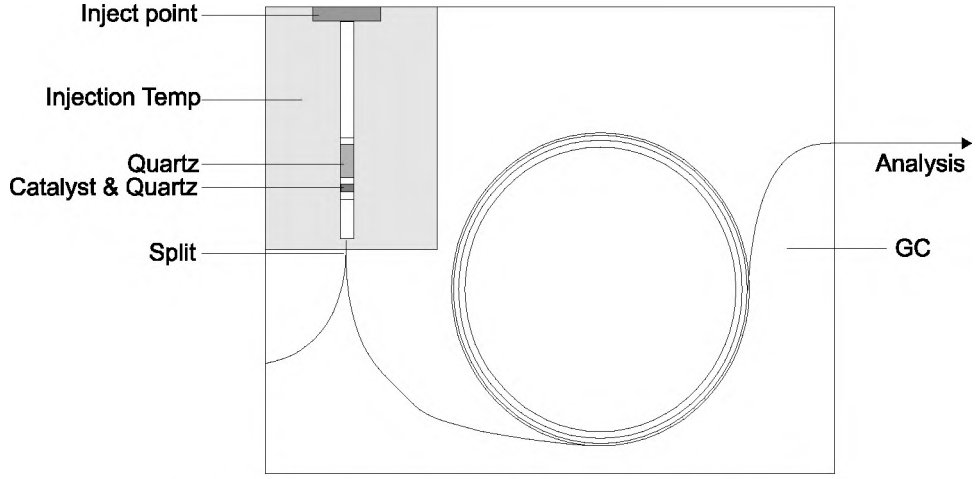

Figure 5.5 *Schematic representation of the micropuls reactor unit*

General procedure for micropuls reactor unit experiments

The micropuls reactor unit described above was used. Experiments were performed using a fractured catalyst (150-425 μm), which was pre-treated at 400°C in the pre-column of the micropuls reactor unit prior to use, to remove physisorbed water from the catalyst. Typically, 5.0 mg of catalyst was diluted in 20.0 mg of quartz powder to form the diluted catalyst mixture (both having a particle size of 150-425 μm) and on top of that 200 mg of quartz (425-850 μm) was mounted. A solution of the epoxide and an internal standard was injected with a syringe through the septum, into the GC-flow system just above the catalyst bed in the carrier gas (nitrogen). An immediate product analysis was performed using the analytical column of the GC. With an attached autosampler a series of consecutive injections could be carried out. Typically, a 10 or 20% (m/m) solution of substrate and internal standard (in a mass ratio of 1:1) were used in injections of 2.0 μl.

Micropuls reactor unit experiments with styrene oxide ***1***

The general procedure described above was used. 5.0 mg of catalyst was diluted in 20.0 mg of quartz to form the diluted catalyst mixture and on top of that 200 mg of quartz was placed. Injections of 2.0 μl of a 10 or 20% (m/m) solution of styrene oxide **1** and 2-methyl-

naphtalene (in a mass ratio of 1:1) in hexane were injected into the GC-flow system. Results are given in Figure 5.1 and Figure 5.2.

Micropuls reactor unit experiments with α-pinene oxide **3**

The general procedure described above was used. 5.0 mg of catalyst was diluted in 20.0 mg of quartz to form the diluted catalyst mixture and on top of that 200 mg of quartz was placed. Injections of 2.0 µl of a 20% (m/m) solution of α-pinene oxide **3** and 2-methylnaphtalene (in a mass ratio of 1:1) in hexane were injected into the GC-flow system. Results are given in Figure 5.3 and Figure 5.4.

5.5 REFERENCES

[1] Personal communication by Dr. M.J.G. Janssen (Exxon Chemical Europe).
[2] Coopmans, J.F.; Mars, P.; De Groot, R.L. *Ind. Eng. Chem. Res.* **1992**, *31*, 2093.

6 Pinacol Rearrangement via Catalytic Flash Vacuum Thermolysis using Solid Acids

6.1 Introduction

The Pinacol rearrangement is the acid-catalyzed reaction of vicinal diols, which results in dehydration and the migration of an alkyl or aryl group, or a hydrogen atom, to form an aldehyde or ketone.[1] The name is derived from the material used in the earliest recorded example,[2] viz. the rearrangement of pinacol **1** into pinacolone **2** using sulfuric acid (Scheme 6.1). All classes of vicinal diols (i.e. primary, secondary, tertiary, alkyl- or aryl-substituted) may undergo a Pinacol rearrangement. Many acids and solvent have been employed, but sulfuric acid remains the most commonly used catalyst. The selection of reagents and conditions is important as they can completely alter the outcome of the reaction. Pinacol **1** may be converted quantitatively into pinacolone **2** using 25% sulfuric acid,[3] but **1** may also serve as the starting material for the synthesis of 2,3-dimethylbutadiene by a slow distillation of a mixture of **1** and a catalytic amount of HBr.[4]

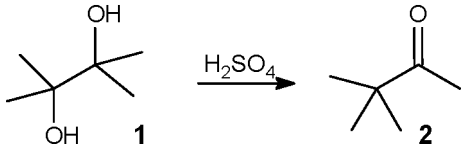

Scheme 6.1 *The rearrangement of pinacol* **1** *into pinacolone* **2**

The Pinacol rearrangement and the acid-catalyzed rearrangement of epoxides (cf. Chapters 3 and 4) are closely related processes which outcome is highly dependent upon the substrates, reagents and conditions used. In some cases epoxides have been isolated from diols under Pinacol rearrangement conditions[5] and they are implicated as reactive intermediates in other instances. Similarly, treatment of an epoxide with aqueous acid may cause opening of the epoxide to the vicinal diol either prior to, or in competition with, rearrangement of the epoxide. If the equilibrium shown in Scheme 6.2 is reached more rapidly than rearrangement can occur, then the two substrates (viz. diol and epoxide) are synthetically equivalent for most purposes. The

merger of the two processes is promoted by strong acids and substrates bearing cation-stabilizing substituents. Mild acids and good nucleophiles, on the other hand, will favor covalent bond-forming reactions, such as the formation of a halohydrin upon treatment of an epoxide with HX. These covalent products may be isolable or may serve as intermediates leading to rearranged products under the conditions employed for their formation. The rearrangement step itself may be regarded as the interaction of an intramolecular nucleophile (the migrating group and its bonding electron pair) with an adjacent electrophilic center. This center may range from a formal cation (as displayed in Scheme 6.2) to a carbon which bears a leaving group suitable for a S_N2 substitution.

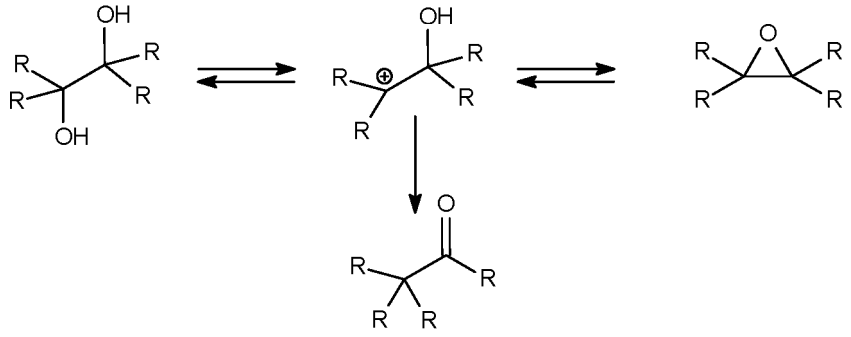

Scheme 6.2 *Formation of a carbonyl compound from a diol or an epoxide via a common intermediate*

Only a very few mechanistic features are general for all diols under all conditions. In fact, the same substrate may yield different products when subjected to seemingly similar reaction conditions. This is illustrated by the example in Scheme 6.3, where the diol **3** gives the ketone **4** when treated with concentrated sulfuric acid, but predominantly aldehyde **5** when reacted with 40% sulfuric acid. Several detailed mechanistic studies are treated in two reviews by Collins[6,7] and the general conclusions may be summarized as follows: *i.* Pinacol rearrangements are exclusively intramolecular; *ii.* the course of the Pinacol rearrangement usually depends on which hydroxyl group is most easily removed, which may be predicted on the basis of the stability of the intermediate; *iii.* the group which preferentially migrates is the one which stabilizes a positive charge best, although stereochemical and conformational effects, rapid equilibration of intermediate carbocations or interconversion of products may give complications; *iv.* inversion or racemization may be observed at the migration terminus.

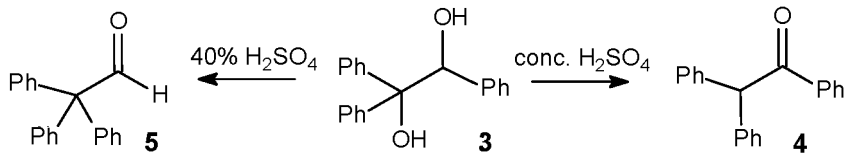

Scheme 6.3 *Different product formation depending on reaction conditions*

Concerning the migratory aptitudes in Pinacol rearrangements a few observations can be made, although these are by no means conclusive. Phenyl and hydrogen appear to be similar in the rate of migration and the migration of a hydrogen is some 20 times faster than that of a methyl group. The *tert*-butyl group has been reported to migrate much more rapidly than other simple alkyl groups (*tert*-butyl:ethyl:methyl = >4000:17:1).[8] Cyclopropyl substituents shift more readily than simple alkyl groups and without ring opening of the cyclopropyl moiety.[9]

Sulfuric acid in various concentrations is the most commonly used catalyst in the Pinacol rearrangement (*vide supra*), but also a few reports have appeared using solid acids as catalysts in this reaction, such as zeolites,[10] montmorillonites[11] and SAPO molecular sieves.[12] Some of these catalysts were able to alter the outcome of the Pinacol rearrangement by shifting the product composition[11] and reduce the formation of unwelcome side-products.[12] It is essential to exclude these competitive processes and to control both regio- and stereoselectiviy in order to maximize the synthetic utility of Pinacol rearrangements. The two factors influencing the regio-selectivity (i.e. which hydroxyl is lost and which adjacent group migrates) are to some extent predictable and, in favorable circumstances, controllable. But the control of stereoselectivity is more problematic.[1] These factors and the fact that many diols are generally expensive as they are not easily accessible, have prevented the use of the Pinacol rearrangement in multi-step organic syntheses and in industrial processes.

Objective and approach

Clay minerals are powerful solid acid catalysts for a large variety of organic transformations (cf. Chapter 2). So far, however, clays have only scarcely been used in the Pinacol rearrangement. The aim of the present study is to investigate the Pinacol rearrangement using clays as solid acid catalysts under flash vacuum thermolysis conditions. Various natural and synthetic clays were tested and, in addition, also amorphous (silica) aluminas have been employed. The activity of the catalysts will be discussed in terms of their acidity and their porosity. Because of the analogy with the epoxide rearrangement reaction (cf. Scheme 6.2) the results of the solid acid-catalyzed Pinacol rearrangement under flash vacuum thermolysis conditions will be compared with those of the structurally related epoxide rearrangement reactions under similar reaction conditions (cf. from Chapter 4).
The diols used comprise one aromatically substituted diol, viz. 1-phenyl-1,2-ethanediol **6**, one simple aliphatic diol, viz. 1,2-octane diol **9**, one diol having both a phenyl and an aliphatic substituent, viz. 2-phenyl-1,2-propane diol **13** and one

complex aliphatic diol, viz. α-pinane *cis*-diol **18**. Diols **6**, **9** and **18** were chosen because their epoxide counterparts were studied in Chapter 4. Phenylacetaldehyde **7** and campholenic aldehyde **17** are important fine chemical products and may be synthesized from 1-phenyl-1,2-ethanediol **6** and α-pinane *cis*-diol **18**, respectively.

6.2 PINACOL REARRANGEMENT VIA CATALYTIC FVT

Pinacol rearrangement reactions were carried out using the catalytic flash vacuum thermolysis set-up described in the Experimental section. Experiments were performed at 0.05 mbar with 100 mg of a fractured catalyst (150-425 μm), which was pre-treated at 400°C and 0.05 mbar prior to use to remove physisorbed water from the catalyst. Substrates were vaporized at an appropriate temperature (see Experimental section) in about 45 min. Typically, a series of runs was performed using the same catalyst batch while the reaction temperature was varied. The temperatures in such a series were varied according to a hysteresis loop, going from 400°C to 200°C and back to 400°C. In this manner a possible deactivation would be detectable by comparing the results of two experiments carried out at the same reaction temperature. Deactivation was visibly observed, however, by blackening of the catalyst after use. Control experiments were performed under identical condition but without a catalyst.

6.2.1 Rearrangement of 1-phenyl-1,2-ethanediol

1-Phenyl-1,2-ethanediol **6** was taken as a model substrate, as Pinacol rearrangement of this diol (Scheme 6.4) may lead to the commercially interesting phenylacetaldehyde **7**, which is rather acid labile and usually rapidly trimerizes or polymerizes under homogeneous acidic conditions. Phenylacetaldehyde **7** was prepared successfully from styrene oxide via catalytic flash vacuum thermolysis (cf. Chapter 4). However, starting from the diol instead of the epoxide, the rearrangement could result in a different product composition.

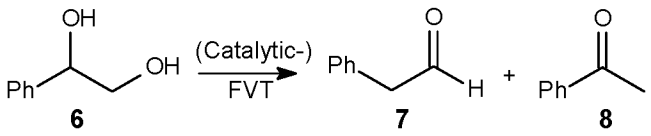

6 **7** **8**

Scheme 6.4 *Rearrangement of 1-phenyl-1,2-ethanediol* **6** *under (Catalytic) FVT conditions*

The thermal reactivity of 1-phenyl-1,2-ethanediol **6** was determined in some control experiments (entries 1-3 in Table 6.1). Diol **6** proved to be very stabile as only 3% of **6** was converted at 400°C to give phenylacetaldehyde **7** with 100% selectivity. At lower reaction temperatures no conversion was observed.

The results obtained with natural and synthetic clays, and amorphous (silica) aluminas as solid acid catalysts in the rearrangement of 1-phenyl-1,2-ethanediol **6** under catalytic FVT conditions are collected in Table 6.1 (entries 4-38), Table 6.2 and Table 6.3, respectively. Most of these solid acids proved to be effective catalysts in this transformation as the conversions were, usually, considerably higher than in the absence of a catalyst.

Table 6.1 *Rearrangement of 1-phenyl-1,2-ethanediol* **6** *under Catalytic FVT conditions using natural clays*

Entry	Catalyst[a]	Temp.[b] (°C)	Conversion[c] (%)	Selectivity[c] (%) 7	8
1	none	400	3	100.0	
2		300	0	-	-
3		200	0	-	-
4	F-1	400	100	99.0	
5		300	94	99.5	
6		200	66	100.0	
7		300	65	100.0	
8		400	100	99.0	1.0
9	F-13	400	100	89.4	
10		300	100	100.0	
11		200	100	100.0	
12		300	100	99.7	0.3
13		400	100	99.6	0.4
14	F-105SF	400	100	99.5	
15		300	100	100.0	
16		200	100	100.0	
17		300	100	100.0	
18		400	100	99.5	0.5
19	F-24	400	100	100.0	
20		300	95	78.8	
21		200	86	99.2	0.5
22		300	100	100.0	
23		400	100	99.1	0.9
24	F-25	400	100	97.8	0.3
25		300	100	99.8	0.1
26		200	94	100.0	
27		300	96	100.0	
28		400	99	95.7	
29	Montmorillonite K-10	400	100	100.0	
30		300	93	100.0	
31		200	86	100.0	
32		300	94	100.0	
33		400	100	99.4	0.6
34	Montmorillonite KSF	400	100	66.2	
35		300	45	100.0	
36		200	9	100.0	
37		300	40	98.2	1.8
38		400	58	97.8	2.4

[a] 100 mg of catalyst was used and 100 mg of substrate per run. [b] Oven temperature; The substrate was vaporized at 100°C; 0.05 mbar pressure. [c] Conversions and selectivities determined by GC.

Table 6.2 *Rearrangement of 1-phenyl-1,2-ethanediol* **6** *under Catalytic FVT conditions using synthetic clays*

Entry	Catalyst[a]	Temp.[b] (°C)	Conversion[c] (%)	Selectivity[c] (%) 7	8
1	Mg-saponite\Al^{3+}	400	95	100.0	
2		300	61	100.0	
3		200	37	100.0	
4		300	34	100.0	
5		400	73	98.3	0.7
6	Zn-saponite\Al^{3+}	400	94	98.1	0.4
7		300	74	68.8	
8		200	41	100.0	
9		300	25	97.6	
10		400	69	98.0	0.7
11	Mg-saponite\H^{+}	400	76	100.0	
12		300	15	100.0	
13		200	2	100.0	
14		300	7	100.0	
15		400	44	86.2	
16	Zn-saponite\H^{+}	400	35	95.7	
17		300	11	100.0	
18		200	2	100.0	
19		300	5	100.0	
20		400	17	88.2	
21	Mg-stevensite	400	74	88.8	0.7
22		300	22	100.0	
23		200	16	52.2	
24		300	20	72.5	
25		400	74	94.0	0.9
26	Zn-stevensite	400	6	49.1	14.5
27		300	0	-	-
28		200	0	-	-
29		300	6	88.7	
30		400	12	66.9	

[a] 100 mg of catalyst was used and 100 mg of substrate per run. [b] Oven temperature; The substrate was vaporized at 100°C; 0.05 mbar pressure. [c] Conversions and selectivities determined by GC.

A series of runs was performed using the same catalyst batch while the reaction temperature was varied according to a hysteresis loop, going from 400°C to 200°C and back to 400°C. In the first run the conversions were mostly very high at the highest temperature (400°C), reaching 100% using the natural clays, amorphous alumina B698D-24 and amorphous silica-alumina HA-SHPV (Table 6.1 and Table 6.3). Also with the remaining catalysts acceptable conversions were obtained and only with the Zn-stevensite and Zn-saponite\H^{+} low conversions of 35 and 6% were observed, respectively. However, when this temperature was used again in the fifth run with the same catalyst batch the conversions were, in some cases, notably lower. This was most evident for synthetic clays, amorphous (silica) aluminas and montmorillonite KSF. A similar effect can be noticed by comparing the second and

fourth run (300°C). The only two catalysts that gave complete conversions in all five runs with the same batch of catalyst were the natural clays F-13 and F-105SF. Other very active catalysts were the natural clays F-24, F-25 and montmorillonite K-10, which showed conversions of 86, 94 and 86%, respectively at the lowest reaction temperature of 200°C. The lowest conversions were found with the Zn-stevensite and the saponites having H^+ as the interlayer cation (Table 6.2).

Table 6.3 *Rearrangement of 1-phenyl-1,2-ethanediol* **6** *under Catalytic FVT conditions using amorphous (silica) aluminas*

Entry	Catalyst[a]	Temp.[b] (°C)	Conversion[c] (%)	Selectivity[c] (%) 7	8
1	B698D-24	400	100	94.2	
2		300	78	85.3	
3		200	57	100.0	
4		300	65	98.0	
5		400	90	98.0	
6	B698D-25	400	96	90.8	0.2
7		300	47	93.1	
8		200	30	93.2	
9		300	33	95.7	0.6
10		400	62	93.7	0.3
11	HA-SHPV	400	100	96.6	
12		300	84	97.7	
13		200	50	100.0	
14		300	56	100.0	
15		400	86	99.1	0.4

[a] 100 mg of catalyst was used and 100 mg of substrate per run. [b] Oven temperature; The substrate was vaporized at 100°C; 0.05 mbar pressure. [c] Conversions and selectivities determined by GC.

The selectivity for phenylacetaldehyde **7** was usually very high and often exceeded 99%. The rearrangement of 1-phenyl-1,2-ethanediol **6** proceeds with a high selectivity because the electron-releasing phenyl group promotes the release of an hydroxyl group from the carbon to which it is attached by stabilizing the developing electron deficient center. After migration of an adjacent hydride to this positive center and release of the product from the catalyst surface the catalytic center may be regenerated. Acetophenone **8** is the minor by-product in this catalytic rearrangement of 1-phenyl-1,2-ethanediol **6**. This ketone arises when the electron deficient center is generated at the other carbon of the diol. From this relatively unstable primary cationic intermediate two products may be formed: ketone **8** after a hydride shift and aldehyde **7** after a phenyl migration.

The type and number of acidic sites of the various solid catalysts has been semi-quantitatively determined using infrared analyses of adsorbed pyridine (cf. Chapter 2). These studies showed that montmorillonite K-10, Zn-saponite\H^+ and the F-1 clay

possess predominantly Lewis acidic character, whereas the amorphous alumina B698D-25 and the F-13 and F-25 natural clays display mainly Brønsted acidity. Other catalysts studied contain a slightly larger number of Lewis acidic sites. The relative acidity of most catalysts is in the same order of magnitude. The highest acidity is observed for the amorphous silica-aluminas B698D-25 and HA-SHPV and the synthetic clay Mg-saponite\$Al^{3+}$. The synthetic clay Mg-saponite\$H^{+}$ and the F-13 natural clay display lower acidity than the other solid catalysts. Stevensite materials have a considerable lower acidity, and it is known[13] that this (low) acidity is mainly of the Lewis type.
These acidic properties are only partly reflected in the results obtained in the Pinacol rearrangement of **6**. The B698D-25 amorphous silica-alumina possesses the highest acidity, but this catalyst is by no means the most active one. The highest conversions were observed for clays F-13, F-105SF, followed by F-24, F-25 and montmorillonite K-10. Compared with these catalysts the amorphous (silica) aluminas and the saponites gave lower conversions, although some of them have an acidity even stronger than these natural clays.
Some correlation was found for the synthetic clays, since the clay with the highest total acidity (Mg-saponite\$Al^{3+}$) also gave the higher conversions in the series of synthetic clays. The order of acidity for the other synthetic clays correlates also rather well, although not completely (e.g. Zn-saponite\$Al^{3+}$ > Mg-saponite\$H^{+}$ > Zn-saponite\$H^{+}$ > the stevensites) with the observed conversions for these catalysts.
However, a consistent correlation between the acidic properties of the various catalysts and their catalytic activity is not present.

There are some indications that the active surface area may play some role in the rearrangement of **6** to **7**. KSF montmorillonite with small active surface area (20-40 m^2/g) exhibits a distinctly lower catalytic activity than the other natural clay catalysts, which all have a larger active surface area (> 200 m^2/g). Contradictorily, the magnesium-clays have a much larger active surface area (411-575 m^2/g) than their zinc-counterparts (244-165 m^2/g), but their catalytic activities were rather similar. In this case the differences in the surface area may therefore be outweighed by other factors effecting the catalytic activity in this rearrangement.

A comparison of the catalytic FVT experiments with styrene oxide (Chapter 4) and phenyl-1,2-ethanediol **6** shows that the outcome of the reaction is very similar but not identical. For the epoxide the conversions at a given temperature were notably higher, particularly when the saponite clays were used at 200°. For styrene oxide conversions were obtained ranging from 83-63% whereas for the diol **6** conversions

were determined ranging from 41-2%. A similar difference was observed for the amorphous (silica) aluminas, but for the natural clays the difference was less pronounced since for both the epoxide and diol high conversions were obtained at 400, 300 and 200°C. The overall conclusion is that styrene oxide is more reactive than the structurally related diol **6** applying catalytic flash vacuum thermolysis.

6.2.2 Pinacol Rearrangement of 1,2-octanediol

The Pinacol rearrangement of aliphatic diols is usually accompanied by a wide product distribution because aliphatic substituents usually do not direct the rearrangement to one reaction path as aryl substituents do. 1,2-Octane diol **9** was included in this study as an aliphatic diol, because the rearrangement of the corresponding epoxide was investigated in Chapter 4.

Control experiments, without catalysts, showed that **9** is quite inert under thermal conditions, as only 4% was converted at 400°C and 14% at 600°C (Table 6.4, entries 1-5). The main products were identified as octanal **10**, 2-octanone **11** and 1-octyne **12** (Scheme 6.5). The results obtained in the rearrangement of 1-octane diol **9** under catalytic FVT conditions using natural and synthetic clays, and amorphous (silica) aluminas as solid acid catalysts are collected in Table 6.4, Table 6.5 and Table 6.6, respectively.

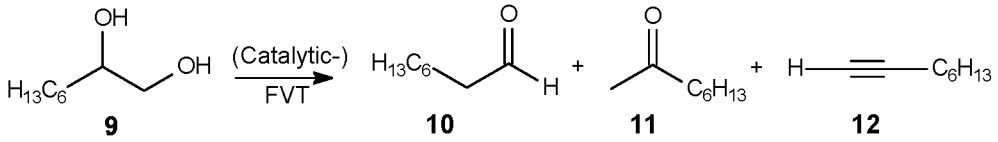

Scheme 6.5 *Rearrangement of 1,2-octanediol* **9** *under Catalytic FVT conditions*

Five runs were performed using the same batch of catalyst while the reaction temperature was varied according to a hysteresis loop, going from 400°C to 200°C and back to 400°C. In the first run with a given catalyst the conversions at 400°C were usually higher than in the fifth run (at the same temperature). This was true for all the catalysts, except for the F-13 clay and Zn-stevensite where in the last run the same or a slightly higher conversion were observed. Some deactivation may also be noticed by comparing the conversions of the second and fourth run (300°C) for all catalysts. The best conversions were obtained for the F-clays, montmorillonite K-10, the amorphous alumina B698D-24 and the amorphous silica-alumina HA-SHPV. Complete conversions were only observed for the F-13 and F-105SF clays at 400°C. Moderate catalytic activities were observed for the saponite clays, montmorillonite KSF and the amorphous silica-alumina B698D-25. The lowest conversions were found using the stevensites as catalysts.

Table 6.4 *Rearrangement of 1,2-octanediol* **9** *under Catalytic FVT conditions using natural clays*

Entry[d]	Catalyst[a]	Temp.[b] (°C)	Conversion[c] (%)	Selectivity[c] (%)		
				10	**11**	**12**
1	None (blanc expts)	200	4			
2		300	4			
3		400	4	5		
4		500	6	35	7	
5		600	14	56	13	
6	F-1	400	91	80	6	3
7		300	39	79	4	3
8		200	19	20		
9		300	44	80	5	2
10		400	71	82		4
11	F-13	400	100	59	6	4
12		300	94	77	5	2
13		200	49	18	1	3
14		300	88	79	5	2
15		400	100	73	7	3
16	F-105SF	400	100	69	7	3
17		300	87	80	6	1
18		200	38	23	1	4
19		300	71	77	6	2
20		400	95	78	8	3
21	F-24	400	91	76	5	5
22		300	64	78	4	3
23		200	31	16	3	5
24		300	45	77	5	3
25		400	78	81	7	3
26	F-25	400	97	75	6	4
27		300	66	75	4	2
28		200	27	22	1	2
29		300	51	73	5	2
30		400	89	79	7	2
31	Montmorillonite K-10	400	95	79	8	3
32		300	88	80	7	2
33		200	13	17	2	2
34		300	43	76	7	3
35		400	92	80	8	3
36	Montmorillonite KSF	400	47	33	3	1
37		300	8	49	4	
38		200	3			
39		300	5	38	2	
40		400	20	75	7	2

[a] 100 mg of catalyst was used and 100 mg of substrate per run. [b] Oven temperature; The substrate was vaporized at 100°C; 0.05 mbar pressure. [c] Conversions and selectivities determined by GC. [d] The best results are marked by shading of the entry number.

The selectivity for the products **10**, **11** and **12** shows some correlation with the reaction temperature applied. Octanal **10**, the main product in most cases, was formed with a selectivity up to 82%. The selectivity for aldehyde **10** was quite acceptable (57-88%) at 300 and 400°C but decreased sharply (0-36%) when the reaction temperature was lowered to 200°C. 2-Octanone **11** was only obtained in

small amounts with the highest selectivity at the higher reaction temperatures. 1-Octyne **12** was observed only in minute amounts at 400°C, but totally absent at lower reaction temperatures. The acetylene by-product is probably formed by a dehydratation process which is similar to that observed for the formation of phenylacetylene from styrene oxide (cf. Scheme 4.5 in Chapter 4).

Table 6.5 *Rearrangement of 1,2-octane diol* **9** *under Catalytic FVT conditions using synthetic clays*

Entry	Catalyst[a]	Temp.[b] (°C)	Conversion[c] (%)	Selectivity[c] (%)		
				10	**11**	**12**
1	Mg-sap\Al3+	400	60	78	6	2
2		300	16	66	4	
3		200	7	10		
4		300	15	64	5	
5		400	46	79	6	1
6	Zn-sap\Al3+	400	45	74		3
7		300	15	69		
8		200	8			
9		300	13	68		
10		400	26	71		2
11	Mg-sap\H+	400	15	81	6	1
12		300	5	40		
13		200	4			
14		300	4	17		
15		400	11	63	5	
16	Zn-sap\H+	400	13	39	6	
17		300	5	30		
18		200	5			
19		300	4	18		
20		400	10	34	6	
21	Mg-stevensite	400	31	68		2
22		300	8	43		
23		200	5			
24		300	11	44		
25		400	27	57		1
26	Zn-stevensite	400	5	6	2	
27		300	3			
28		200	3			
29		300	4			
30		400	7	7		

[a] 100 mg of catalyst was used and 100 mg of substrate per run. [b] Oven temperature; The substrate was vaporized at 100°C; 0.05 mbar pressure. [c] Conversions and selectivities determined by GC.

Comparison of the results obtained for the diols **6** and **9** shows that the selectivity for the aldehyde is much lower for the aliphatic diol **9** than for diol **6**. Clearly, the directing effect of the phenyl group in substrate **6** is responsible for this difference in behavior.

The acidic properties of the catalysts (See Section 6.2.1 and Chapter 2) are reflected only to a limited extent in the rearrangement of 1,2-octanediol **9**. The highest

conversions were observed with the F clays, montmorillonite K-10, B698D-24 and HA-SHPV. The clay that has the highest acidity (Mg-saponite\Al^{3+}), however, exhibits only moderate activity in the rearrangement of **9**. As may be anticipated on the basis of acidity, the clays with the weakest acidity, the stevensites, showed the lowest activity.

Table 6.6 *Rearrangement of 1,2-octane diol* **9** *under Catalytic FVT conditions using amorphous (silica) aluminas*

Entry[d]	Catalyst[a]	Temp.[b] (°C)	Conversion[c] (%)	Selectivity[c] (%)		
				10	**11**	**12**
1	B698D-24	400	92	78	10	5
2		300	42	74	10	2
3		200	9	28	4	
4		300	15	63	5	
5		400	86	79	10	4
6	B698D-25	400	57	72	8	4
7		300	27	66	6	3
8		200	14	17	1	1
9		300	21	59	6	1
10		400	47	75	9	2
11	HASHPV	400	88	74	10	3
12		300	43	70	10	3
13		200	13	36	6	
14		300	39	72	10	4
15		400	77	76	10	3

[a] 100 mg of catalyst was used and 100 mg of substrate per run. [b] Oven temperature; The substrate was vaporized at 100°C; 0.05 mbar pressure. [c] Conversions and selectivities determined by GC. [d] The best results are marked by shading of the entry number.

As already concluded for diol **6**, there are also indications here that the active surface area may be a factor in the rearrangement reaction of diol **9**. KSF montmorillonite showed a distinctly lower catalytic activity than the other natural clay catalysts, which all have a considerably larger active surface area. In contrast, the Mg-saponites, which have a much larger active surface area than their zinc-counterparts, have similar catalytic activities as the Zn-saponites. Clearly, there must be other features, which contribute to the differences in the catalytic activity.

A comparison of the results obtained for 1,2-octanediol **9** and 2-hexyloxirane reveals that the outcome is rather similar, but not the same. The major differences were encountered for HA-SHPV, B698D-24 and the saponites with H^+ as the interlayer cation, where the conversions were substantially higher for the epoxide than for the diol. 1-Octyne **12** was generated to a moderate extent from the epoxide, whereas from the diol **9** only minute amounts of this alkyne were produced. The octyne is obtained by a dehydration process; possibly the water released during the Pinacol rearrangement blocks this dehydration in the case of diol **9**. It should be noted that

the liberated water during the Pinacol rearrangement influences the formation of octanal only marginally. Clearly, no catalyst deactivation has occurred.

6.2.3 Pinacol Rearrangement of 2-phenyl-1,2-propanediol

In this Section a diol is investigated having both an aliphatic and an aryl substituent, viz. 2-phenyl-1,2-propanediol **13**. Control experiments, without catalysts, showed that **13** is not very reactive under thermal conditions, as only 15% was converted at 400°C (Table 6.7, entry 3). The main products were identified as 2-phenylpropanal **14** and 1-phenyl-2-propanone **15** (Scheme 6.6). In Table 6.7 the results obtained in the Pinacol rearrangement of **13** under catalytic FVT conditions using various solid acid catalysts are collected.

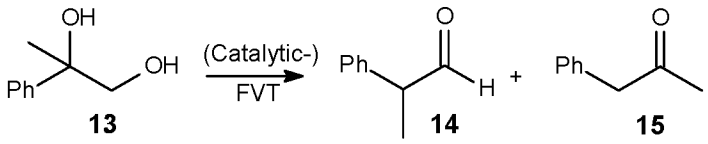

13 **14** **15**

Scheme 6.6 *Rearrangement of 2-phenyl-1,2-propanediol* **13** *under Catalytic FVT conditions*

Also here five runs were performed using the same batch of catalyst while the reaction temperature was varied according to a hysteresis loop. For four catalysts, viz. F-105SF, montmorillonite K-10, B698D-24 and HA-SHPV, the conversions obtained were very high during all five runs and often even reached completion. The other solid acid catalysts used (montmorillonite KSF, Mg- and Zn-saponite\H$^+$) showed clear signs of deactivation as the conversions were markedly lower when a certain temperature was used again in a later run. The conversions observed in the Pinacol rearrangement of **13** were substantially higher than for the aliphatic diol **9**, and in the same range as for aryl-substituted diol **6**. This shows that the presence of the aryl substituent enhances the reactivity of a diol in this rearrangement significantly by stabilizing the cationic intermediate.

The selectivity for the products **14** and **15** correlated nicely with the reaction temperature. 2-Phenylpropanal **14**, the main product in most cases, was formed in selectivities of up to 100%, especially at lower reaction temperatures. At higher temperatures the selectivity for the aldehyde was notably lower particularly for the amorphous alumina B698D-24 and the amorphous silica-alumina HA-SHPV, where the selectivities for **14** varied between 96 and 13%, and between 96 and 9%, respectively. 1-Phenyl-2-propanone **15** was mostly obtained with low selectivities at 200°C, but at 400°C appreciable amounts of this ketone were obtained. These observations are in accordance with the stabilizing effect of the phenyl group on the adjacent carbocation that is produced by expelling the hydroxyl group on that particular carbon. Eventually, this stabilized carbocation leads to aldehyde **14**. The

route via the alternative primary carbocation leading to ketone **15** is clearly less favored.

Table 6.7 *Rearrangement of 2-phenyl-1,2-propanediol* **13** *under thermal and Catalytic FVT conditions using various solid acid catalysts*

Entry[d]	Catalyst[a]	Temp.[b] (°C)	Conversion[c] (%)	Selectivity[c] (%)	
				14	**15**
1	None (blanc)	200	6		
2		300	2	100	
3		400	15	86	
4	F-105SF	400	100	49	51
5		300	100	92	8
6		200	100	100	
7		300	99	94	4
8		400	99	78	21
9	Montmorillonite K-10	400	100	72	29
10		300	98	93	4
11		200	97	100	
12		300	97	98	2
13		400	100	91	9
14	Montmorillonite KSF	400	94	76	4
15		300	64	88	10
16		200	31	100	
17		300	61	89	
18		400	68	89	
19	Mg-saponite\H$^+$	400	94	74	16
20		300	66	83	4
21		200	36	97	
22		300	54	83	3
23		400	70	80	4
24	Zn-saponite\H$^+$	400	82	82	3
25		300	46	91	
26		200	19	97	
27		300	31	89	
28		400	55	81	
29	B698-D24	400	98	13	62
30		300	100	56	31
31		200	100	96	3
32		300	100	75	24
33		400	100	25	60
34	HA-SHPV	400	99	9	55
35		300	100	61	26
36		200	100	96	2
37		300	100	83	17
38		400	100	32	57

[a] 100 mg of catalyst was used and 100 mg of substrate per run. [b] Oven temperature; The substrate was vaporized at 100°C; 0.05 mbar pressure. [c] Conversions and selectivities determined by GC. [d] The best results are marked by shading of the entry number.

6.2.4 Pinacol Rearrangement of α-pinane *cis*-diol

In this section the behavior of α-pinane cis-diol **18**, which is a synthetic equivalent of α-pinene oxide **16**, is studied under catalytic FVT conditions using the same set of solid acid catalysts. The Pinacol rearrangement of diol **18** is expected to proceed via the same type of intermediates as proposed in the rearrangement of epoxide **16**. However, the product composition may differ significantly. The focus will be especially on the selectivity for campholenic aldehyde **17**, which is an important intermediate in the flavor and fragrance industry.

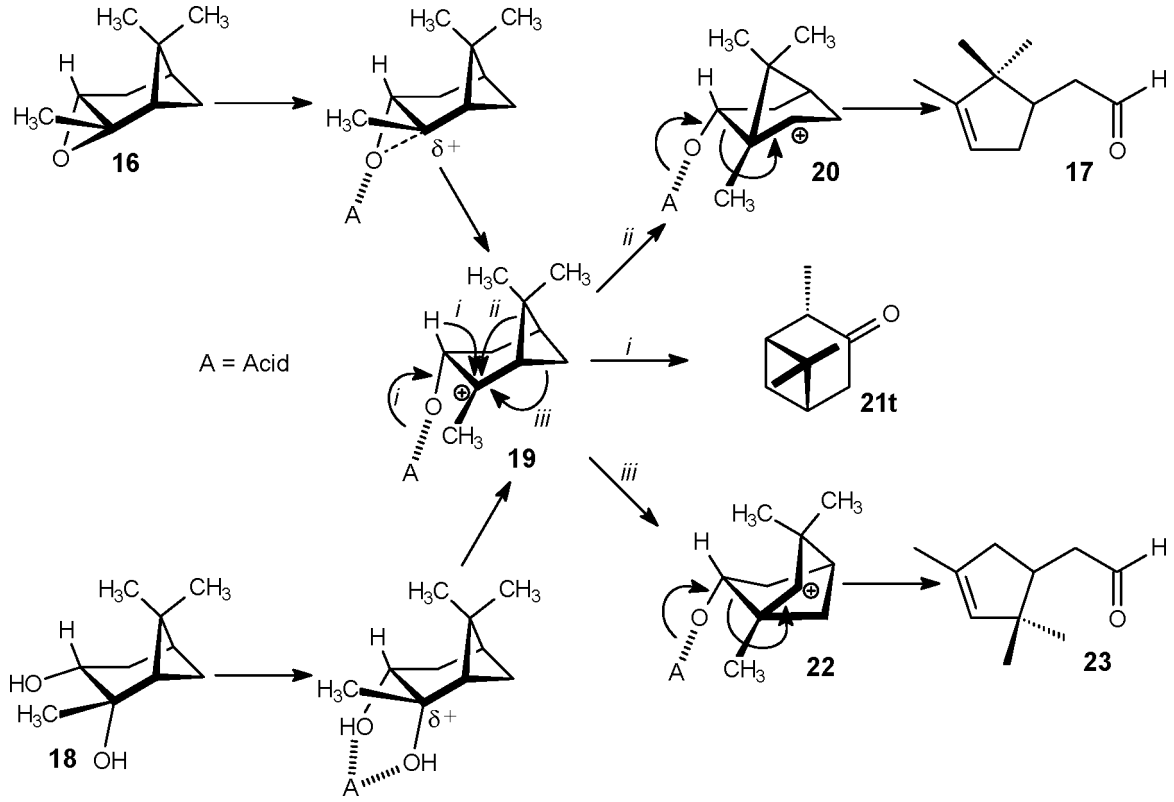

Scheme 6.7 *Isomerization of α-pinene oxide* **16** *and α-pinane diol* **18**

The main reaction pathways and the resulting reaction products for the acid-catalyzed isomerization of α-pinene oxide **16**[14] and α-pinane *cis*-diol **18** are depicted in Scheme 6.7. The top half of the scheme has already been discussed in Chapter 4 (Scheme 4.8). In the bottom half the conceivable intermediates from the diol **18** are given. Here, the essential point is that interaction of the diol with the acidic sites of the catalysts leads to tertiary carbocation **19** by the preferential removal of the tertiary hydroxyl group. The same intermediate is generated from epoxide **16**, whereby the two substrates are integrated in one scheme. The formation of a secondary carbocation by elimination of the alternative hydroxy group leads to other products. However, it may be expected, due to the lower stability of this secondary carbocation, that these side reactions will be of less importance. On the basis of this scheme, the products campholenic aldehyde **17**, pinocamphone **21** and 2-(2,2,4-

trimethyl-3-cyclopentenyl)acetaldehyde **23** are predicted. In actual practice the product mixture contained the three just mentioned compounds and, in addition, α-pinene oxide **16**, *p*-cymene **24**, pinocarveol **25** and exo-isocamphanone **26**. The formation of epoxide **16** can be accounted for by elimination of water from diol **18**, probably via intermediate **19**, by a reversal of the steps **16** to **19**. Compounds **24**, **25** and **26** were also encountered in the catalytic FVT reaction of epoxide **16** and can be explained as described in Chapter 4 (Section 4.2.4, Scheme 4.9 and 4.10).

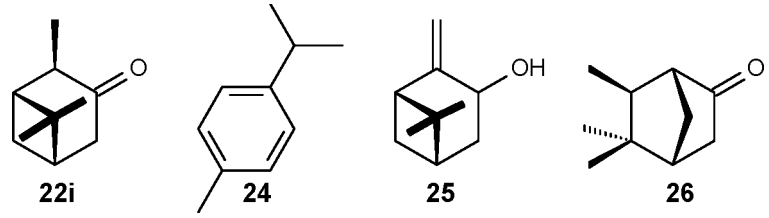

22i **24** **25** **26**

Control experiments, in the absence of catalysts, showed that *cis*-diol **18** is not very reactive under thermal conditions, as only 2% was converted at 300°C and 9% at 400°C. Only at more elevated reaction temperatures (i.e. 500-700°C) a substantial conversion could be accomplished (Table 6.8, entries 1-7). The main products were campholenic aldehyde **17** and pinocamphanone **21**, while compounds **16**, **24**, **23**, **25** and **26** were identified as minor products. The results obtained in the rearrangement of α-pinane *cis*-diol **18** under catalytic FVT conditions with various solid acid catalysts are collected in Table 6.8.

The same catalyst batch was used in seven consecutive runs in this rearrangement of **18** while the reaction temperature was varied according to a hysteresis loop. At 400 and 300°C high conversions were obtained with natural clay catalysts and amorphous (silica) aluminas, but the use of the two saponites gave only moderate to poor conversions at 300°C, while at 400°C also these catalysts showed a high activity. The saponites showed almost no activity at 200 and 150°C. Deactivation of the catalysts in the reaction of diol **18** was also observed, but only to a small extent as the conversions were slightly lower when a given reaction temperature was used again in a later run. Visually, the catalysts changed color from white or light gray to black after use. Using other substrates these signs of deactivation were usually more pronounced (Sections 6.2.1 - 6.2.3, and with epoxides in Chapter 4). The observation that the conversion hardly decreased after several runs with the same catalyst batch supports the assumption that the release of water during the Pinacol rearrangement does not block the catalytic sites. Water released in the Pinacol rearrangement is supposed to desorb as easy from the catalytic sites under the FVT conditions as did the physisorbed water during the catalyst pre-treatment at 400°C and 0.05 mbar.

Table 6.8 *Rearrangement of α-pinane diol* **18** *under Catalytic FVT conditions using various solid acid catalysts*

Entry	Catalyst[a]	Temp.[b] (°C)	Conversion[c] (%)	Selectivity[c] (%)								
				17	16	24	23	25	21t	21i	26	Others[d]
1	none	150	2									100
2		200	1									100
3		300	2	25					40			35
4		400	9	24	7		3	9	43			15
5		500	61	23	6	1	3	5	47	3		9
6		600	85	18	2	1	4	1	31	2	1	38
7		700	90	17	6	2	4	5	6		2	58
8	F-105SF	400	100	5	3	27	3		14		9	40
9		300	100	12	10	14	6		19		15	25
10		200	96	23	10	14	17		14		3	19
11		150	83	20	1	8	21		6	1		41
12		200	82	29	5	9	18	1	16	2	2	17
13		300	99	20	5	10	7		27		15	16
14		400	100	10	6	20	4	1	17		15	27
15	Montm. K-10	400	100	9	6	31	4		17		12	22
16		300	99	21	7	10	7		27	6	11	11
17		200	80	28	5	10	18	1	18	1	2	15
18		150	41	22	1	7	21		8	1		36
19		200	57	28	3	6	15		22		2	24
20		300	98	26	3	7	7		31		10	15
21		400	100	14	5	14	5		22		16	25
22	Mg-saponite\ Al^{3+}	400	100	18	7	26	9		19		7	14
23		300	81	29	4	13	15	1	21		4	13
24		200	21	28	3	8	16	2	23		1	18
25		150	6	19		8	15		17			41
26		200	15	27	2	5	14	3	26	2	2	18
27		300	73	30	2	10	14	2	25	3	4	10
28		400	96	24	4	15	11	1	25	5	7	8
29	Mg-saponite\ H^{+}	400	92	25	5	15	14		23		2	10
30		300	25	29	2	9	17	2	20		1	17
31		200	2									100
32		150	2									100
33		200	2	17			11		17			56
34		300	20	31	2	7	18	3	21	2	1	14
35		400	71	29	3	9	15	2	25	3	2	12
36	B698D-24	400	100	10	3	23	4		19		11	24
37		300	95	21	3	11	7	1	25		13	13
38		200	64	27	2	7	13	2	25		6	14
39		150	32	22	1	4	17		18			29
40		200	56	26	1	4	10	2	27	3	6	18
41		300	93	22	2	9	6	1	28	6	14	12
42		400	99	15	4	19	5	1	23	5	11	16
43	HA-SHPV	400	100	13	4	18	4		22		11	21
44		300	92	25	2	8	6		30		11	11
45		200	55	28	1	6	11		29		5	15
46		150	19	23			14		27			30
47		200	50	23	1	3	8		26	3	5	30
48		300	87	26	1	6	6	2	33	6	11	8
49		400	98	19	3	10	4	1	28	7	11	14

[a] 100 mg of catalyst 100 mg of substrate per run. [b] Oven temperature; The substrate was vaporized at 90°C. [c] Conversions and selectivities determined by GC. [d] 'others' refers to various unidentified products.

The selectivity for campholenic aldehyde **17** ranged from 5 to 31% for the catalysts employed (Table 6.8). In general, the selectivity towards **17** was low to moderate at high reaction temperatures and somewhat higher at lower temperatures. This observation holds for all the catalysts, but the yields of **17** never reached the values close to those found for the selectivities because the conversions dropped markedly at these lower reaction temperatures.
A second major product was *trans*-pinocamphone **21t** (Scheme 6.7), which was formed especially at higher temperatures, although this temperature dependence differed for each catalyst. The selectivities for **21t** ranged between 6 and 33%. *Iso*-pinocamphone **21i** was also formed, particularly at higher temperatures. Compound **21i** cannot be produced directly from the carbocationic intermediate **19** but is probably formed via epimerization of **21t** (see discussion in Chapter 4, Section 4.2.4).
The isomer of **17**, 2-(2,2,4-trimethyl-3-cyclopentenyl)acetaldehyde **23**, is another main product (Scheme 6.7). The selectivity for **23** correlates with the reaction temperature as higher selectivities were found at lower temperatures, and vice versa. The selectivity for **23** ranged from 4 to 21%. The selectivities for *p*-cymene **24**, pinocarveol **25** and exo-isocamphanone **26** were the other way around: the largest fractions of these three compounds were obtained at the more elevated temperatures. Although their temperature dependence is similar, the selectivities for these products did differ significantly, viz. for **24**: 3-31%, for **26**: 0-16%, and for **25**: 3% throughout.

It is of interest to compare the results obtained for epoxide **16** (see Chapter 4) and diol **18** in these catalytic FVT experiments. The data shown in the tables reveal that the results are similar, but not identical. Starting from the epoxide the conversions are generally much higher. Especially at lower temperatures the difference is substantial. Starting from the epoxide the product ratio of the two major products, viz. campholenic aldehyde **17** and *trans*-pinocamphone **21t** is mostly ca. 2:1, whereas for the diol this ratio amounts to ca. 1:1. This is the most striking difference between the diol and the epoxide experiments in terms of selectivity, which must find its origin in the nature of the respective reaction intermediates or in the binding of the substrates to the catalytic surface. With regard to the latter possibility a considerable difference can be envisaged, viz. the diol **8** is in fact bound to the catalyst surface in a bidentate manner, whereas the epoxide **16** is only attached via the epoxide oxygen (monodentate). Of course, the intrinsic difference between the diol and the epoxide has to be taken into account as well. The annelated oxirane ring in **16** enforces a distinct conformation of the cyclohexene skeleton; a strain effect that is absent in the diol (Scheme 6.8). Thus, a higher reactivity is expected for the epoxide. Assuming that the alkyl and hydride shift take place in a concerted manner, the difference in

attachment to the surface and the effect of the annelation strain in the epoxide, may result in a pronounced migration rate difference of the alkyl group and the hydride, leading to different product ratios. However, why the alkyl shift is preferred over the hydride shift in the case of the epoxide, is not clear.

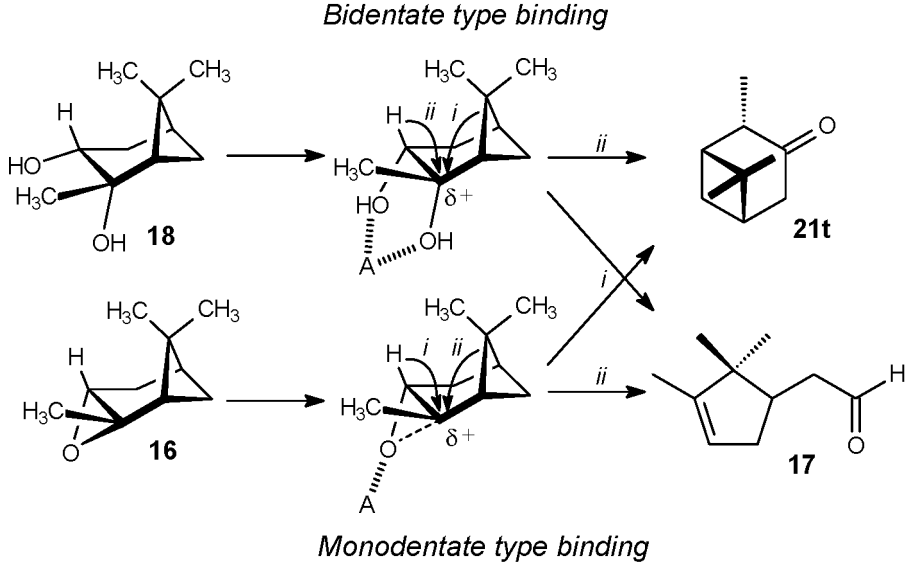

Scheme 6.8 *Isomerization of α-pinene oxide* **16** *and α-pinane diol* **18** *via different intermediates*

To shed some light on the effect of the bidentate binding of the diol, a model reaction was designed involving the behavior of α-pinane sulfite **27** under catalytic FVT conditions. This sulfite **27** to a certain extent is a model compound for the bidentate binding of the diol to the catalyst surface. It is well known that glycol sulfites readily loose sulfur dioxide when thermolyzed.[15] The annelation strain of the sulfite is minimal. Assuming monodentate binding of **27** at the catalytic surface, loss of sulfur dioxide during thermolysis and either a concurrent alkyl migration or hydride shift to the tertiary incipient carbocationic center leads to the respective products **17** and **21t**. This process, which is assumed to have a concerted character, bears some analogy with the product formation from the diol.

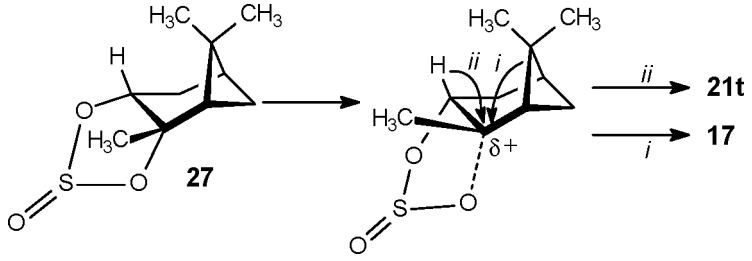

Scheme 6.9 *Reaction of α-pinane sulfite* **27** *and a mechanism leading to two of its products*

The results obtained for the rearrangement of α-pinane sulfite **27** under catalytic FVT conditions using several solid acid catalysts are collected in Table 6.9. In the absence of a catalyst the thermolysis needs to be carried out at temperatures higher than 400°C. In the presence of catalysts excellent conversions were obtained even at

temperatures as low as 200°C. Besides products **17** and **21t**, the same series of compounds is obtained as for the thermolysis of diol **18** and epoxide **16**. It is quite rewarding to find that at maximum conversions the product ratio of **17** and **21t** was always about 1:1, very similar to that observed for the thermolysis of diol **18**. This observation gives some support to mechanistic discussions rationalizing the difference in behavior of epoxide **16** and diol **18** under catalytic FVT conditions.

Table 6.9 *Reaction of α-pinane sulfite* **27** *under Catalytic FVT conditions using various solid acid catalysts*

Entry	Catalyst[a]	Temp.[b] (°C)	Conversion[c] (%)	Selectivity[c] (%)									
				17	**16**	**24**	**23**	**25**	**21t**	**21c**	**26**	**18**	**Others[d]**
1	None (blanc)	200	4										100
2		300	4	35	9	2	5		35				14
3		400	27	19	1	1	3	1	68				7
4		500	95	4		1	1		92				2
5		600	100	2	5		4	1	83				5
6	F-105SF	400	100	12	4	30	5		15	3	8		24
7		300	97	8	4	29	3		17		8	9	22
8		200	81	10	3	38	4		8	1	2	12	21
9		300	96	10	3	26	4		19	4	7	11	15
10		400	98	8	2	22	4		23	5	11	12	14
11	Montm. K-10	400	100	9	5	30	2		14	4	13		24
12		300	100	18	11	26	3		15	4	13		11
13		200	91	28	9	34	4		10	1	3		11
14		300	100	22	9	21	4		17	4	14		10
15		400	100	11	5	27	3		16	5	15		18
16	Mg-saponite\Al^{3+}	400	100	17	6	31	4		17	4	8		13
17		300	99	26	6	28	6		16	3	7		9
18		200	81	19	2	23	4		5	1	1		44
19		300	95	29	4	26	8		18		5		11
20		400	100	22	4	25	5		21	5	9		8
21	Mg-saponite\H^{+}	400	100	24	6	22	7		27	5	3		8
22		300	71	28	3	25	11		22	1	1		9
23		200	11	35	4	30	13		14				4
24		300	48	31	2	24	13		24				5
25		400	97	22	1	16	7		23	2	1		28
26	B698D-24	400	99	9	2	37	1		12	2	7		29
27		300	97	15	3	36	3		12	4	13		16
28		200	87	23	2	37	3		9	1	9		16
29		300	96	15	2	32	3		14	4	14		16
30		400	98	13	3	32	3		17	4	11		17

[a] 100 mg of catalyst was used and 100 mg of substrate per run. [b] Oven temperature; The substrate was vaporized at 70°C. [c] Conversions and selectivities determined by GC. [d] 'others' refers to various unidentified products.

6.3 CONCLUSIONS

The Pinacol rearrangement of a series of diols, viz. 1-phenyl-1,2-ethanediol **6**, 1,2-octane diol **9**, 2-phenyl-1,2-propane diol **13** and α-pinane *cis*-diol **18**, was investigated under catalytic FVT conditions employing various natural and synthetic clays as well as amorphous (silica) aluminas as the solid acids. Rearrangement of 1-phenyl-1,2-

ethanediol **6** preferentially leads to the rather labile phenylacetaldehyde **7** in very high selectivities. Thermolysis of 1,2-octane diol **9** produced three rearrangement products, viz. octanal **10**, 2-octanone **11** and 1-octyne **12** of which the aldehyde is the major product. Thermolysis of 2-phenyl-1,2-propane diol **13** gave two products, viz. 2-phenylpropanal **14** and 1-phenyl-2-propanone **15** of which the aldehyde is the predominant one, especially at lower thermolysis temperatures. At higher temperatures substantial amounts of ketone **15** were formed. α-Pinane *cis*-diol **18** gave a range of products of which campholenic aldehyde **17** and pinocamphone **21** are the most important ones. The results of the thermal rearrangement of diols were compared with those of the structurally related epoxides, viz. styrene oxide, 2-hexyloxirane and α-pinane oxide **16**, respectively. The outcome of the thermolysis reaction of diols and epoxides are similar, but not identical. For epoxides the conversions were usually higher, especially at lower thermolysis temperatures. The resulting product mixture had in most cases a different composition. This was most pronounced with 1,2-octane diol **9** and α-pinane *cis*-diol **18**. For diol **9** the aldehyde **10** was the main product whereas for the corresponding epoxide considerable amounts of 1-octyne (a dehydration product) were formed. Comparison of thermolysis of α-pinene oxide **16** and α-pinane *cis*-diol **18** revealed that the ratio of the produced campholenic aldehyde **17** and trans-pinocamphone **21t** is ca. 2:1 for the epoxide, and about 1:1 for the diol. This difference was tentatively explained by the different type of binding to the catalyst surface, bidentate-like for the diol and in a monodentate manner for the epoxide. Moreover, the effect of the annelation strain in epoxide **16** on the reactivity of this compound has to be taken into account. It may effect the formation of the respective reaction intermediates. Some support for the binding modes was obtained from the results of the thermolysis of α-pinane sulfite **27**, which serves as a model for the bidentate binding of diol **18**.

The overall conclusions are that the highest conversions are obtained for the natural clays F-13, F-105SF, F-24, F-25, montmorillonite K-10, amorphous alumina B698D-24, and the amorphous silica-alumina HA-SHPV as solid acid catalysts in catalytic FVT. There was no consistent correlation between the acidity of the catalysts and their catalytic activity. The active surface area of the catalysts may have some influence on the catalyst performance, but this effect is not very large.

Industrial perspective

In this chapter the use of the Pinacol rearrangement applying solid acis in the gas phase (catalytic FVT) for the synthesis of fine chemicals was studied. To this aim two industrially important products were chosen, namely phenylacetaldehyde **7** and campholenic aldehyde **17**. It was shown that the first aldehyde can conveniently be

prepared from 1-phenyl-1,2-ethane diol **6** in high yields (99%) using various solid acid catalysts at moderate reaction temperatures. The yield and purity of **7** obtained during this catalytic thermolysis process is much higher than in the commercial process, which involves the oxidation of the 2-phenyl-1-ethanol. Due to the lability of the product the purity of the aldehyde is 85% at best in the oxidation process.[16] Synthesis of phenylacetaldehyde **7** from styrene oxide, which has been described in Chapter 4, has similar high selectivities for the aldehyde. In view of the better availability of styrene oxide this route is strongly preferred.

Campholenic aldehyde **17** is one of the major products from the catalytic thermolysis of α-pinane *cis*-diol **18**. A highest selectivity of 31% is obtained here. This reaction is less attractive for the synthesis of campholenic aldehyde **17** than the solid acid catalyzed thermolysis of α-pinene oxide **16**. However, both thermolysis approaches cannot compete with the current commercial process, which involves rearrangement of α-pinene oxide **16** in benzene with $ZnCl_2$ as the catalyst.[17]

In spite of the conclusion that catalytic FVT in its current state of development is not an alternative for the current processes, benefits of the catalytic flash vacuum thermolysis using solid acids are clearly the absence of any aggressive reagent and solvent, which improves the ease and safety of operation. Moreover, with the methodology described here no waste salts are produced.

6.4 EXPERIMENTAL SECTION

General remarks

Reported percentages are molar percentages (% $^{m}/_{m}$). Gas chromatographic (GC) analyses were performed on a Hewlett-Packard HP5890II gas chromatograph (flame ionization detector, FID) equipped with an HP-3396II integrator, using a capillary column (HP-1, 25 m x 0.31 mm x 0.17 μm) and nitrogen at 2 ml/min (0.5 atm) as the carrier gas or on a Hewlett-Packard HP6890 gas chromatograph (flame ionization detector, FID) equipped with an HP-6890 integrator, using a capillary column (HP-1, 25 m x 0.32 mm x 0.17 μm) and hydrogen at 3.2 ml/min (0.53 atm) as the carrier gas. The GC temperature programs employed were either from 75°C (5 min isothermal) to 250°C at 15°C/min followed by 3 min at 250°C (isothermal) or from 100°C to 250°C at 15°C/min followed by 10 min at 250°C (isothermal). FT-IR spectra were recorded on a Biorad FTS-25 spectrophotometer. ^{1}H- and ^{13}C-NMR spectra were recorded on a Bruker AM-400 and a Bruker AC-100 at T=298 K. Chemical shifts were reported against $Si(CH_3)_4$. Mass spectrometric (MS) analyses were measured with a double focussing VG Analytical 7070E mass spectrometer or a Varian Saturn II GC-MS set-up equipped with an HP-1 capillary column and Varian 8100 autosampler.

Column chromatography at ambient pressure was carried out using Merck Kieselgel 60. Thin layer chromatography (TLC) was carried out on Merck precoated silicagel 60 F254 plates (0.25 mm) using the eluents indicated. Spots were visualized with UV or molybdate spray.

Dichloromethane was distilled from calcium hydride. Commercially available starting materials were used as received.

Origin of the catalysts

Amorphous alumina B698D-24, amorphous silica-alumina B698D-25 and the acid-treated natural F-clays were received as generous gifts from Engelhard De Meern B.V. Amorphous silica-alumina HA-SHPV was obtained as a generous gift from AKZO Nobel Chemicals. Commercial natural clays montmorillonite K-10 and montmorillonite KSF are produced by Süd Chemie and were obtained via Aldrich Chemical Company. Prior to use montmorillonite K-10 was washed in hot demineralized water and subsequently dried to remove any residual mineral acid that may have been present due to the acid-treatment during its preparation. Synthetic clay materials were prepared and donated by the Department of Inorganic Chemistry and Heterogeneous Catalysis of the University of Utrecht. All saponites used had a Si/Al ratio of 7.9 and are described as M-saponite\C^+, where M represents the octahedral cation and C^+ the interlayer cation.

All catalysts were pressed (3 tons), sieved into the desired particle size (150-425 μm), and stored at ambient pressure. Catalysts were used after a pre-treatment: An amount of catalyst was mounted onto a quartz porous filter in the middle of a quartz (FVT-)tube. Using the catalytic Flash Vacuum Thermolysis set-up (*vide infra*) the catalyst was equilibrated at a temperature of 400°C and a vacuum of 0.05 mbar during 15-20 min to remove physisorbed water.

Catalytic Flash Vacuum Thermolysis set-up

The Catalytic Flash Vacuum Thermolysis apparatus, as developed at the Department of Organic Chemistry of the University of Nijmegen, is described and schematically depicted in the Experimental Section of Chapter 4.

General procedure for catalytic flash vacuum thermolysis experiments

The Catalytic Flash Vacuum Thermolysis set-up described above was used. Typically, 100 mg of a fractured catalyst with a sieve fraction of 150-425 μm was placed on a porous filter in the center of the quartz tube. The catalyst was equilibrated at a temperature of 400°C and a vacuum of 0.05 mbar during 15-20 min to remove physisorbed water. The temperature of the oven was adjusted to the desired temperature. The substrate was placed in the sample flask. The vacuum gauge was carefully opened until maximum vacuum was achieved after which the receiving cooler was filled with CO_2/acetone (-78°C). The substrate (usually 50 or 100 mg) was vaporized at room temperature or with the aid of a sublimation oven, at such a rate that evaporation was complete in 45 min. After another 10 min, the system was flushed with nitrogen. Products were rinsed from the receiving cooler with an appropriate solvent and analyzed by gas chromatography. Thermal (control) experiments were carried out under identical conditions, however, without a catalyst.

Catalytic-FVT of 1-phenyl-1,2-ethanediol ***6***

Experiments were carried out according to the general procedure described above. 1-phenyl-1,2-ethanediol **6** was vaporized at 100°C and thermolyzed over 100 mg of catalyst in about 40 min. The products were rinsed from the receiving cooler with dichloromethane and analyzed by gas chromatography. Results are collected in Table 6.1, Table 6.2 and Table 6.3.

Catalytic-FVT of 1,2-octane diol ***9***

Experiments were carried out according to the general procedure described above. 1,2-Octene diol **9** was vaporized at 100°C and thermolyzed over 100 mg of catalyst in about 60 min. The products were rinsed from the receiving cooler with dichloromethane and analyzed by gas chromatography. Results are collected in Table 6.4, Table 6.5 and Table 6.6.

Catalytic-FVT of 2-phenyl-1,2-propane diol ***13***

Experiments were carried out according to the general procedure described above. 2-Phenyl-1,2-propane diol **13** was vaporized at 100°C and thermolyzed over 100 mg of catalyst in about 60 min. The products were rinsed from the receiving cooler with dichloromethane and analyzed by gas chromatography. Results are collected in Table 6.7.

Catalytic-FVT of α-pinane cis-*diol* ***18***

Experiments were carried out according to the general procedure described above. α-Pinane *cis*-diol **18** was vaporized at 90°C and thermolyzed over 100 mg of catalyst in about 50 min. The products were rinsed from the receiving cooler with dichloromethane and analyzed by gas chromatography. Results are collected in Table 6.8. Selected samples were analyzed using GC-MS configured with an appropriate library at IFF.

α-Pinane sulfite ***27***

The synthesis of **27** was carried out following a literature procedure.[15a] Thionyl chloride (2.98 g) in diethyl ether (10 ml) was gradually added to a solution of α-pinane cis-diol **18** (4.0 g, 23.5 mmol) and pyridine (5.7 g) in diethyl ether (75 ml) at 0°C. The mixture was stirred for an additional hour and filtered. Extraction of the inorganic residue with water (on the filter) left some organic material undissolved and this material was dissolved in diethyl ether. The combined ethereal solutions were washed with water, dried ($MgSO_4$) and concentrated *in vacuo*. The crude product was purified by column chromatography (hexane: ethyl acetate = 20:1) and subsequently recrystallized from hexane to yield **27** (3.41 g, 67%) as white crystals. M.p.: 92°C.

Analytical data are in agreement with literature.[18,19]

Catalytic-FVT of α-pinane sulfite ***27***

Experiments were carried out according to the general procedure described above. α-Pinane sulfite **27** was vaporized at 70°C and thermolyzed over 100 mg of catalyst in about 50 min. The products were rinsed from the receiving cooler with dichloromethane and analyzed by gas chromatography. Results are collected in Table 6.9.

6.5 REFERENCES

1 Rickborn, B. 'The Pinacol Rearrangement' in *Comprehensive Organic Synthesis; Carbon-Carbon σ-Bond Formation,* Trost, B.M. Ed., Vol. 3, Pergamon Press, Oxford, 1991, Section 3.2.

2 Fittig, R. *Justus Liebigs Ann. Chem.* **1860**, *114*, 54.

3 Adams, R.; Adams, E.W. *Org. Synth.* **1925**, *5*, 87.

4 Allen, C.F.R.H.; Bell, A. *Org. Synth., Coll. Vol.* **1955**, *3*, 312.

5 a) Gebhart jr., H.J.; Adams, K.H. *J. Am. Chem. Soc.* **1954**, *76*, 3925. b) Matsumoto, K. *Tetrahedron* **1968**, *24*, 6851.; c) Pocker, Y.; Ronald, B.P. *J. Am. Chem. Soc.* **1970**, *92*, 3385.

6 Collins, C.J.; Eastham, J.F. in *The Chemistry of Functional Groups; The Carbonyl Group*, Patai, S. Ed., Wiley-Interscience, New York, 1966, Chapter 15.

7 Collins, C.J. *Q. Rev.* **1960**, *14*, 357.

8 Stiles, M.; Mayer, R.P. *J. Am. Chem. Soc.* **1959**, *81*, 1497.

9 Shono, T.; Fujita, K.; Kumai, S.; Watanabe, T.; Nishiguchi, I. *Tetrahedron Lett.* **1972**, *13*, 3249.

10 Bezouhanova, C.P.; Jabur, F.A. *J. Mol. Catal.* **1994**, *87*, 39.

11 Gutierrez, E.; Ruiz-Hitzky, E. *Mol. Cryst. Liq. Cryst. Inc. Nonlin. Opt.* **1988**, *161*, 453.

12 Jabur, F.A.; Penchev, V.J.; Bezoukhanova, C.P. *J. Chem. Soc., Chem. Commun.* **1994**, 1591.

13 Leliveld, B.R.G.; Kerkhoffs, M.J.H.V.; Broersma, F.A.; van Dillen, J.A.J.; Geus, J.W.; Koningsberger, D.C. *J. Chem. Soc., Faraday Trans.* **1998**, *94*, 315.

14 Erman, W.F. 'Chemistry of the Monoterpenes' in *Studies in Organic Chemistry*, Vol. 11, Part B, Marcel Dekker Inc., New York, 1985, p969.

15 a) Price, C.C.; Berti, G. *J. Am. Chem. Soc.* **1954**, *76*, 1211. b) Berti, G. *J. Am. Chem. Soc.* **1954**, *76*, 1213. c) Price, C.C.; Berti, G. *J. Am. Chem. Soc.* **1954**, *76*, 1207.

16 Personal communication by Dr. J.G. de Vries (DSM).

17 Personal communication by Dr. A.J.A. van der Weerdt (Quest International).

18 a) Coxon, J.M.; Dansted, E.; Hartshorn, M.P.; Richards, K.E. *Tetrahedron* **1968**, *24*, 1193. b) Brice, M.D.; Coxon, J.M.; Dansted, E.; Hartshorn, M.P.; Robinson, W.T. *J. Chem. Soc. D.* **1969**, 356.

19 Hellier, D.G.; Motevalli, M. *Acta Crystallogr. Sect. C: Cryst. Struct. Commun.* **1995**, *51*, 116.

7 RETRO DIELS-ALDER REACTIONS CATALYZED BY SOLID ACIDS

7.1 INTRODUCTION

The Diels-Alder reaction is the addition of an alkene to a 1,3-diene to form a cyclohexene and it is formally called a [4+2]-cycloaddition because 4 π electrons from the diene and 2 π electrons from the alkene (commonly called the dienophile) are directly involved in the bonding change.[1] The reverse reaction, i.e. the formation of a diene and an alkene from a cyclohexene, is called the retro Diels-Alder reaction (Scheme 7.1). The Diels-Alder reaction is a stereospecific and suprafacial addition with respect to both the dienophile as the diene.[1] Generally, the highest occupied molecular orbital (HOMO) of the diene reacts with the lowest unoccupied molecular orbital (HUMO) of the dienophile. An efficient overlap is feasible when these frontier orbitals have the proper geometric configuration and their energy difference is small. Frontier orbital concepts may also serve to explain the very strong catalysis of certain Diels-Alder reactions by Lewis acids.[2] These acids coordinate with a nucleophilic substituent, e.g. a carbonyl function, which is conjugated with the olefinic bond of the dienophile. This coordination leads to an increase of the electron withdrawing capacity of the substituent and decreases the LUMO energy. As a result, the activation energy for cycloaddition is lowered and the reaction rate is enhanced.[1]

Scheme 7.1 *The (retro) Diels-Alder reaction*

The Diels-Alder reaction is probably the most extensively studied organic transformation and has been widely used in the synthesis of natural and unnatural products.[3,4] Also industrially, the Diels-Alder reaction is an extremely important synthetic conversion and is applied in many processes, for example in the preparation of certain insecticides and in coke-forming processes by condensation of various olefins, diolefins and aromatics.[5] Lewis acids that are used traditionally in Diels-Alder reactions include $ZnCl_2$, $SnCl_4$ and $AlCl_3$. Many studies[6] aimed at enhancement of the rate and/or the regio- and stereoselectivity as well as the π-

diastereofacial selectivity of Diels-Alder reactions. These studies include high pressure technique,[7] solvent effects,[8] microwave[9] and ultrasonic activation,[10] enzymes,[11] antibodies,[12] metals,[13] polymer-bound dienophiles[14] and the use of heterogeneous Lewis acids such as alumina,[15] silicagel,[16] silica-aluminas,[17] zeolites,[18] supported Lewis acids[19] and clays.[20]

The retro Diels-Alder reaction is particularly useful as a protecting strategy in those cases where a reactive π-system would interfere with a desired group transformation during modification of either the diene or the dienophile fragment.[21,22] Such a strategy involves *i.* masking of an olefinic or acetylenic bond using the Diels-Alder reaction; *ii.* execution of the desired group transformations of the cycloadduct and *iii.* deprotection using the retro Diels-Alder reaction restoring the unsaturated moiety. The activation barrier for the retro reaction is dependent on various factors. The stability of the diene and the dienophile is important as the equilibrium may be shifted towards fragmentation when the fragments are lower in energy than the cycloadduct. A diene is particularly stabilized when it forms part of an aromatic ring system. Also the release of ring strain and conjugative stabilization of the dienophile are important parameters.[23] For this reason cyclopentadiene has sometimes been replaced by pentavulvene,[24] furan[25] and anthracene.[26] These dienes may be split off in the liquid phase already at 150-200°C, whereas for the release of cyclopentadiene much higher temperatures are required in the gas-phase (viz. 350-600°C[27]). These alternative dienes, however, can not always conveniently be applied in the Diels-Alder reactions, and are therefore less frequently used in the protection of dienophiles than cyclopentadiene.

Lowering of the activation energy of the retro Diels-Alder reaction may also be achieved by the use of catalysts. Catalysts that have been applied successfully include copper (II) salts,[28] sulphonic acid resins,[28] dimethylaluminum chloride[29] and borontrifluoride-etherate [30] in the liquid phase (static thermolysis) and several solid acids in combination with Flash Vacuum Thermolysis (dynamic thermolysis).[31]

The retro Diels-Alder reaction may be accomplished applying either static or dynamic thermolysis. In static thermolysis in the liquid phase the starting material and formed products stay at a high temperature during the whole process. This method is not suitable for the preparation of thermally labile products as they will undergo further intra- as well as intermolecular reactions, leading to complex mixtures.[32] In a dynamic process the substrate is distilled or sublimed through a hot zone, e.g. a quartz tube heated in an oven, and the products formed are trapped at low temperatures immediately after they leave the hot zone. By careful selection of the reaction parameters (dimensions of the hot zone, appropriate temperature, flow and pressure) the substrate can be subjected to adjust the amount of thermal energy

required to undergo the desired reaction. The residence time of the substrate in the hot zone plays a crucial role in determining the optimum product formation. The shorter the contact time the smaller the probability that primary product molecules can undergo secondary reactions. Sufficiently short contact times may be achieved when dynamic or gas flow pyrolysis is performed under low or medium pressures (10^{-1} – 10^{-3} mbar).[32] Due to very short contact times involved this pyrolytic methodology is commonly known as the Flash Vacuum Thermolysis (FVT) or Pyrolysis (FVP) technique[33]. Another important aspect of the use of low pressure is the high dilution implying that intermolecular reactions are highly unlikely, thus preventing the formation of by-products. The temperatures needed to effect the retro Diels-Alder reaction of cyclopentadiene derivatives using the FVT technique are generally quite high (350-600°C). In many cases lower temperatures are desired for the preparation of thermally labile products. Inorder to execute the retro Diels-Alder reactions at lower temperatures and with higher selectivities Van der Waals[31] investigated the possible use of solid acids (zeolites, clays and amorphous (silica) aluminas) as catalysts under Flash Vacuum Thermolysis conditions. This process is denoted as 'Catalytic-Flash Vacuum Thermolysis' (see also Chapters 4 and 6).

In the aforementioned study[31], epoxy enedione **1** was used as model compound and it was shown that the temperature required to effect complete conversion decreased dramatically, viz. from 470°C in the uncatalyzed case to 270°C using an amorphous (silica) alumina (Scheme 7.2). Both clays and zeolites were less efficient catalysts. The selectivity towards **2** was generally very high, but in some cases some unidentified side products were obtained as well. Obviously, cyclopentadiene **3** was also formed in this reaction, but due to its high volatility it can only be trapped in the nitrogen cooled trap protecting the vacuum pump and therefore it does not contaminate the product. (See the Experimental Section in Chapter 4.)

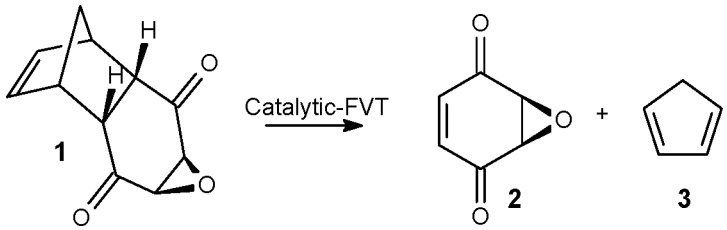

Scheme 7.2 *The retro Diels-Alder reaction of epoxy enedione* **1** *under Catalytic-FVT conditions*

In order to further investigate the application of solid acid catalysts in retro Diels-Alder methodology, the much more sensitive tricyclodecenone epoxides **4** were subjected to catalytic FVT, applying a variety of solid acids.[31] The results were quite unexpected. The thermolysis temperatures needed to achieve complete conversion, decreased from 450°C to 300°C for most catalysts, however, hardly any retro Diels-Alder reaction was observed. Virtually independent of the nature of the substituent

(R) on the 6-position in compounds **4** isomeric cage compounds were obtained. The expected cycloreversion products **6** and **7** were present in only minor amounts (Scheme 7.3). Van der Waals was unable to establish the structure of these cage compounds unambiguously, but proposed structure **5** (for R = CO_2Et, **5a**) based on NMR data.[31]

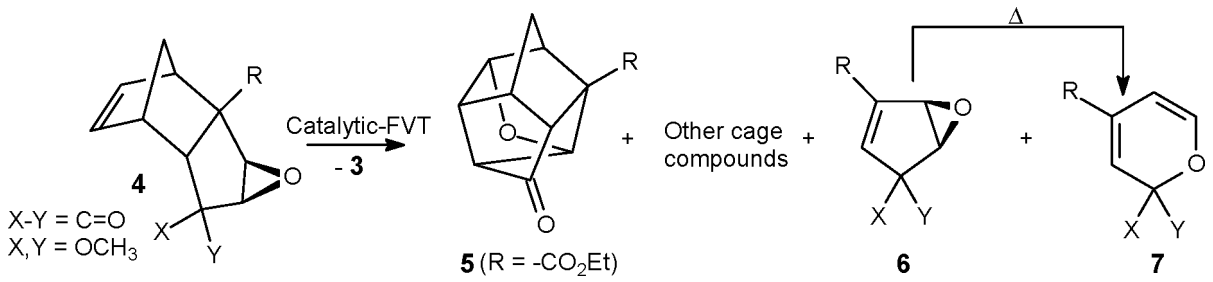

Scheme 7.3 *The retro Diels-Alder reaction of tricyclodecenone epoxides* **4** *and the formation of cage compounds* **5** *under Catalytic-FVT conditions*

Objective and approach

The aim of the present study was to proceed with the investigation of the retro Diels-Alder reaction applying solid acid catalysts both in the liquid and gas phase. Various natural and synthetic clay materials were tested and, in addition, also amorphous (silica) aluminas were employed. In contrast to the studies carried out by Van der Waals (*vide supra*) the catalysts used here were pre-heated at standard conditions to avoid the presence of any surfacial water. A series of simple tricyclic and bicyclic esters **8** and **10** were selected as substrates both in solution and gas phase studies. In addition, the catalytic thermolysis of tricyclodecenone epoxide ester **4a** was studied in more detail in order to unequivocally establish the structure of the produced cage compound and to unravel the mechanistic pathways leading to this product.

7.2 SOLID ACID CATALYZED SOLUTION PHASE RETRO DIELS-ALDER REACTIONS

Solution phase Retro Diels-Alder reactions were carried out using a variety of clay catalysts in toluene as the solvent and at reaction temperatures between 20 and 110°C. Some simple bi- and monocyclic compounds without sensitive substituents were investigated to establish the general applicability of this method. The catalysts used in solution were in most cases not pre-heated prior to their use, with a few exceptions (*vide infra*) where the catalysts were pre-heated at 125°C. The catalysts used in this section comprise an amorphous alumina (B698D-24) and several natural clays. All these materials have a strong to moderate acidity (see Chapter 2) and a specific surface area between 220 and 300 m^2/g, with the exception of Montmorillonite KSF which has a substantial lower surface area (20-40 m^2/g) (see

Chapter 2). In solution phase reactions the diene and dienophile may still stay in contact when one of them is not withdrawn from the equilibrium. In the present study, the equilibrium was shifted into the desired direction by applying a suitable trapping agent, which reacts either with the released diene or dienophile.

The bicyclic 4-oxatricyclodecenedione **8** was used as the first substrate in the cycloreversion reaction. The released cyclopentadiene is trapped with an excess of dimethyl fumarate **9**. The products obtained were maleic anhydride **11** as the released dienophile, compound **10** as the trapped diene and tricyclic lactone **12** as an unexpected product. A variety of catalysts was used in this reaction. A blanc experiment, with no catalyst present, was performed as well. The results are collected in Table 7.1.

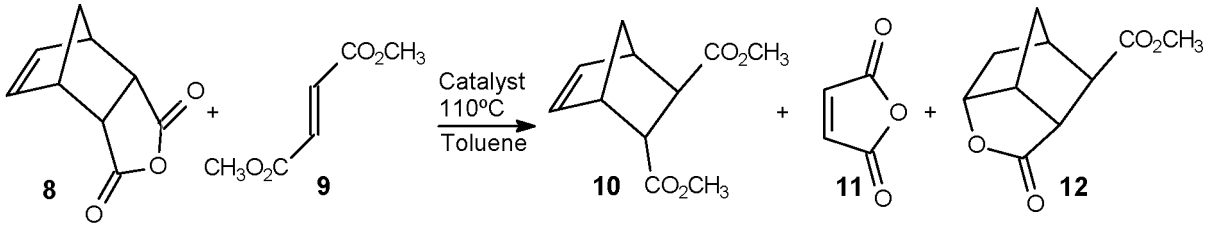

Table 7.1 *The reaction of* **20** *as a function of reaction time and type and amount of catalyst*

Entry	Catalyst[a]	Mass Ratio[b]	Reaction Time (h)	Conversion[c] (%)	Selectivity[c] (%)	
					10 and 11	12
1	None	-	96	7	91	
2	B698D-24	1	150	25	100	
3	B698D-24	2	189	43	100	
4	B698D-24	5	189	74	91	
5	B698D-24	10	69	97	100	
6	Montmorillonite K-10	5	120	45	2	49
7	Montmorillonite KSF	5	93	24	11	22
8	Grade F-1	5	91	23	23	21

[a] Catalyst used as received. [b] Mass ratio stands for the ratio [mass catalyst]/[mass substrate].
[c] Conversions and selectivities determined by GC analysis.

In the uncatalyzed reaction of **8** at 110°C a very low conversion of 7% was observed after a reaction time of 96 h. The major products **10** and **11** (91%) originated from the expected retro Diels-Alder reaction (entry 1). The conversions in the presence of a solid acid catalyst were substantially higher and ranged from 23 to 97% after long reaction times (entries 2-8). The highest selectivities towards products **10** and **11** were observed for the amorphous silica-alumina B698D-24, but the conversions were generally low after a very long reaction time. Only when using a very large amount of this catalyst an almost complete conversion was achieved after 69 h (entry 5). When no trapping agent **9** was added to the reaction mixture only starting material and no retro Diels-Alder products were observed.

In those cases where a clay material was used as the catalyst, an additional product was isolated (entries 6-8), which was characterized as lactone **12**. This lactone is

formed from the trapped diene product **10** by intramolecular addition of the *endo*-ester function to the C_4-C_5 norbornene double bond. This unexpected lactonization reaction of the strained γ,δ-unsaturated methyl ester **10** was investigated in more detail. In order to determine the scope of this transformation also some additional substrates were included in this study. The results for the cyclization reaction of the γ,δ-unsaturated geometrically rigid methyl ester **10** into the lactone **12** are collected in Table 7.2.

Table 7.2 *The lactonization reaction of the rigid γ,δ-unsaturated methyl ester* **10** *into* **12** *as a function of temperature and amount and type of catalyst*

Entry	Catalyst[a]	Mass Ratio[b]	Temp. (°C)	Yield[c](%)
1	Montmorillonite K-10	5	110	91
2	idem	5	75	99
3	idem	5	20	0
4	idem	1	75	7
5	Montmorillonite KSF	5	110	95
6	Grade F-1	5	110	92
7	Grade F-13	5	110	89

[a] Catalyst used as received. [b] Mass ratio stands for the ratio [mass catalyst]/[mass substrate]. [c] Yield determined by GC analysis.

Yields of up to 99% were obtained in the lactonization reaction of **10** depending upon the exact reaction conditions. The data in Table 7.2 reveal that the reaction temperature is an important parameter. When employing montmorillonite K-10 as the catalyst in a mass ratio of 5 and toluene as the solvent the conversion to product **12** was complete after 3 to 4 h, whereas at 70°C this conversion was reached only after 4 days. At room temperature the reaction did not proceed at all. For all four natural clays tested the yields did not vary much and ranged from 89 to 99%.

The reaction of **10** to **12** was also monitored as a function of time. A first order reaction (in substrate **10**) with a rate constant k =4.3 10^{-4} s^{-1} (the average of 3.9 10^{-4} s^{-1} (R = 0.994) and 4.7 10^{-4} s^{-1} (R = 0.997)) was observed applying the following reaction conditions: montmorillonite K-10 in a mass ratio of 5, a temperature of 110°C and toluene as the solvent. When the catalyst montmorillonite K-10 was re-used for a second time a slightly lower rate constant k = 2.6 10^{-4} s^{-1} (R = 0.999) was found (95% conversion in 3 h instead of 2 h). In Figure 7.1 the fraction of **10** that is still present in the reaction mixture is plotted as a function of time to determine the rate constants.

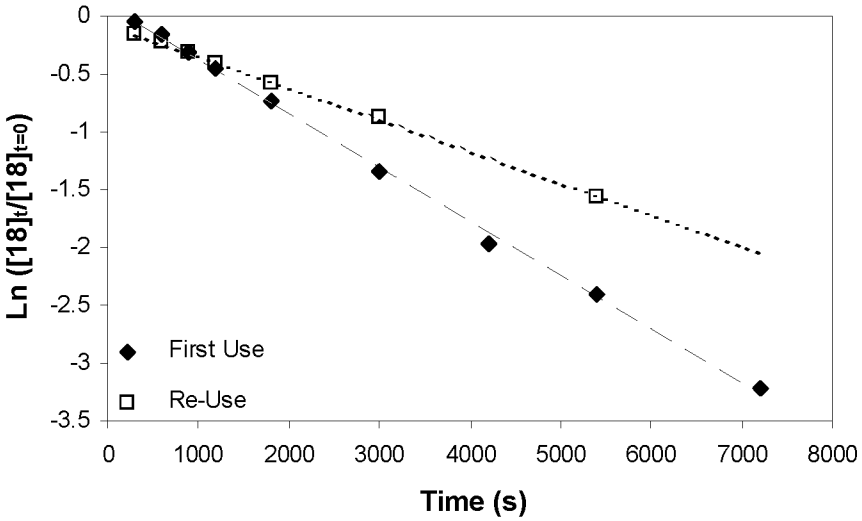

Figure 7.1 *The conversion of the reaction from* **10** *to* **12** *displaced as* $ln([18]_t/[18]_{t=0})$ *as a function of time to determine the reaction constant for both fresh and re-used catalyst. Fresh catalyst:* $k = 4.7.10^{-4}$ s^{-1} ($R^2 = 0.9985$); *Re-used catalyst:* $k = 2.7.10^{-4}$ s^{-1} ($R^2 = 0.9991$); *Reaction conditions: montmorillonite K-10 in mass ratio of 5, toluene as the solvent and a temperature of 110°C.*

When water (0.4 mass equivalent) was added to the reaction mixture, a somewhat lower rate constant was measured (k = 2.0 10^{-4} s^{-1}, R^2 = 0.997). This clearly indicates that a small amount of water does not inhibit the catalytic performance in this transformation, in contrast to what is often seen when clay catalysts are used (cf. Chapter 3 and 4). When the reaction conditions were modified such that water was excluded from the system (nitrogen atmosphere, clay catalyst dried at 125°C prior to use and not allowed to come into contact with air) a rate constant of k = 1.5 10^{-4} s^{-1} (R = 0.954) was observed. However, the observed selectivities with respect to **12** were considerably lower, viz. 63 to 23%, whereas normally the selectivities ranged from 90 to 95%. The drop in selectivity in the absent of water gives a clear support to the proposed reaction mechanism. In this mechanism, as depicted in Scheme 7.4, a Brønsted acidic surface site of the clay acts as a proton donor to the double bond. The electronegative oxygen of the ester moiety binds to the resulting aliphatic carbocation. Upon the addition of water and the expulsion of methanol, lactone **12** is obtained.

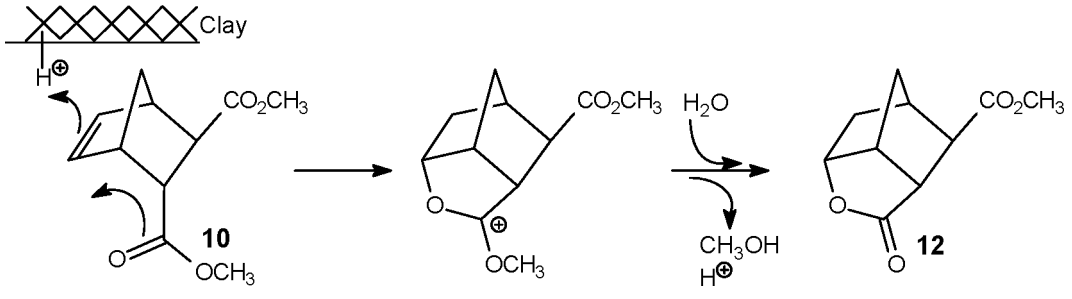

Scheme 7.4 *Proposed mechanism for the formation of* **12** *from* **10**

A reported route to lactone **12** involves the lactonization of the di-acid of **10** using concentrated sulphuric acid.[34] Usually, an intramolecular lactonization reaction of a carboxylic acid with an olefinic bond is accomplished via an iodolactonization reaction.[35,36] A possible route to **12**, having such a iodolactonization step, can start from **10** and involves saponification and iodolactonization, followed by removal of the residual iodine by tributyltin hydride, as in the synthesis of Corey's lactone,[37] or by hydrogenolysis over Pd/C.[38] The application of clays as heterogeneous catalysts in the preparation of lactone **12** from the easily accessible cycloadduct **10** profits from the easy separation of the product from the reaction mixture and avoids the formation of a considerable amount of waste products. This synthesis of **12** using clays as heterogeneous catalysts is a striking example of an environmentally benign process, as the formation of considerable amounts of waste products is avoided.

In order to investigate the scope of this lactonization process, substrates **13**, **15** and **17** were also studied (Table 7.3). Analogously to the lactonization described above, products **14** and **16** were obtained starting from substrates **13** and **15**, respectively. However, yields were relatively low and more detailed studies are needed to optimize these yields. Starting from compound **17** (*trans*-), no lactone could be identified even after prolonged reaction times, instead mixtures of *cis*- and *trans*-**17** were obtained (*trans:cis* = 18:51% to 48:42%). The non-cyclic compound **18** was also subjected to the same reaction conditions, but no lactone was obtained. These results suggest that the lactonization reaction can easily be carried out for geometrically rigid γ,δ-unsaturated esters (viz. substrates **10**, **13** and **15**), but so far no lactones were obtained for more flexible substrates (viz. substrates **17** and **18**). This strong dependence on the rigidity of the substrate indicates that overcoming of the entropy barrier is important.

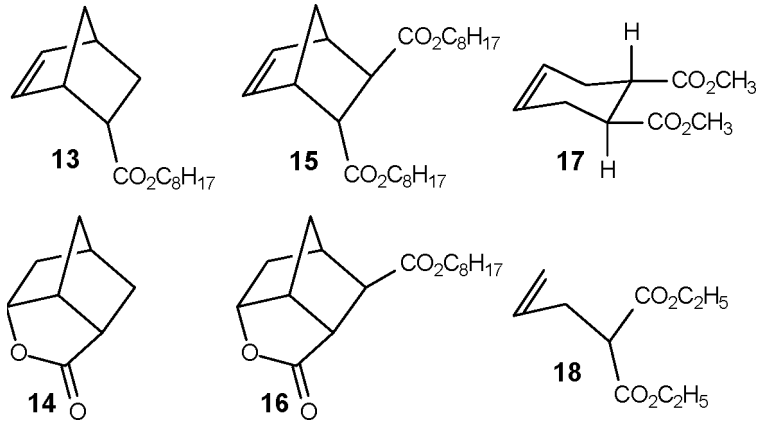

In summary, solid acids can be used to catalyze the retro Diels-Alder reaction in the liquid phase. In the present study a trapping agent was used to avoid the reformation of the original adduct by withdrawing the released cyclopentadiene from the reaction equilibrium. The product of this trapping reaction, the rigid γ,δ-

unsaturated ester **10**, underwent a lactonization reaction to **12**. This solid acid catalyzed lactonization is restricted to rigid γ,δ-unsaturated esters in which the reacting ester group is in close proximity to the olefinic bond. It was shown that the presence of some water is essential for the lactonization reaction to occur.

Table 7.3 *Lactonization reaction of various γ,δ-unsaturated esters*

Entry	Substrate	Product	Catalyst[a]	Mass Ratio[b]	Yield[c] (%)
1	**13**	**14**	Montmorillonite K-10	5	25
2			Montmorillonite KSF	5	[d]
3	**15**	**16**	Montmorillonite K-10	5	47
4	**17**	-	Montmorillonite K-10	5	-[e]
5			Montmorillonite KSF	5	-[e]
6	**18**	-	Montmorillonite K-10	5	-
7			Montmorillonite KSF	5	-

[a] Catalyst used as received; Reaction conditions: toluene as the solvent and a temperature of 110°C. [b] Mass ratio stands for the ratio [mass catalyst]/[mass substrate]. [c] Isolated yield. [d] Not precisely determined. [e] Mixtures of *cis*- and *trans*-**17** were obtained.

The long reaction times and the large amounts of catalyst needed to accomplish an acceptable conversion are drawbacks for the chemistry described in this section. For this reason more attention was given to gas phase reactions using solid acids (Section 7.3).

7.3 SOLID ACID CATALYZED GAS PHASE RETRO DIELS-ALDER REACTIONS

Gas phase retro Diels-Alder reactions were carried out using the catalytic flash vacuum thermolysis set-up described in the Experimental Section of Chapter 4. Experiments were performed at 0.05 mbar with 100 mg or 400 mg of a fractured catalyst (150-425 μm), which was pre-treated at 400°C and 0.05 mbar prior to use in order to remove physisorbed water from the catalyst. It should be noted that the catalysts used in an earlier study by Van de Waals[31] were not pre-heated prior to use. Substrates were vaporized at an appropriate temperature (see Experimental section) in about 45 min. In some cases, a series of runs was performed using the same catalyst batch while the reaction temperature was varied. The temperatures in such a series were varied according to a hysteresis loop, going from 400°C to 150°C. In this manner a possible deactivation would be detectable by comparing the results of two experiments conducted at the same reaction temperature. Control experiments were performed under identical conditions in the absence of a catalyst. The simple bicyclic ester **10** was chosen as substrate. In addition, tricyclodecenone epoxide esters **4a** and **4c** were studied to unequivocally establish the structure of the cage compound, observed by Van der Waals[31], and to shed light on the mechanistic pathway leading to this product.

7.3.1 Retro Diels-Alder Reactions of dimethyl bicyclo[2.2.1]hept-5-ene-2,3-dicarboxylate

A simple cycloadduct **10** was selected as substrate in order to establish the general applicability of the retro Diels-Alder using catalytic FVT. In contrast to the earlier study by Van de Waals[31] the catalysts used here were pre-heated prior to use to remove physisorbed water from their surface. This ensures that the catalysts used have undergone a uniform treatment, which promotes the reproducibility.

The thermal reactivity of dimethyl bicyclo[2.2.1]hept-5-ene-2,3-dicarboxylate **10** under FVT conditions was determined in some control experiments (Table 7.4, entries 1-3). These experiments showed that **10** was almost inert at temperatures around 300°C (0.05 mbar). Only at 500°C (0.05 mbar) a complete conversion was achieved (entries 1-3). Under these conditions the reaction was completely selective to give retro Diels-Alder product **9**. The major product found in solution phase solid acid catalyzed reactions (see Section 7.2), lactone **12**, was not detected in reactions under catalytic FVT conditions. Apparently, the thermolysis takes a different coarse in solution and in the gas phase. It should be noted that in the former case some water is present in contrast to the latter case.

The results obtained using various solid acids in the retro Diels-Alder reaction of **10** under catalytic FVT conditions are collected in Table 7.4. All tested solid catalysts proved to enhance the conversion of **10**.

A series of runs was performed using the same catalyst batch while the reaction temperature was varied according to a hysteresis loop, going from 400°C to 200°C. During the later runs at the same reaction temperature the conversions were generally somewhat lower. This was also noted previously (cf. Section 7.3.2 and Chapter 4) and these observations point to some deactivation of the catalysts.

At temperatures of about 400°C very high conversions were achieved for all acids and substantial differences in catalytic activity of the catalysts were observed only at lower temperatures (200 and 300°C). The amorphous silica-alumina HA-SHPV proved to be the most active catalyst. At 200°C a conversion of 42% was obtained (entry 41). The amorphous alumina B698D-24 and the amorphous silica-alumina B698D-25 also gave some conversion at this temperature (entries 31 and 36). The clay materials were significantly less active and hardly gave any conversion at 200°C. The Zn-saponite and the Zn-stevensite failed completely to catalyze the reaction at this temperature.

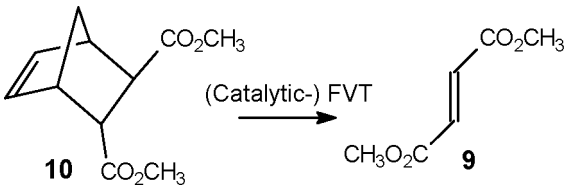

Table 7.4 *The retro Diels-Alder reaction of* **10** *under (Catalytic-) FVT conditions*

Entry	Catalyst[a]	Temp.[b] (°C)	Conversion[c,d] (%)
1	None	300	2
2		400	81
3		500	100
4	Montmorillonite K-10	400	100
5		300	64
6		200	6
7		300	56
8		400	100
9	Mg-saponite\ Al^{3+}	400	100
10		300	28
11		200	3
12		300	21
13		400	96
14	Zn-saponite\ Al^{3+}	400	95
15		300	20
16		200	0
17		300	15
18		400	85
19	Mg-stevensite	400	100
20		300	44
21		200	4
22		300	32
23		400	92
24	Zn-stevensite	400	94
25		300	9
26		200	0
27		300	4
28		400	73
29	B698D-24	400	100
30		300	100
31		200	21
32		300	97
33		400	100
34	B698D-25	400	100
35		300	75
36		200	16
37		300	66
38		400	98
39	HA-SHPV	400	100
40		300	96
41		200	42
42		300	97
43		400	100

[a] 100 mg of catalyst was used and 100 mg of substrate per run. [b] Oven temperature; The substrate was vaporized at 70°C; 0.05 mbar pressure. [c] Conversions and selectivities determined by GC. [d] Selectivity towards **9** was 100%.

The results presented in this section together with the results obtained earlier by Van der Waals[31] on *exo*-4,5-epoxy-*endo*-tricyclo[6.2.1.0.^{2,7}]undec-9-ene-3,6-dione **1** prove that catalytic FVT using various solid acids is a suitable method to achieve a retro Diels-Alder reaction. A major benefit of the catalytic FVT technique compared to solution phase retro Diels-Alder reactions is that no solvents are needed and that labile products may be obtained which would otherwise have undergone secondary reactions in solution phase reactions due to their long residence time in the hot reaction mixture. Catalytic FVT reactions on more complicated substrates, viz. tricyclodecenone epoxides **4**, are described in the next section and these appeared to be more complicated.

7.3.2 Retro Diels-Alder Reactions of Tricyclodecenone Epoxides

The catalytic thermolysis of tricyclodecenone epoxide ester **4a**, which previously had been studied by Van der Waals[31], was investigated in more detail in order to unambiguously establish the structure of the isolated cage compound and to unravel the mechanistic pathways leading to this product. It is important to note that the catalysts were pre-heated prior to use to remove physisorbed water from their surface. This pre-treatment, which was not done in the earlier study by Van de Waals[31] ensures that the catalysts have undergone a uniform treatment, which promotes the reproducibility.

The thermal reactivity of ethyl *exo*-3,4-epoxy-5-oxo-*endo*-tricyclo[5.2.1.0^{2,6}]deca-8-en-2-carboxylate **4a** under FVT conditions was determined in some control experiments (Table 7.5, entries 1-3). These experiments showed that **4a** was completely inert at 300°C, whereas at 500°C complete conversion was achieved. At 450°C a conversion of 83% was observed which is consistent with earlier studies and which established the lower temperature limit for complete conversion of **4a**.[31] In these thermolyses pyrone **7a** was formed predominantly at all temperatures. Appreciable amounts of five-membered ring epoxide **6a**, the primary retro Diels-Alder product, were obtained only at 400°C. At elevated temperatures epoxide **6a** may be transformed into pyrone **7a** via a stereospecific [$4\pi_a+2\pi_a$] opening of **6a** and subsequent recyclization of the intermediate. In these uncatalyzed control experiments no cage compound **5a** was detected.

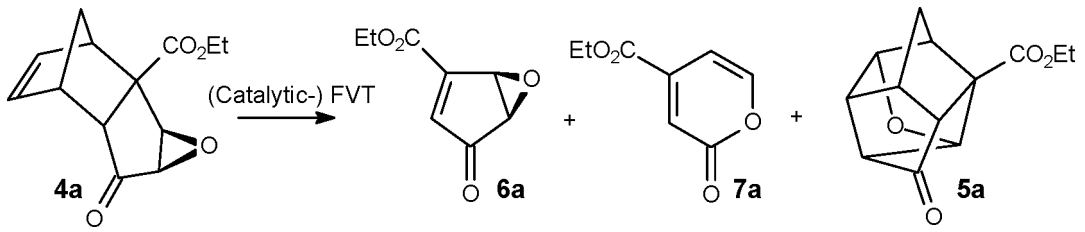

Table 7.5 *Reaction of tricyclodecenone epoxide* **4a** *under (Catalytic) FVT conditions*

Entry	Catalyst[a]	Temp.[b] (°C)	Conversion[c] (%)	Selectivity[c] (%)			Mass Balance[d]
				6a	7a	5a	
1	None	300	0				100
2		400	83	25	75		68
3		500	100		100		74
4	Montmorillonite K-10	400	95	3	49	25	90
5		300	30			49	96
6		200	8			28	100
7		300	17			29	96
8		400	88	5	56	11	84
9	Mg-saponite\Al^{3+}	400	85	7	67	4	80
10		300	5				100
11		200	1			25	78
12		300	2			17	90
13		400	77	24	67	1	88
14	Mg-saponite\H^{+}	400	86	34	57	1	76
15		300	7		2		86
16		200	1				72
17		300	1				96
18		400	80	30	62		88
19	B698D-24	400	90	13	58	15	78
20		300	22			45	96
21		200	17			48	94
22		300	15			41	90
23		400	70	6	75	9	86
24	HA-SHPV	400	92	13	68	9	66
25		300	19		13	46	96
26		200	18			49	100
27		300	12		11	42	100
28		400	73	28	59	5	82
29	F-1[e]	400	98			33	86
30		350	75		24	52	62
31		300	22		23	50	100
32		250	11		9	46	64
33	B698D-24[e]	300	87		12	72	26
34		250	74		4	73	66
35		350	68		25	46	96
36		400	83		49	30	46

[a] 100 mg of catalyst was used and 50 mg of substrate per run, unless mentioned otherwise. [b] Oven temperature; The substrate was vaporized at 120°C (100 mg catalyst) or 150°C (400 mg catalyst); 0.05 mbar pressure. [c] Conversions and selectivities determined by GC. [d] Ratio (in %) of mass before and after thermolysis, uncorrected for loss of cyclopentadiene. [e] 400 mg of catalyst was used and 50 mg of substrate per run.

The results obtained using various solid acids as catalysts in the retro Diels-Alder reaction of tricyclodecenone epoxide **4a** under FVT conditions are given in Table 7.5. All materials tested proved to effect the conversion of **4a**, but some solid acids were only mildly effective.

A series of runs was performed using the same catalyst batch while the reaction temperature was varied. For some catalysts (entries 4-28) this was according to a hysteresis loop, going from 400°C to 200°C. In the first run with a certain catalyst at the highest temperature (400°C) the conversions were generally high. However, when this temperature was used again in the fifth run with the same catalyst batch the conversions were usually lower. A similar effect may be noticed by comparing the second and fourth run (300°C). These observations point to some deactivation of the catalysts, and this is supported by visual blackening of the catalyst materials after use. Elemental analysis of a catalyst (B698D-24) used in this way showed a carbon content of 7%, which was significantly more than found in the fresh catalyst (0.07%). The elemental analysis of the catalyst used showed a carbon/hydrogen ratio corresponding with C_x:H_{2x}. These analyses clearly demonstrated that organic material was deposited on the catalyst.

When 100 mg of catalyst was used (entries 4-28) conversions at 400°C ranged from 85 to 95%, and at 300°C from 5 to 30%. When a four times larger amount of catalyst was used (400 mg, entries 29-36) the conversions at lower temperatures were significantly higher. This was particularly striking for the amorphous alumina B698D-24 that was used in both amounts (compare entries 19-23 and 33-36).

The selectivities with regard to the retro Diels-Alder products **6a** and **7a** and cage compound **5a** were dependent on the reaction temperature. The epoxide **6a** was only found at a thermolysis temperature of 400°C with a catalyst:substrate ratio of 2 (viz. 100 mg catalyst and 50 mg substrate). In general, the selectivity for **6a** was not significantly improved when compared with the uncatalyzed thermal reaction at 400°C (entry 2). The selectivity for pyrone **7a** decreased sharply with decreasing reaction temperature and at 200°C no **7a** was found anymore. Surprisingly, this decrease in selectivity only partly resulted in a higher selectivity for epoxide **6a**. Generally, the selectivity towards **5a** increased appreciably. A maximum selectivity for **5a** of 73% was found with amorphous alumina B698D-24 in a catalyst:substrate ratio of 8 (entry 34).

The total mass of the product mixtures after thermolysis were in most cases not 100%, but the values for the mass balance in Table 7.5 are not corrected for the loss of cyclopentadiene. For instance, the mass balance value of 74% in entry 3 of Table 7.5 corresponds to a yield of 100% of pyrone **7a** since the molmass of **7a** is 28% less than of **4a**. The loss of cyclopentadiene could, however, not explain the low mass balance

values in all cases. Coke formation on the catalyst surface may have contributed to this poor mass balance, which was confirmed analytically by elemental analysis (*vide supra*).

Elucidation of the structure of cage compound 5 and the mechanism of its formation

Cage compound **5a** was hitherto not identified unambiguously. Tentatively, structure **5a** was proposed by Van der Waals[31] on basis of a detailed NMR study. In order to explain its unexpected and surprising formation, which must be attributed to the use of a solid acid, the correctness of structure of **5a** needed to be ensured. For this purpose efforts were made to obtain a crystalline derivative of **5a** in order to allow an X-ray diffraction analysis. To obtain a sizeable amount of the cage compound several catalytic FVT experiments were carried out successively applying the optimal conditions (Table 7.5, entry 33) and using 100 mg of substrate **4a**. Amorphous B698D-24 was used as the catalyst. A pure sample (100 mg) of cage compound was obtained after column chromatography of these combined product mixtures. This compound could not be crystallized and therefore it was derivatized with 2,4-dinitrophenylhydrazine to its hydrazone **19** (Scheme 7.5), which was crystalline. Earlier attempts[31] to obtain a crystalline derivative of the cage compound by reduction of the ketone group and subsequent esterification to form a 3,5-dinitrobenzoate had failed.

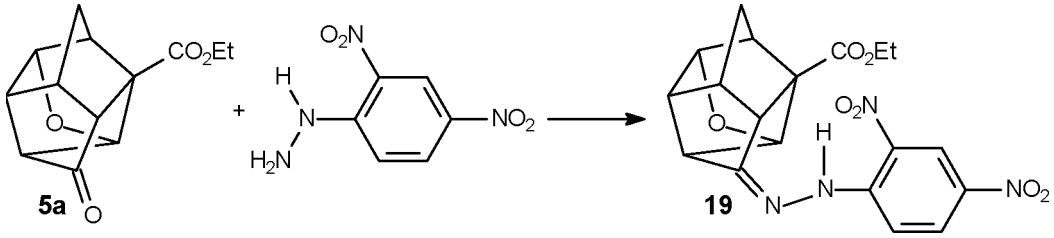

Scheme 7.5 *Derivatization of* **5a** *to its hydrazone* **19**

The 2,4-dinitrophenylhydrazone **19** was recrystallized five times from ethanol and finally once from methanol to afford transparent orange platelet-like crystals. An X-ray diffraction analysis was performed on these crystals, which turned out to be a rather laborious task because the quality of the crystals was poor. The results of the X-ray analysis, however, allowed the indisputable determination of the atom connectivity. The structure of the 2,4-dinitrophenylhydrazone derivative of the cage compound is displayed in Figure 7.2. This structure showed that the previously assigned structure **5a** for the cage compound was indeed correct.

Figure 7.2 *PLUTON drawing of the X-ray structure of the 2,4-dinitrophenylhydrazone* **19**

Tentative mechanisms that might explain the formation of cage compound **5a** from **4a** under catalytic FVT conditions are presented in Scheme 7.6. In these mechanisms the role of the solid acid is essential as its presence is a prerequisite for the formation of **5a**. The structure of **5a** dictates which bonds need to be formed during this process and structural comparison of starting tricyclic epoxide **4a** and the cage product **5a** leads to the conclusion that the oxygen bridge in **5a** originates from the epoxy oxygen. This conclusion inevitably requires inversion of configuration of this oxygen with respect to the carbon to which it is attached (C_3 in epoxide **4a**). This inversion can be accounted for by assuming an inversion of the epoxide function via a six-membered intermediate **20**. Such a transformation is conceivable by the initial coordination of the carbonyl function in **4a** with the solid acid. Instead of promoting the [4π+2π] cycloreversion reaction, epoxide ring opening takes place to form carbonyl ylid type intermediate **20**. The carbonyl ylid type system may then reform the epoxide function but this may results in either *exo*-epoxide **4a** or its isomeric *endo*-epoxide **21**. Cleavage of the C-C bond of an epoxide has precedents in literature,[39,40] but most examples involve cyano substituted epoxides. Moreover, epoxides are known to undergo isomerization via a C-C bond cleavage mechanism under certain thermal conditions.[39,41] Reports concerning a C-C bond cleavage of epoxy ketones giving 1,3-dipoles of the carbonyl ylid type are less frequent.[42]

Conceivable reaction pathways explaining the formation of cage compound **5a** from *endo*-epoxide **21** are depicted as *i*, *ii* and *iii* in Scheme 7.6. In pathway *i* the required bond connection between C_4 and C_8 is realized by initial nucleophilic attack of the

olefinic C_8-C_9 π-system on the C_4 position. Such an unusual frontal nucleophilic substitution with retention of configuration can only have some reality if C_4 already possesses considerable electrophilicity and the oxirane oxygen does not interfere electronically. These conditions are only met when it is assumed that the C_4-O bond is significantly elongated as the result of strong coordination of the epoxide oxygen with the solid acid. Simultaneously or in a fast subsequent reaction the oxygen then releases from the catalyst and forms the required C_9-O bond.

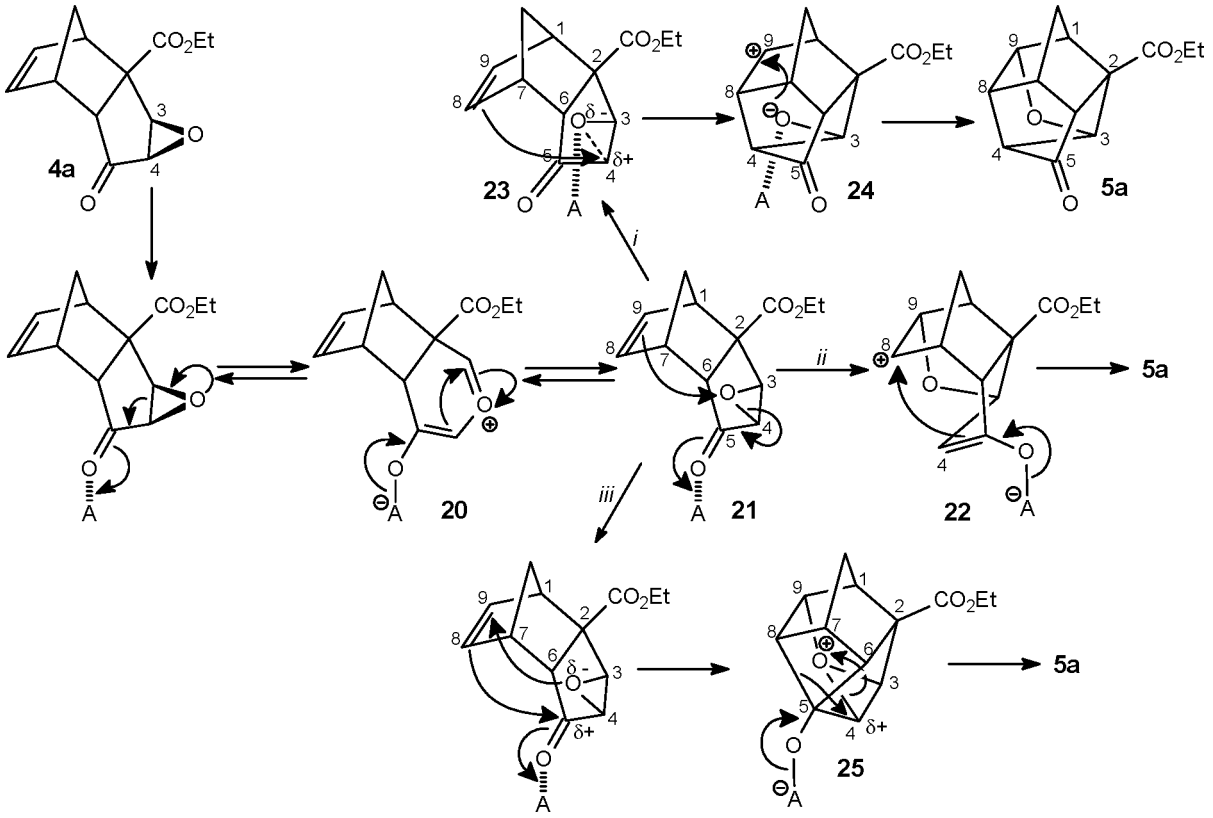

Scheme 7.6 *Possible mechanisms for the formation of cage compound* **5a** *from tricyclodecenone epoxide* **4a**

In pathway *ii* formation of the C_9-O bond is the initial step. As the result of the same strong interaction of the solid acid with the carbonyl function that caused the unusual epoxide inversion, viz. from **4a** to **21**, the epoxide oxygen has gained some electrophilic character. The close proximity of the C_8-C_9 olefinic π-system to this epoxide oxygen combined with the rigid geometry of the overall structure **21** now initiates formation of the C_9-O bond resulting formally in dipolar intermediate **22** which, obviously, is stabilized by formation of the C_4-C_8 bond. This stepwise process probably has considerable concerted character.

The mechanistic pathways *i* and *ii* are nevertheless regarded unlikely for the following reasons. In pathways *i* and *ii* reaction of the olefinic bond with C_4 (pathway *i*) or the epoxide oxygen (pathway *ii*) occurs essentially without activation of this olefinic, electron rich, bond, which is not very probable. Of pathways *i* and *ii*, the first is regarded as the most unlikely, since coordination of the solid catalyst with

the epoxide oxygen has to replace the coordination of the solid acid with the ketone function. Hence both oxygen atoms are coordinated to the acidic surface. However, a strong coordination of the ketone function with the catalyst certainly further opposes the already unfavorable formation of an electrophilic center at C_4 next to the ketone function. Moreover, there is no reason to assume that coordination with the ketone function is less probable for *endo*-epoxide **21** than it is for *exo*-epoxide **4a**.

As the explanations for the formation of cage compound **5a** in pathways *i* and *ii* were unsatisfactory, calculations were performed on this unusual reaction. Relatively simple AM1 calculations as implemented in the MOPAC93 program[43], starting from carbonyl protonated epoxy ketone **21** and taking the ultimate formation of the C_4-C_8 bond in cage compound **5a** as prerequisite, immediately showed the occurrence of a different mechanism represented as pathway *iii* in Scheme 7.6. In this alternative route *iii* considerable polarization of the C_8-C_9 π-system takes place as the result of the close proximity of the epoxide oxygen and electrodeficient carbonyl carbon C_5. Stabilization now occurs by concurrent formation of the C_9-O and C_5-C_8 bond leading to cyclobutanol **25** in a slightly exothermic process. Calculations show that the bond lengths and bond angles in **25** have close to normal values. In this intermediate **25** the electron density is high on the catalyst whilst there is considerable electron deficiency on the epoxide oxygen and the C_4-atom. This combination of charge now allows an energy favorable homoketonization[44] to **5a** in which migration of the C_5-C_8 to C_4 takes place, releasing a considerable amount of strain energy as the result of ring enlargement, viz. from a cyclobutanol to a cyclopentanone.

This pathway *iii* is strongly preferred over the first two as the interaction of the ketone and the epoxide oxygen with the olefinic bond rationalizes the C_9-O bond formation. Moreover, the calculations show that this pathway has a favorable energy profile and probable geometric feasibility. Currently, higher-level computational studies are carried out to gain more detailed insight in this process. [45]

Catalytic FVT of ethyl *exo*-3,4-epoxy-5,5-dimethoxy-*endo*-tricyclo[5.2.1.$0^{2,6}$]deca-8-en-2-carboxylate

Catalytic FVT experiments were also performed with dimethyl ketal tricyclo-decenone epoxide **4b**. The results are collected in Table 7.6. The results obtained for **4b** clearly differed from those starting from **4a**. At moderate temperatures (up to 300°C) fair amounts of the deprotected compound **4a** were obtained accompanied by small fractions of cage compound **5a** formed from **4a** when B698D-24 was used as the catalyst. At higher temperatures a moderate selectivity towards the secondary retro Diels-Alder product (after rearrangement into its pyrone isomer) **7b** was observed. No 5-ring ketal epoxide (**6b**) or the ketal of cage compound (**5b**) were observed.

It was hoped that these experiments would provide clear evidence for the coordinating role of the carbonyl group at C_5. However, because of the formation of **4a** such conclusions cannot be drawn unambiguously. The product composition is different; therefore acetalization does change the catalytic FVT behavior considerably.

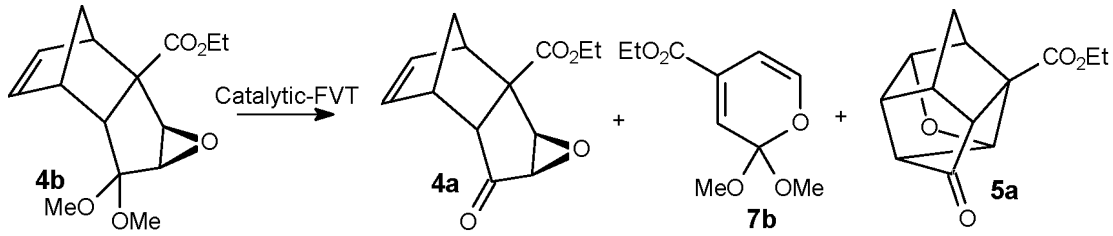

Table 7.6 *Reaction of tricyclodecenone epoxide* **4b** *under Catalytic FVT conditions*

Entry	Catalyst[a]	Temp.[b] (°C)	Conversion[c] (%)	Selectivity[c] (%)			Mass Balance[d]
				4a	7b	5a	
1	F-1	300	36	19			24
2		250	14	21			100
3		350	18	11	22		-[e]
4		400	38		63		76
5	B698D-24	150	76	32		13	30
6		250	79	3		6	72
7		300	5	40			66
8		400	51		80		78

[a] 400 mg of catalyst was used and 50 mg of substrate per run. [b] Oven temperature; The substrate was vaporized at 150°C; 0.05 mbar pressure. [c] Conversions and selectivities determined by GC. [d] Ratio (in %) of mass before and after thermolysis, uncorrected for loss of cyclopentadiene. [e] Not determined.

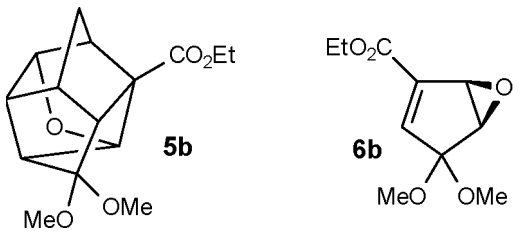

Table 7.6 shows that the conversion tends to decrease when the same catalyst batch is reused. This is most evident from the comparison of entries 1 and 6 with entries 3 and 7, respectively (Table 7.6). In these cases the increase in reaction temperature is not sufficient to compensate the effect of considerable catalyst deactivation. Apparently, the most reactive catalytic sites are only accessible during these first runs and are deactivated rapidly. This is confirmed by the experimentally established coke formation on the catalysts.

Catalytic FVT of *exo*-5-*tert*-Butyl-*endo*-4,5-epoxy-*endo*-tricyclo[5.2.1.$0^{2,6}$]dec-8-en-3-one

The mechanism that is proposed (Scheme 7.6) for the formation of oxacage **5a** from the tricyclodecenone *exo*-epoxide **4a** requires the inversion of the *exo*-epoxide

function as the first step. In order to further substantiate the occurrence of such an *endo*-epoxide in this transformation, *endo*-epoxide **4c** was synthesized independently and its thermal behavior studied under catalytic FVT conditions. As a consequence of the synthetic route to such an *endo*-epoxide a *tert*-butyl group at the C_5 position and the absence of the ester function at C_6 had to be accepted. The synthesis of this *endo*-epoxide **4c** is reported in Section 7.3.3. Catalytic FVT experiments with tricyclodecenone *endo*-epoxide **4c** were performed under identical conditions as for **4a** using amorphous alumina B698D-24 as the catalyst. The results are given in Table 7.7.

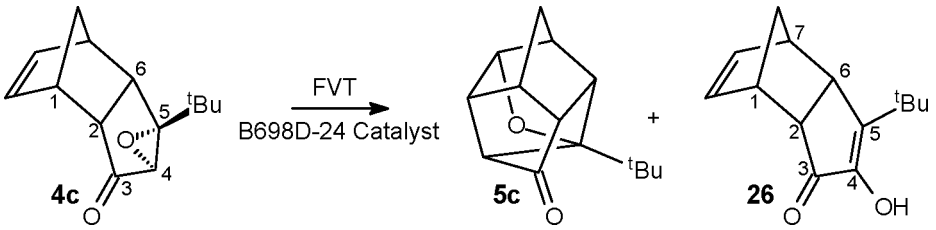

Table 7.7 *Reaction of tricyclodecenone endo-epoxide* **4c** *under Catalytic FVT conditions*

Entry	Catalyst[a]	Temp.[b] (°C)	Conversion[c] (%)	Selectivity[c] (%)		Mass Balance[d]
				5c	26	
1	B698D-24	300	86	78	7	25
2		350	83	76	8	53
3		300	58	59	16	72
4		300	30	43	27	78

[a] 400 mg of catalyst was used and 40 mg of substrate per run. [b] Oven temperature; The substrate was vaporized at 70°C; 0.05 mbar pressure. [c] Conversions and selectivities determined by GC. [d] Ratio (in %) of mass before and after thermolysis.

The results in Table 7.7 show that cage compound **5c** is indeed obtained with relatively high efficiency, which however decreased slightly when the catalyst batch was used more than once (compare entries 1 and 4). The mass balance on the other hand increased when the same batch of catalyst is reused. This had also been observed and discussed for other substrates (*vide supra*). The high yield of oxygen cage **5c** clearly substantiates the intermediacy of such an *endo*-epoxide in the formation of cages **5** as proposed in Scheme 7.6.

Besides cage compound **5c** also 5-*tert*-butyl-4-hydroxy-tricyclodecadienone **26** could be isolated and characterized. The amount of **26** increased with the increasing number of catalytic cycles. A mechanism that explains the formation of **26** from **4c** involves an epoxide rearrangement reaction (cf. Chapters 3 and 4) to form a 1,2-diketone, which leads to **26** after a keto-enol isomerization. According to spectral data the keto-enol equilibrium is completely on the enol side. In this rearrangement, which is induced by complexation of the solid acid catalyst with the epoxide oxygen, a hydride migrates to give a 1,2-diketone. Migration of the *tert*-butyl group, which would have yielded a 1,3-diketone isomer or its enol isomer (4-*tert*-butyl-5-hydroxy-tricyclodecadienone), was not observed. This is in line with the expectation because a

hydride migrates generally more easily than an alkyl group in the epoxide rearrangement (cf. Chapters 3 and 4). The structure of **26** was established unequivocally by 2D-NMR analysis. The NOESY spectrum showed an interaction between the hydrogens of the *tert*-butyl group and H_7 and this proved indisputably that **26** was obtained since this interaction is not possible with its 4-*tert*-butyl-5-hydroxy-isomer. An alternative explanation for the formation of **26** from **4c** may involve the hydrolysis of the epoxide from the *exo*-face to give the corresponding 1,2-trans-diol followed by a pinacol rearrangement and concurrent release of water to give **26**. The catalytic FVT conditions, however, practically exclude this possibility in view of the pre-treatment of the catalyst, which removes all physisorbed water.

Catalytic FVT experiments using some differently substituted tricyclodecenone epoxides **4d** (R: CH_2OH, X-Y: C=O; Scheme 7.3) and **4e** (R: CH_2OAc, X-Y: C=O; Scheme 7.3) showed that also in these cases moderate yields of cage compounds **5** were formed. However, in all these cases the product mixtures obtained could not be separated and it was therefore not possible to identify and characterize their components.

7.3.3 Synthesis of Tricyclic *exo*-epoxides 4a, 4b, 4d, 4e and Tricyclic *endo*-epoxide 4c

The tricyclic *exo*-epoxides **4** were prepared following the reaction sequences depicted in Scheme 7.7 and Scheme 7.8. Ethyl *exo*-3,4-epoxy-5-oxo-*endo*-tricyclo[5.2.1.$0^{2,6}$]deca-8-en-2-carboxylate **4a** was synthesized from benzoquinone **27**.[46,47,48,49c] The readily available cycloadduct **28** was epoxidized to **1** under nucleophilic conditions. This epoxy enedione **1** was transformed into tricyclic enone **29** via a base-induced Favorski type ring-contraction.[46,49] Tricyclodecenone *exo*-epoxide **4a** was obtained from **29** after epoxidation.

Various (protected) derivatives of tricyclodecenone *exo*-epoxide **4a** were prepared according to Verlaak *et al.*[49] Compound **4a** was converted into its dimethoxy acetal **4b** in order to prevent reduction of the C_3-ketone moiety in the subsequent reaction with lithium aluminiumhydride to the primary alcohol **4f**. Deprotection yielded **4d**, which was transformed into acetate **4e** by treatment with acetic anhydride and DMAP in the presence of base.

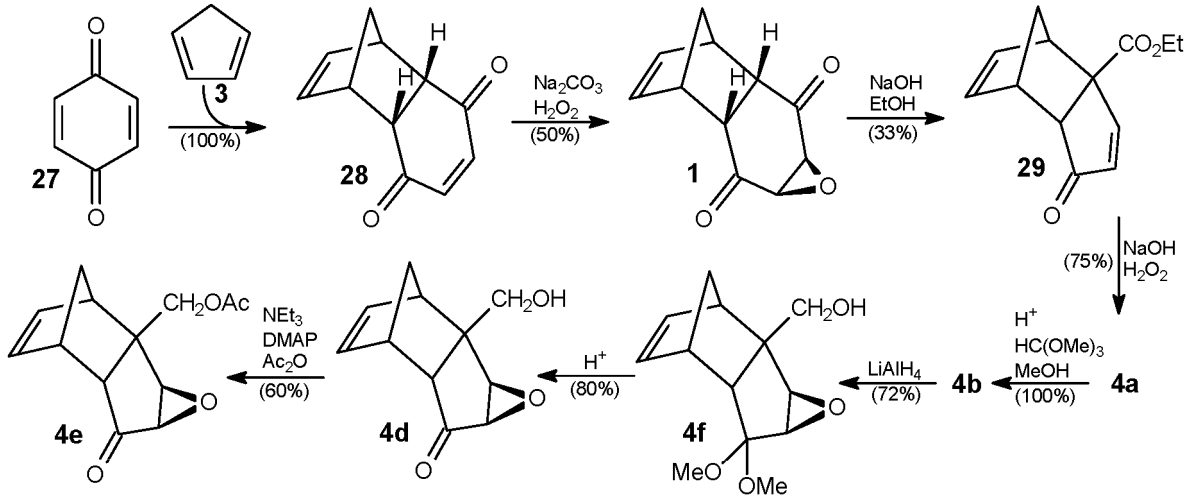

Scheme 7.7 *Synthesis of various tricyclodecenone exo-epoxides* **4**

Tricyclodecenone *endo*-epoxide **4c** was synthesized starting from dicyclopentadiene **30**, which was oxidized with selenium oxide to give tricyclodecenol **31**. After oxidation of **31** to give **32** the enone double bond of **32** was epoxidized to yield tricyclodecenone *exo*-epoxide **33**. The key step in the reaction sequence towards the tricyclodecenone *endo*-epoxide **4c** involves the nucleophilic addition of *tert*-butyl lithium to the carbonyl moiety of **33** followed by a Payne rearrangement to yield the inverted *endo*-epoxide **34**.[50,51] In the final step, the alcohol moiety of **34** was oxidized with PCC to yield tricyclodecenone *endo*-epoxide **4c**.

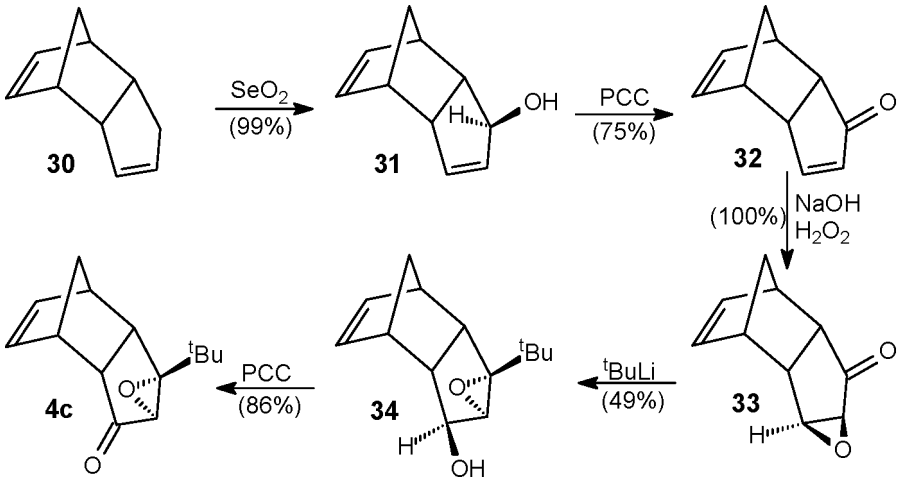

Scheme 7.8 *Synthesis of tricyclodecenone endo-epoxide* **4c**

7.4 CONCLUSIONS

The retro Diels-Alder reaction was investigated using solid acid catalysts in the liquid phase as well as under flash vacuum thermolysis conditions. Various natural and synthetic clay materials were tested and, in addition, also amorphous (silica) aluminas were employed. The simple tricyclic and bicyclic esters **8** and **10** and tricyclodecenone epoxides **4** were used as substrates.

Solid acids can be used to catalyze the retro Diels-Alder reaction in the liquid phase. Surprisingly, the rigid γ,δ-unsaturated ester **10** undergoes a lactonization reaction to **12**. It was shown that also other rigid γ,δ-unsaturated esters may react in this manner, but flexible γ,δ-unsaturated esters did not. In the proposed mechanism for the formation of lactones **12** catalyzed by solid acids water is essential, which was confirmed experimentally.

A reported route to lactone **12** involves a multi-step synthesis that is not only laborious but also gives rise to large amounts of waste salts. Our alternative synthesis of **12** is a nice example of an environmentally benign process.

Catalytic FVT using various solid acids is a suitable method to achieve retro Diels-Alder reactions of simple cycloadducts as demonstrated by the results with dimethyl bicyclodicarboxylate **10** presented here together with results obtained earlier by Van der Waals[31] with epoxy enedione **1**. In contrast to solution phase experiments a lactonization of **10** was not observed in gas phase reactions. Catalytic flash vacuum thermolysis reactions of various tricyclodecenone epoxides **4** proved to be rather complex since in many cases besides minor amounts of retro Diels-Alder products cage compounds were obtained as the major products. The basic structure of these unexpected cage products **5** have been indisputably established by means of an X-ray diffraction analysis of a hydrazone derivate of **5a**. The mechanism explaining the formation of cage compounds **5** involves an initial isomerization of the *exo*-epoxide into the *endo*-isomer via a carbonyl ylid type intermediate. The product forming step is a reaction of the olefinic bond with the *endo*-epoxide, which probably takes place on the catalyst surface.

When solid acids are used under catalytic FVT conditions the retro Diels-Alder reaction may be achieved at much lower thermolysis temperatures. This may allow otherwise thermally difficult transformations, and clearly is advantageous for industrial applications applying a retro Diels-Alder strategy in a (multi-step) synthesis.

7.5 EXPERIMENTAL SECTION

General remarks

Reported percentages are molar percentages (% $^{m}/_{m}$). Gas chromatographic (GC) analyses were performed on a Hewlett-Packard HP5890II gas chromatograph (flame ionization detector, FID) equipped with an HP-3396II integrator, using a capillary column (HP-1, 25 m x 0.31 mm x 0.17 μm) and nitrogen at 2 ml/min (0.5 atm) as the carrier gas or on a Hewlett-Packard HP6890 gas chromatograph (flame ionization detector, FID) equipped with an HP-6890 integrator, using a capillary column (HP-1, 25 m x 0.32 mm x 0.17 μm) and hydrogen at 3.2 ml/min (0.53 atm) as the carrier gas. The GC temperature programs employed were

either from 75°C (5 min isothermal) to 250°C at 15°C/min followed by 3 min at 250°C (isothermal) or from 100°C to 250°C at 15°C/min followed by 10 min at 250°C (isothermal). FT-IR spectra were recorded on a Biorad FTS-25 spectrophotometer. ^{1}H- and ^{13}C-NMR spectra were recorded on a Bruker AM-400 and a Bruker AC-100 at T=298 K. Chemical shifts were reported against $Si(CH_3)_4$. Mass spectrometric (MS) analyses were measured with a double focusing VG Analytical 7070E mass spectrometer or a Varian Saturn II GC-MS set-up equipped with an HP-1 capillary column and Varian 8100 autosampler.
Column chromatography at ambient pressure was carried out using Merck Kieselgel 60. Thin layer chromatography (TLC) was carried out on Merck precoated silicagel 60 F254 plates (0.25 mm) using the eluents indicated. Spots were visualized with UV or molybdate spray. Dichloromethane and hexane were distilled from calcium hydride, ethyl acetate from potassium carbonate and toluene from sodium. Commercially available starting materials were used as received.

Origin of the catalysts
Amorphous alumina B698D-24, amorphous silica-alumina B698D-25 and the acid-treated natural F-clays were received as generous gifts from Engelhard De Meern B.V. Amorphous silica-alumina HA-SHPV was obtained as a generous gift from AKZO Nobel Chemicals. Commercial natural clays montmorillonite K-10 and montmorillonite KSF are produced by Süd Chemie and were obtained via Aldrich Chemical Company. Prior to use montmorillonite K-10 was washed in hot demineralized water (to remove any residual mineral acid that could be present due to the acid-treatment involved in its preparation) and subsequently dried. Synthetic clay materials were prepared and donated by the Department of Inorganic Chemistry and Heterogeneous Catalysis of the University of Utrecht. All saponites used had a Si/Al ratio of 7.9 and are described as M-saponite\C^{+}, where M represents the octahedral cation and C^{+} the interlayer cation.
Catalysts used in catalytic FVT experiments were pressed (3 tons), sieved into the desired particle size (150-425 μm), and stored at ambient pressure. Catalysts were used after a pre-treatment: An amount of catalyst was placed on a quartz porous filter in the middle of a quartz (FVT-)tube. Using the catalytic Flash Vacuum Thermolysis set-up (*vide infra*) the catalyst was equilibrated at a temperature of 400°C and a vacuum of 0.05 mbar during 15-20 min to remove physisorbed water. Catalysts used in solution phase reactions were employed as powders and used as obtained from the suppliers.

Catalytic Flash Vacuum Thermolysis set-up
The Catalytic Flash Vacuum Thermolysis apparatus, as developed at the Department of Organic Chemistry of the University of Nijmegen, is described and schematically depicted in the Experimental Section of Chapter 4.

Retro Diels-Alder reaction in solution of 4-oxatricyclo[5.2.1.0^{2,6}]dec-8-ene-3,5-dione ***8***
An amount of catalyst (100, 200 or 500 mg) was weighed into a glass round-bottom flask. Toluene (12 ml) and dimethyl fumarate **9** (720 mg) as the trapping agent were added and the

mixture was heated to 110ºC under reflux using an oil bath. Finally, a toluene solution of **8** (165 mg in 5 ml) was added. The mixture was stirred magnetically. The reaction was monitored by taking small aliquots, which were, after filtration, subjected to GC analysis. Results are collected in Table 7.1.

General procedure for the lactonization reaction

An amount of catalyst was weighed into a glass round-bottom flask. Toluene was added and the mixture was heated to 110ºC under reflux using an oil bath. Then, a toluene solution of the substrate was added. The mixture was stirred magnetically. The reaction was monitored by taking small aliquots, which after filtration were subjected to GC analysis.

*Lactonization reaction of dimethyl bicyclo[2.2.1]hept-5-ene-2,3-dicarboxylate **10***

Experiments were carried out following the general procedure described above. To the catalyst (100 or 500 mg) toluene (15 ml), and a toluene solution of **10** (100 mg in 5 ml) were added. Samples were analyzed using gas chromatography after filtration. When GC-analysis showed the absence of starting material the mixture was filtered and concentrated *in vacuo*, which resulted in the isolation of **12**, which was not purified further. Results are collected in Table 7.2.

*Methyl 5-oxo-4-oxatricyclo[4.2.1.0^{3,7}]nonane-9-carboxylate **12***

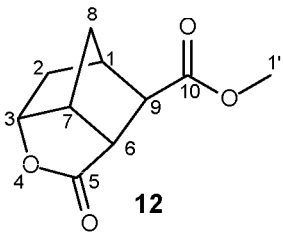

12

^{1}H-NMR (400 MHz, $CDCl_3$, ppm): δ 4.80 (dd, $J_{2endo\text{-}3}$=7.7 Hz, J=5.2 Hz, 1H, H_3), 4.10 (t, $J_{1'\text{-}2'}$=6.7 Hz, 2H, $H_{1'}$), 3.22 (dd, J=4.6 Hz, J=4.7 Hz, 1H, H_7) {decoupling at 4.80 results in d, J=4.7 Hz}, 3.08 (d, J=4.6 Hz, 1H, H_6) {decoupling at 4.80 ppm results in dd, J=1.9 and J=4.9 Hz}, 2.76 (bs, 1H, H_1) {decoupling at 4.80 ppm results in d, J=2.8 Hz}, 2.74 (bs, 1H, H_9), 1.85 (ddd, J=4.0 Hz, $J_{2endo\text{-}3}$=7.7 Hz, $J_{2endo\text{-}2exo}$=14.2 Hz, 1H, H_{2endo}) {decoupling at 4.80 ppm results in dd, J=4.0 Hz and 14.2 Hz}, 1.79 (d, $J_{8a\text{-}8s}$=11.3 Hz, 1H, H_{8a}), 1.67-1.63 (m, 2H, $H_{2'}$), 1.59 (dd, J=3.9 Hz, $J_{2endo\text{-}2exo}$=14.2 Hz, 1H, H_{2exo}), 1.53 (d, $J_{8a\text{-}8s}$=11.3 Hz, 1H, H_{8s}), 1.36-1.28 (m, 10H, $H_{3'}$, $H_{4'}$, $H_{5'}$, $H_{8'}$ and $H_{7'}$), 0.88 (t, $J_{7'\text{-}8'}$=6.7 Hz, 3H, $H_{8'}$). NOE contacts (max distance ~4Å): H_1 couples with H_{2endo}, H_{8a}, H_{8s} and H_9; H_{2endo} couples with H_1 and H_3; H_{2exo} couples with H_{8s}; H_3 couples with H_{2endo}, H_7 and H_{8s}; H_6 couples with H_7, H_{8a} and H_9; H_7 couples with H_3, H_6, H_{8a} and H_{8s}; H_{8a} couples with H_1, H_6, H_7 and H_{8s}; H_{8s} couples with H_1, H_{2exo}, H_3, H_7 and H_{8a}; H_9 couples with H_1 and H_6; $H_{1'}$ couples with $H_{2'}$ and $H_{3'\text{-}7'}$; $H_{2'}$ couples with $H_{1'}$ and $H_{3'\text{-}7'}$; $H_{3'\text{-}7'}$ couples with $H_{1'}$, $H_{2'}$ and $H_{8'}$; $H_{8'}$ couples with $H_{3'\text{-}7'}$. ^{13}C-NMR (100 MHz, $CDCl_3$, ppm): δ 179.2 (s, C_{10}), 172.0 (s, C_5), 80.0 (d, C_3), 65.5 (t, $C_{1'}$), 50.2 (d, C_7), 45.9 (d, C_6), 42.3 (d, C_1), 40.8 (d, C_9), 38.0 (t, C_2), 35.6 (t, C_8), 31.7 (t, $C_{6'}$), 29.1 (t, $C_{4'}$ and $C_{5'}$), 28.5 (t, $C_{2'}$), 25.8 (t, $C_{3'}$), 22.6 (t, $C_{7'}$), 14.0 (q, $C_{8'}$). IR (CCl_4, cm^{-1}): ν 2959, 2931, 2858 (C-H sat), 1790 (C=O lactone), 1736 (C=O ester). EI/GC-MS: *m/e* (%) 295 (8, M^++1), 165 (41, M^+ - OC_8H_{17}, 137 (12, M^+ - $CO_2C_8H_{17}$), 93 (27, M^+ - CO_2 C_8H_{17} - CO_2). HRMS/EI: *m/e* calculated for $C_{17}H_{26}O_4$: 294.1831 amu. Found: 294.1830 ± 0.0011 amu.

Lactonization reaction of methyl bicyclo[2.2.1]hept-5-ene-2-carboxylate ***13***

Experiments were carried out according to the general procedure described above. To the catalyst (1.0 g) toluene (15 ml), and a toluene solution of **13** (180 mg in 5 ml) were added. Samples were analyzed, after filtration, using gas chromatography. When GC-analysis showed the absence of starting material the mixture was filtered and concentrated *in vacuo* and the crude mixture was purified by column chromatography (hexane: ethyl acetate = 4:1) to yield **14** as a colorless oil. Results are collected in Table 7.3.

4-oxatricyclo[4.2.1.0^{3,7}]nonan-5-one ***14***

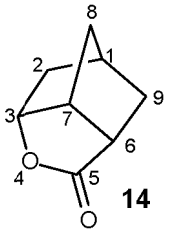

^{1}H-NMR (400 MHz, $CDCl_3$, ppm): δ 4.78 (dd, J=5.4 Hz, J=7.5 Hz, 1H, H_3), 3.19 (dd, J=4.7 Hz, J=4.7 Hz, 1H, H_7), 2.54 (dd, J=4.6 Hz, J=11.3 Hz, 1H, H_6), 2.45 (bs, 1H, H_1), 1.97 (tt, J=3.3 Hz, J=12.1 Hz, 1H, H_{9exo}), 1.78-1.72 (m, 2H, H_{2exo} and H_{9endo}), 1.60 (bs, 2H, H_{2endo} and H_{8a}), 1.53 (dd, J=1.5 Hz, J_{8a-8s}=14.2 Hz, 1H, H_{8s}). NOE contacts (max distance ~4Å): H_1 couples with H_{2exo}, H_{2endo}, H_{8a}, H_{8s}, H_{9endo} and H_{9exo}; H_{2exo} couples with H_1, H_3 and H_{8s}; H_{2endo} couples with H_1 and H_{2exo}; H_3 couples with H_{2exo} and H_7; H_6 couples with H_7, H_{8a} and H_{9exo}; H_7 couples with H_3, H_6 and H_{8a}; H_{8a} couples with H_1, H_6, H_7, H_{8s} and H_{9exo}; H_{8s} couples with H_1, H_{2exo} and H_{8a}; H_{9exo} couples with H_1, H_7 and H_{9endo}; H_{9endo} couples with H_1 and H_{9exo}. ^{13}C-NMR (100 MHz, $CDCl_3$, ppm): δ 181.4 (s, C_5), 80.8 (d, C_3), 46.4 (d, C_7), 39.0 (d, C_6), 38.0 and 37.8 (t, C_2 and C_8), 36.4 (d, C_1), 34.4 (t, C_9).). IR (CCl_4, cm^{-1}): ν 2966 (C-H sat), 1792 (C=O). EI/GC-MS: *m/e* (%) 139 (19, M^+ +1), 138 (1, M^+), 110 (33, M^+ - CO), 94 (7, M^+ - CO_2). HRMS/EI: *m/e* calculated for $C_8H_{10}O_2$: 138.06808 amu. Found: 138.06808 ± 0.00092.

Lactonization reaction of dioctyl bicyclo[2.2.1]hept-5-ene-2,3-dicarboxylate ***15***

Experiments were carried out according to the general procedure described above. To the catalyst (750 mg) toluene (15 ml), and a toluene solution of **25** (150 mg in 5 ml) were added. After filtration samples were analyzed using gas chromatography. When GC-analysis showed the absence of starting material the mixture was filtered and concentrated *in vacuo* and the crude mixture was purified by column chromatography (hexane: ethyl acetate = 4:1) to yield **16** as a colorless oil. Results are collected in Table 7.3.

Octyl 5-oxo-4-oxatricyclo[4.2.1.0^{3,7}]nonane-9-carboxylate ***16***

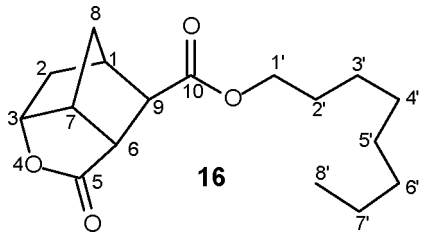

^{1}H-NMR (400 MHz, $CDCl_3$, ppm): δ 4.81 (dd, J=5.1 Hz, J=7.8 Hz, 1H, H_3), 3.73 (s, 3H, $H_{1'}$), 3.23 (dd, J=4.6 Hz, J=4.7 Hz, 1H, H_7), 3.06 (d, J=4.6 Hz, 1H, H_6), 2.77 (d, J=2.3 Hz, 1H, H1), 2.75 (bs, 1H, H_9), 1.86 (ddd, J=4.0 Hz, $J_{2endo-3}$=7.8 Hz, $J_{2endo-2exo}$=14.3 Hz, 1H, H_{2endo}), 1.79 (d, J_{8a-8s}=11.3 Hz, 1H, H_{8a}), 1.58 (dd, J=3.3 Hz, $J_{2endo-2exo}$=14.2 Hz, 1H, H_{2exo}), 1.55 (d, J_{8a-8s}=11.9 Hz, 1H, H_{8s}). ^{13}C-NMR (100 MHz, $CDCl_3$, ppm): δ 178.9 (s, C_{10}), 172.3 (s, C_5), 79.9 (d, C_3), 52.2 (d, C_7), 49.9 (q, $C_{1'}$), 45.7 (d, C_6), 42.4 (d, C_1), 40.5 (d, C_9), 37.8 (t, C_2), 35.5 (t, C_8). IR (CCl_4, cm^{-1}): ν 2993, 2954. (C-H sat), 1786 (C=O lactone), 1739 (C=O ester). EI/GC-MS: *m/e* (%) 197 (M^+ +1, 100), 196 (M^+, 5), 165 (7, M^+ - OCH_3), 152 (9, M^+ - CO_2) 137 (10, M^+ - CO_2CH_3), 93 (M^+ - CO_2CH_3 - CO_2). HRMS/EI: *m/e* calculated for $C_{10}H_{12}O_4$: 196.0736 amu. Found: 196.07355 ± 0.00096 amu.

General procedure for catalytic flash vacuum thermolysis experiments

The Catalytic Flash Vacuum Thermolysis set-up as described above was used. Typically, 100 mg or 400 mg of a fractured catalyst with a sieve fraction of 150-425 μm was placed on a porous filter in the center of the quartz tube. The catalyst was equilibrated at a temperature of 400°C and a vacuum of 0.05 mbar during 15-20 min to remove physisorbed water. The thermolysis oven was brought to the desired temperature and the substrate was weighted into the substrate flask. The vacuum gauge was carefully opened until maximum vacuum was achieved after which the receiving cooler was filled with CO_2/acetone (-78°C). The substrate (usually 50 or 100 mg) was vaporized at room temperature or with the aid of a sublimation oven, at such a rate that evaporation was complete in 45 min. After another 10 min, the system was flushed with nitrogen. Products were rinsed from the receiving cooler with an appropriate solvent and analyzed by gas chromatography. Thermal control experiments were carried out under identical conditions, however, without a catalyst.

Catalytic-FVT of dimethyl bicyclo[2.2.1]hept-5-ene-2,3-dicarboxylate ***10***

Experiments were carried out according to the general procedure described above. Di-ester **10** was vaporized at 70°C and thermolyzed over 100 mg of catalyst in about 40 min. The product mixture (starting material **10** and retro Diels Alder product **9**) was rinsed from the receiving cooler with dichloromethane and analyzed by gas chromatography. Results are collected in Table 7.4.

Analytical data of the *dimethyl fumarate* **9** were in agreement those of an authentic sample.

Catalytic-FVT of ethyl exo-*3,4-epoxy-5-oxo*-endo-*tricyclo[5.2.1.0^{2,6}]deca-8-en-2-carboxylate* ***4a***

Experiments were carried out according to the general procedure described above. **4a** was vaporized at 120°C and thermolyzed over 100 mg or 400 mg of catalyst in about 40 min. The products were rinsed from the receiving cooler with dichloromethane and analyzed by gas chromatography. Several product mixtures were combined and separated by column chromatography (hexane: ethyl acetate = 5:1) to give products **5a**, **6a** and **7a**. Results are collected in Table 7.5.

Analytical data of *cyclopentenone epoxide* **6a** and *pyrone* **7a** were in agreement with literature.[31]

Ethyl 11-oxo-4-oxapentacyclo[6.3.0.0^{2,6}.0^{3,10}.0^{5,9}]undecane-2-carboxylate ***5a***

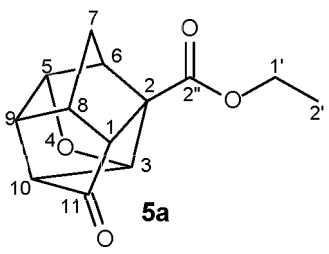

5a

^{1}H-NMR (400 MHz, $CDCl_3$, ppm): δ 4.98 (dd, J=1.2 Hz, J=1.8 Hz, 1H, H_3), 4.84 (d, J=3.1 Hz, 1H, H_5), 4.16 (q, $J_{1'-2'}$=7.1 Hz, 2H, $H_{1'}$), 2.91 (bs, 1H, H_6), 2.60-2.70 (m, 2H, H_8 and H_9), 2.37 (d, J=2.0 Hz, 1H, H_1), 2.24 (d, J=3.5 Hz, 1H, H_{10}), 1.86 (d, J_{7a-7s}=11.5 Hz, 2H, H_{7s}), 1.74 (d, J_{7a-7s}=11.5 Hz, 2H, H_{7a}), 1.26 (t, $J_{1'-2'}$=7.1 Hz, 3H, $H_{2'}$). ^{13}C-NMR (100 MHz, $CDCl_3$, ppm): δ 209.2 (C_{11}), 171.7 ($C_{2''}$), 81.5 and 85.3 (C_3 and C_5), 61.3 (C_2), 61.0 ($C_{1'}$), 52.0, 53.0 and 55.1 (C_1, C_9 and C_{10}), 40.4 and 41.9 (C_6 and C_8), 32.0 (C_7), 14.1 ($C_{2'}$). IR ($CHCl_3$, cm^{-1}): ν 2984 (C-H sat), 1778 (C=O ketone), 1728 (C=O ester); EI/GC-MS: *m/e* (%) 235 (6, M^++1), 234 (6, M^+), 206 (M^+ - CH_2CH_2), 189 (72, M^+ - OEt), 177 (26, M^+ - CO - Et), 161 (59, M^+ - CO_2Et), 132 (59, M^+ - CO - CO_2Et), 66 (74, Cp^+). HRMS/EI: *m/e* calculated for $C_{13}H_{14}O_4$: 234.0892 amu. Found: 234.0892 amu.

Ethyl 11-[2-(2,4-dinitrophenyl)hydrazono]-4-oxa-pentacyclo[6.3.0.0^{2,6}.0^{3,10}.0^{5,9}]undecane-2-carboxylate ***19***

To **5a** (32.3 mg, 0.138 mmol) dissolved in ethanol (0.5 ml) was added at room temperature under stirring 0.70 ml of the following mixture[52]: conc. H_2SO_4 (2.02 ml), DNPH (dinitrofenylhydrazine, 0.13 mmol, 0.335 g), ethanol (5.9 ml) and water (2.4 ml). A yellow precipitate was formed immediately and GC analysis showed a complete conversion after 4.5 h. The precipitate was filtered (Hirsch funnel), washed on the filter with water, an aqueous sodium bicarbonate solution and water and then dissolved in dichloromethane. After drying ($MgSO_4$) and concentrating *in vacuo* **19** (17 mg, 30%) was obtained. Recrystallization (5x) from ethanol and finally from methanol (1x), each time removing the supernatant, afforded yellow platelet-like crystals.

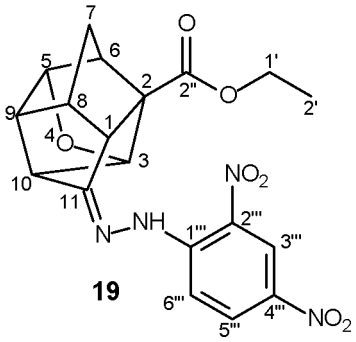

M.p.: 186°C. ^{1}H-NMR ($CDCl_3$, 400 MHz, ppm): δ 11.09 (s, 1H, NH), 9.13 (d, $J_{3'''-5'''}$=2.5 Hz, 1H, $H_{3'''}$), 8.31 (dd, $J_{5'''-6'''}$=9.6 Hz, $J_{3'''-5'''}$=2.5 Hz, 1H, $H_{5'''}$), 7.92 (d, $J_{5'''-6'''}$=9.6 Hz, 1H, $H_{6'''}$), 4.97 (s, 1H, H_3 or H_5), 4.86 (d, J=3.0 Hz, 1H, H_3 or H_5), 4.18 (q, $J_{1'-2'}$=7.1 Hz, 2H, $H_{1'}$), 3.05 (bs, 1H, H_9), 2.95 (s, 1H, H_6 or H_8), 2.83 (s, 1H, H_6 or H_8), 2.60-2.70 (m, 2H, H_1 and H_{10}), 1.83 (d, J_{7a-7s}=11.6 Hz, 1H, H_{7a} or H_{7s}), 1.78 (d, J_{7a-7s}=11.5 Hz, 1H, H_{7a} or H_{7s}), 1.26 (t, $J_{1'-2'}$=7.1 Hz, 3H, $H_{2'}$); ^{13}C-NMR ($CDCl_3$, 100 MHz, ppm): δ 172.0 (C_{11}), 162.9 ($C_{2''}$), 145.2 ($C_{1'''}$), 137.8 ($C_{2'''}$), 130.0 ($C_{5'''}$), 129.0 ($C_{4'''}$), 123.5 ($C_{3'''}$), 116.3 ($C_{6'''}$), 85.2 and 84.0 (C_3 and C_5), 61.6 (C_2), 61.4 ($C_{1'}$), 54.1, 53.3, 45.1, 44.4 and 43.4 (C_1, C_6, C_8, C_9 and C_{10}), 31.2 (C_7), 14.2 ($C_{2'}$). IR (KBr, cm^{-1}): ν 3431 (imine N-H stretch), 3110 (Ar-H), 2990, 2931, 2883 en 2850 (C-H sat), 1721 (C=O), 1656 (imine C=N-R), 1623 and 1344 (nitro), 1510 en 1526 (imine -N-H bend). EI/MS: *m/e* (%) 414 (100, M^+), 385 (27, M^+ - Et), 369 (21, M^+ - OEt), 189 (89, M^+ - $NHC_6H_3(NO_2)_2$ – CH_2CH_2), 77 (31, $C_6H_5^+$), 30 (14, NO^+), 29 (46, Et^+). HRMS/EI: *m/e* calculated for $C_{19}H_{18}N_4O_7$: 414.1175 amu. Found: 414.1175 ± 0.0012 amu.

Catalytic-FVT of ethyl exo-*3,4-epoxy-5,5-dimethoxy*-endo-*tricyclo[5.2.1.0^{2,6}]deca-8-en-2-carboxylate* ***4b***

Experiments were carried out according to the general procedure described above. Carboxylate **4b** was vaporized at 150°C and thermolyzed over 400 mg of catalyst in about 40 min. The products were rinsed from the receiving cooler with dichloromethane and analyzed by gas chromatography. Results are collected in Table 7.6.

Catalytic FVT of exo-*5*-tert-*butyl*-endo-*4,5-epoxy*-endo-*tricyclo[5.2.1.0^{2,6}]dec-8-en-3-one* ***4c***

Experiments were carried out according to the general procedure described above. Epoxy ketone **4c** (40 mg) was vaporized at 70 °C and thermolyzed over 400 mg of B698D-24 catalyst. The cooler was rinsed with dichloromethane and the reaction products were analyzed using gas chromatography. A series of four runs of 40 mg substrate each was performed to obtain a preparatively useful amount of the mixture of products. The reaction mixture was purified by chromatography (hexane: ethyl acetate = 6:1), preparative thin layer chromatography (hexane: ethyl acetate = 2.5:1) and again preparative thin layer chromatography (chloroform:

benzene: ethyl acetate = 4:1:1) to yield **5c** and **26** as a yellowish oil and white solid, respectively. Results are collected in Table 7.7.

*5-(*tert*-butyl)-4-oxapentacyclo[6.3.0.0^{2,6}.0^{3,10}.0^{5,9}]undecan-7-one* **5c**

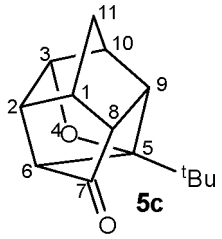

^{1}H-NMR (400 MHz, $CDCl_3$, ppm): δ 4.64-4.62 (m, 1H, H_3), 2.66-2.62 (m, 2H, H_2, H_9), 2.60-2.58 (m, 1H, H_{10}), 2.44 (bs, 1H, H_1), 2.13 (d, $J_{2,6}$=4.0 Hz, 1H, H_6), 2.10-2.08 (m, 1H, H_8), 1.75 (d, $J_{11a,11s}$=6.8 Hz, 1H, H_{11s}), 1.58 (d, $J_{11a,11s}$=6.8 Hz, 1H, H_{11a}), 1.00 (s, 9H, tBu). NOE contacts (max distance ~4Å): H_1 couples with H_2, H_8, H_{11s} and H_{11a}; H_2 and H_9 couple with H_1, H_3 H_8, H_{10}, and H_{tBu}; H_6 couples with H_2 and H_{tBu}; H_8 couples with H_1, H_9 and H_{11a}; H_{10} couples with H_8, H_{11a} and H_{11b}; H_{11s} couples with, H_1, H_3 and H_{10}; H_{11a} couples with H_1, H_8 and H_{10}; H_{tBu} couples with H_8, H_9 and H_{10}. ^{13}C-NMR (100 MHz, $CDCl_3$, ppm): δ 214.2 (s, C_7), 96 (s, C_5), 52.5 (d, C_8), 52.2 (d, C_6), 48.6 (d, C_{10}), 46.6 and 46.2 (d, C_9 and C_2), 39.4 (d, C_1), 33.4 (s, $\underline{C}(CH_3)_3$), 33.1 (t, C_{10}), 26.0 (q, $C(\underline{C}H_3)_3$). IR (CCl_4, cm^{-1}): ν 2962 (C-H sat), 1766 (C=O). EI/GC-MS: *m/e* (%) 218 (6, M^+), 203 (4, M^+ - CH_3), 190 (5, M^+ - CO), 161 (7, M^+ - ^{t}Bu), 109 (100, M^+ - ^{t}Bu – CO – CH_2). HRMS/EI: *m/e* calculated for $C_{14}H_{18}O_2$: 218.13068 amu. Found: 218.13045 ± 0.00082 amu.

*5-(*tert*-butyl)-4-hydroxy-*endo*-tricyclo[5.2.1.0^{2,6}]deca-4,8-dien-3-one* **26**

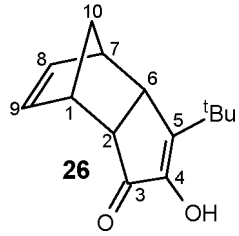

^{1}H-NMR (400 MHz, $CDCl_3$, ppm): δ 5.91 (dd, $J_{8,9}$=5.6 Hz, $J_{1,9}$=2.9 Hz, 1H, H_9), 5.77 (dd, $J_{8,9}$=5.6 Hz, $J_{7,8}$=2.9 Hz, 1H, H_8), 5.19 (s, 1H, OH, exchanges with water), 3.21 (t, $J_{6,7}$=4.5 Hz, 1H, H_6), 3.14 (bs, 1H, H_1), 3.03 (bs, 1H, H_7), 2.74 (t, $J_{1,2}$=4.9 Hz, 1H, H_2), 1.78 (d, $J_{10a,10s}$=8.5 Hz, 1H, H_{10s}), 1.61 (d, $J_{10a,10s}$=8.5 Hz, 1H, H_{10a}), 1.05 (s, 9H, tBu). NOE contacts (max distance ~4Å): H_1 couples with H_2, H_{10s}, H_{10a} and H_{tBu}; H_2 couples with H_1, H_6 and H_{10a}; H_6 couples with H_2, H_7, H_{10a} and H_{tBu}; H_7 couples with H_6, H_8, H_{10a}, H_{10s} and H_{tBu}; H_8 couples with H_7, H_9, H_{tBu} and weakly with H_{10s}; H_9 couples with H_1, H_8 and weakly with H_{10s}; H_{10a} couples with H_1, H_2, H_6, H_7 and H_{10s}; H_{10s} couples with H_1, H_7 and weakly with H_8 and H_9; H_{tBu} couples with H_6, H_7 and H_8. ^{13}C-NMR (100 MHz, $CDCl_3$, ppm): δ 203.5 (s, C_3), 153 (s, C_5), 150 (s, C_4), 132.6 and 132.3 (d , C_8 and C_9), 52.1 (t, C_{10}), 47.2, 45.1, 43.6 and 42.7 (C_1, C_2, C_6 and C_7), 33.9 (s, $\underline{C}(CH_3)_3$), 28.5 (q, $C(\underline{C}H_3)_3$). IR (CCl_4, cm^{-1}): ν 3478 (OH), 2960, 2932, 2871 (C-H sat), 1701 (C=O). EI/GC-MS: *m/e* (%) 218 (6, M^+), 203 (11, M^+ - CH_3), 190 (59, M^+ - CO), 161 (4, M^+ - ^{t}Bu), 152 (27, M^+ - Cp), 110 (100, M^+ +1 – Cp - 3x CH_3), 66 (52, Cp). HRMS/EI: *m/e* calculated for $C_{14}H_{18}O_2$: 218.13068 amu. Found: 218.13045 ± 0.00082 amu.

endo-*Tricyclo[6.2.1.0^{2,7}]undeca-4,9-diëen-3,6-dione* ***28***

Cyclopentadiene (70 g, 1.06 mol) was added dropwise under stirring in 30 min to a solution of *p*-benzoquinone **27** (132 g, 1.22 mol) in methanol (660 ml) at 0-5°C. The mixture was stirred for 2.5 h at room temperature. The resulting brown liquid was concentrated *in vacuo* to yield **28** (206 g) as a brown solid, which was not further purified.

Analytical data were in agreement with literature.[31]

exo-4,5-Epoxy-endo-tricyclo[6.2.1.0^{2,7}]undeca-9-en-3,6-dione ***1***

An aqueous solution of sodium carbonate (30 g in 120 ml) was added to an acetone solution of crude *endo*-tricyclo[6.2.1.0^{2,7}]undeca-4,9-dien-3,6-dione **28** (106 g, 0.608 mol, in 250 ml) and the solution was cooled to 6°C. Hydrogen peroxide (35%, 200 ml) was added slowly in 2 h at 16°C. The mixture was poured into water (1.5 l) after 2.5 h and filtered. Water (200 ml) was added to the residue and the mixture was extracted with dichloromethane (6x200 ml). The combined organic layers were dried ($MgSO_4$) and concentrated *in vacuo* to yield **1** (57 g, 50%) as a slightly yellow solid, which was not further purified.

Analytical data were in agreement with literature.[31]

Ethyl 5-oxo-endo-*tricyclo[5.2.1.0^{2,6}]deca-3,8-diene-2-carboxylate* ***29***

An aqueous 10% sodium hydroxide solution (17 ml) was added slowly to an ethanol solution of *exo*-4,5-epoxy-*endo*-tricyclo[6.2.1.0^{2,7}]undeca-9-en-3,6-dione **1** (25 g, 0.13 mol, in 250 ml) while stirring at room temperature. The mixture was kept at this temperature. After GC analysis showed the absence of the starting material, the brown mixture was concentrated *in vacuo*, dissolved in water and extracted with diethyl ether (200 ml). The water layer was extracted with diethyl ether (3x200 ml) and the combined organic layers were washed with water (3x100 ml), dried (Na_2SO_4) and concentrated *in vacuo*. The crude product was purified by column chromatography (*n*-hexane: ethyl acetate = 10:1) to give **29** (10.4 g, 33.4%) as a yellow oil.

Analytical data were in agreement with literature.[31,46]

Ethyl exo-*3,4-epoxy-5-oxo*-endo-*tricyclo[5.2.1.0^{2,6}]deca-8-en-2-carboxylate* ***4a***

Aqueous solutions of sodium hydroxide (0.59 g in 75 ml) and hydrogen peroxide (35%, 36 ml) were added slowly to a solution of ethyl 5-oxo-*endo*-tricyclo[5.2.1.0^{2,6}]deca-3,8-diene-2-carboxylate **12** (9.9 g, 45.4 mmol) in a mixture of dichloromethane (180 ml) and methanol (200 ml). The mixture was kept at room temperature. After 140 min the layers were separated and the water/methanol layer was extracted with dichloromethane (3x150 ml). The combined dichloromethane layers were washed with water (3x150 ml), dried ($MgSO_4$) and concentrated *in vacuo* to yield **4a** (8.21 g, 77%). Recrystallization from ethanol gave **4a** (7.92 g, 75%) as white needles. M.p.: 120°C.

Analytical data were in agreement with literature.[31,48]

Ethyl exo-*3,4-epoxy-5,5-dimethoxy*-endo-*tricyclo[5.2.1.0^{2,6}]deca-8-en-2-carboxylate* ***4b***

To ethyl-*exo*-3,4-epoxy-5-oxo-*endo*-tricyclo[5.2.1.0^{2,6}]deca-8-en-2-carboxylate **4a** (5.8 g, 25 mmol) dissolved in methanol (300 ml) was added cold methanol (5 ml) saturated with hydrogen chloride in one portion and subsequently trimethyl orthoformiate (10.6 g, 100 mmol) in one portion. After 9 h of heating under reflux conditions potassium hydroxide was added to the solution until pH~9. The mixture was extracted with dichloromethane (3x100 ml), dried ($MgSO_4$) and concentrated *in vacuo* to yield **4b** (7.0 g, 100%) as a colorless oil, which crystallized upon standing and subsequently recrystallized from 2-propanol.

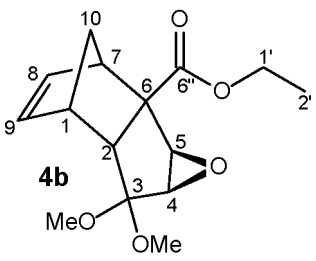

M.p.: 38°C. ^{1}H-NMR (100 MHz, $CDCl_3$, ppm): δ 6.09-6.28 (m, 2H, H_8 and H_9), 4.29 (q, $J_{1'-2'}$=7.1 Hz, 2H, $H_{1'}$), 3.30 and 3.37 (s, 6H, 2x -OCH_3), 3.08-3.48 (m, 5H, H_1, H_3, H_4, H_6 and H_7), 1.59 (s, 2H, H_{10}), 1.34 (t, $J_{1'-2'}$=7.1 Hz, 3H, $H_{2'}$). ^{13}C-NMR (25 MHz, $CDCl_3$, ppm): δ 173.4 ($C_{2''}$), 131.1 and 139.2 (C_8 and C_9), 106.4 (C_5), 64.3 (C_2), 61.7 and 62.0 (C_3 and C_4), 61.1 ($C_{1'}$), 59.0 (C_6), 50.0 and 50.6 (2x -OCH_3), 49.7 (C_1 or C_7), 48.6 (C_{10}), 45.5 (C_1 or C_7), 14.3 ($C_{2'}$). IR (CH_2Cl_2, cm^{-1}): ν 3000-2929 (C-H sat), 1725 (C=O); EI/GC-MS: *m/e* (%) 281 (2, M^+ +1), 249 (49, M^+ - OCH_3), 215 (11, M^+ - Cp), 207 (47, M^+ - CO_2Et), 185 (90, M^+ - Cp – Et), 183 (100, M^+ - Cp - OCH_3), 66 (50, Cp). Analysis calculated for $C_{15}H_{20}O_5$: C 64.27%, H 7.19%. Found: C 63.97%, H 7.15%.

2-Hydroxymethyl-exo-*3,4-epoxy-5,5-dimethoxy*-endo-*tricyclo[5.2.1.0^{2,6}]deca-8-ene* ***4f***

Ethyl *exo*-3,4-epoxy-5,5-dimethoxy-*endo*-tricyclo[5.2.1.0^{2,6}]deca-8-en-2-carboxylate **4b** (1.00 g, 3.57 mmol) in dry diethyl ether (10 ml) was added in 5 min to $LiAlH_4$ (0.16 g, 4.3 mmol) in dry diethyl ether (30 ml). TLC analysis showed the absence of the starting material after 5 min. The mixture was quenched with ethyl acetate and water and 0.2 N HCl was added until pH~8. The water layer was extracted with diethyl ether (3x), which was dried ($MgSO_4$) and concentrated *in vacuo* to give **4f** (0.77 g, 91%) as a colorless oil.

Analytical data were in agreement with literature.[31]

2-Hydroxymethyl-exo-*3,4-epoxy*-endo-*tricyclo[5.2.1.0^{2,6}]deca-8-en-5-one* ***4d***

To an acetone solution of 2-hydroxymethyl-*exo*-3,4-epoxy-5,5-dimethoxy-*endo*-tricyclo-[5.2.1.0^{2,6}]deca-8-ene **4f** (0.77 g, 3.24 mmol, in 20 ml) was added 4 M HCl (0.5 ml). After 30 min of stirring sodium bicarbonate and magnesium sulfate were added until pH~5 and stirring was continued for another 30 min. The mixture was filtered and concentrated *in vacuo* to give **4d** (0.51 g, 83%) as a thick yellow oil, which solidified upon standing.

Analytical data were in agreement with literature.[31]

2-Methylacetoxy-exo-*3,4-epoxy*-endo-*tricyclo[5.2.1.0^{2,6}]deca-8-en-5-one* ***4e***

2-Hydroxymethyl-*exo*-3,4-epoxy-*endo*-tricyclo[5.2.1.0^{2,6}]deca-8-en-5-one **4d** (0.78 g, 4.08 mmol) in dichloromethane (20 ml) was stirred for 1.5 h at room temperature together with acetic anhydride (10 ml, 10.7 mmol), triethylamine (0.6 ml, 4.2 mmol) and DMAP (96 mg, 0.78 mmol). The mixture was concentrated *in vacuo* and dissolved in dichloromethane and water. Sodium bicarbonate was added until pH~8 and the excess sodium bicarbonate was removed by filtration. The filtrate was extracted with diethyl ether (3x) and the combined organic layers were washed with brine, dried and concentrated *in vacuo* to yield **4e** (0.57 g, 60%) as white crystals. M.p.: 60°C.

Analytical data were in agreement with literature.[31]

endo-*Tricyclo[5.2.1.0^{2,6}]deca-4,8-dien-3-ol* ***31***

Dicyclopentadiene **30** (95 ml, 0.72 mol) was added to a suspension of SeO_2 (33 g, 0.30 mol) in dioxane (250 ml) and water (25 ml). The reaction mixture was heated at reflux temperature for 3 h. The mixture was allowed to cool to room temperature and then filtered. The filtrate

was poured out in water (800 ml) and subsequently extracted with diethyl ether (3x). The combined organic layers were dried over $MgSO_4$ and concentrated *in vacuo*. The crude reaction product was purified by distillation under reduced pressure, to give **31** (44 g) as a yellow oil, which solidified upon standing. B.p.: 84 °C/3.6 mbar.
Analytical data were in agreement with literature.[53]

endo-*Tricyclo[5.2.1.0^{2,6}]deca-4,8-dien-3-one* **32**
A solution of **31** (20.4 g, 138 mmol) in dichloromethane (75 ml) was added to a suspension of PCC (44.8 g, 208 mmol) in dichloromethane (250 ml) at 0 °C under a nitrogen atmosphere. The reaction mixture was stirred for 4 h, filtered and concentrated *in vacuo*. The residue was dissolved in diethyl ether and extracted with saturated aqueous ammonium chloride (2x) and 5% aqueous ammonium hydroxide (2x). After drying over $MgSO_4$ and filtration over a short column of silica 60 and concentration *in vacuo*, **32** (15.1 g, 75%) was obtained as a light yellow oil, which solidified upon standing.
Analytical data were in agreement with literature.[50]

exo-*4,5-Epoxy*-endo-*tricyclo[5.2.1.0^{2,6}]deca-4,8-dien-3-one* **33**
30% hydrogenperoxide (30 ml) and 0.2 M aqueous sodium hydroxide (40 ml) were added to a solution of **32** (9.05 g, 62 mmol) in a mixture of dichloromethane/methanol (1:1, 150 ml) at room temperature. After stirring for 45 min the reaction mixture was poured out in dichloromethane (350 ml). After washing with brine (3x), drying over $MgSO_4$ and concentration *in vacuo*, **33** (10.4 g, 100%) was obtained as a white solid.
Analytical data were in agreement with literature.[31]

exo-*5*-tert-*Butyl*-endo-*4,5-epoxy*-endo-*tricyclo[5.2.1.0^{2,6}]dec-8-en-3-ol* **34**
A 1.5 M solution of *tert*-butyllithium (4.5 ml, 6.7 mmol) in hexane was added to a solution of **33** (1.00 g, 6.17 mmol) in freshly distilled tetrahydrofurane (60 ml) at 0°C and under an argon atmosphere. After 30 min, stirring was continued at room temperature. After another 60 min an additional amount of *tert*-butyllithium (1.0 ml, 1.5 mmol) was added at 0 °C. The reaction mixture was stirred for an additional 2 h at room temperature, quenched with saturated aqueous ammonium chloride and extracted with diethyl ether (2x). The combined organic layers were dried over $MgSO_4$ and concentrated *in vacuo*. The crude reaction product was purified by flash chromatography (chloroform: benzene: ethyl acetate = 4:1:1) to yield **34** (0.67 g, 49%) as a colorless oil.
Analytical data were in agreement with literature.[50,51]

exo-*5*-tert-*Butyl*-endo-*4,5-epoxy*-endo-*tricyclo[5.2.1.0^{2,6}]dec-8-en-3-one* **4c**
A solution of **35** (0.64 g, 2.9 mmol) in dichloromethane (10 ml) was added to a suspension of PCC (1.18 g, 5.4 mmol) in dichloromethane (15 ml) at room temperature under a nitrogen atmosphere. The reaction mixture was stirred for 5 h, diluted with diethyl ether (100 ml), filtrated over a short column of silica 60 and concentrated *in vacuo*. The resulting solid was recrystallized from hexane to yield **4c** (0.55 g, 86%) as white crystals.

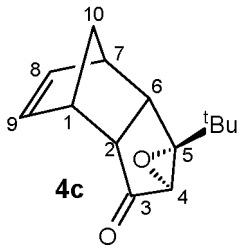

M.p.: 84-85 ºC. ^{1}H-NMR (400 MHz, $CDCl_3$, ppm): δ 6.16 (dd, $J_{8,9}$=5.4 Hz, $J_{7,8}$=2.9 Hz, 1H, H_8), 5.77 (dd, $J_{8,9}$=5.4 Hz, $J_{1,9}$=2.3 Hz, 1H, H_9), 3.13-3.08 (m, 2H, H_7 and H_6), 3.02-2.99 (m, 3H, H_1, H_2 and H_4), 1.54 and 1.44 (ABq, J_{AB}=8.3 Hz, 2H, H_{10a} and H_{10s}), 1.04 (s, 9H, tBu). ^{13}C-NMR (100 MHz, $CDCl_3$, ppm): δ 207.7 (s, C3), 136.7 (d, H8), 132.7 (d, H9), 73.7 (s, C5), 62.2 (d, C4), 55.8 (d, C2), 46.8, 43.8 and 40.5 (d, C1, C6 and C7), 32.6 (s, $\underline{C}(CH_3)_3$), 26.4 (q, $C(\underline{C}H_3)_3$). IR (CCl_4, cm^{-1}): ν 2968, 2940, 2870 (C-H sat), 1741 (C=O). EI/GC-MS: *m/e* (%) 218 (5, M^+), 203 (3, M^+ - CH_3), 161 (14, M^+ - ^{t}Bu), 153 (59, M^+ +1 - Cp), 66 (83, Cp). HRMS/EI: *m/e* calculated for $C_{14}H_{18}O_2$: 218.13068 amu. Found: 218.13024 ± 0.00082 amu.

7.5.1 Crystal structure of Ethyl 11-[2-(2,4-dinitrophenyl)hydrazono]-4-oxa-pentacyclo[6.3.0.0^{2,6}.0^{3,10}.0^{5,9}]undecane-2-carboxylate 19

Ethyl 11-[2-(2,4-dinitrophenyl)hydrazono]-4-oxa-pentacyclo[6.3.0.0^{2,6}.0^{3,10}.0^{5,9}]undecane-2-carboxylate ***19***

An irregularly shaped crystal platelet of dimensions 0.52 x 0.16 x 0.08 mm was mounted on a glassfiber and the structure of **19** was determined at 293K. Crystal data are given in Table 7.8.

Table 7.8 Crystal data and structure refinement for compound **19**

Crystal colour / shape	Transparent orange / irregular platelet
Crystal size	0.52 x 0.16 x 0.08 mm
Empirical formula	$C_{38}H_{36}N_8O_{14}$
Formula weight	828.75 g/mol
Temperature	293(2) K
Radiation / Wavelength	CuKα (graphite monochrom.) / 1.54184 Å
Crystal system	Orthorhombic
Space group	Pcab
Unit cell dimensions	a = 13.0469(12) Å
(21 reflections, 19.821 < θ < 25.561)	b = 16.1444(11) Å
	c = 36.706(3) Å
Volume	7731.5(10) Å^3
Z	8
Calculated density	1.424 Mg/m^3
Absorption coefficiënt	0.940 mm^{-1}
Diffractometer / scan	Enraf-Nonius CAD4 / ω
F(000)	3456
θ–range for data collection	4.52 to 70.45 deg.
Index ranges	0≤ h≤15, -19≤k≤ 0, -44≤l≤44
Reflections collected / unique	14525 / 7352 [R(int) = 0.2289]
Reflections observed	1704 ([Io>2σ(Io)])
Absorption correction	Semi-empirical from ψ-scans
Range of relat. transm. Factors	1.187 and 0.910
Refinement method	Full-matrix least-squares on F^2
Computing	SHELXL-97 (Sheldrick, 1997)
Data / restraints / parameters	7352 / 92 / 543
Goodness-of-fit on F^2	1.189
SHELXL-97 weight parameters	0.100000
Final R indices [I>2σ(I)]	R_1 = 0.1650, wR_2 = 0.3286
R indices (all data)	R_1 = 0.3925, wR_2 = 0.4061
Largest diff. peak and hole	0.812 and -0.383 e/Å^3

7.6 REFERENCES

1 Carey, F.A.; Sundberg, R.J. in *Advanced Organic Chemistry, Part A: Structure and Mechanisms* 3rd edn., Plenum Press, New York, 1990, p625.

2 Laszlo, P.; Lucche, J. *Actual. Chim.* **1984**, 42.

[3] Fringuelli, F.; Taticchi, A. in *Dienes in the Diels-Alder Reaction*, Wiley-Interscience, New York, 1990.

[4] Carruthers, W. in *Cycloaddition Reactions in Organic Synthesis*, Pergamon, Oxford, 1990.

[5] Tedder, J.M.; Nechvatal, A.; Jubb, A.H. in *Industrial Products; Basic Chemistry*, Part 5, Wiley, New York, 1975.

[6] Pindur, U.; Lutz, G.; Otto, C. *Chem. Rev.* **1993**, *93*, 741.

[7] a) Jenner, G. in *Pericyclic Reactions; Organic High-Pressure Chemistry*, Le Noble, W.G. Ed., Elsevier, 1989. b) McCabe, J.R.; Eckert, C.A. *Acc. Chem. Res.* **1974**, *7*, 251.

[8] a) Breslow, R. *Acc. Chem. Res.* **1991**, *24*, 159. b) Blake, J.F.; Jorgensen, W.L. *J. Am. Chem. Soc.* **1991**, *113*, 7430. c) Desimoni, G.; Pasini, D.; Righetti, P.P. *Tetrahedron* **1992**, *48*, 1667.

[9] Cativiela, C.; García, J.I.; Pires, E.; Royo, A.J.; Figueras, F. *Appl. Catal. A: General* **1995**, *131*, 159.

[10] Chew, S.; Ferrier, J. *J. Chem. Soc., Chem. Commun.* **1986**, 911.

[11] Rao, K.R.; Srinivasan, T.N.; Bhanumathi, N. *Tetrahedron Lett.* **1990**, *31*, 5959.

[12] Hilvert, D.; Hill, K.W.; Nared, K.D.; Bartlett, P.A.; Schultz, P.G. *J. Am. Chem. Soc.* **1989**, *111*, 9261.

[13] a) Bakhtiar, R.; Drader, J.J.; Jacobson, D.B. *J. Am. Chem. Soc.* **1992**, *114*, 8304. b) Lautens, M.; Tam, W.; Edwards, L.G. *J. Org. Chem.* **1992**, *57*, 8.

[14] Yedidia, V.; Leznoff, C.C. *Can. J. Chem.* **1980**, *58*, 1144.

[15] a) McGinnis, M.B.; Vagle, K.; Green, J.F.; Tan, L.C.; Palmer, R.; Siler, J.; Pagni, R.M.; Kabalka, G.W. *J. Org. Chem.* **1996**, *61*, 3496. b) Pagni, R.M.; Kabalka, G.W.; Hondroginannis, G.; Bains, S.; Anosike, P.; Kurt, R. *Tetrahedron* **1993**, *49*, 6743. c) Wali, A.; Satish, S. *Indian J. Chem. B* **1992**, *31B*, 207. d) Kabalka, G.W.; Pagni, R.M.; Bains, S.; Hondrogiannis, G.; Plesco, M.; Kurt, R.; Cox, D.; Green, J. *Tetrahedron Asymm.* **1991**, *2*, 1283.

[16] Conrads, M.; Mattay, J.; Runsink, J. *Chem. Ber.* **1989**, *122*, 2207.

[17] Matsumoto, Y.; Mita, K.; Hashimoto, K.; Tokoroyama, T. *Appl. Catal. A.: General* **1995**, *131*, L1.

[18] a) Narayana Murthy, Y.V.S.; Pillai, C.N.; *Synth. Commun.* **1991**, *21*, 783. b) Cativiela, C.; Figueras, F.; Fraile, J.M.; Garcia, J.I.; Mayoral, J.A.; de Ménorval, L.C.; Pires, E. *Appl. Catal. A: General* **1993**, *101*, 253.

[19] a) García, J.I.; Mayoral, J.A.; Pires, E.; Brown, D.R.; Massam, J. *Catal. Lett.* **1996**, *37*, 261. b) Cativiela, C.; Figueras, F.; García, J.I.; Mayoral, J.A., Pires, E.; Royo, A.J. *Tetrahedron Assym.* **1993**, *4*, 621. c) Cativiela, C.; Fraile, J.M.; García, J.I.; Mayoral, J.A., Pires, E.; Royo, A.J.; Figueras, F.; de Ménorval, L.C. *Tetrahedron* **1993**, *49*, 4073. d) Fraile, J.M.; Garcia, J.I.; Mayoral, J.A.; Royo, A.J. *Tetrahedron Asymm.* **1996** , *7*, 2263.

[20] a) Adams. J.M.; Dyer, S.; Martin, K.; Matear, W.A., McCabe, R.W. *J. Chem. Soc. Perkin Trans 1* **1994**, 761. b) Cativiela, C.; Fraile, J.M.; Gracia, J.I.; Mayoral, J.A.; Figueras, F.; de Menorval, L.C.; Alonso, P.J. *J. Catal.* **1992**, *137*, 394. c) Laszlo, P.; Moison, H. *Chem. Lett.* **1989**, 1031. d) Nagakura, M.; Kai, Y.; Yoshitomi, K. *Yukagaku* **1975**, *24*, 253. e) Balogh, M.; Laszlo, P. 'Diels-Alder Reactions' in *Organic Chemistry Using Clays*, Springer Verlag, Berlin, 1993, p95.

[21] Ichihara, A. *Synthesis* **1987**, 207.

[22] Klunder, A.J.H.; Zhu, J.; Zwanenburg, B. *Chem. Rev.* **1999**, *99*, 1163.

[23] Griesbeck, A.G. *J. Prakt. Chem.* **1993**, *335*, 489.

[24] Kresze, G.; Rau, S.; Sabelus, G.; Götz, H. *J. AM. Chem. Soc.* **1987**, *109*, 2469.

[25] a) Houwen-Claassen, A.A.M. *Thesis*, University of Nijmegen, The Netherlands, 1990. b) Jenner, G.; Papadopoulos, M.; Rimmelin, J. *J. Org. Chem.* **1983**, *48*, 748.

[26] Sauer, J. *Angew. Chem. Int. Ed. Engl.* **1967**, *6*, 16.

[27] Cope, A.C.; Haven jr., A.C.; Ramp, F.L.; Trumbull, E.R. *J. Am. Chem. Soc.* **1952**, *74*, 4867.

[28] a) Grieco, P.A.; Parker, D.T.; Cornwell, M.; Ruckle, R. *J. Am. Chem. Soc.* **1987**, *109*, 5859. b) Grieco, P.A.; Clark, J.D. *J. Org. Chem.* **1990**, *55*, 2271.
[29] a) Grieco, P.A.; Abood, N. *J. Org. Chem.* **1989**, *54*, 6008. b) Grieco, P.A.; Abood, N. *J. Chem. Soc., Chem. Commun.* **1990**, 410.
[30] Marchand, A.P.; Vidyasagar, V. *J. Org. Chem.* **1988**, *53*, 4412.
[31] Van der Waals, A.C.L.M *Thesis*, University of Nijmegen, The Netherlands, 1997.
[32] Klunder, A.J.H., Zwanenburg, B. 'Gas Phase Thermolysis in Natural Product Synthesis' in *Gas Phase Reactions in Organic Synthesis*, Vallée, Y. Ed., Gordon and Breach Science Publishers, Amsterdam, 1997, p107.
[33] a) Brown, R.F.C. 'Cleavage of Carbocyclic Systems with Related Heterocyclic Examples' in *Pyrolytic Methods in Organic Chemistry; Organic Chemistry Monographs*, Vol. 41, Academic Press, New York, 1980, p259. b) Wiersum, U.E. *Recl. Trav. Chim. Pays-Bas* **1982**, *101*, 365.
[34] a) Bin Sadikun, A.; Davies, D.I. *J. Chem. Soc. Perkin Trans. 1* **1982**, 2461. b) Fieser, L.F.; Williamson, K.L. *Organic Experiments*, 7th Ed., D.C. Heath and Company, Lexington, 1992, p283.
[35] Carey, F.A.; Sundberg, R.J. in *Advanced Organic Chemistry, Part A: Structure and Mechanisms* 3rd edn., Plenum Press, New York, 1990, p181.
[36] Janssen, A.J.M. *Thesis*, University of Nijmegen, The Netherlands, 1991.
[37] Corey, E.J.; Weinshenker, N.M.; Schaaf, T.K.; Huber, W. *J. Am. Chem. Soc.* **1969**, *91*, 5675.
[38] Ortuño, R.M.; Alonso, D.; Cardellach, J.; Font, J. *Tetrahedron* **1987**, *43*, 2191.
[39] Huisgen, R. *Angew. Chem.* **1977**, *89*, 589.
[40] a) Eberbach, W.; Burchhardt, B.; Trostmann, U. *Tetrahedron Lett.* **1979**, 4049. b) Klärner, F-G.; Golz, T.; Uhländer, C.; Yaslak, S. *Tetrahedron Lett.* **1996**, *37*, 1385.
[41] a) Dahmen, A.; Hamberger, H.; Huisgen, R.; Markowski, V. *J. Chem. Soc., Chem. Commun.* **1971**, 1192. b) Huisgen, R.; Markowski, V. *J. Chem. Soc., Chem. Commun.* **1977**, 440.
[42] a) Ullman, E.F.; Milks, J.E. *J. Am. Chem. Soc.* **1962**, *84*, 1315. b) Ullman, E.F.; Milks, J.E. *J. Am. Chem. Soc.* **1964**, *86*, 3814.
[43] Stewart, J.J. *J. Computer-Aided Molecular Design* **1990**, *4*, 1.
[44] Klunder, A.J.H.; Zwanenburg, B. *Chem. Rev.* **1989**, *89*, 1035.
[45] Borkent, J.H. Centre for Molecular and Biomolecular Informatics, University of Nijmegen, The Netherlands.
[46] Herz, W.; Iyer, V.S.; Gopal Nair, M. *J. Org. Chem.* **1975**, *40*, 3519.
[47] Klunder, A.J.H.; de Valk, W.C.G.M.; Verlaak, J.M.J.; Schellekens, J.W.M.; Noordik, J.H.; Parthasarathi, V.; Zwanenburg, B. *Tetrahedron* **1985**, *41*, 963.
[48] Zhu, J. *Thesis*, University of Nijmegen, The Netherlands, 1995.
[49] a) Klunder, A.J.H.; Bos, W.; Verlaak, J.M.J.; Zwanenburg, B. *Tetrahedron Lett.* **1981**, *22*, 4553. b) Verlaak, J.M.J.; Klunder, A.J.H.; Zwanenburg, B. *Tetrahedron Lett.* **1982**, *23*, 5463. c) Verlaak, J.M.J. *Thesis*, University of Nijmegen, The Netherlands, 1983.
[50] Dols, P.P.M.A. *Thesis*, University of Nijmegen, The Netherlands, 1993.
[51] Dols, P.P.M.A.; Arnouts, E.G.; Rohaan, J.; Klunder, A.J.H.; Zwanenburg, B. *Tetrahedron* **1994**, *50*, 3473.
[52] Behforouz, M.; Bolan, J.L.; Flynt, M.S. *J. Org. Chem.* **1985**, *50*, 1186.
[53] Takano, S.; Inomata, K.; Takahashi, M.; Ogasawara, K. *Synlett.* **1991**, 636.

SUMMARY

This thesis deals with possible applications of mineral solid acids such as amorphous aluminas and natural or synthetic clay materials as catalysts in environmentally benign fine chemical transformations.

Chapter 1 gives an introduction to the background of the research described in this thesis. Some general topics concerning heterogeneous catalysis are described as well as the central theme of the IOP-Catalysis program. The aims of the research and the outline of the thesis are described.

In **Chapter 2** the chemical, textural and structural properties of solid acids, such as amorphous alumina, amorphous silica-alumina, clays and zeolites are discussed. In addition, possible applications of these materials are briefly treated. Furthermore, the solid acid catalysts used in this thesis are characterized by means of nitrogen adsorption (BET), aluminum MAS NMR and DRIFT infrared analysis of adsorbed pyridine.

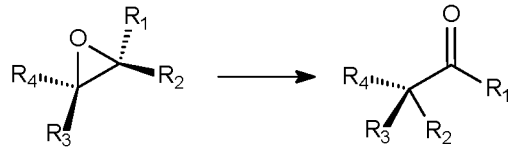

Scheme 1 *Isomerization of epoxides into carbonyl compounds*

In **Chapter 3** the use of various solid acid catalysts in the isomerization of epoxides to carbonyl compounds (Scheme 1) in liquid phase reactions is treated. The epoxides used in this chapter have one or more aromatic substituents (viz. styrene oxide **1**, *cis*- and *trans*-stilbene oxide and tetraphenyloxirane) or is a complex aliphatic epoxide (α-pinene oxide **3**). Styrene oxide **1** rearranges to the rather labile phenylacetaldehyde **2** as the major product. The best results, in terms of high reaction rates and high product selectivities (99%), were achieved with montmorillonite K-10 as the catalyst. Reactions on a larger (multigram) scale showed that at higher substrate concentrations the reaction time required was longer and that the selectivity towards **2** was lower due to an increased formation of secondary reaction products. The method described allows the synthesis of **2** in a high purity and with a simple filtration as the only work-up step, whereas in the current commercial process a maximum purity of 85% is achieved. Rearrangement of the sensitive α-pinene oxide **3** resulted in a broad range of products. Campholenic aldehyde **4** was the major

product with a maximum selectivity of 55%, using Mg-stevensite. The catalysts that gave very high conversion rates (i.e. the natural clays) showed only moderate selectivities of up to 40%. The method used allows the synthesis of **4** avoiding the use of a classical Lewis acid and with filtration as the only work-up step, thus reducing the amount of waste.

The established acidic properties of the catalysts are only partly reflected in the results obtained in the isomerization reaction of epoxides. Accessibility to catalytic surface sites is a very important feature and this is observed in some cases, as the unequal surface area of several catalysts seems to be of influence on the catalytic activity.

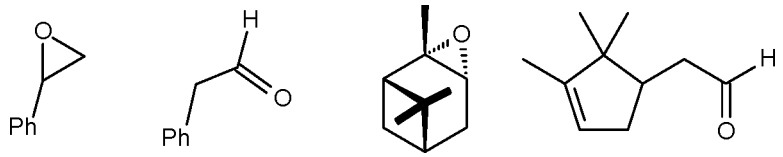

1 **2** **3** **4**

In **Chapter 4**, the isomerization of epoxides under catalytic flash vacuum thermolysis conditions is described, using various solid acid catalysts. The substrates used to investigate the isomerization reaction were similar to those in Chapter 3, but, in addition, several aliphatic epoxides (viz. cyclohexene oxide and 1-octene oxide) and an epoxide having an additional polar functionality (methyl 3-phenyl-2-oxirane-carboxylate) are used. Under catalytic flash vacuum thermolysis conditions phenyl-acetaldehyde **2** is also the major product from styrene oxide **1** with selectivities typically between 97 and 99.5%. At very high temperatures also some phenyl-acetylene was produced via a dehydration mechanism. It was shown for montmorillonite K-10 that the epoxide rearrangement can be used to prepare **2** in a substrate/catalyst ratio of up to 20. As in Chapter 3, rearrangement of α-pinene oxide **3** resulted in a broad spectrum of products of which campholenic aldehyde **4** was the principal component and a maximum selectivity of 60% was achieved using the B698D-24 amorphous alumina at 150°C. The selectivity for **4** usually reached a maximum at the lowest reaction temperatures. Methyl 3-phenyl-2-oxiranecarboxy-late **5** was smoothly isomerized into methyl 2-oxo-3-phenylpropanoate **6** with a very high selectivity (Scheme 2). Apparently, the presence of an electronegative function in the epoxide does not impede the epoxide rearrangement reaction using solid acid catalysts.

No consistent correlation was found between the catalytic activity and the acidity of the catalysts or the active surface area.

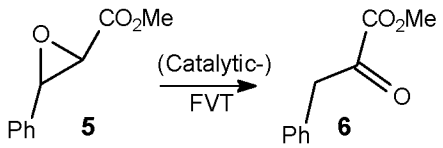

Scheme 2 *Isomerization of epoxide* **5** *under catalytic FVT conditions*

The use of a puls flow system incorporated in a gas chromatograph as a model for a fixed bed reactor is described in **Chapter 5**. Various solid acid catalysts were employed under normal pressure and flow conditions in the epoxy/carbonyl rearrangement reactions of styrene oxide **1** and α-pinene oxide **3**. The outcome of the reaction was dependent on the type of catalyst, the temperature and the amount of substrate. The highest conversions of **1** were achieved at higher temperatures and some catalysts (viz. F-105SF and HA-SHPV) were still able to give complete conversions after many consecutive runs, thus showing minor deactivation. The selectivity for **2** increased with the number of runs until a maximum was reached, which ranged from 45 to 73% (F-105SF). Rearrangement of α-pinene oxide **3** resulted in a broad spectrum of products of which campholenic aldehyde **4** was the principal component. The selectivity for **4** increased with the number of consecutive runs and a maximum of 58% was reached using HA-SHPV as the catalyst.
A comparison with the catalytic FVT methodology (Chapter 4) shows that there is a profound effect of pressure. Using the micropuls reactor unit the conversions for both **1** and **3** varied within a much broader range, the selectivity for **2** was much lower and the selectivity for **4** was in the same order of magnitude.
The results indicate that the desired epoxide rearrangement reactions can be performed at ambient pressure. Hence, a fixed bed reactor is the best option for scaling-up, although for the production of phenylacetaldehyde **2** from **1** the catalytic FVT method, viz. much higher product purity, low waste production, high conversion and selectivity, is more advantageous. For the conversion of α-pinene oxide **3** the outcome of the reaction under ambient pressure is in the same range as was accomplished under catalytic FVT conditions. Here a fixed bed reactor seems an attractive option.

Chapter 6 deals with the application of various solid acid catalysts in the pinacol rearrangement under catalytic flash vacuum thermolysis (Scheme 3). This rearrangement was studied, because of its mechanistic similarities with the epoxide rearrangement. A pronounced difference, however, between these types of reactions is the formation of water during the pinacol rearrangement, but it turned out that the liberated water does not hamper the catalytic performance. The diols employed, viz. 1-phenyl-1,2-ethanediol, 1,2-octane diol, 2-phenyl-1,2-propane diol and α-pinane *cis*-

diol, may be considered as the diol analogs of the epoxides used in Chapter 4. Rearrangement of 1-phenyl-1,2-ethanediol preferentially leads to phenylacetaldehyde **2** in very high selectivities. In view of the better availability of epoxide **1** the preparation of **2** from **1** is strongly preferred. α-Pinane *cis*-diol gave on thermolysis a range of products of which campholenic aldehyde **4** and pinocamphone are the most important ones.

There was no consistent correlation between the acidity of the catalysts and their catalytic activity. The active surface area of the catalysts may have some influence on the catalyst performance, but this effect is not very pronounced.

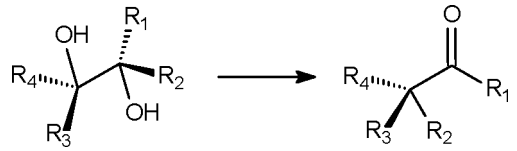

Scheme 3 *The pinacol rearrangement of diols into carbonyl compounds*

The outcome of the thermolysis reaction of diols and epoxides are similar, but not identical. The conversions were usually higher for epoxides, especially at lower thermolysis temperatures. The resulting product mixtures had in most cases a different composition. This was most pronounced with 1,2-octane diol and α-pinane *cis*-diol. Comparison of the results of α-pinane *cis*-diol with α-pinene oxide **3** reveals that the ratio of the products campholenic aldehyde **4** and trans-pinocamphone are different. This is tentatively explained by a different type of binding to the catalyst surface, bidentate-like for the diol and in a monodentate manner for the epoxide. Moreover, the effect of the annelation strain in the epoxide on the reactivity of this compound has to be taken into account, to explain the difference in product formation.

In **Chapter 7**, various solid acid catalysts are used in the liquid phase and under catalytic flash vacuum thermolysis conditions to study the retro Diels-Alder reaction. Our study shows that they can indeed be used to catalyze the retro Diels-Alder reaction in the liquid phase. Surprisingly, the rigid γ,δ-unsaturated ester **7** underwent a lactonization reaction to **8** (Scheme 4). It was shown that also other rigid γ,δ-unsaturated esters may react in this manner, but flexible γ,δ-unsaturated esters did not. Water is essential in the proposed mechanism for the solid acid catalyzed formation of lactones **8**, which is confirmed experimentally.

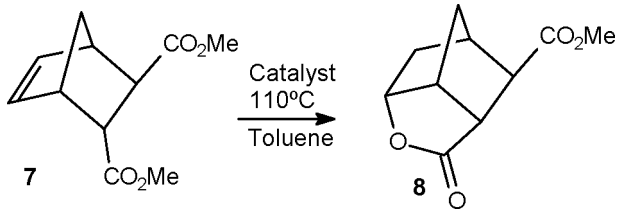

Scheme 4 *Lactonization reaction of rigid γ,δ-unsaturated ester* **7**

Catalytic FVT using various solid acids is a suitable method to achieve retro Diels-Alder reactions of simple cycloadducts as demonstrated by the results obtained in this and earlier studies. Catalytic FVT reactions on various tricyclodecenone epoxides **9** proved to be rather complex since in many cases cage compounds **10** were obtained as the major products besides minor amounts of retro Diels-Alder products (Scheme 5). The structures of these unexpected cage products **10** have been indisputably established by means of an X-ray diffraction analysis of a hydrazone derivate of **10a**. The mechanism explaining the formation of cage compounds **10** involves an initial isomerization of the tricycli-*exo*-epoxide into the *endo*-isomer **11** via a carbonyl ylid type intermediate. The product-forming step is a reaction of the olefinic bond with the oxygen of the *endo*-epoxide, which probably takes place on the catalyst surface.

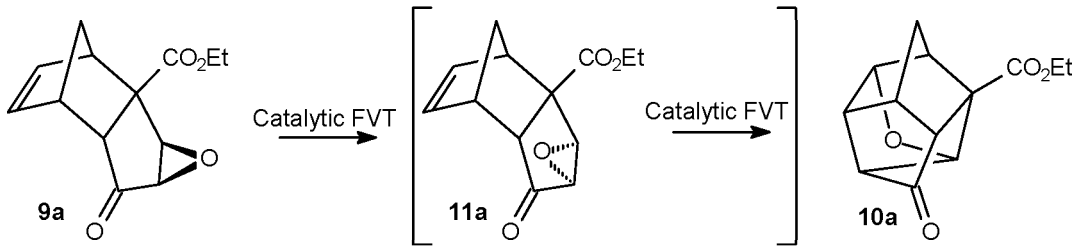

Scheme 5 *Formation of cage compound* **10a** *from tricyclodecenone* exo-*epoxide* **9a**

In summary, the studies described in this thesis show that the use of mineral solid acids, such as amorphous aluminas and natural or synthetic clay materials, as catalysts in isomerization reactions of various epoxides has attractive features from an environmental point of view.

SAMENVATTING

In dit proefschrift worden mogelijke toepassingen beschreven van vaste minerale zuren, zoals amorfe alumina's en natuurlijke en synthetische kleien, in milieu-vriendelijke fijnchemische processen.

Hoofdstuk 1 geeft een inleiding voor het in dit proefschrift beschreven onderzoek. Een aantal algemene onderwerpen betreffende heterogene katalyse worden behandeld, evenals het centrale thema van het IOP-Katalyse programma. De doelen van het onderzoek en de indeling van het proefschrift worden beschreven.

In **Hoofdstuk 2** worden the chemische en morfologische eigenschappen beschreven van belangrijke vaste minerale zuren, zoals amorfe alumina, amorfe silica-alumina, kleien en zeolieten. Tevens worden mogelijke toepassingen van deze materialen kort behandeld. Bovendien wordt aangegeven hoe de in dit proefschrift gebruikte vaste zure katalysatoren zijn gekarakteriseerd middels stikstof adsorptie (BET), aluminium MAS NMR en DRIFT infrarood analyse van geadsorbeerd pyridine.

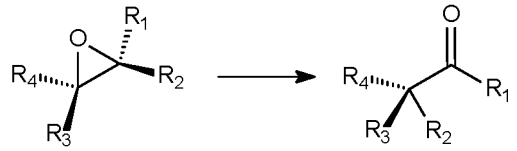

Schema 1 *Isomerisatie van epoxides naar carbonyl verbindingen*

Hoofdstuk 3 behandelt het gebruik van verscheidene vaste zure katalysatoren voor de isomerisatie van epoxides naar carbonyl verbindingen (Schema 1) in vloeistoffase reacties. De gebruikte epoxides hebben één of meer aromatische substituenten (namelijk: styreenoxide **1**, *cis*- en *trans*-stilbeenoxide en tetrafenyloxiraan) of is een complex alifatisch epoxide (α-pineenoxide **3**). Styreenoxide **1** isomeriseert naar het nogal labiele fenylacetaldehyde **2** als belangrijkste product. De beste resultaten, in termen van snelle reacties en hoge productselectiviteiten (99%), werden verkregen met montmorillonite K-10 as katalysator. Uit reacties op grotere schaal bleek dat de vereiste reactietijd langer is bij hogere substraat concentraties en dat de selectiviteit naar **2** lager is ten gevolge van een toename in de vorming van secondaire reactieproducten. Fenylacetaldehyde **2** kan met de beschreven methode worden bereid met een hoge zuiverheid, waarbij slechts één simpele filtratie als de enige opwerkstap nodig is. In het huidige commerciële proces kan slechts een maximale zuiverheid van 85% worden behaald. Isomerisatie van het reactieve α-pineenoxide **3**

gaf een grote verscheidenheid aan producten. Kamfoleenaldehyde **4** was het belangrijkste product met een maximum selectiviteit van 55%, indien Mg-stevensiet als katalysator werdgebruikt. Katalysatoren die in staat waren hoge conversies te geven (de natuurlijke kleien) gaven slechts bescheiden selectiviteiten (tot 40%). Op deze wijze kan **4** worden gesynthetiseerd zonder gebruik van klassieke Lewiszuren en met filtratie als de enige opwerkstap, waardoor de hoeveelheid afvalstoffen aanzienlijk is vermindert.

In de resultaten van de isomerisatiereacties van epoxides worden de gemeten zure eigenschappen van de katalysatoren slechts beperkt teruggevonden. Toegankelijkheid van het substraat tot katalytische centra op het oppervlak is zeer belangrijk. Dit wordt in een aantal gevallen teruggevonden, aangezien het verschil in actief oppervlak van een aantal katalysatoren van invloed lijkt te zijn op de katalytische activiteit.

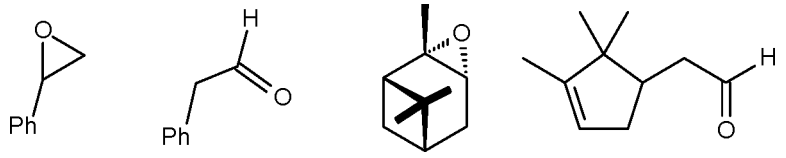

1 **2** **3** **4**

In **Hoofdstuk 4** wordt de isomerisatie van epoxides onder katalytische flits-vacuüm-thermolyse condities beschreven met verscheidene vaste zure katalysatoren. De gebruikte substraten zijn deels hetzelfde als in Hoofdstuk 3, maar tevens zijn een aantal alifatische epoxides (cyclohexeenoxide en 1-octeenoxide) en een epoxide met een additionele polaire functie (methyl 3-fenyl-2-oxiraancarboxylaat) gebruikt. Fenylacetaldehyde **2** is ook onder katalytische flits-vacuüm-thermolyse condities het hoofdproduct uitgaande van styreenoxide **1**, gewoonlijk met een selectiviteit tussen 97 en 99.5%. Bij zeer hoge temperaturen wordt tevens een weinig fenylacetyleen gevonden, dat via een dehydratie mechanisme wordt gevormd. Voor montmorillonite K-10 is aangetoond dat de epoxide omlegging gebruikt kan worden voor een praktische bereiding van **2** met een substraat/katalysator verhouding van 20. Net als in Hoofdstuk 3 gaf de isomerisatie van α-pineenoxide **3** een grote verscheidenheid aan producten, waarvan kamfoleenaldehyde **4** de hoofdcomponent is. Een maximale selectiviteit van 60% kon worden behaald met de amorfe alumina B698D-24 bij 150°C. De selectiviteit naar **4** bereikte gewoonlijk een maximum bij de laagste reactietemperaturen. Methyl 3-fenyl-2-oxiraancarboxylaat **5** kan gemakkelijk worden geïsomeriseerd naar methyl 2-oxo-3-fenylpropanoaat **6** met een zeer hoge selectiviteit (Schema 2). Blijkbaar vormt de aanwezigheid van een electronegatieve functie in het epoxide geen beletsel voor deze door vaste zure gekatalyseerde isomerisatie van epoxides.

Geen consistente correlatie kon gevonden worden tussen de katalytische activiteit en de zuurtegraad van de katalysatoren of de oppervlaktegrootte.

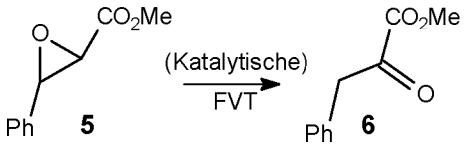

Schema 2 *Isomerisatie van epoxide* **5** *onder katalytische FVT condities*

In **Hoofdstuk 5** wordt het gebruik van een puls-flow-systeem in een gaschromatograaf als een model voor een fixed-bed-reactor beschreven. Verscheidene vaste zure katalysatoren zijn gebruikt onder normale druk en flow condities in de epoxide/carbonyl omleggingsreacties van styreenoxide **1** en α-pineenoxide **3**. De uitkomst van de reacties was afhankelijk van het type katalysator, de temperatuur en de substraathoeveelheid. De hoogste conversies van **1** werden behaald bij hogere temperaturen en een tweetal katalysatoren, namelijk F-105SF en HA-SHPV. Zelfs na vele achtereenvolgende runs waren deze nog in staat complete conversies te bewerkstelligen, hetgeen wijst op een geringe deactivering tijdens dit proces. De selectiviteit naar **2** nam toe met het aantal runs totdat er een maximum werd bereikt, welke tussen de 45 en 73% (F-105SF) lag. Isomerisatie van α-pineenoxide **3** gaf een grote verscheidenheid aan producten waarvan kamfoleenaldehyde **4** de belangrijkste is. De selectiviteit naar **4** nam toe met het aantal achtereenvolgende runs en een maximum van 58% werd bereikt met HA-SHPV als de katalysator.
Een vergelijking met de katalytische FVT methode (Hoofdstuk 4) toont aan dat het drukverschil van grote invloed is. Met de micropulsreactor varieerden de conversies van zowel **1** als **3** binnen een veel bredere marge, was de selectiviteit naar **2** veel lager. De selectiviteit naar **4** was daarentegen in dezelfde orde van grootte.
De resultaten laten zien dat de gewenste epoxide omleggingsreacties kunnen worden uitgevoerd bij normale druk. Een fixed-bed-reactor is daarom de beste optie voor opschaling, hoewel voor de productie van fenylacetaldehyde **2** vanuit **1** de katalytische FVT methode (namelijk de veel hogere productzuiverheid, weinig afvalstoffen, hoge conversie en selectiviteit) grotere voordelen heeft. De conversies van α-pineenoxide **3** zijn onder gewone druk ongeveer gelijk aan die onder katalytische FVT condities. Een fixed-bed-reactor lijkt hier een aantrekkelijke optie.

Hoofdstuk 6 gaat over het gebruik van vaste zure katalysatoren in de pinacol omlegging van 1,2-diolen onder katalytische flits-vacuüm-thermolyse condities (Schema 3). Deze omlegging is bestudeerd, omdat deze mechanistische overeenkomsten heeft met de epoxide omlegging. Echter een belangrijk verschil is dat tijdens de pinacol omlegging water wordt gevormd. Het bleek echter dat het

vrijkomende water de katalytische activiteit niet beïnvloedt. De gebruikte diolen (1-fenyl-1,2-ethaandiol, 1,2-octaandiol, 2-fenyl-1,2-propaandiol en α-pinaan-*cis*-diol) kunnen min of meer worden beschouwd als synthetisch analoga van de epoxides beschreven in Hoofdstuk 4. Omlegging van 1-fenyl-1,2-ethaandiol geeft hoofdzakelijk fenylacetaldehyde **2** met zeer hoge selectiviteiten. Echter een voorkeur voor de bereiding van **2** vanuit styreenoxide **1** ligt voor de hand, aangezien dit epoxide veel beter verkrijgbaar is. α-Pinaan-*cis*-diol gaf na thermolyse allerlei producten waarvan kamfoleenaldehyde **4** en pinokamfon de belangrijksten zijn.
Een consistente correlatie kon niet gevonden worden tussen de katalytische activiteit en de zuurheid van de katalysatoren. De oppervlaktegrootte van de katalysatoren leek van invloed te zijn op de katalytische activiteit, maar dit effect was niet groot.

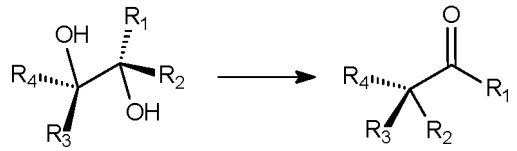

Schema 3 *De pinacol omlegging van diolen naar carbonylverbindingen*

De uitkomsten van de thermolyse reacties van diolen en epoxides zijn vergelijkbaar, maar niet identiek. Voor de epoxides waren de conversies normaliter hoger, zeker bij de lagere temperaturen. De resulterende productmengsels hadden in de meeste gevallen een verschillende samenstelling. Dit was het duidelijkst bij 1,2-octaandiol en α-pinaan-*cis*-diol. Vergelijking van de resultaten van α-pinaan-*cis*-diol met α-pineen-oxide **3** laat zien dat de verhouding van de producten kamfoleenaldehyde **4** en *trans*-pinokamfon verschillend zijn. Dit wordt verklaard met een verschillende soort binding aan het katalysatoroppervlak, bidentaatachtig voor het diol en monodentaat-achtig voor het epoxide. Daarnaast moet rekening gehouden worden met het effect van de extra ringspanning die inherent is aan de epoxide functie die van invloed lijkt te zijn op de productvorming.

In **Hoofdstuk 7** worden vaste zure katalysatoren gebruikt voor de bestudering van de retro Diels-Alder reactie zowel in de vloeistoffase als onder katalytische-flits-vacuüm-thermolyse-condities. Onze studie toont aan dat zij inderdaad toegepast kunnen worden om de retro Diels-Alder reactie te katalyseren in de vloeistoffase. Verrassenderwijze onderging de starre γ,δ-onverzadigde ester **7** een lactonisatie-reactie naar **8** (Schema 4). Aangetoond is dat ook andere starre γ,δ-onverzadigde esters op deze wijze kunnen reageren, maar flexibele γ,δ-onverzadigde esters niet. Water is essentieel in het voorgestelde mechanisme voor deze door vaste zuren gekatalyseerde vorming van lactonen **8**, hetgeen experimenteel bevestigd werd.

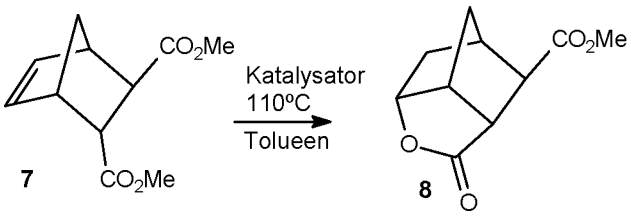

Schema 4 *Lactonisatiereactie van starre γ,δ-onverzadigde ester* **7**

Katalytische FVT met vaste zuren is een geschikte methode om de retro Diels-Alder reactie van eenvoudige cycloadducten bij relatief lage temperaturen te kunnen realiseren. Dit is aangetoond in de deze en eerdere studies. Katalytische FVT reacties aan verscheidene tricyclodecenon-epoxides **9** bleken niet te leiden tot een efficient retro Diels-Alder proces. Vermoedelijk als gevolg van de bijzondere structuur van deze epoxiden werden hierbij kooiverbindingen **10** als hoofdproduct verkregen (Schema 5). De structuren van deze onverwachte kooiverbindingen **10** zijn ondubbelzinnig bepaald middels een Röntgendiffractie analyse van een hydrazon-derivaat van **10a**. Het mechanisme dat de vorming van **10** verklaart behelst eerst een isomerisatie van het *exo*-epoxide **9** naar het *endo*-isomeer **11** via een carbonyl ylide type intermediair, waarna in een productvormende stap een reactie van de olefinische binding met het de zuurstof van het *endo*-epoxide plaatsvindt, waarschijnlijk op het katalysatoroppervlak.

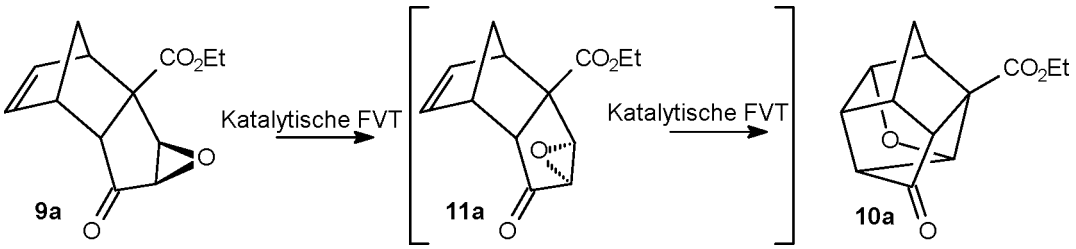

Schema 5 *Vorming van kooiverbinding* **10a** *vanuit tricyclodecenone epoxide* **9a**

Samenvattend kan gezegd worden dat de studie beschreven in deze dissertatie laat zien dat vaste minerale zuren, zoals amorfe alumina's en natuurlijke en synthetische kleien, goed gebruikt kunnen worden voor de omlegging van verscheidene typen epoxiden, met name vanuit het oogpunt van milieuvriendelijkheid.

LIST OF PUBLICATIONS & PRESENTATIONS

a-Oxo Sulfines and their Synthetic Behaviour
R.C. de Laet, A.J.J.M. van Breemen, A.J. Derksen, M. van Klaveren and B. Zwanenburg, *Phosphorus, Sulfur and Silicon*, **1993**, *74*, 371-372.

Behaviour of Steps on the (001) face of $K_2Cr_2O_7$ Crystals
A.J. Derksen, W.J.P. van Enckevort, M.S. Couto, *J. Phys. D: Appl. Phys.* **1994**, *27*, 2580-2591.

Impurity Blocking of Growth Steps: Experiments and Theory
W.J.P. van Enckevort, A.C.J.F. van der Berg, K.B.G. Kreuwel, A.J. Derksen, M.S. Couto, *J. Cryst. Growth.* **1996**, *166*, 156-161.

Isomerization of Tricyclodecenone Epoxides to Oxa-pentacyclo-undecanones using Flash Vacuum Thermolysis with Solid Acid Catalysts
A.J. Derksen, A.C.L.M. van der Waals, M.H.A. van Ham, M. Van Dongen, R. de Gelder, A.J.H. Klunder, B. Zwanenburg, in preparation.

Nucleophilic Substitution Reactions of Thiopyrans
A.J. Derksen, R.C. de Laet, B. Zwanenburg
Oral presentation at the Shell Sittingbourne Research Centre during the study tour of chemistry students to the United Kingdom, United Kingdom, April 1993.

Nucleophilic Substitution Reactions of Thiopyrans
A.J. Derksen, R.C. de Laet, B. Zwanenburg
Poster presentation during "209th American Chemical Society National Meeting", in Anaheim, California (USA), April 1995.

Application of Environmentally Benign Solid Acid Catalysts in the Synthesis of Fine Chemicals
A.J. Derksen, A.J.H. Klunder, B. Zwanenburg
Poster presentation during "11th International Conference on Organic Synthesis", in Amsterdam, The Netherlands, June-July 1996.

Application of Environmentally Benign Solid Acid Catalysts in the Synthesis of Fine Chemicals
A.J. Derksen, A.J.H. Klunder, B. Zwanenburg
Poster presentation at several universities and companies during the study tour of the Department of Organic Chemistry to South Africa, South Africa, March-April 1997.

Environmentally Benign Solid Acid Catalysts in the Synthesis of Fine Chemicals
A.J. Derksen, A.C.L.M. van der Waals, A.J.H. Klunder, B. Zwanenburg
Oral presentation during the annual NSR meeting, Nunspeet, The Netherlands, October 1997.

Synthesis of Fine Chemicals by the Application of Environmentally Benign Solid Acid Catalysts
A.J. Derksen, A.J.H. Klunder, B. Zwanenburg
Oral presentation during the 6th Bologna-Nijmegen Minisymposium, Nijmegen, The Netherlands, September 1998.

CURRICULUM VITAE

André Derksen werd op 6 september 1971 geboren in Nijmegen. In juni 1989 behaalde hij aan het R.K. Elshofcollege te Nijmegen het VWO-diploma. In datzelfde jaar begon hij aan de studie scheikunde aan de Katholieke Universiteit Nijmegen, waarvoor hij in 1990 het propeadeutisch examen haalde (cum laude). In augustus 1994 haalde hij het doctoraal examen met als uitgebreide hoofdrichting Organische Chemie (Prof. Dr. B. Zwanenburg) en als nevenrichting Vaste Stof Chemie (Prof. Dr. P. Bennema, Dr. W.J.P. van Enckevort). Voordat hij afstudeerde verrichte hij bij de vakgroep Vaste Stof Chemie onder leiding van Dr. H.L.M. Meekes vier maanden onderzoek in opdracht van de Holland Sweetener Company.

Van november 1994 tot november 1998 was hij als Assistent in Opleiding (AIO) verbonden aan het NSR Center for Molecular Structure, Design and Synthesis bij de vakgroep Organische Chemie. Onder leiding van Prof. Dr. B. Zwanenburg en Dr. A.J.H. Klunder verrichte hij het in dit proefschrift beschreven promotieonderzoek. Het onderzoek werd verricht in het kader van het IOP-Katalyse waarbij werd samengewerkt met de Universiteit van Utrecht (Prof. Dr.Ir. J.W. Geus) en waarbij er regelmatig werd gerapporteerd aan vertegenwoordigers van de Nederlandse chemische industrie. Tijdens zijn studie en promotieonderzoek was hij betrokken bij het practicum onderwijs aan eerste en tweede jaars scheikunde studenten.